WBS: 1.2.3.9
QA: N/A

Civilian Radioactive Waste Management System
Management & Operating Contractor

Geology/Hydrology Environmental Baseline File

B00000000-01717-5700-00027 REV 01, DCN 1

June 1999

Prepared for:

U.S. Department of Energy
Yucca Mountain Site Characterization Office
P.O. Box 30307
North Las Vegas, Nevada 89036-0307

Prepared by:

TRW Environmental Safety Systems Inc.
1261 Town Center Drive
Las Vegas, Nevada 89134-6352

Under Contract Number
DE-AC08-91RW00134

DISCLAIMER

This report was prepared as an account of work sponsored by an agency of the United States Government. Neither the United States Government nor any agency thereof, nor any of their employees, nor any of their contractors, subcontractors or their employees, makes any warranty, express or implied, or assumes any legal liability or responsibility for the accuracy, completeness, or any third party's use or the results of such use of any information, apparatus, product, or process disclosed, or represents that its use would not infringe privately owned rights. Reference herein to any specific commercial product, process, or service by trade name, trademark, manufacturer, or otherwise, does not necessarily constitute or imply its endorsement, recommendation, or favoring by the United States Government or any agency thereof or its contractors or subcontractors. The views and opinions of authors expressed herein do not necessarily state or reflect those of the United States Government or any agency thereof.

Civilian Radioactive Waste Management System
Management & Operating Contractor

Geology/Hydrology
Environmental Baseline File

B00000000-01717-5700-00027 REV 01, DCN 1

June 1999

Prepared by:

David F. Fenster

D.F. Fenster
Site Description and Regulatory Documents

6/17/99
Date

Checked by:

J.R. McCleary

J.R. McCleary
Senior Staff,
Natural Environment Program Operations

6/17/99
Date

Approved by:

R.C. Quittmeyer

R.C. Quittmeyer
Technical Lead,
Site Description and Regulatory Documents

6/17/99
Date

CHANGE HISTORY

Revision	Document Change Notice	Date	Description of Change
00	N/A	September 1997	Initial Issue. Note that Revision 00 did not use a Document Identifier number.
01	N/A	March 1999	Complete revision to update document with more recent results of site characterization, especially as presented in the *Yucca Mountain Site Description,* REV 00 (CRWMS M&O 1998)
01	01	June 1999	Cover page changed to correct quality designation. Pages in reference section changed to correct typographic errors and traceability numbers. Other minor changes were made to address comments resulting from the Yucca Mountain Site Characterizaiton Office acceptance review.

PREFACE

The objective of the *Geology/Hydrology Environmental Baseline File* is to provide information on the Yucca Mountain site in a manner that will be useful for the preparation of the Environmental Impact Statement for the Yucca Mountain Site. As such, the *Geology/Hydrology Environmental Baseline File* is primarily a summary of the *Yucca Mountain Site Description* (CRWMS M&O 1998) and other important references that synthesize the results of site characterization studies or present other important information. This baseline file contains information on the geology, hydrology, natural resources, and rock and soil properties of the Yucca Mountain site. Section 1, Regional and Site Geology, focuses on geomorphology, stratigraphy, and structural geology and tectonics including volcanism and seismic hazards. Section 2, Hydrology, discusses the hydrology of surface water, the unsaturated zone, and the saturated zone. Section 3, Natural Resources, contains discussions of natural resources that occur in the Southern Great Basin such as metallic mineral, industrial rocks and minerals, hydrocarbon and geothermal resources. Section 4, Geoengineering, discusses the stratigraphic framework for rock testing, rock structure properties from field studies, laboratory properties of rock core samples, rock mass properties, in situ stress conditions, excavation characteristics, and engineering properties of surficial deposits.

The Environmental Programs Department of the U.S. Department of Energy's Civilian Radioactive Waste Management System Management and Operations Contractor performed an analysis according to Quality Administrative Procedure 2-0, *Conduct of Activities*, of the request by the U.S. Department of Energy to complete environmental and engineering baseline files. This analysis documented that this activity is not quality affecting and thus is not subject to the *Quality Assurance Requirements and Description* (DOE 1998). This environmental baseline file was prepared and reviewed under Civilian Radioactive Waste Management System Management and Operating Contractor procedure PRO-TS-003, *Development of Technical Documents Not Subject to QARD Requirements.*

In accordance with PRO-TS-003, Jefferson R. McCleary checked the document. On behalf of Robert W. Craig of the U.S. Geological Survey, John S. Stuckless and William W. Dudley, Jr. provided technical reviews. On behalf of Lee Morton, Edward W. McCann provided technical review for the CRWMS M&O Environmental Programs Department. In addition to the Lead Preparer, David F. Fenster, contributions to the document were also made by George H. Davis (Section 2) and Gerald P. Kashatus (Section 3).

INTENTIONALLY LEFT BLANK

CONTENTS

CONTENTS (Continued)

CONTENTS (Continued)

FIGURES

FIGURES (Continued)

INTENTIONALLY LEFT BLANK

TABLES

INTENTIONALLY LEFT BLANK

ACRONYM LIST

BP	Before present
CFu	Crater Flat unit
CHn	Calico Hills nonwelded ash flow tuff
DOE	U.S. Department of Energy
ESF	Exploratory Studies Facility
Ga	billion years ago
ka	thousand years ago
ky	thousands of years
kyr	thousand years
Ma	million years ago
M&O	Civilian Radioactive Waste Management System Management and Operating Contractor
MAP	mean annual precipitation
M_d	duration magnitude (a measure of earthquake size)
M_I	intensity derived magnitude (a measure of earthquake size)
M_L	local magnitude (a measure of earthquake size)
M_S	surface-wave magnitude (a measure of earthquake size)
M_w	moment magnitude (a measure of earthquake size)
NRC	U.S. Nuclear Regulatory Commission
PGA	peak ground acceleration
PGV	peak ground velocity
PTn	Paintbrush nonwelded bedded tuffs
Tac	Calico Hills Formation
Tcb	Bullfrog Tuff
Tcp	Prow Pass Tuff
Tct	Tram Tuff
TCw	Tiva Canyon welded tuff
Tma	Ammonia Tanks Tuff
Tmr	Rainier Mesa Tuff
Tpc	Tiva Canyon Tuff
Tpp	Pah Canyon Tuff
Tpt	Topopah Spring Tuff
Tptpll	Topopah Spring Tuff, lower lithophysal zone
Tptpln	Topopah Spring Tuff, lower nonlithophysal zone
Tptpmn	Topopah Spring Tuff, middle nonlithophysal zone
Tptpul	Topopah Spring Tuff, upper lithophysal zone
Tpy	Yucca Mountain Tuff
TSw	Topopah Spring welded devitrified ash flow tuff

INTENTIONALLY LEFT BLANK

1. REGIONAL AND SITE GEOLOGY

1.1 REGIONAL AND SITE GEOMORPHOLOGY

1.1.1 Regional Geomorphology and Topography

The Yucca Mountain region is located within the Great Basin subprovince of the Basin and Range physiographic province which encompasses nearly all of Nevada as well as adjacent parts of Utah, Idaho, Oregon, and California. The region surrounding Yucca Mountain can be further subdivided into several well-defined physiographic areas that reflect regional variations in their geologic characteristics. These areas include: the north-northeast-trending basins and ranges of the central Great Basin; the smaller, more arcuate, and more closely spaced basins and ranges of the southeast Great Basin; the massive ranges and deep basins of the southwest Great Basin (Inyo-Mono terrane); and the highly variable terrane of the Walker Lane belt (Figure 1-1). The southern margin of the Great Basin subprovince is considered to be the Garlock fault (see Figure 1-11) and its projection toward the northeast. The northeastern part of the Mojave Desert, characterized by relatively small, irregularly shaped basins and ranges, is located south of the Garlock fault (CRWMS M&O 1998, p. 3.4-1).

The mountain ranges of the Great Basin are mostly tilted fault-bounded blocks that often extend for more than 80 km (50 miles), are generally 8 to 24 km (5 to 15 miles) wide, rise 300 to 1,500 m (1,000 to 5,000 ft) above the floors of the intervening basins, and occupy approximately 40 to 50 percent of the total land area. The deep structural depressions forming the basins contain sedimentary deposits of late Tertiary and Quaternary ages ranging in thickness from a few hundred meters to more than 3 km. The ground surfaces of closed basins are nearly level to gently sloping, and are commonly partly covered by playas. Open basins are generally moderately to deeply dissected with surface water drainage located parallel to the basin axis. Geomorphic processes in the southern Great Basin are determined largely by climate, existing topography, rock type, and, to a lesser degree, tectonic activity. Late Cenozoic extensional tectonism, volcanism, and semiarid to arid climatic conditions have combined to produce a structurally dominated landscape of high relief, with rugged uplands separated by gently sloping lowland basins. Within this landscape, erosion and erosional processes are concentrated in the high, steep, and relatively wet uplands, whereas deposition and depositional processes are generally concentrated in the low, gently sloping, and relatively arid lowlands (CRWMS M&O 1998, pp. 3.4-1 to 3.4-2).

The Yucca Mountain area is located within the Walker Lane belt, which is a major structural feature considered to be a zone of transition between the combined central and southeastern parts of the Great Basin, characterized by dip-slip normal faulting and typical basin-and-range topography; and the southwestern Great Basin, characterized by both dip-slip and right-lateral strike-slip faulting and by irregular high relief topography (Carr, W.J. 1984, pp. 21, 26; Figure 1-1). Yucca Mountain is situated just south of the central southwestern Nevada volcanic field, which consists of a series of volcanic centers from which large volumes of pyroclastic flow

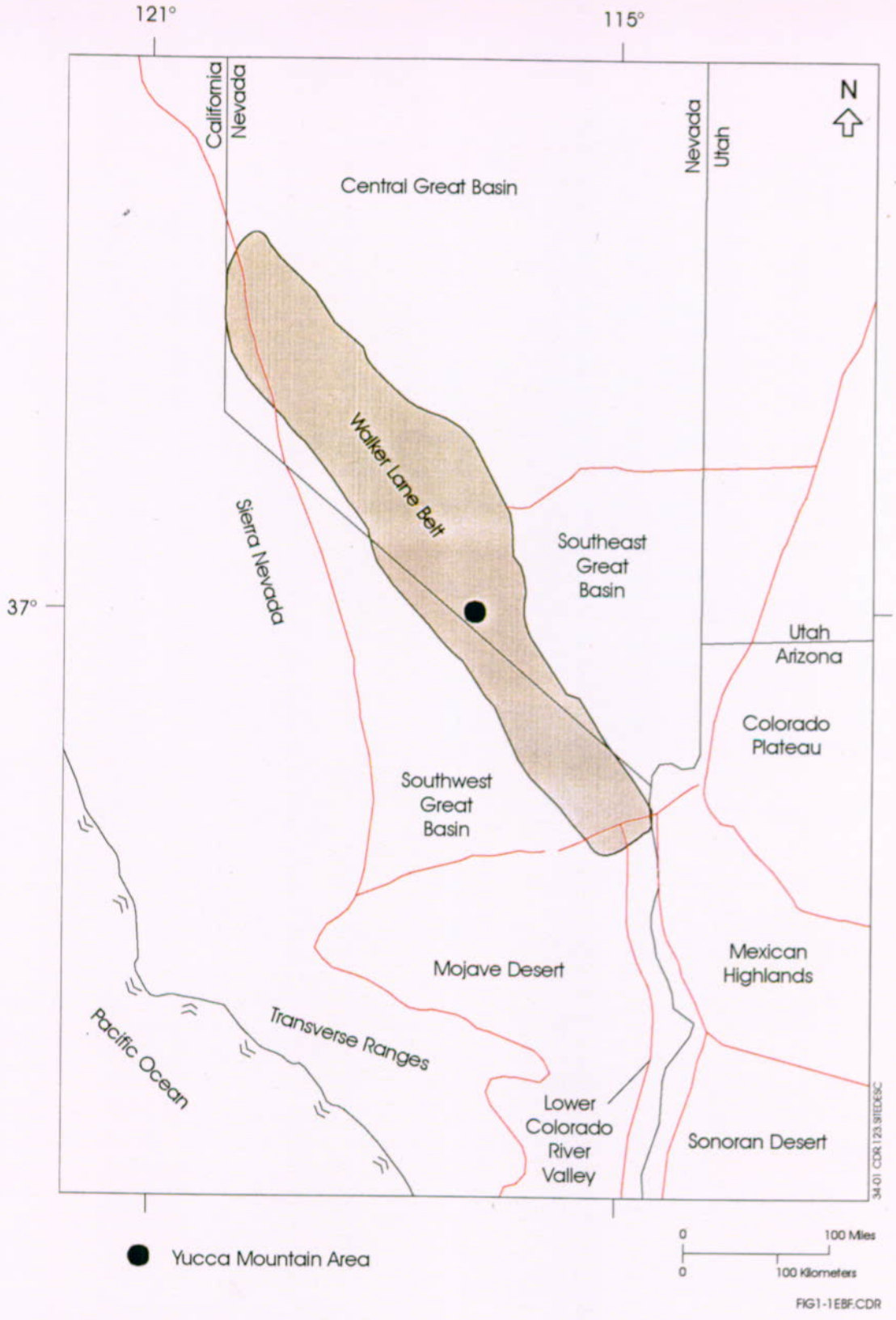

Source: CRWMS M&O (1998, Figure 3.4-1)

Figure 1-1. Generalized Physiographic Subdivisions and Location of the Walker Lane Belt in the Region Surrounding the Yucca Mountain Area

and fallout tephra deposits were erupted from about 14.0 to 11.5 million years ago (Ma) (Sawyer et al. 1994, pp. 1304-1305, 1311-1312,1314; see also Section 1.2.2). Accordingly, Yucca Mountain and many of the adjacent landforms carry the imprint of the area's extensive volcanic history as well as its deformational history. The geologic relations suggest that many (and perhaps most) of these landscape features took on their basic topographic form during the period 12.7 to 11.7 Ma (CRWMS M&O 1998, p. 3.4-2).

In addition to tectonics, another factor affecting the geomorphology of the Yucca Mountain region is climate. Climatic conditions in the Yucca Mountain region, and over Nevada and much of the southwestern United States, are described in several publications that address this general subject (see CRWMS M&O 1998, Section 4 references). In general, the climate of south-central Nevada can be characterized as arid to semiarid, with average annual precipitation ranging from 100 to 200 mm (4 to 8 in.) in most lowland areas, 200 to 400 mm (8 to 16 in.) over parts of the uplands, and more than 400 mm (16 in.) along some mountain crests. This climate exists because the Sierra Nevada (Figure 1-1) effectively prevents moist air from moving toward the east from the west. Precipitation from Pacific air masses that reaches the potential repository area accounts for about 50 percent of the total amount, and occurs during the months of November through April. Precipitation in the form of snow is infrequent. Sections 2.1 and 2.3.1 contain more detailed discussions of precipitation and climate at the Yucca Mountain site.

Section 2.1 also contains information on the surface water hydrology of the Yucca Mountain site and region.

1.1.2 Geomorphology and Topography of the Yucca Mountain Area

Yucca Mountain is located in southern Nevada in the southern part of the Great Basin. The area is bordered on the west and south by Death Valley and by the Mojave Desert of California, a part of the Sonoran Section of the Basin and Range Province (Figure 1-1). The main drainage system of the Yucca Mountain region is the Amargosa River, north, east, and southeast of Beatty, Nevada. When rain is sufficient to induce drainage, the Amargosa River (Figure 1-2) carries runoff from the region south into the southern part of Death Valley.

The Yucca Mountain region, including the Timber Mountain area, the Calico Hills, and the mesas that lie to the north of Timber Mountain, drains ultimately to the Amargosa Valley. Yucca Mountain drains into partially filled alluvial basins from both the east and west flanks of the mountain. The southern half of Crater Flat, west of Yucca Mountain, drains south into the Amargosa Desert west of the Lathrop Wells cinder cone. The Amargosa River is not a perennial flowing stream system in the Yucca Mountain region today, and carries significant runoff only as a result of extraordinarily large precipitation events.

Yucca Mountain is an irregularly shaped upland, 6 to 10 km wide and about 40 km long. The crest of the mountain ranges between elevations of 1,500 and 1,430 m above sea level, about 650 m higher than the floors of adjacent washes in Crater Flat and Jackass Flats. The uplands of the Yucca Mountain area are composed of three general landform types: ridge crests, valley bottoms, and intervening hillslopes (DOE 1988, p. 1-27). The dominantly north-trending, en echelon pattern of ridges and valleys is controlled by westward-dipping, high-angle faults (Day et al. 1998). The fault blocks, composed of fine-grained volcanic rocks (mostly welded tuffs),

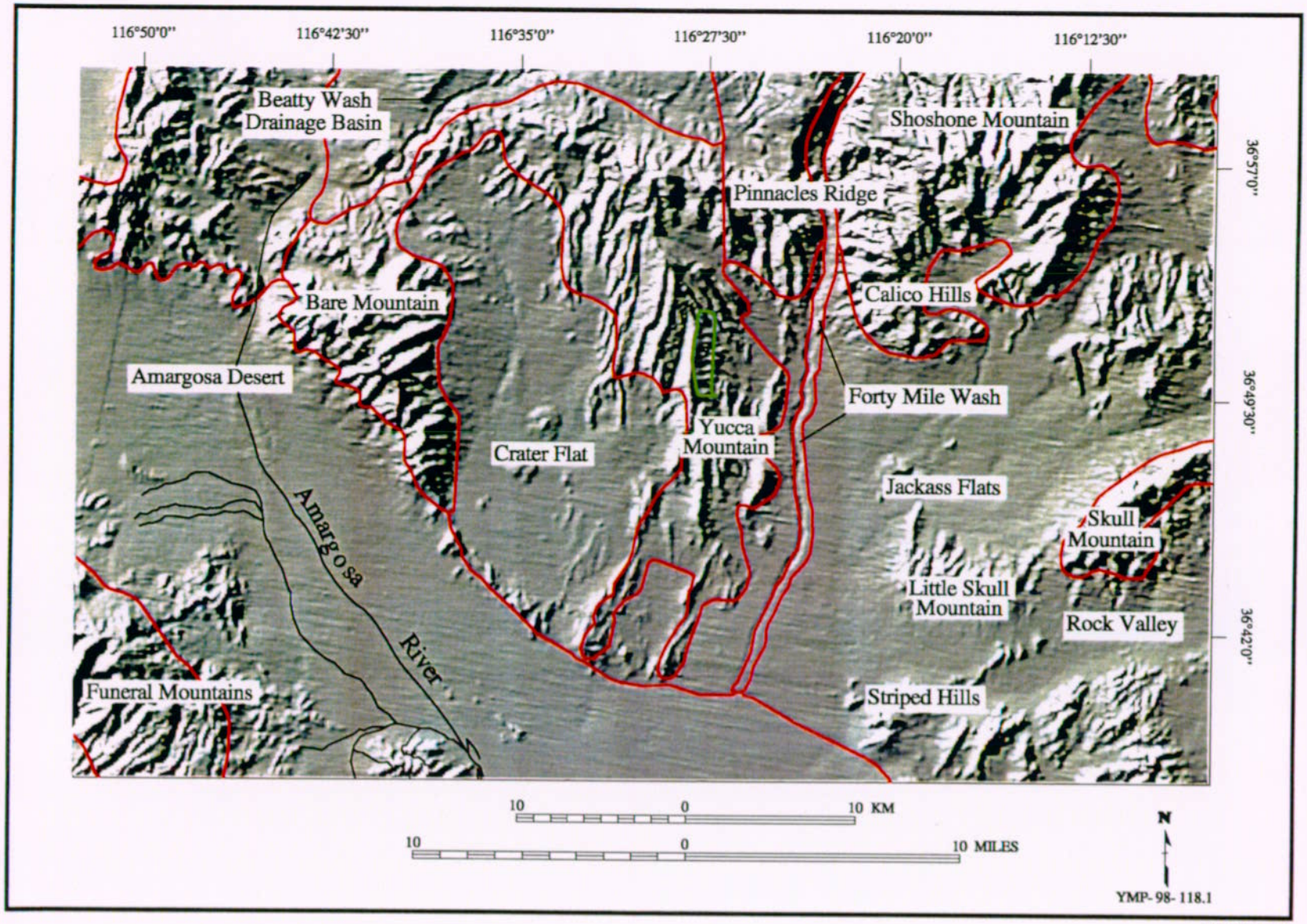

Source: CRWMS M&O (1998, Figure 3.4-2)

NOTE: The proposed repository block is outlined in green.

Figure 1-2. Local Physiographic Subdivisions of the Yucca Mountain Area

are tilted eastward, so that the fault-bounded west-facing slopes are generally high, steep, and straight, whereas the east-facing slopes are more gentle and are commonly deeply dissected. The ridge crests are mostly angular and rugged with the exception of the caprock-protected dip slopes that characterize some of the areas along the ridge crests. The valleys are generally narrow and V-shaped along their upper and middle reaches, but locally contain flat, alluviated floors in their lower reaches. Valley morphology ranges from shallow, straight, steeply sloping gullies and ravines to relatively deep, bifurcating, gently sloping valleys and canyons. The hillslopes between ridge crests and valley floors typically include at least three general forms: narrow upper convexities, extensive straight segments, and broad lower concavities.

The open basins flanking Yucca Mountain, including Crater Flat and Jackass Flats (Figure 1-2), are floored almost entirely by gentle piedmont slopes. These piedmonts are dissected Pleistocene surfaces juxtaposed against slightly dissected to undissected Holocene surfaces. It is not unusual for the older surfaces, which generally lie close to the mountain fronts, to be both overlain by younger deposits and incised by younger channels. In contrast, in areas lying along and adjacent to the basin axes, younger deposits typically bury older deposits and the slopes are dominated by active or recently abandoned alluvial surfaces. Thin, discontinuous sheets of fluvially reworked eolian sand occur locally across the basin floors. In Crater Flat, immediately west of Yucca Mountain, four volcanic cones and associated lava flows reach heights ranging from 27 to 140 m above the alluviated surface of the central basin area. These basalts are discussed in more detail in Section 1.3.3.2.

Fortymile Wash is a conspicuous north to south drainage that lies between Pinnacles Ridge and Yucca Mountain on the west, and Shoshone Mountain, Calico Hills, and the western extremity of Jackass Flats on the east (Figure 1-2). Most of the runoff from Yucca Mountain originates in small tributaries entering the west side of this drainage system. Across the west margin of Jackass Flats, Fortymile Wash has cut a nearly linear channel, 150 to 600 m wide and as much as 25 m deep. Farther to the south and southwest, the wash merges with the general level of the land surface near the northeast margin of the Amargosa Desert. The Amargosa Desert occupies a broad north-west trending basin. Ephemeral streams draining the Yucca Mountain area are tributary to the Amargosa River, which terminates in the internal drainage of Death Valley.

Both Bare Mountain and Pinnacles Ridge are triangular shaped uplands in the Yucca Mountain area (Figure 1-2). The eastern flank of Bare Mountain is well-defined by the high-angle, east-dipping Bare Mountain fault which was active during the Quaternary Period.

Differential vertical movement along high-angle normal faults has probably been the dominant factor in the development of the topographic features that now characterize the Yucca Mountain area (Figure 1-3). Structural studies (e.g., Scott and Bonk 1984; Simonds et al. 1995; Day et al. 1998) show that bedrock (mostly tuffs of Miocene age) is displaced several hundred meters (maximum ~600 m) along many of the faults that occur within or along the flanks of Yucca Mountain, thereby producing offsets that are still highly visible in the landscape. Displacements of Late Quaternary surficial deposits have also taken place along some of these faults, but these are generally less than 3 m cumulative displacement (Menges and Whitney 1996, Table 4.2.1), which is an important consideration in studies dealing with the influence of tectonic movements on future erosion in the area.

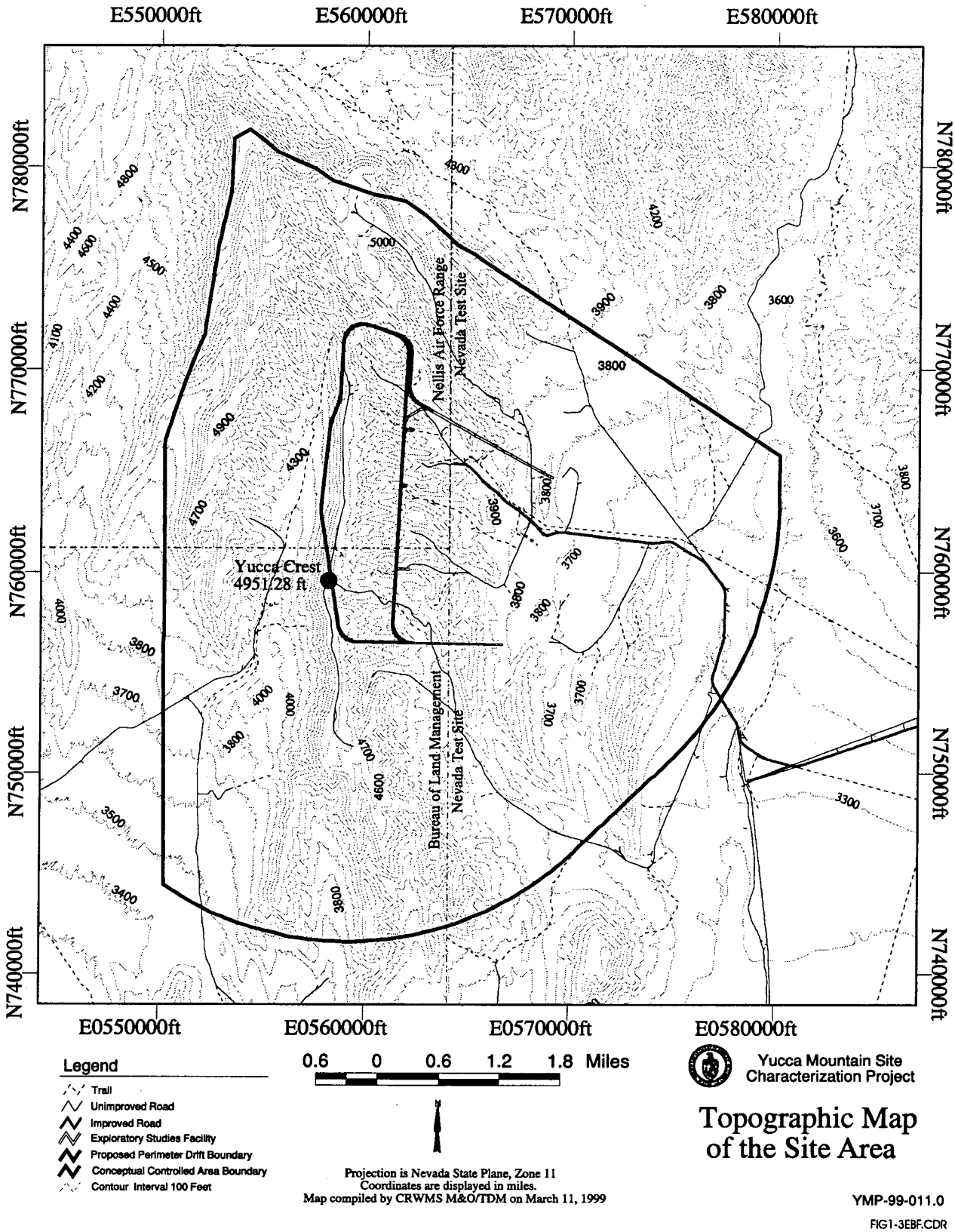

Source: CRWMS M&O (1998 Figure 3.8-1)

Figure 1-3. Simplified Topographic Map of the Site Area

Yucca Mountain is composed of Miocene-age silicic volcanic ash flow and ash fall deposits. A younger phase of volcanism is represented by a series of small volume basaltic volcanic centers that formed during the Pliocene and Quaternary, primarily in Crater Flat, on the west side of Yucca Mountain. The volcanic landforms associated with the 3.7 Ma centers in central Crater Flat have been severely modified by erosion. The volcanic centers dated at approximately 1 Ma form the topographically prominent cinder cones in Crater Flat (Perry et al. 1998, pp. 2-25 to 2-30). The topography of these volcanic centers indicate that the base level for Crater Flat has not changed significantly during the Quaternary. The basalt flows at both the Red Cone and Black Cone centers have neither been buried by alluvium nor has the fill been eroded to expose the base of these flows. The 1 Ma cones and flows show moderate dissection. The youngest volcanic feature, the late Quaternary center at Lathrop Wells, shows little post depositional erosional modification. Geomorphic features that indicate erosion and cone degradation, such as rills on the cone surface or marginal cone aprons, are not generally present on the cinder cone (Wells et al. 1990, p. 551).

1.1.3 Geomorphic Processes and Erosion at the Site

Surficial mapping of Quaternary deposits in the Yucca Mountain site area has been described in detail in the *Yucca Mountain Site Description* (CRWMS M&O 1998, Section 3.4.3). Surficial deposits in the Yucca Mountain area include alluvium that underlies alluvial fan and fluvial terrace surfaces and is deposited along active washes, colluvium and debris-flow deposits that occur along the base and mantle the lower parts of the hillslopes, areas of mixed bedrock and thin colluvium, and eolian deposits. Colluvium includes those sediments deposited by rainwash, sheetwash, or slow continuous downhill creep. Eolian sediments are wind blown deposits, generally sand and silt. Based on mapping investigations, geomorphic processes at the site have resulted in both erosion and deposition during the Quaternary Period.

Potential erosion at the Yucca Mountain site is a regulatory concern that has been addressed by the Yucca Mountain Site Characterization Project (YMP 1993). Additional detailed mapping of surficial geologic deposits, the dating of these deposits and of bedrock surfaces using multiple dating techniques, and related investigations of geomorphic features and processes indicate that the erosion rate at Yucca Mountain is relatively low compared with other areas within the United States and around the world (YMP 1993, Tables 2 and 3).

Surface exposure dating and ages of basaltic flows and cones show that erosion of topographic highs in the vicinity of Yucca Mountain proceeded very slowly. Erosion at Black Cone, located in Crater Flat, was evaluated where the flows have been dated at approximately 1 Ma using K-Ar and cosmogenic beryllium (Beryllium-10). The maximum erosion rate at this site is 0.02 cm/1,000 year (kyr) (CRWMS M&O 1998, Section 3.4.5.2, p. 3.4-39). Using this erosion rate, the total eroded material from the flow surface is about 17 cm. This low quantity of erosional lowering of the crest of a pressure ridge on the Black Cone flows indicates that erosion of such volcanic features occurs very slowly in this area and that volcanic rocks are relatively insensitive to the range of climatic conditions that have existed in the Yucca Mountain area since the mid-Quaternary. Both the cinder cones dated as approximately 1 Ma and the Lathrop Well cinder cone dated at 75 to 80 thousand years ago (ka) have retained much of their original morphology. In the case of the latter, Wells et al. (1990, p. 552) had concluded that the cone is virtually

unmodified by erosion such that the morphology is similar to the 15 to 20 ka cone of the Cima volcanic field.

Two styles of erosion have been examined in the Yucca Mountain area: erosion rates on bedrock outcrops on ridge crests and erosion rates on hillslopes by removal of colluvial materials. Rock samples obtained from outcrops along an east-west profile along two ridges were analyzed for Beryllium-10. These analyses indicate that the vertical erosion rates on bedrock on the summit of Yucca Mountain range from <0.10 to 0.30 cm/kyr averaged over the Quarternary Period (CRWMS M&O 1998, p. 3.4-40).

The erosion rate calculated using the cation ratio dating curve of Harrington and Whitney (1987, pp. 968-969) averages about 0.2 cm/kyr (0.02 to 0.60 cm/kyr) for the Yucca Mountain hillslopes. When the ages of the boulder deposits are calculated using either the recalibrated cation ratio dating curve or calculated using the cosmogenic nuclide exposure ages, the long-term average erosion rates for Yucca Mountain hillslopes are still less than 0.5 cm/kyr (CRWMS M&O 1998, p. 3.4-44).

A maximum erosion rate was calculated for a time interval (17 to 2 ka) during the last climatic transition from wet and cool to warm and dry. This resulted in a bounding value of 1.8 cm/kyr for erosion of unconsolidated hillslope material. This rate would decrease to about 1.2 cm/kyr if the alluvial depositional unit is assumed to have been derived from hillslope bedrock outcrops. This erosion rate, calculated for a period of maximum hillslope stripping, provides a maximum erosion rate compared with the average values given above for the middle and late Quaternary. The erosion rate for the complete climatic cycle for the Yucca Mountain hillslopes is 1.1 cm/kyr for unconsolidated material and 0.7 cm/kyr for hillslope bedrock, during the period from 17 to 2 ka (CRWMS M&O 1998, pp. 3.4-44 to 3.4-45).

These data and studies of sand and gravel deposits at the Yucca Mountain site indicate that fluvial (stream) processes have been intermittent and have not resulted in significant erosion and sediment deposition during the Quaternary Period (last 1.6 Ma). The predominantly semiarid to arid climates of the past and present have tended to preserve the landscape of the region surrounding Yucca Mountain (DOE 1988, p. 1-29). The prevailing conditions have induced a slow rate of weathering on the bedrock slopes. The flow of surface water is intermittent, and subject to flash flood episodes, typically occurring in response to small, intense storms of brief duration. Because of a lack of perennial streams, sediment transport is slow and discontinuous. Colluvial wedges, talus cones, alluvial fans, and alluviated valley floors are the common depositional features of the area.

1.2 REGIONAL AND SITE STRATIGRAPHY

1.2.1 Regional Stratigraphy and Lithology

The stratigraphy and lithology of the regional geologic setting are relevant to the assessment of Yucca Mountain because these geological elements are a product of the history of deformation that has affected the site. The stratigraphy and lithology also constitute the framework for understanding structural geology and tectonics, including volcanism; geoengineering properties;

mineral resource evaluation; hydrology; and geochemistry. The following section provides a description of regional rock stratigraphic units.

Units are grouped according to age and chronostratigraphic boundaries, from oldest to youngest. The units are defined in terms of group and formation names, but are described as lithosomes. Thus, bodies of rock are characterized in terms of gross lithology, thickness, mineralogy, and lateral variations in these parameters, all of which reflect their genesis and depositional environments.

The stratigraphy of the southern Great Basin comprises highly variable lithologies, ranging in age from Precambrian (older than 570 million years) to Holocene (younger than 10,000 years). The stratigraphic sequence with formation names is illustrated in Figures 1-4a through 1-4c. These rocks fall into general groups (based on similarities in age, lithology, and history) that are described individually in the following sections. The regional stratigraphy is discussed in greater detail in the *Yucca Mountain Site Description* (CRWMS M&O 1998, Section 3.2.2).

1.2.1.1 Precambrian Rocks

Precambrian rocks occur in two major assemblages: an older, metamorphosed basement assemblage (no basal contact is exposed), and a younger, metasedimentary assemblage, the uppermost unit of which grades upsection into Cambrian strata. The older assemblage consists chiefly of quartzofeldspathic gneisses and quartz-feldspar-mica schists of metasedimentary or metaigneous origin. The rocks are typically intruded by migmatitic veins or larger, deformed bodies of granite or pegmatite. These old metamorphic rocks are well-exposed in the core of the Panamint Range (CRWMS M&O 1998, Figure 3.2-3), and have been radiometrically dated by Rb-Sr whole-rock and U-Pb zircon methods at about 1.7 billion years ago (Ga) (CRWMS M&O 1998, p. 3.2-4).

These metamorphic rocks are unconformably overlain by the Pahrump Group (Figure 1-4a), which is characterized by high-grade metamorphism in the central Panamint Range and in the northern Funeral Mountains where the Pahrump Group is most widely exposed (CRWMS M&O 1998, Figure 3.2-3). Older Precambrian metamorphic and younger Precambrian igneous rocks are exposed extensively in eastern Clark County and southeastern Lincoln County (Stewart 1980, p. 9).

Schist, gneiss, and gneissic quartz monzonite are exposed in the Bullfrog Hills and the Trappman Hills of southern Nye County.

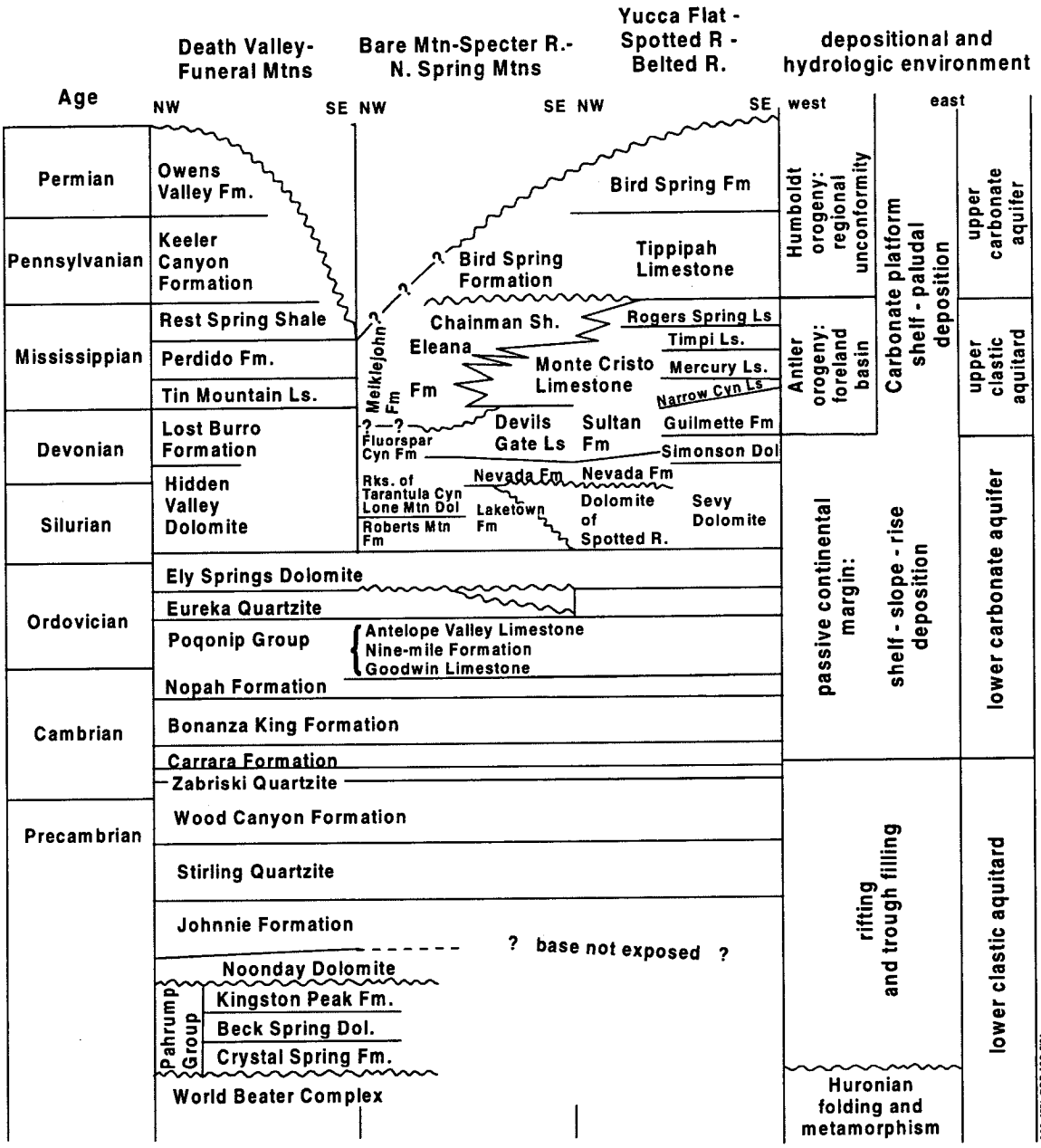

FIG1-4aEBF.CDR

Source: CRWMS M&O (1998, Table 3.2-1)

Figure 1-4a. Precambrian and Paleozoic Stratigraphic Units of the Yucca Mountain Region

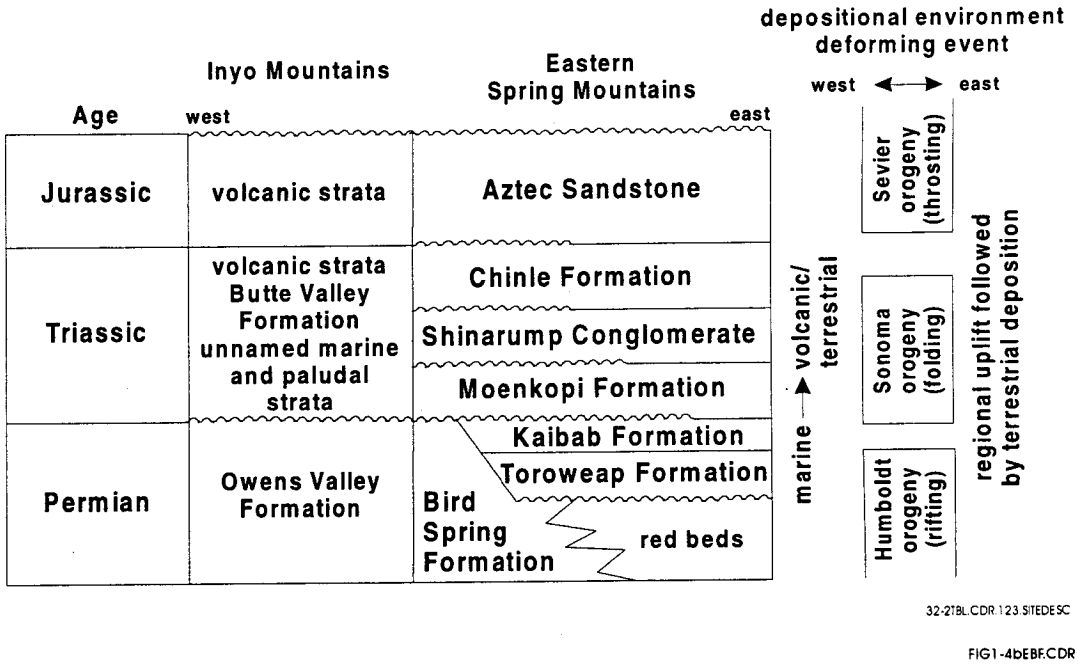

Source: CRWMS M&O (1998, Table 3.2-2)

Figure 1-4b. Late Paleozoic and Mesozoic Stratigraphic Units of the Yucca Mountain Region

The Pahrump Group is overlain at an erosional unconformity by upper Proterozoic units, the Noonday Dolomite and the Johnnie Formation, which in turn are capped by the Stirling Quartzite and the Wood Canyon Formation, which spans the Proterozoic-Cambrian boundary (Figure 1-4a). The upper Proterozoic formations are widely exposed in the Panamint Range of the Inyo-Mono terrane, in the Spring Mountains section of the Walker Lane, in the Funeral Mountains, and at Bare Mountain, the Striped Hills, and the Specter Range (CRWMS M&O 1998, Figure 3.2-3; exposures in the Striped Hills and the Specter Range are too small to show at the scale of the figure). Regionally, the upper Proterozoic units thicken and become increasingly calcareous across Nevada to the northwest (Stewart 1970, pp. 64-68; Diehl 1976, p. SR106). They form the basal units of a marine depositional environment characterized by passive tectonic conditions and simple lithologies, chiefly siliciclastic rocks that grade upward into Paleozoic carbonate rocks.

1.2.1.2 Paleozoic Rocks

Paleozoic rocks in the Yucca Mountain region comprise three lithosomes: a lower, Cambrian through Devonian carbonate lithosome; a middle, Mississippian fine-grained siliciclastic lithosome; and an upper, Pennsylvanian to mid-Permian carbonate lithosome. The lower carbonate lithosome represents deposition in a deep marine passive continental margin (outer shelf to upper rise) setting that was simply an evolutionary deepening of the late Proterozoic environment. By late Devonian time, these conditions were interrupted by the Antler orogeny, the main result of which, in the Yucca Mountain region, was an influx of clay, silt, and sand into the depositional record. A carbonate platform (continental shelf) depositional environment was reestablished in Pennsylvanian time across much of the region, except in the area of the Inyo-Mono terrane, where a deeper trough or slope environment was formed.

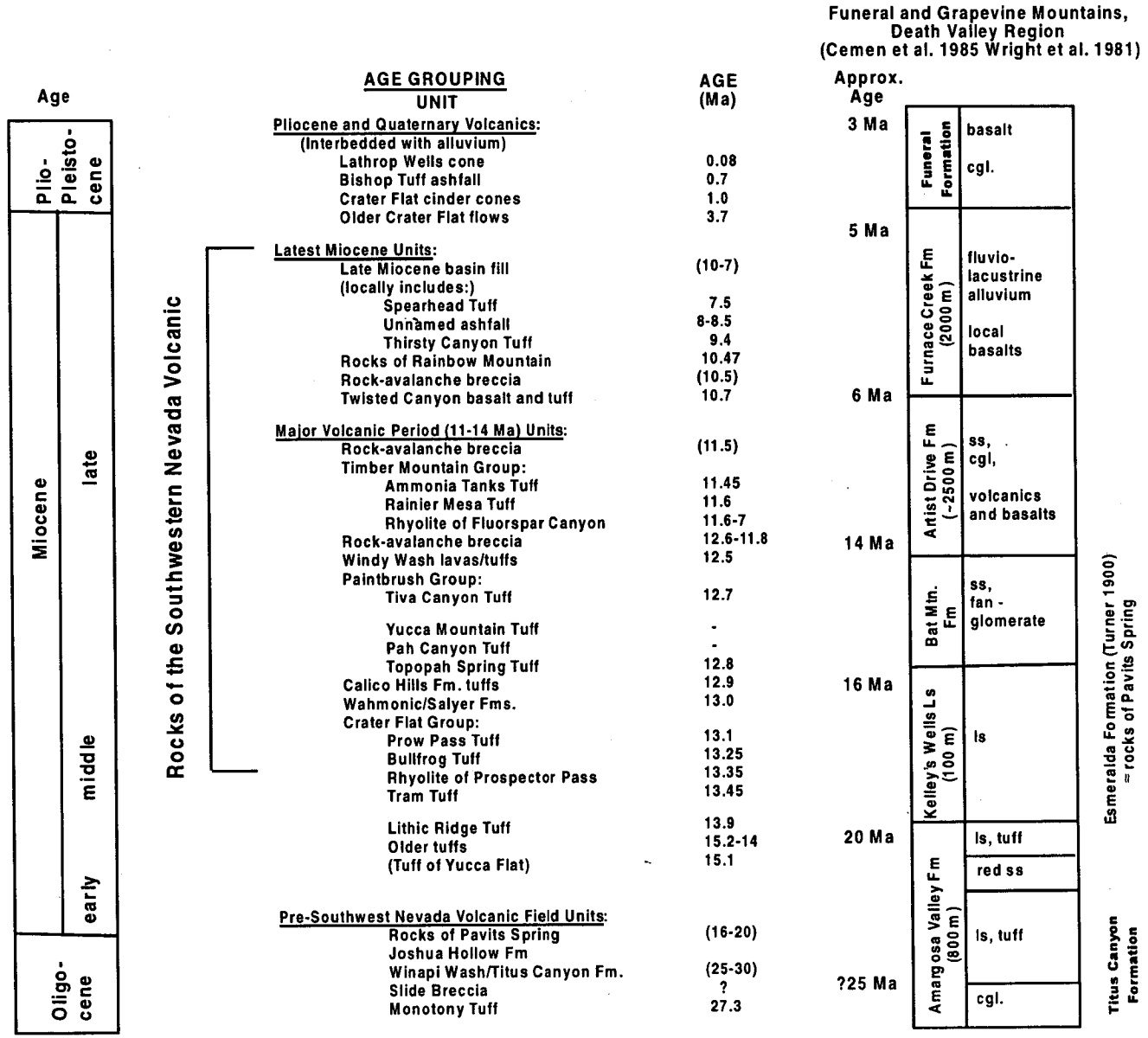

Source: CRWMS M&O (1998, Table 3.2-3)

Figure 1-4c. Tertiary and Quaternary Stratigraphic Units of the Yucca Mountain Region

Lower Cambrian through Devonian Sedimentary Rocks

The base of the lower carbonate lithosome is represented by a shallow water, mixed clastic to carbonate succession. This succession is capped by a thick interval of monotonous dark-gray Cambro-Ordovician limestone, dolomite, and minor shale. Taken as a group, sedimentary rocks of late Precambrian and early Cambrian age are present throughout the southern Great Basin. They consist of a westward-thickening prism of shallow marine quartzite, siltstone, shale, and carbonate. Limestone and dolomite occur in layers ranging from less than 1 to 100 m thick. This system has been interpreted as deposited in a shallow marine environment (Stewart 1980, p. 14). Winograd and Thordarson (1975, p. C11) consider all clastic sedimentary rocks of this age (late Precambrian through early Cambrian) in the Great Basin as aquitards. Stratigraphic formations include the Noonday Dolomite, Johnnie Formation, Stirling Quarzite, the Wood Canyon Formation, Zabriskie Quartzite, and the lower part of the Carrara Formation (Figure 1-4a).

Middle Cambrian through Devonian rocks are exposed throughout the southern Great Basin. Rocks of this age group consist of carbonate and shale with interbedded quartzite and sandstone and are interpreted as the deposits of a passive continental marginal miogeosyncline. Total thickness of the Devonian section ranges from about 500 ft in western Utah to at least 5,000 ft in central Nevada (Stewart 1980, p. 32). Strata of middle Cambrian through Devonian age are known as the Lower Carbonate Aquifer (Winograd and Thordarson 1975, p. C11).

Mississippian Siliclastic Sedimentary Rocks

The mountain-building event known as the Antler orogeny created a marked change in the depositional environment in southern Nevada in late Devonian and early Mississippian time. The orogeny formed a north-northeast trending highland, adjacent to the Roberts Mountains Thrust, which extended from west of the site through northern Nevada. Large volumes of sediment eroded into a foreland basin in the eastern half of the Great Basin. These rocks consist of thick flysch deposits adjacent to the Antler Highland and shallow-water shelf carbonates farther east. The Mississippian section along the west side of Yucca Flat is mostly the shaley, western facies represented by the Eleana Formation. The upper part of the Eleana Formation is represented farther west and south by the Chainman Shale, a monotonous siltstone or mudstone that crops out in the Calico Hills (CRWMS M&O 1998, p. 3.2-10). A section of upper Devonian to lower Mississippian strata above the Guilmette Formation at Shoshone Mountain may be a transitional facies between the Eleana turbidite to the northwest and the carbonate-platform facies of the Spotted Range to the southeast. Winograd and Thordarson (1975, p. C11) considered Mississippian rocks in the southern Great Basin as the Upper Clastic Aquitard.

Pennsylvanian through Permian Sedimentary Rocks

Rocks of Pennsylvanian to Permian age in the Yucca Mountain region are represented at the Nevada Test Site by the Tippipah Limestone and the Bird Spring Formation (Figure 1-4a). The Pennsylvanian section is about 1,000 m thick at the Nevada Test Site. Carbonate deposition continued into the Permian (CRWMS M&O 1998, pp. 3.2-10). Winograd and Thordarson (1975, p. C11) considered Pennsylvanian-Permian rocks in the southern Great Basin as the Upper Carbonate Aquifer.

1.2.1.3 Mesozoic Rocks

The only Mesozoic sedimentary rocks present in the broader region around the site are in Clark County, where they consist of continental and marine sandstone, siltstone, and limestone of the Triassic and Jurassic Aztec Sandstone, Chinle Formation, and Moenkopi Formation (Figure 1-4b). Tschanz and Pampeyan (1970, p. 65) report the presence of cobble conglomerate deposits, which they informally call "older clastic rocks," in the Spotted, Pintwater, and Northern Desert Ranges of southwestern Lincoln County.

Approximately 30 separate, Mesozoic to Tertiary granitic plutons are exposed in Esmeralda County, Nevada, west of Yucca Mountain and in the northeastern part of the Nevada Test Site, northeast of Yucca Mountain in Nye and Lincoln counties. These plutons vary in size and some have an area of less than one square kilometer. The Inyo Batholith in Nevada and California is the largest, with an outcrop area of approximately 1,000 square-km (400 square miles) (Albers and Stewart 1972, p. 28).

The restricted extent of Mesozoic age sedimentary rocks suggests that throughout much of the Mesozoic Era, the southern Great Basin was an emergent area and no deposition occurred. In addition, the Mesozoic Era was characterized in the region by the development of complex fold and thrust structures, such as the Keystone Thrust (Stewart 1980, pp. 76-77).

1.2.1.4 Tertiary Sedimentary Rocks

Tertiary sedimentary rocks crop out throughout the southern Great Basin, and consist of poorly to moderately consolidated alluvial deposits and fresh water limestones (Figure 1-4c; CRWMS M&O 1998, Figure 3.2-8; Jayko 1990, p. 215; Taylor, W.J. 1990, Figure 2, p. 183). Thicknesses of these deposits are variable but can reach 1,000 m. These rocks are commonly found interbedded with volcanic deposits, and are interpreted as early, extensional, basin fill deposits (Stewart and Diamond 1990, pp. 468-471).

1.2.1.5 Tertiary and Quaternary Igneous Rocks

Yucca Mountain is located on the southern flank of a cluster of four calderas in the southwestern Nevada volcanic field which erupted between approximately 14 and 11.4 Ma (See Sections 1.2.2 and 1.3.2). The deposits from these eruptions are a complex mixture of pyroclastic flow and ash-fall deposits, epiclastic deposits, and subsidiary lavas.

Following the cessation of large-scale pyroclastic eruptions at approximately 7.5 Ma, the dominant form of volcanism in the southern Great Basin has been scattered, small volume, basaltic or bimodal basaltic-andesitic lava and scoria eruptions. The Lathrop Wells cinder cone appears to have erupted about 75 ka. Other volcanic centers are scattered throughout the region, including within the southwestern Nevada volcanic field (CRWMS M&O 1998, p. 3.9-5).

1.2.1.6 Tertiary and Quaternary Surficial Deposits

Late Tertiary to Quaternary surficial deposits occur as unconsolidated alluvial fan, pediment, and basin fill deposits throughout much of the region. Thickness or character of the deposits is highly variable, depending on the location.

1.2.2 Site Stratigraphy and Lithology

The description of site stratigraphy presented below has evolved as a result of extensive surface and subsurface studies since the late 1970s (CRWMS M&O 1998, Sections 3.4 and 3.5). Locations of Yucca Mountain Project boreholes at the site and the Exploratory Studies Facility (ESF) location are shown on Figure 1-5. A simplified geologic map shows the distribution of major lithostratigraphic units in the vicinity of the Yucca Mountain site (Figure 1-6). The stratigraphic sequence in the site region consists, from oldest (deep) to youngest (shallow), of: pre-Cenozoic sedimentary and metasedimentary rocks; mid-Tertiary siliceous volcanic rocks; late Miocene to Quaternary basalts; and late Tertiary to late Quaternary surficial deposits.

1.2.2.1 Pre-Cenozoic Rocks

Pre-Cenozoic rocks, believed to consist primarily of Paleozoic sedimentary strata, underlie the pyroclastic rocks at Yucca Mountain, but little detailed information on their thickness, lithology, and contact relations with overlying stratigraphic units is available. This is due to their occurring at depth and the fact that these rocks have been penetrated at the site by only one borehole. Borehole UE-25 p#1, located about 2 km east of Yucca Mountain, penetrated carbonate rocks in the depth interval 1,244 to 1,807 m (Carr, M.D. et al. 1986, p. 17). The location of borehole UE-25 p#1 and the elevation of the Tertiary volcanics/Paleozoic carbonate unconformity (425 ft. below mean sea level) is shown on Figure 1-7. Exposures of complexly deformed Paleozoic rocks occur at scattered localities in the Yucca Mountain area, including the Calico Hills to the east (Figure 1-6), Bare Mountain to the west (Figure 1-2), and the Striped Hills to the south, and similar strata may extend beneath the potential repository site. The Paleozoic rocks penetrated in borehole UE-25 p#1 (interval 1,244 to 1,807 m) are almost entirely dolomites that have been correlated with the Lone Mountain Dolomite and Roberts Mountains Formation on the basis of lithologic similarities with exposures of these two formations at Bare Mountain and the presence of Silurian age conodonts (Carr, M.D. et al. 1986, pp. 16-23). The Tertiary-Paleozoic contact had previously been interpreted as a detachment fault by some investigators (Scott 1990, pp. 258, 273). Based on current information, such as extensive geological mapping and a seismic reflection profile across Crater Flat (Brocher and Hunter 1996, pp. 148-150), this surface is an unconformity cut by high-angle faults (CRWMS M&O 1998, pp. 3.3-24 to 3.3-26). Two representations of the Paleozoic surface are incorporated into the three-dimensional Geologic Framework and Integrated Site Model of Yucca Mountain. One interpretation is derived from gravity data, whereas the other interpretation also incorporates major offset along the block-bounding faults (Figure 1-7; CRWMS M&O 1997b, pp. 29-31, Plates 43A and 43B). Seismic reflection data are inconclusive as to the thickness and extent of the pre-Cenozoic rocks beneath Yucca Mountain; however, a substantial thickness is assumed to be present.

1.2.2.2 Mid-Tertiary Siliceous Volcanic Rocks

Volcanic rocks ranging in age from more than 14 to about 11.4 Ma (Sawyer et al. 1994, pp. 1304-1305, 1311-1312, 1314) form the bulk of the stratigraphic section at Yucca Mountain. The sequence consists of a series of welded and nonwelded silicic pyroclastic flow and fallout tephra deposits (terms now commonly used in preference to "ash-flow" and "ash-fall" tuffs) and volcanic breccias erupted from nearby calderas in the southwestern Nevada volcanic field (Section 1.3; CRWMS M&O 1998, Sections 3.5 and 3.9.2). Extensive studies have led to a

detailed subdivision of lithostratigraphic units in the Yucca Mountain area and a standardized nomenclature for the site that provide a consistent basis for correlation and for development of the geologic framework and hydrogeologic and thermomechanical models for Yucca Mountain and the potential repository site area (see Sawyer et al. 1994, p. 1305; Buesch, Spengler et al. 1996, pp. 5-8, 21, 24-25; CRWMS M&O 1998, Section 3.5, Tables 3.5-1 and 3.5-2). The principal Mid-Tertiary volcanic stratigraphic units logged in drillholes and mapped on the surface and in the ESF are shown on a stratigraphic column, a site geologic map, and a cross section in Figures 1-8, 1-9, and 1-10, respectively. Information on these units is summarized below in descending order:

Unit	Symbol	Age (Ma)
Timber Mountain Group	Tm	
Ammonia Tanks Tuff	Tma	11.45
Rainier Mesa Tuff	Tmr	11.6
Post-Tiva Canyon pre-Rainier Mesa tuffs	Tmblt1-Tplt5	12.5
Paintbrush Group	Tp	
Tiva Canyon Tuff	Tpc	12.7
Yucca Mountain Tuff	Tpy	–
Pah Canyon Tuff	Tpp	–
Topopah Spring Tuff	Tpt	12.8
Calico Hills Formation	Tac	12.9
Crater Flat Group	Tc	13.1
Prow Pass Tuff	Tcp	–
Bullfrog Tuff	Tch	13.25
Tram Tuff	Tct	13.45
Lithic Ridge Tuff	Not Subdivided	14.0
Pre-Lithic Ridge volcanics	Not Subdivided	>14.0

The Lithic Ridge Tuff and Pre-Lithic Ridge volcanics have been penetrated by only a few boreholes and these units have not been subdivided. Locally, the water table occurs within the Crater Flat Group, Calico Hills Formation, and Topopah Spring Tuff (see Section 2.2). These and the overlying units have been penetrated by a large number of boreholes. The Topopah Spring Tuff and younger units have been mapped in the ESF and on the surface. The stratigraphic units above the Lithic Ridge tuff are described in more detail below from oldest to youngest.

Crater Flat Group–The Crater Flat Group consists of three formations of rhyolitic, moderate to large volume, pyroclastic flow deposits and interstratified bedded tuffs that are distinguished by the stratigraphic relations and petrologic and geochemical characteristics. In ascending order these are the Tram, Bullfrog, and Prow Pass Tuffs (CRWMS M&O 1998, Section 3.5.3.5, p. 3.5-20). The Tram Tuff thins rapidly to the north from Drill Hole Wash (CRWMS M&O 1997b, Section 7.1, p. 29). The Bullfrog Tuff becomes thicker to the southwest.

Source: CRWMS M&O (1998, Figure 3.7-1)

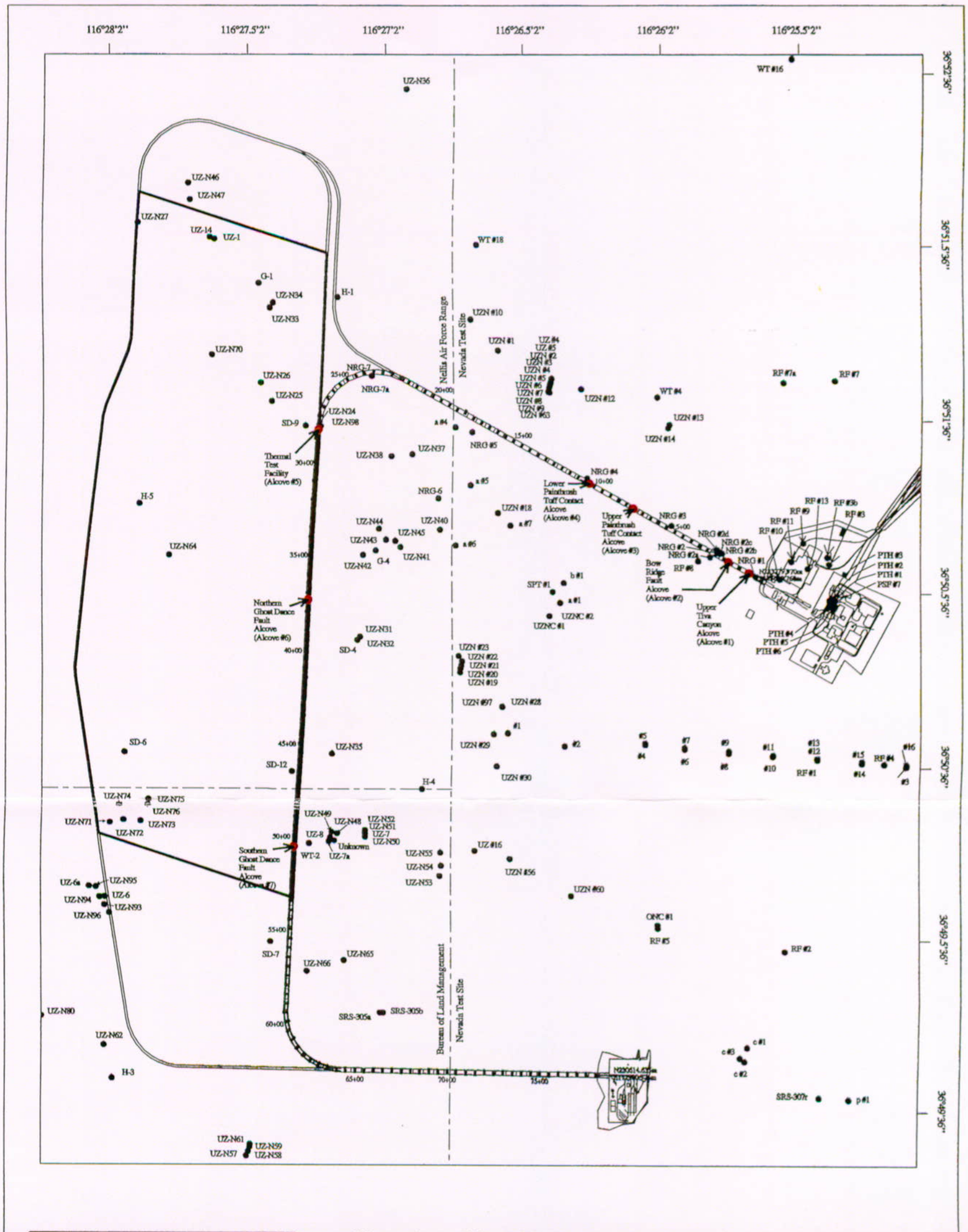

1000 0 1000 2000 FEET

300 0 300 600 METERS

Yucca Mountain Site Characterization Project

PROPOSED REPOSITORY SITE INVESTIGATION AREA

Legend

- Existing Borehole
- Test Alcove
- Proposed North & South Portal Operations Facilities
- Proposed Repository Block
- Proposed Extension of Repository Block
- ESF Tunnel
- Reference Tic Interval 50 Meter in ESF
- Contour Interval 100 Feet

Projection is Transverse Mercator with coordinates based on Nevada State Plane Coordinate System, Central Zone.

Map compiled by CRWMS M&O/TDM on March 12, 1999.

YMP- 98- 115.2

FIG1-5EBF.CDR

Figure 1-5. Plan Map Showing the Exploratory Studies Facility and YMP Boreholes

INTENTIONALLY LEFT BLANK

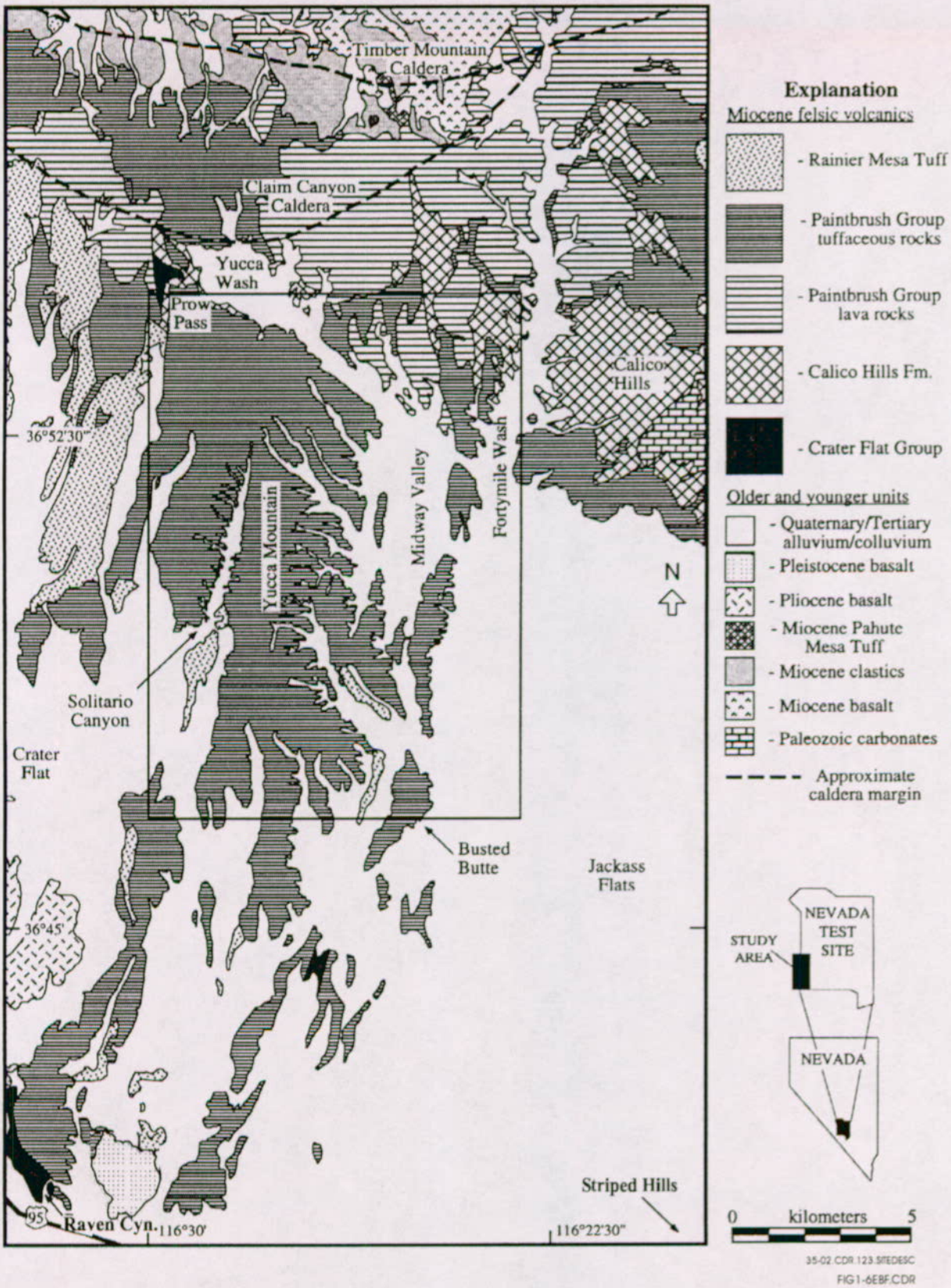

Source: CRWMS M&O (1998, Figure 3.5-2)

Figure 1-6. Simplified Geologic Map Showing Distribution of Major Lithostratigraphic Units

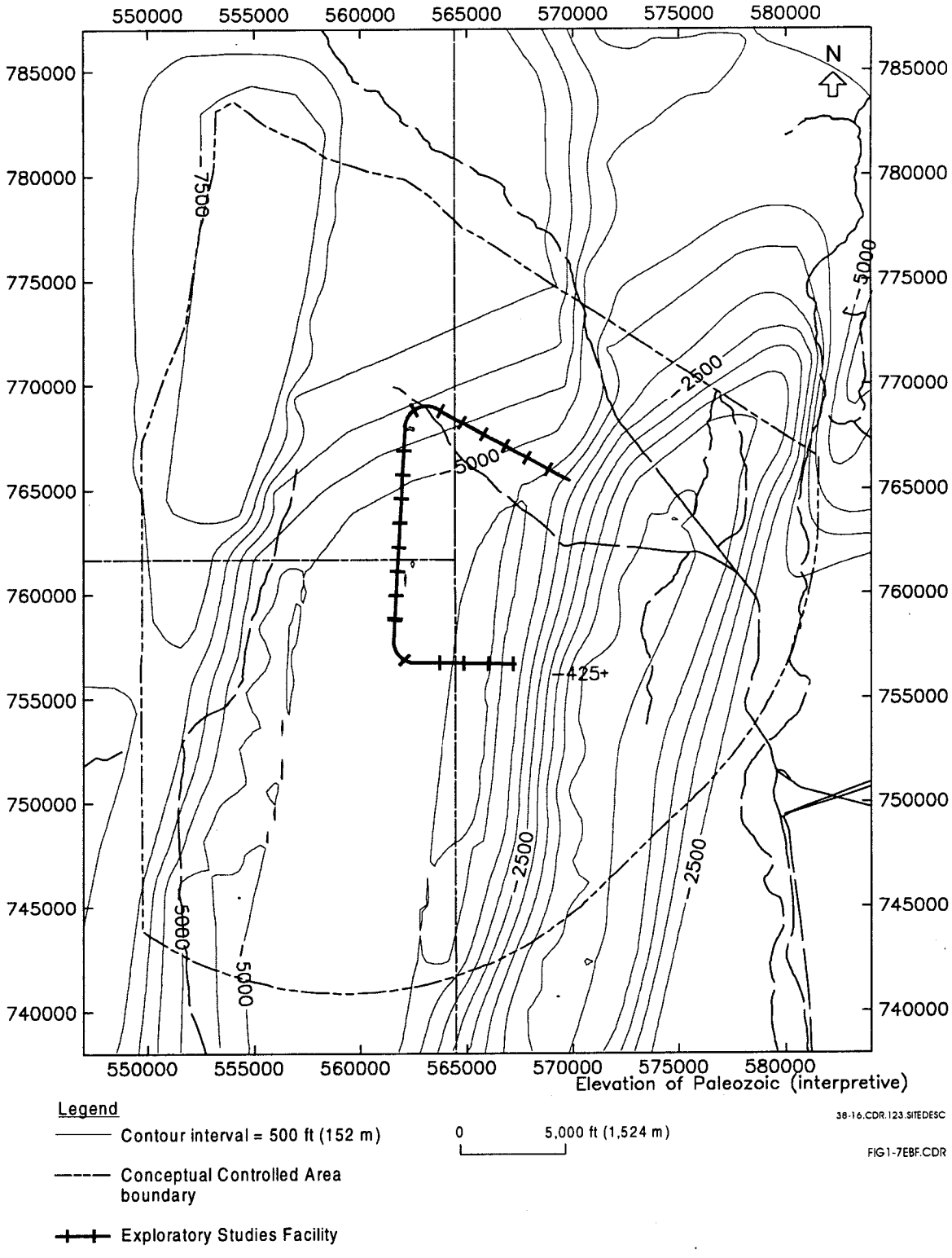

Source: CRWMS M&O (1998, 3.8-16)
NOTE: 425+ - - Elevation of unconformity in Borehole UE-25 p#1 (ft. below mean sea level)

Figure 1-7. Interpretive Structure Contour Map of the Tertiary-Paleozoic Unconformity

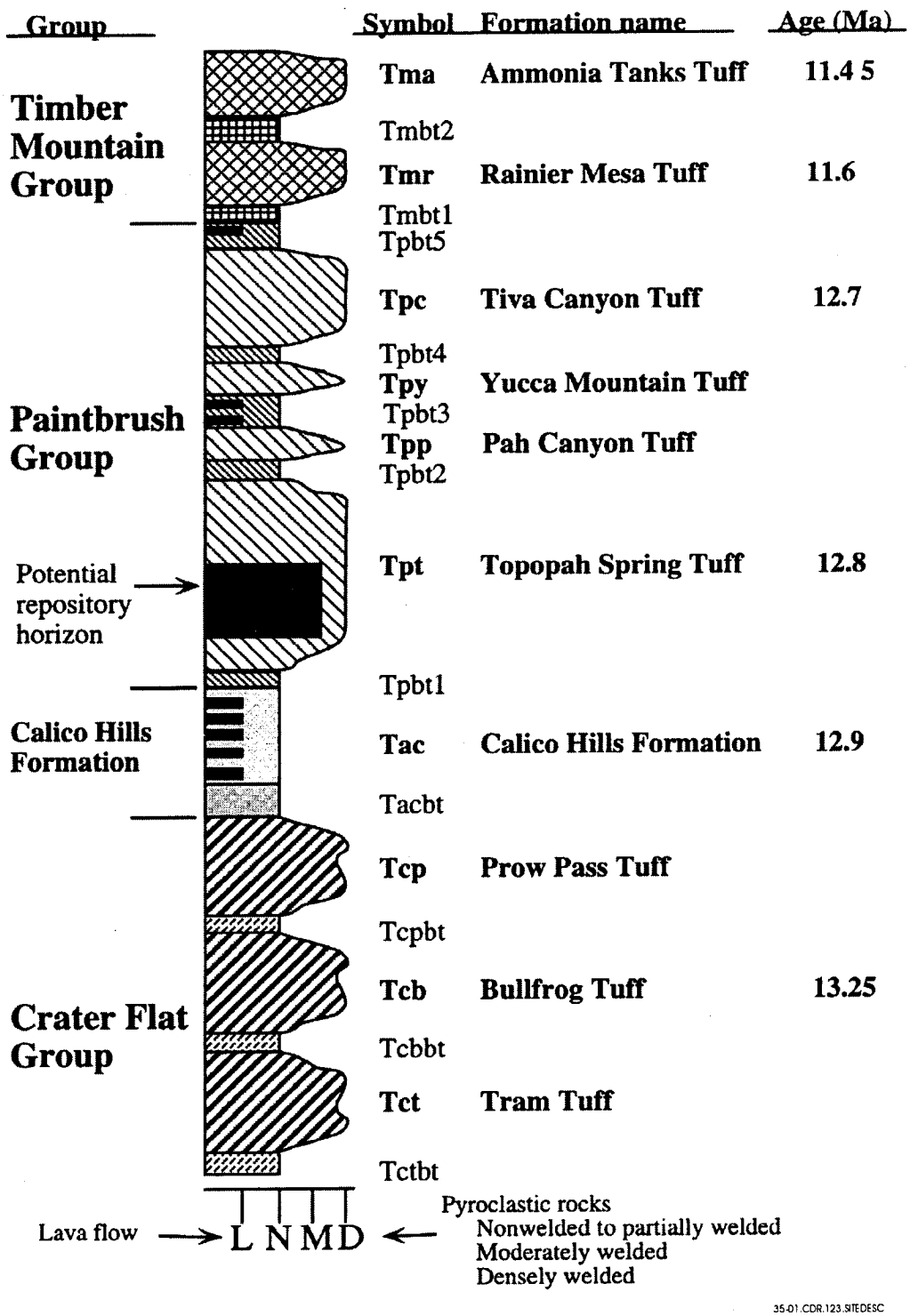

Source: CRWMS M&O (1998, Figure 3.5-1)

Figure 1-8. Principal Stratigraphic Units at Yucca Mountain

Calico Hills Formation–The Calico Hills Formation is a series of rhyolite tuffs and lavas that resulted from post-Crater Flat Group volcanism at approximately 12.9 Ma (Sawyer et al. 1994, p. 1310). Five pyroclastic units, overlying a bedded tuff unit and a locally occurring basal sandstone unit, have been distinguished in the Yucca Mountain area by Moyer and Geslin (1995, pp. 5-8). The formation thins southward across the potential repository site area, from composite thicknesses of as much as 460 m (1,500 ft) to only about 15 m (50 ft) (CRWMS M&O 1998, p. 3.5-23). The pyroclastic units are composed of one or more pyroclastic flow deposits separated by pumice- and lithic-fallout tephra deposits. CRWMS M&O (1997b, p. 28) reports this unit as 250 m thick at borehole USW G-2 and thinning to the south and west. This unit was originally logged as 288.7 m thick, but that included the underlying bedded tuff (Maldonado and Koether 1983, p. 15).

Paintbrush Group–The Paintbrush Group consists of primary pyroclastic flow and fallout tephra deposits, lava flows, and secondary volcaniclastic deposits from eolian and fluvial processes (Buesch, Spengler et al. 1996, p. 9). In ascending order, the group consists of four formations that include the Topopah Spring, Pah Canyon, Yucca Mountain, and Tiva Canyon tuffs. This series of tuffs and lava flow deposits is one of the most widespread and voluminous caldera-related assemblages in the southwestern Nevada volcanic field (Sawyer et al. 1994, p. 1307). The Topopah Spring Tuff forms the host rock for the potential radioactive waste repository. Locations of eruptive centers for the Topopah Spring and Pah Canyon tuffs are uncertain, but the Claim Canyon caldera is identified as the source of the Tiva Canyon and possibly the Yucca Mountain tuffs (Figure 1-6; Sawyer et al. 1994, p. 1308). The four formations of the Paintbrush Group are listed below:

1. **Topopah Spring Tuff**–The Topopah Spring Tuff has a maximum thickness of about 380 m (1,250 ft) in the vicinity of Yucca Mountain (CRWMS M&O 1998, p. 3.5-25). This unit is approximately 288 m (946 ft) thick at borehole USW G-2 (Maldonado and Koether 1983, p. 15). South of USW G-2, in the repository area, the Topopah Spring Tuff is more than 335 m thick, then thins to 244 m (800 ft) near borehole WT-17 (CRWMS M&O 1997b, p. 28). The formation is divided into two members—an upper crystal-rich member and a lower crystal-poor member—each of which is divided into numerous subunits based on variations in crystal content, phenocryst assemblage, pumice composition, distribution of welding and crystallization zones, depositional features, and fracture characteristics. Vitric zones are distinguished by the preservation of the volcanic glass to form rocks with a vitreous luster. The vitric zones at the top and bottom of the tuff are divided primarily on the degrees of welding that range from a densely welded subzone, which forms a vitrophyre, through a moderately welded subzone, to a nonwelded subzone. The vitrophyre near the base is identified as an important thermal-mechanical unit. The top of the Topopah Spring Tuff is defined as a thin (2 cm), very fine grained ash bed that is overlain by a thin (2 cm) lithic-rich fallout tephra. These subunits have been noted in core from boreholes across Yucca Mountain and in surface exposures from the southwestern flank of the mountain along Solitario Canyon to north of Yucca Wash near Fortymile Wash.

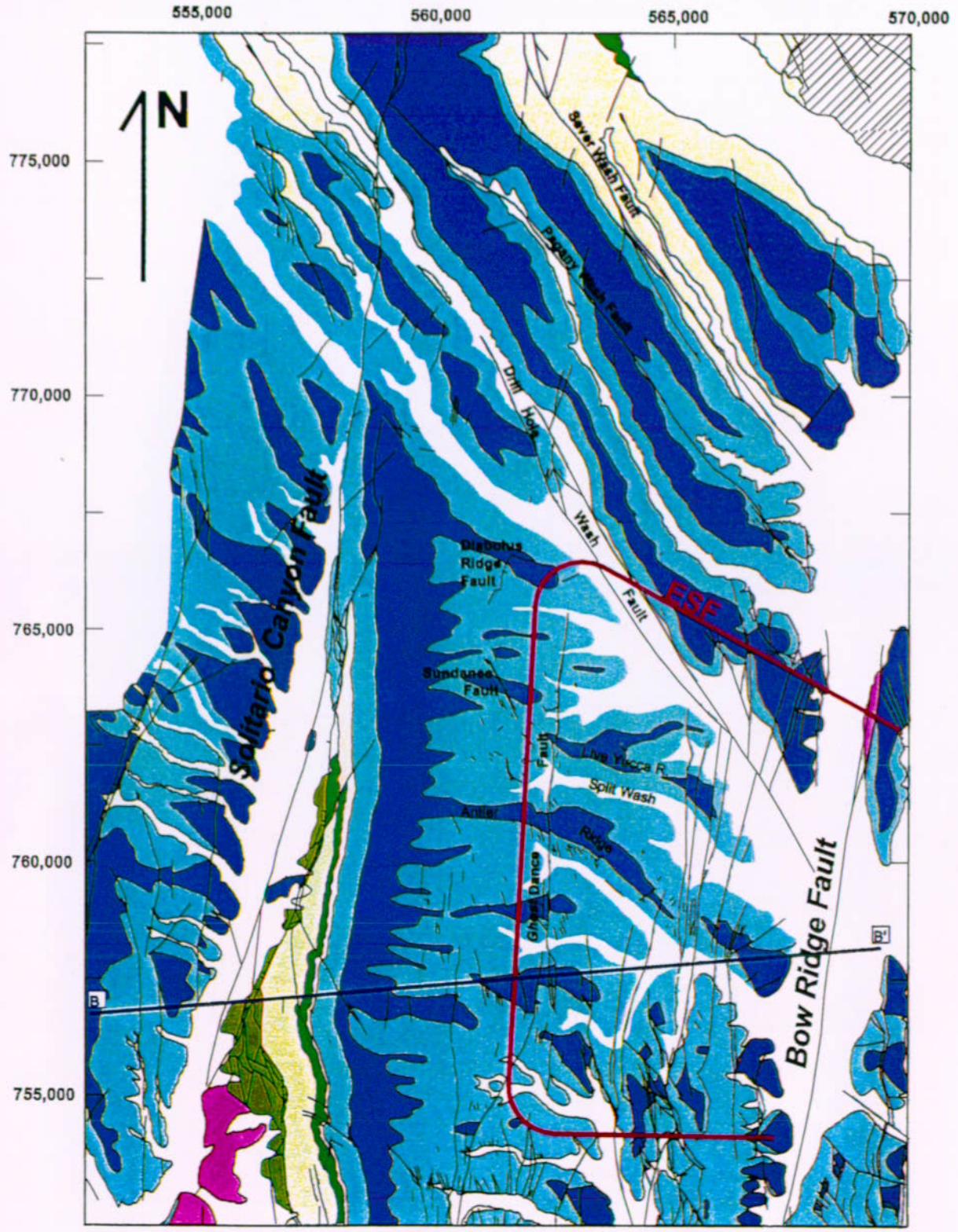

Source: CRWMS M&O (1998, Figure 5.3-2)

Bedrock Geologic Map of the Central Block Area, Yucca Mountain, Nevada

Explanation

Quaternary

- Alluvium & Colluvium

Tertiary

- Rainier Mesa Tuff
- Comb Peak Rhyolite

Tiva Canyon Tuff

- Crystal - rich member
- Crystal - poor member

Pah Canyon, Yucca Mountain Tuffs - undivided

Topopah Spring Tuff

- Crystal - rich member
- Crystal - poor member

- Tiva Canyon & Topopah Spring Tuff (lenses in fault zone)

0 1 km

03-02.CDR.123.SIEDKSC

FIG1-9EBF.CDR

Figure 1-9. Simplified Geologic Map of Yucca Mountain

INTENTIONALLY LEFT BLANK

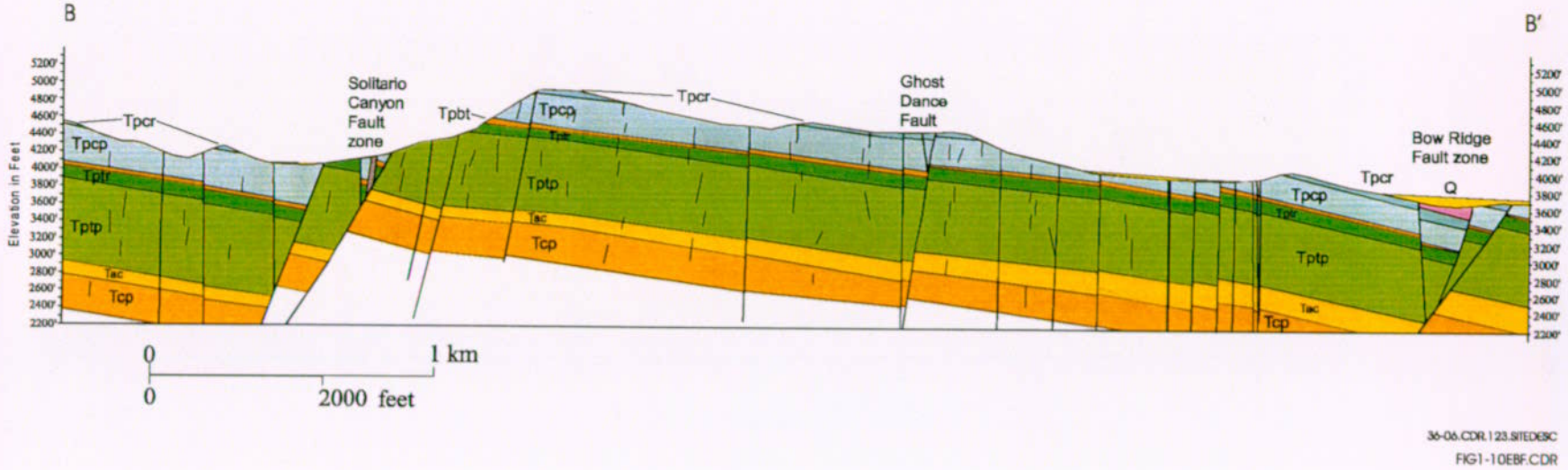

Source: CRWMS M&O (1998, Figure 3.6-6)

Figure 1-10. Simplified East-West Geologic Cross-Section Across Yucca Mountain

2. **Pah Canyon Tuff**–The Pah Canyon Tuff is a simple cooling unit composed of multiple pyroclastic units. The formation reaches its maximum thickness of 70 m (225 ft) in the northern part of Yucca Mountain, and thins southward. The Pah Canyon varies from nonwelded to moderately welded (CRWMS M&O 1998, p. 3.5-25).

3. **Yucca Mountain Tuff**–The Yucca Mountain Tuff is a simple cooling unit that is nonwelded throughout much of the Yucca Mountain area, but is partially or moderately welded where it thickens in the northern part of Yucca Mountain. The tuff, which varies in thickness from 0 to 45 m (0 to 150 ft), locally includes a thin (few centimeters), pumice-fallout bed at the base of the pyroclastic flow deposit (CRWMS M&O 1998, p. 3.5-26).

4. **Tiva Canyon Tuff**–The Tiva Canyon Tuff is a large-volume, regionally extensive, compositionally zoned (from rhyolite to quartz latite) tuff sequence that forms most of the rocks exposed at the surface of Yucca Mountain (Scott and Bonk 1984, p. 2; Day et al. 1998). Thicknesses range from less than 50 m to as much as 175 m (165 to 575 ft) (CRWMS M&O 1998, p. 3.5-26). Separation of the formation into crystal-rich and crystal-poor members and into zones within each of these members is based on similar criteria and characteristics as discussed above for the Topopah Spring Tuff. This unit is thickest in the potential repository area (CRWMS M&O 1997b, p. 27).

Post-Tiva Canyon, pre-Rainier Mesa Tuffs–A sequence of pyroclastic flow and fallout tephra deposits occurs between the top of the Tiva Canyon Tuff and the base of the Rainier Mesa Tuff (a formation in the Timber Mountain Group) in the vicinity of Yucca Mountain. Rocks in this stratigraphic position occur in the subsurface beneath alluvial deposits in Midway Valley, on the east flank of Yucca Mountain (Carr, W.J. 1992, pp. A-12, A-16). The sequence ranges in thickness from 0 to 61 m (0 to 200 ft) and is intermediate in composition between the Tiva Canyon and Rainier Mesa tuffs (CRWMS M&O 1998, p. 3.5-27). Some of these units have been placed in the Timber Mountain Group and others in the Paintbrush Group (Buesch, Spengler et al. 1996, p. 5). The part of this sequence in the Paintbrush Group includes the Comb Peak Rhyolite.

Timber Mountain Group–The Timber Mountain Group includes all of the quartz-bearing pyroclastic flow and fallout tephra deposits that were erupted from the Timber Mountain Caldera complex (Figure 1-6; Sawyer et al. 1994, p. 1308). The complex consists of two overlapping, resurgent calderas: an older caldera formed by the eruption of the Rainier Mesa Tuff, and a younger, nested caldera formed by eruption of the Ammonia Tanks Tuff (CRWMS M&O 1998, Section 3.5.3.9).

1. **Rainier Mesa Tuff**–This formation is not present across much of Yucca Mountain, but is locally exposed in wedges on the downthrown sides of large normal faults (CRWMS M&O 1997b, Section 7.1, p. 27; Day et al. 1998, cross sections A-A', B-B' C-C'; Gibson et al. 1992, pp. 49, 63, 66-67). The tuff is nonwelded and vitric at the base and grades upward into partially to moderately welded, devitrified tuff. This unit is useful in constraining the younger limit of faulting in the area.

2. **Ammonia Tanks Tuff**–The Ammonia Tanks Tuff is not present across Yucca Mountain, but is exposed in the southern part of Crater Flat and is described here for completeness. It has been penetrated by one borehole in the Crater Flat area. The formation consists of welded to nonwelded rhyolite tuff with thickness ranging up to about 215 m (705 ft) (CRWMS M&O 1998, p. 3.5-28).

1.2.2.3 Mid-Tertiary Basalt

Miocene basalt comprises a relatively small volume of rock. It occurs as a dike intruded along the Solitario Canyon Fault and as several dikes located along northwest-striking faults on the eastern flank of Jet Ridge (Day et al. 1998, p. 7). These basalts are not important from a stratigraphic perspective but are important for an understanding of site tectonics. Basalts are discussed in the context of volcanic hazards in Section 1.3.3.

1.2.2.4 Late Tertiary to Quaternary Surficial Deposits

Surficial mapping of Quaternary deposits in the area surrounding the Yucca Mountain site has been progressively refined over the years. The results of several investigations are discussed in detail in CRWMS M&O (1998, Section 3.4.3.1, Table 3.4-1). Physical and morphological characteristics of landscape elements, such as landform, drainage network, soils, elevation above modern washes, desert pavement, desert varnish, depositional environment, and lithology have been combined with improved radiometric dating techniques to establish a standardized subdivision of stratigraphic units that is now being applied in the large-scale mapping and related studies of surficial deposits at Yucca Mountain. In general, these units have been classified as stream (alluvial) deposits, hillslope (colluvial) deposits, spring deposits, and wind blown sand (eolian) deposits. General characteristics of surfaces and soils developed on surficial deposits and geomorphic surfaces are discussed in detail in the *Yucca Mountain Site Description* (CRWMS M&O 1998, Section 3.4.3). Available numerical and relative age data are presented in Table 1-1.

Table 1-1. Ranges in Age Dates for Tertiary-Quaternary Surficial Deposits at Yucca Mountain

Mapping Unit	Geologic Age	Age Range
Q7	Latest Holocene	Historic
Q6	Late Holocene	Historic-3 ka
Q5	Middle Holocene	3-7 ka
Q4	Early Holocene	7-10 ka
Q3	Late Pleistocene	10-128 ka
Q2	Middle Pleistocene	128-736 ka
Q1	Early Pleistocene	736-1650 ka (1.6-1.7 Ma)
Q0	Pliocene	1.65-5.0 Ma (5.0-5.5 Ma)

Source: CRWMS M&O (1998, Table 3.4-4)

NOTE: Modified from Morrison 1991b.

The Quaternary landscape in the Yucca Mountain area has been dominated by physical weathering, and colluvial, eolian, and alluvial processes. These geomorphic processes have responded to climatic changes and have been influenced by the topography of the mountain and adjacent basins that have been formed by extensional tectonic processes over the past 14 Ma. Patterns of Quaternary deposits reflect both the tectonic environment and climatic history in the area.

One noteworthy map pattern at Yucca Mountain is the preservation of early and middle Quaternary colluvial deposits on many hillslopes. These deposits have been dated by cosmogenic isotopes, cation ratio dating, and uranium series dating on colluvial soils. The preservation of older Quaternary deposits indicates that hillslope erosion processes have been ineffective in eroding colluvial deposits that were weathered from bedrock during the colder, pluvial climatic episodes (Whitney and Harrington 1993, pp. 1015-1017). The slow removal of hillslope colluvium is also reflected in the lack of either large or steep alluvial fans at the base of the slopes at Yucca Mountain. The lack of fans along the base of tilted fault blocks is a strong indication of very low rates of tectonic activity. As discussed in CRWMS M&O (1998, Section 3.10.6.2), Quaternary slip rates are generally 0.01 mm/yr or less for the faults in the site area.

Another interpretation can be made from the preservation of older Quaternary deposits at Yucca Mountain: The amount of climatic time that erosional processes dominate the landscape is less than the time during which hillslopes are mostly stable. Recent studies by Paces et al. (1997, p. 3) of the paleo-discharge deposits south of Yucca Mountain suggest that this scenario may be valid. Climatic conditions appear to have been wetter and cooler than the present for a substantial portion of the last 200,000 years. The preservation of essentially unconsolidated sand (indicating drier, windy interpluvial conditions) on the slopes of Busted Butte underscores again the ineffective hillslope erosional processes during the last half of the Quaternary (approximately 760,000 years based on the age of buried Bishop Tuff).

1.3 STRUCTURAL GEOLOGY AND TECTONICS

1.3.1 Regional Structural Geology and Tectonics

Yucca Mountain lies within the Walker Lane, an approximately 100 km-wide structural belt along the western side of the Basin and Range province (Figure 1-11). This belt extends northwestward from the vicinity of Las Vegas, Nevada, sub-parallel to the Nevada-California border, into northern California. The domain is generally characterized as an assemblage of crustal blocks separated by discontinuous northwest-striking right-lateral faults and northeast-striking left-lateral faults (Stewart 1988, p. 4). Because of its structural heterogeneity, the Walker Lane is recognized as a tectonic terrane distinct from the Basin and Range only at the regional scale. The local, northwest-striking faults give the domain its overall structural grain and they obscure basin and range structure to varying degrees.

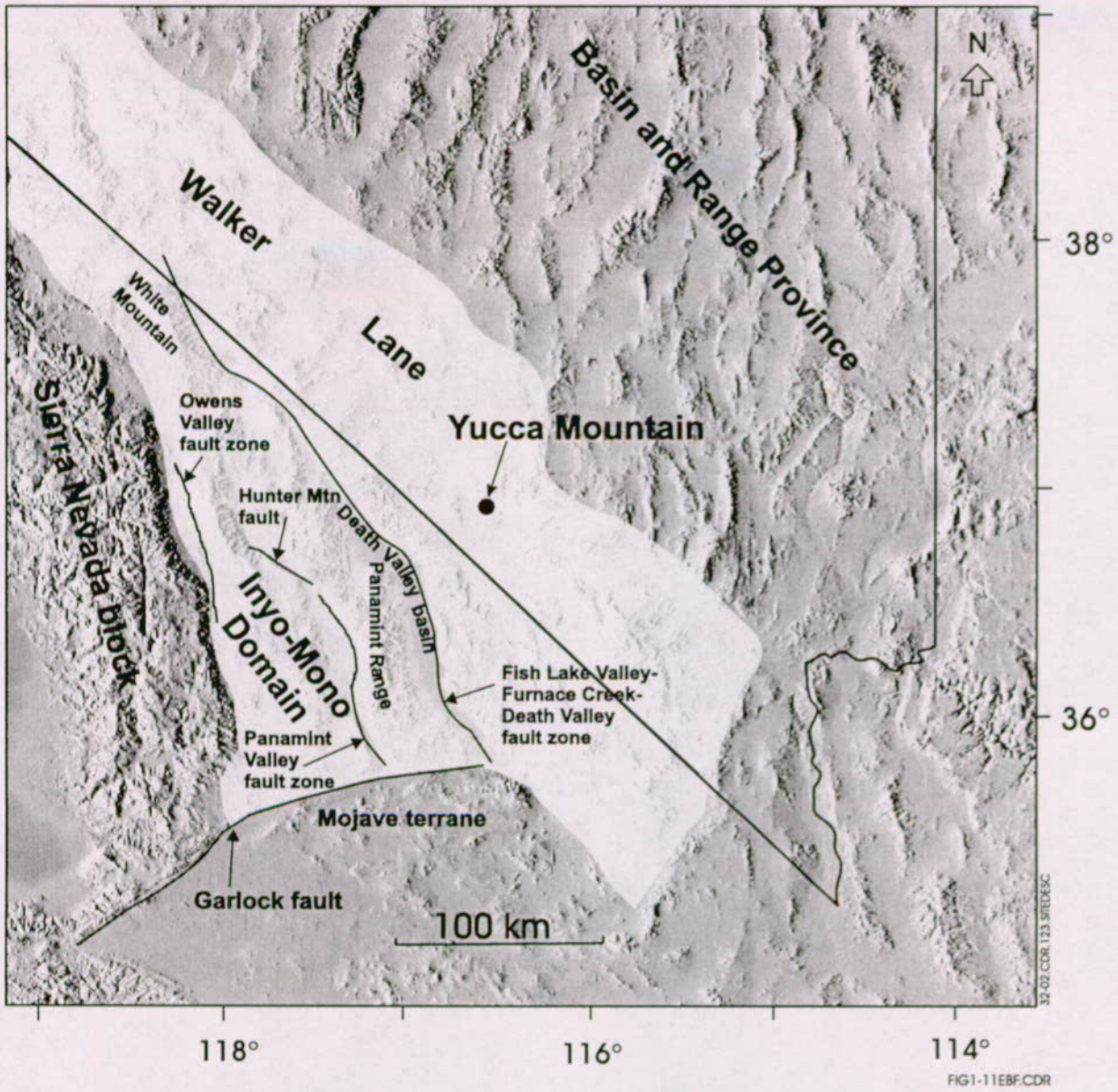

Source: CRWMS M&O (1998, Figure 3.2-2)
NOTE: Light screen highlights the Walker Lane and, to the west of Death Valley basin, the Inyo-Mono Domain.

Figure 1-11. Structural Geologic Setting of Yucca Mountain

The Inyo-Mono terrane includes all the extended crust west of the Furnace Creek-Death Valley fault zone, east of the Sierra Nevada front, and north of the Garlock fault and the Mojave terrane (Figures 1-1 and 1-11). It includes modern basins and ranges with great structural relief, including the Death Valley basin and the Panamint Range. Because of its ongoing tectonic activity and exposure of deep-seated crustal rocks, the Inyo-Mono terrane is an important part of the regional geologic setting of Yucca Mountain; it contains some of the more tectonically active structures in the Yucca Mountain region. Both the Sierra Nevada block and the Mojave terrane are tectonically isolated crustal elements that are not related to the tectonic evolution of Yucca Mountain.

The geologic setting of Yucca Mountain is characterized structurally by two distinctly different styles of tectonic deformation: an early compressional "mountain building" style of regional folding and overthrusting, and a later extensional "basin forming" style of regional normal and strike-slip faulting. The shortening style has affected pre-Cenozoic rocks. It records orogenic events that occurred during Paleozoic deposition, and a peak event that occurred in the Mesozoic that terminated marine deposition. The sedimentary marine rocks described in Section 1.2.1.2 were folded and deformed by thrust faulting during the mountain building event known as the Antler orogeny that occurred during the late Devonian to early Mississippian (Figure 1-12). The Antler orogeny is significant in the Yucca Mountain region for two reasons: (1) the fine-grained, terrigenous lithology of the Eleana (and especially the Chainman Shale) lithosome forms a major Paleozoic aquitard north and east of Yucca Mountain, and (2) the subsequent juxtaposition of three distinct but coeval facies (Antler-derived clastic debris, black Chainman Shale, Mississippian, and older carbonates) aids in recognizing the structural configurations that formed during the subsequent Sevier-Cordilleran orogeny.

Mountain building in the near vicinity of Yucca Mountain began with eastward-encroaching uplift in latest Permian to Triassic time and culminated during the Mesozoic with the Sevier orogeny (Stewart 1980, p. 77). In plate tectonic terms, mountain building due to convergence-related compression began in late Permian to Triassic time in an area west of Yucca Mountain (Figure 1-12). The Sonoma orogeny resulted in uplift and folding in the west, which in turn resulted in erosion from the uplifted area and the formation of a regional unconformity. The Permian marine carbonate platform and continental shelf deposits toward the east were overlain by marine followed by volcanic strata in the area of the Inyo Mountains, and by non-marine strata to the east in the area of the eastern Spring Mountains. The Sevier orogeny resulted in a broadly north-to-northeast trending fold-thrust system. The thrust sheets are typically complicated by overturned or dismembered folds and local reverse or overthrust faults. The major thrusts are continuous on strike for distances of more than 100 km and have stratigraphic juxtapositions that indicate translations of tens of kilometers. The history of thrust faulting in the Yucca Mountain region, and the identity of each fault from place to place, is uncertain because of erosion, subsequent extension, and wide coverage by Miocene volcanic rock.

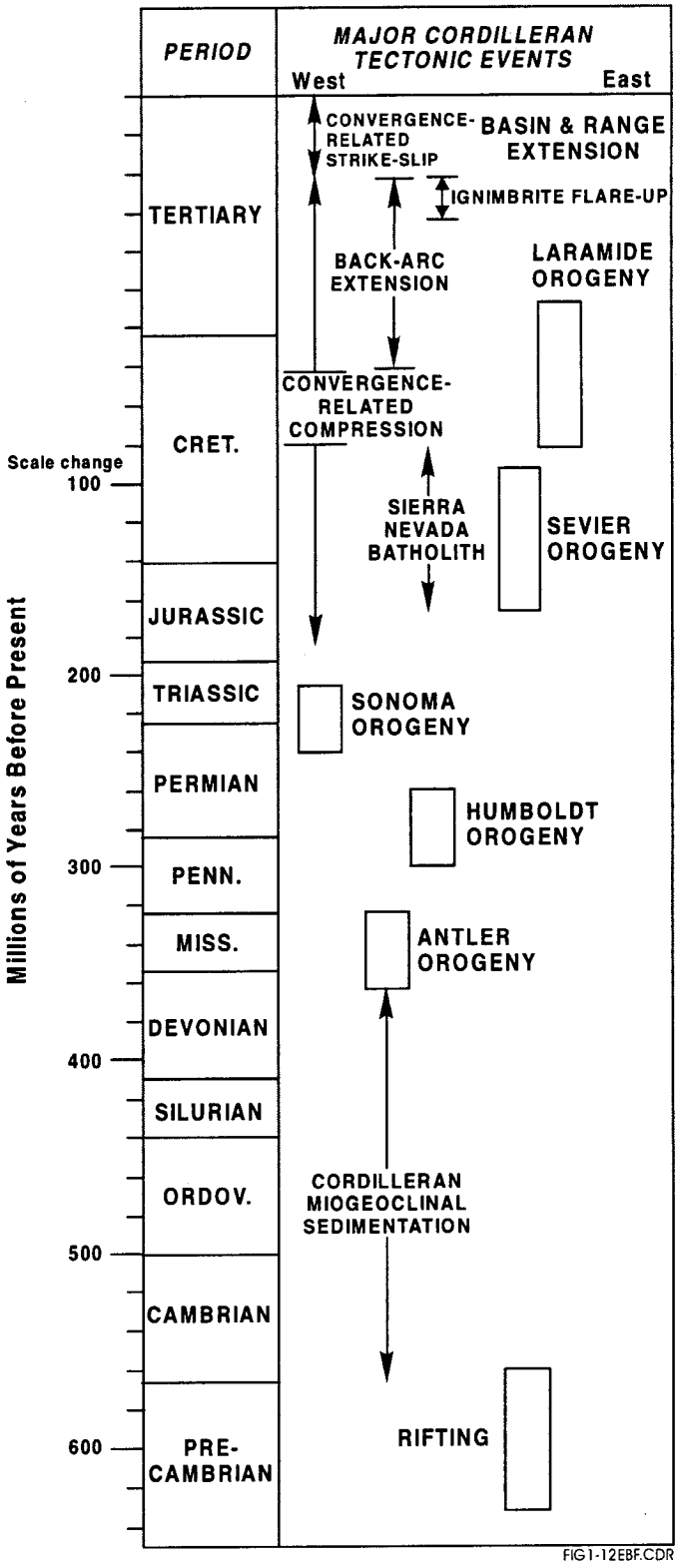

Source: Modified after French, D.E., *Assessment of Hydrocarbon Resources of the Yucca Mountain Vicinity, Nye County, Nevada,* in review, Figure 12

NOTE: Fold and thrust structures formed during the Antler through Laramide orogenies. Fault-block structures were overprinted on these during the Basin-Range extension.

Figure 1-12. Tectonic History of the Great Basin Region

Despite this earlier compressional deformation, the Great Basin has long been recognized as an area where the major landforms have been created by extensional tectonic processes. Several extensional mechanisms and amounts of extension have been proposed. Relatively high-angle, planar, normal faults that cut the brittle (seismogenic) crust can accommodate a maximum of 10 to 15 percent extension. Normal faults that are at a high angle at the surface and curve to lower angles with depth (listric faults) may accommodate much greater amounts of extension. Very low-angle detachment-fault models have been developed that suggest extensive tectonic thinning of the brittle crust, accommodating extension of 200 percent or more (Figure 1-13). Normal faulting (extensional tectonics) in the Great Basin was recognized by some of the earliest studies of the area. The amount of extension, however, has been a matter of debate. The timing of extension and rates of extension are also not fully understood. In parts of the Basin and Range, extensional faulting may have occurred in the late Eocene (40 Ma) and evidence exists for Oligocene normal faulting in the region (Reynolds 1969, p. 220). Most of the extension in the region occurred in the last 20 million years (Miocene to Holocene).

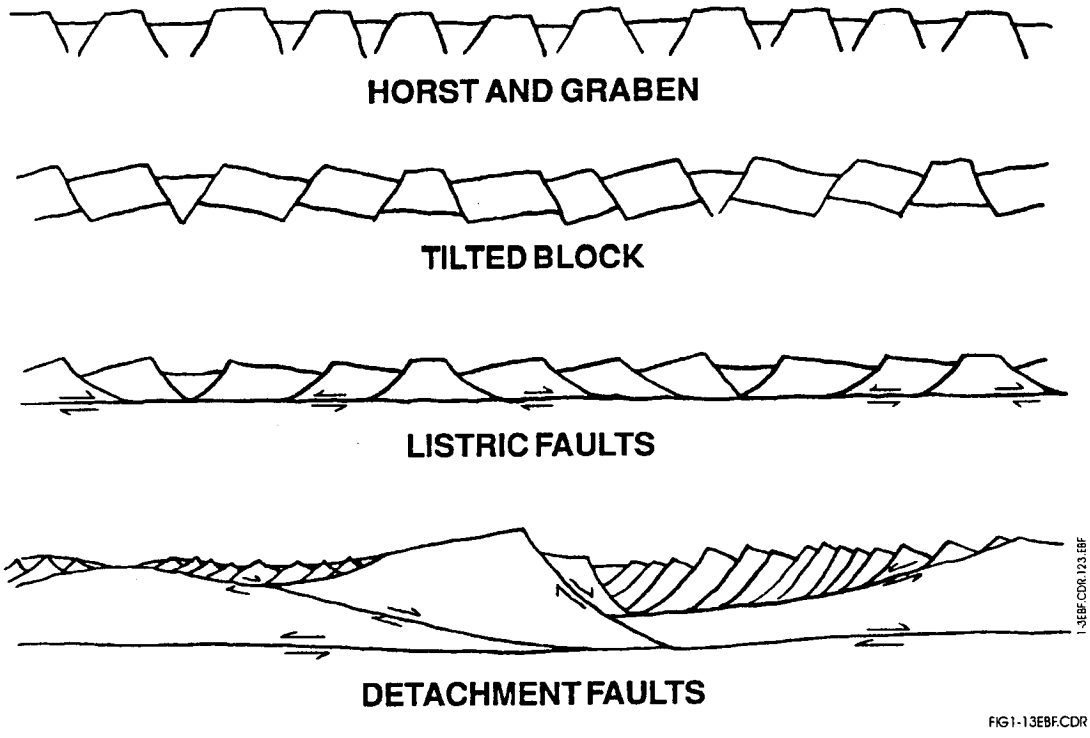

Source: Modified from Stewart (1988) and Scott (1990)

NOTE: The Geometry of the Horst and Graben and the Tilted Block models allows for fairly limited extension (approximately 15 percent), while that of the Listric Faults and Detachment Faults models allows for progressively greater amounts of extension. Using detachment models, Wernicke et al. (1988) has proposed up to 300 percent extension for parts of the Basin and Range.

Figure 1-13. Schematic Illustration of Some of the Mechanisms and Geometric Configurations Proposed for Extensional Faulting in the Basin and Range

Extension was probably not uniform across the region in time or space. While back arc extension was occurring toward the western part of the area, deformation and uplift due to the Laramide orogeny was occurring in eastern Wyoming, Colorado, and Utah (Figure 1-12). Several authors (Scott 1990, p. 279; Noble et al. 1991, p. 930) have suggested that major extension migrated westward from Yucca Mountain after about 11.5 Ma. Extension may also have been nonuniform from north to south. Duebendorfer and Black (1992, pp. 1108-1109) present evidence that structures trending generally east-west may have accommodated different amounts of extension to the north and south.

The typical Basin and Range structures, tilted fault block ranges with relatively large displacement, high-angle normal faults exposed at the surface, bounding one or both sides of each range, were well developed in this area by approximately 11 Ma. Extension in the Yucca Mountain region was active by Oligocene time (Axen et al. 1993, pp. 57, 59-60, 66-67). This early phase of extension, sometimes referred to as "pre-basin and range extension" (Zoback et al. 1981, p. 409), continued into Middle Miocene time. By early Miocene time (and likely by middle-late Oligocene), the characteristic features of the Walker Lane had been established, namely discontinuous northwest striking and northeast striking high-angle strike slip faults (Hardyman and Oldow 1991, p. 279). Deep-seated detachment may also have been a significant mechanism of Eocene-Oligocene extension in this region. By about 15 Ma, the tectonic setting of Yucca Mountain already had its main extensional features established, namely a basin and range structural pattern defined chiefly by north-south oriented basins or troughs, and fault zones associated with the Walker Lane, namely the Rock Valley fault zone and the Las Vegas Valley shear zone and, perhaps, dextral faulting in the Funeral Mountains area.

The late Oligocene-early Miocene interval was punctuated by deposition of ash flow tuffs (Axen et al. 1993, pp. 56-57) derived from eruptions east and north of Yucca Mountain. The advent of siliceous volcanism marks an important tectonic development in the early phase of extension; it signals the beginning of regional crustal heating that culminates in the so-called "ignimbrite flareup" (Figure 1-12). The culminating tectonic event of the region and, coincidentally, the initiating event for structural formation of Yucca Mountain, was the creation of the southwestern Nevada volcanic field. Figure 1-14 shows part of the southwestern Nevada volcanic field near the Yucca Mountain site. The southwestern Nevada volcanic field was produced by a succession of at least five voluminous and numerous smaller eruptions. The greatest of these eruption events created the volcanic rocks (the Paintbrush and Timber Mountain Groups) that have formed Yucca Mountain. The Paintbrush Group (potential repository host rock) was deposited between 12.8 and 12.7 Ma (Sawyer et al. 1994, p. 1305). It was faulted to roughly its present configuration by about 11.6 Ma when the overlying Timber Mountain Group eruptions began. Scott (1990, pp. 273, 279) has suggested that rates of fault movement were highest between 13 and 11.5 Ma and have decreased since that time.

While Miocene extension appears to have been extensive and rapid, Pliocene and later extension appears to have had a different style. Unruh (1991, p. 1403) presents convincing evidence for a Cordillera-wide uplift event starting about 5 Ma. The extension accompanying this uplift is more evenly distributed and is accommodated on high angle normal faults that are coincident with the Miocene faults at the surface. This model is consistent with current seismicity of the Basin and Range, which indicates high-angle faulting to depths of 15 km or more.

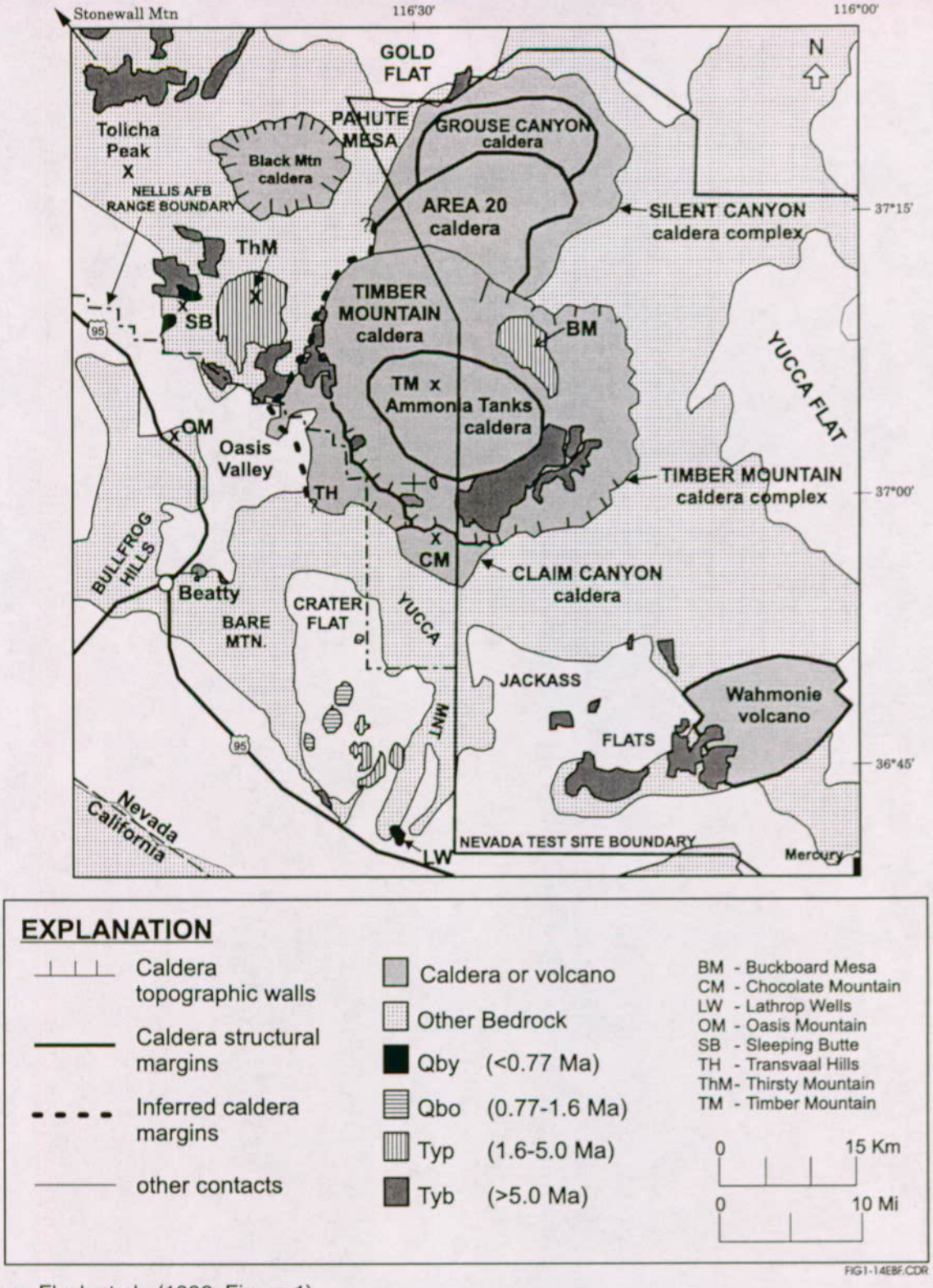

Source: Fleck et al. (1996, Figure 1)

NOTE: Qby = young Quaternary basalt, Qbo = older Quaternary basalt, Typ = Tertiary basalt (Pliocene), Tyb = Tertiary basalt (late Miocene)

Figure 1-14. Calderas of the Southwest Nevada Volcanic Field Near Yucca Mountain

Regionally significant faults are those structures that exhibit styles of deformation and rupture histories characteristic of tectonic subprovinces in the Great Basin. Those faults located in the southern Walker Lane may be significant in terms of potential seismic activity. Faults that contribute to the seismic hazard to Yucca Mountain are discussed in section 1.3.2.

The Walker Lane belt has a long and complex deformational history. Some of the Cenozoic deformation probably took place on preexisting structures and has been characterized by strike-slip faulting, oroflexural folds, and large-scale extension (Stewart 1988, pp. 1, 15). The current style of deformation in the Walker Lane belt probably began approximately 5 Ma in response to the right-lateral relative shear motion of the Pacific and North American plates and gravity-driven extension caused by Cordillera-wide uplift. In the modern stress field, northwest-striking faults move with right-lateral strike-slip or oblique-slip.

In the southern Walker Lane belt and in the Inyo-Mono terrane to the west, there are three major faults along which right-lateral shear is distributed. From west to east, these are the Owens Valley, the Panamint Valley-Hunter Mountain, and the Death Valley-Furnace Creek fault systems (Figure 1-11).

Contemporary Stress and Strain in the Yucca Mountain Region

Measurements and inferences of the tectonic stress field in the southern part of the northern Basin and Range province indicate that the direction of minimum principal compressive stress is near horizontal and trends N60°-70°W (Zoback 1989, p. 7120). The maximum principal compressive stress ranges from vertical to horizontal resulting in a mix of normal, oblique, and strike-slip focal mechanisms for earthquakes (see Section 1.4.1.1). Hydraulic fracturing stress measurements in boreholes USW G-1 and USW G-2 at Yucca Mountain formed part of the basis for and are consistent with the regional observations (Stock et al. 1985, p. 8691). These measurements were taken over a depth range of 646-1288 m and show a near horizontal minimum principal compressive stress oriented at N60°-65°W. Information on *in situ* stress measurements taken in the ESF is summarized in Section 4.6.

Data have also been collected to evaluate contemporary strain in the Yucca Mountain vicinity. Results from a trilateration network with a 50 km aperture (Savage, Lisowski et al. 1994, p. 18106) show no significant deformation for the 1983-1993 monitoring period, except for that associated with the June 1992 earthquake near Little Skull Mountain (See Section 1.4.1.2). Measurements were initially made using a Geodolite. In later years, Global Positioning Satellite (GPS) techniques were used. This network was resurveyed in 1998. After removal of deformation from the Little Skull Mountain earthquake and strain accumulation effects related to faulting in the Inyo-Mono domain to the west, results continue to show no significant deformation in the vicinity of Yucca Mountain (Savage, Svarc et al. 1998, p. F203).

Wernicke et al. (1998) also collected strain data for the Yucca Mountain vicinity for the period 1991-1997 using GPS instruments. They interpret their data to show west-northwest elongation at an average annual rate of 1.7±0.3 mm (50±9 nanostrain/yr) (Davis et al. 1998, p. F203). This rate is about an order of magnitude larger than that obtained by Savage, Lisowski et al. (1994) and Savage, Svarc et al. (1998) for the same area. They are also about an order of magnitude larger than the long-term rates determined from studies of slip rate for local Quaternary faults.

The discrepancy between the two data sets is unresolved and depends to some degree on the manner in which deformation associated with the Little Skull Mountain earthquake is treated. Studies to better define the Little Skull Mountain deformation are ongoing and collection of crustal strain data is continuing.

Marrett et al. (1998, p. F203) also evaluated stain for the Yucca Mountain area. They examined fracture data from the ESF, regional fault data, and seismicity data. Their analysis indicates elongation of 5 to 20 nanostrain/yr.

1.3.2 Site Structural Geology and Tectonics

1.3.2.1 Faulting at Yucca Mountain

Yucca Mountain is the erosional remnant of a volcanic plateau consisting of a series of north-trending, eastward tilted structural blocks that had been segmented by west-dipping, high-angle normal faults during a period of major extensional deformation sometime between the times of eruption of the Tiva Canyon Tuff (12.7 Ma) and the Rainier Mesa Tuff (11.6 Ma). The faults were mapped by Scott and Bonk (1984), and, more recently, have been mapped in greater detail as part of the site characterization program (Day et al. 1998). CRWMS M&O (1998, pp. 3.6-1 to 3.6-4) describes the approaches to mapping.

The north-trending, block-bounding faults that are at or near Yucca Mountain, are from west to east, the North and South Crater Flat, Windy Wash, Fatigue Wash, Solitario Canyon, Iron Ridge, Stagecoach Road, Bow Ridge, and Paintbrush Canyon faults (Figure 1-15). The Ghost Dance fault, an intrablock fault just east of the potential repository block, does not appear to have displaced Quaternary surficial deposits. Mapping in the ESF has shown that the Ghost Dance fault has a consistent dip of 80 to 90 degrees from the surface to the depth of the potential repository, based on two crossings of the fault in alcoves and one in the main drift (CRWMS M&O 1998, p. 3.6-24). The Midway Valley fault has been inferred from geophysical data. In addition, several pre-Quaternary (not labeled on Figure 1-15) northwest-trending faults have been identified within valleys along the east side of the mountain, the most prominent being the Sevier Wash, Pagany Wash, and Drill Hole Wash faults. A northwest-trending shear zone, the Sundance fault, has been the subject of differing interpretations since it was first identified by Spengler, Braun et al. (1994, pp. 9-11; Figure 1-15). A systematic investigation by Potter et al. (1995, p. 1) found that the northwest-striking fault zone can be traced for only about 750 m, as compared with 4.5 km or more suggested by previous workers. The maximum width of the Sundance fault zone is about 75 m and the cumulative northeast-side-down vertical displacement across the fault zone does not exceed 11 m (Potter et al. 1995, p. 1). Individual faults in the zone are vertically and laterally discontinuous. There is no field evidence for significant strike-slip displacement. Southeast of the mapped extent of the Sundance fault zone, the Ghost Dance fault can be projected along an essentially straight trend beneath Quaternary deposits in Split Wash with no apparent offset along the Sundance trend (Potter et al. 1995, p. 1; Day et al. 1998; CRWMS M&O 1998, pp. 3.6-24 to 3.6-25). There is no evidence to indicate Quaternary displacement. Faulting at Yucca Wash appears to be absent, based on observations during detailed mapping in that area (CRWMS M&O 1998, p. 3.6-9).

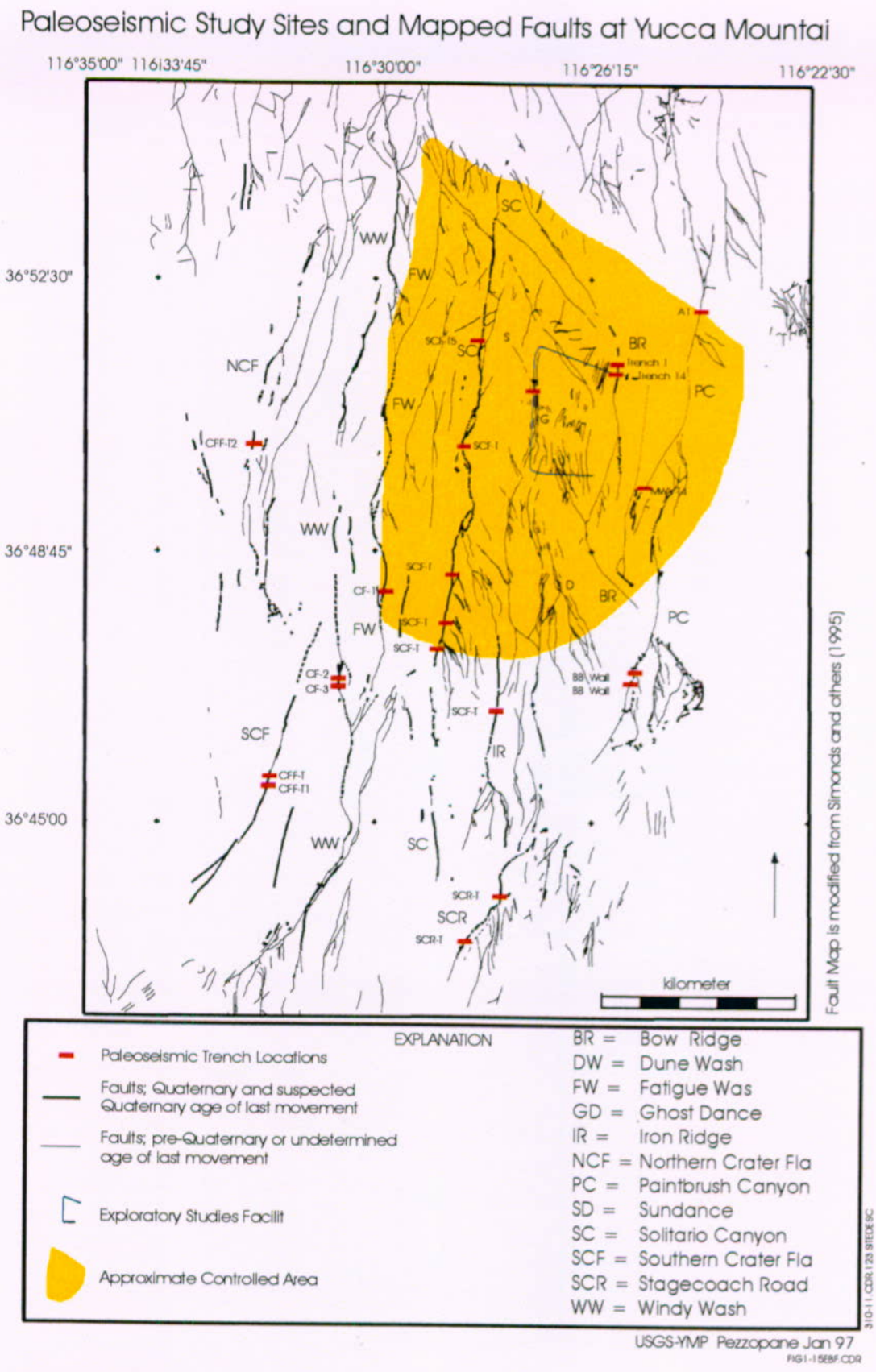

Source: CRWMS M&O (1998, Figure 3.10-11)

Figure 1-15. Mapped Faults At and Near the Yucca Mountain Site

The north-trending, block-bounding faults displace bedrock down-to-the-west; displacements are dominantly dip-slip with varying amounts of left-oblique slip (Simonds et al. 1995, map). Estimates of the amount of bedrock displacement that took place on the major faults over the last approximately 12 million years range from less than 100 m to as much as 600 m. Displacement increases southward along each of these faults. Dips of the fault planes are generally within the range of 60 to 70 degrees.

Scott and Bonk (1984) mapped many subsidiary faults with small displacements between the major north-trending faults. More recent large-scale geologic mapping (Day et al. 1998) and related stratigraphic studies have emphasized the complex geometry of the dominant faults and fault zones. Uncertainty concerning the geometry of faults and fault zones increases with distance away from control points, such as exposures in the ESF and intersections with boreholes, and is also due to uncertainties in interpreting geophysical data.

The northwest-trending faults are thought to be strike-slip faults; fault plane surfaces locally display slickensides that are nearly horizontal, and vertical displacements generally are less than 5 to 10 m (Scott et al. 1984, pp. 2, 8; Simonds et al. 1995, map). Assuming that the northwest trending faults (Sevier Wash, Pagany Wash, and related faults) moved laterally as indicated by the slickenslides, the geometry of the dipping beds they cut and the relative apparent vertical offsets require right lateral slip. This is consistent with the stress field of the Walker Lane. Horizontal displacements are estimated to be about 40 m on each fault (Scott et al. 1984, p. 18). O'Neill et al. (1992, Figure 3, p. 12) had concluded that the northwest-trending faults have some extensional component related to the left-oblique component of displacement along the north-trending faults.

1.3.2.2 Quaternary Faulting History

Quaternary faults at the Yucca Mountain site and in the surrounding region may be defined as relevant earthquake sources for the purpose of analyzing the potential hazards posed by vibratory ground motion and fault displacement at the Yucca Mountain site. Known and suspected Quaternary faults are discussed in the *Yucca Mountain Site Description* (CRWMS M&O 1998, Section 3.10.68). Both the historical record of seismicity in the southern Great Basin and paleoseismic information based on the geologic record are used for extrapolation of the fault displacement and vibratory ground motion hazards into the future. The six teams of experts considered these faults in their evaluation of relevant earthquake sources (CRWMS M&O 1998, Section 3.10.9.2) (also see Section 1.4.3 below).

The north-trending, block-bounding faults at the site show evidence of activity during Quaternary time, with total displacements estimated to be less than about 8 m on the Paintbrush Canyon fault over the past 700 ka (CRWMS M&O 1998, p. 3.10-50). Since the late Quaternary (<128 ka), displacements as much as 2.7 m have occurred, but more commonly they are in the < 1.0 to 2.5 m range. There is no clear evidence that movement along the northwest-trending faults has taken place during the Quaternary; Quaternary alluvial terraces in the floors of the washes do not appear to be displaced by these features (Menges and Whitney 1996, p. 4.2-21; Simonds et al. 1995, map).

The characteristics of selected north-trending and northwest-trending faults near the site are summarized on Table 1-2. Although most of the deformation on these structures occurred during the Miocene, in conjunction with regional extension and silicic volcanism, seven to eight faults display evidence of multiple surface rupture during the middle to late Quaternary, depending on whether the northern and southern Crater Flat faults are distinguished as separate structures (Table 1-2). Most of these Quaternary faults form the structural boundaries of large east-dipping fault blocks (Figure 1-15). Several faults, such as the Ghost Dance and Midway Valley faults are located in the interior of fault blocks. These structures are generally short in length, are associated with small cumulative bedrock offsets, and have poor topographic expression. These faults generally lack evidence for significant Quaternary displacements other than possible minor fracturing of Quaternary units (Menges and Whitney 1996, p. 4.2-22).

As a result of fault investigations in the Yucca Mountain region, approximately 100 individual faults were considered as possible sources of seismicity and potentially significant levels of ground motion (see CRWMS M&O 1998, Subsection 3.10.7; Pezzopane 1996, pp. 11-1 to 11-3). Calculations to determine which faults may have the capability of generating at least 0.1 g peak horizontal acceleration at the 84th percentile level of confidence (a standard commonly used for seismic design basis ground motions for critical facilities) further identified those features that should be taken into specific account for evaluating fault displacement and ground motion hazards at Yucca Mountain. As a result, 67 faults, or combinations of faults, have been distinguished as "relevant" or "potentially relevant" sources of seismicity, depending on whether there is demonstrable or only questionable evidence of Quaternary movement. Two or more closely related faults that are aligned end to end are combined in some cases. This was done because if ruptures were to occur simultaneously along their entire length, the resulting ground motion would be substantially greater than if rupture occurred on only one of the faults (see CRWMS M&O 1998, Table 3.10-11; Pezzopane 1996, Table 11-1). Additional structures at greater distances were also identified as being relevant and include the Pahranagat, Owens Valley, Garlock, White Mountains-Cedar Mountain, and San Andreas faults (CRWMS M&O 1998, Table 3.10-11). Figure 1-15 shows the locations of those faults generally within 20 km of the site and Figure 1-16 shows the locations of faults within 100 km of the site. Known or suspected Quaternary faults are listed and described in detail in CRWMS M&O (1998, Table 3.10-11, Section 3.10.6.8).

1.3.2.3 Folding at Yucca Mountain

Folding has played a minor role in structural deformation at Yucca Mountain and adjacent areas during Tertiary time. Several broad anticlines and synclines have been mapped in Tertiary volcanic rocks in Crater Flat basin to the west. These structures trend easterly, at high angles to the strikes of the major intrabasin faults, for distances of a few kilometers and with amplitudes measured in tens to hundreds of meters. These folds are interpreted to be the result of changes in dip-slip offset along the strikes of intrabasin faults (Faulds et al. 1994, p. 2).

Weakly expressed small anticlinal folds (amplitudes of a few tens of meters) have been mapped in Rock Valley (Sargent and Stewart 1971, map). These structures were developed concomitantly with the strike-slip faulting that took place in this area.

Table 1-2. Summary of Characteristics of Selected Faults at Yucca Mountain

Fault	Surface Characteristics	Evidence of Quaternary Activity	Average Dip of Fault	Sense of Displacement	Amount of Displacement (bedrock)	Amount of Displacement (Quaternary)	Fault Length
Northern and Southern Crater Flat fault zone	Two faults 300-600 m apart, bedrock faults, bedrock scarps, subtle scarps and lineaments in Al, Br/Al fault contacts	Lineaments in Al, subtle scarps and fractures in Al.	70° west	Oblique, left-lateral	Unknown, down to the west	Less than 1 m, late Quaternary	1 km min, 20 km max
Windy Wash fault	Prominent fault-line scarp, east-facing scarps in Al, Br/Al fault contacts, merges with Fatigue Wash fault	Two trenches show multiple events, fractures and scarps in Al, basalt ash in fault plane	63° west	Dip-Slip	Increases to south to-500 m, down to the west	1.0 m, late Quaternary, <0.1 m, Holocene	3 km min, 25 km max
Fatigue Wash fault	Bedrock fault, fault-line scarp, scarps, and lineament in Al, bedrock scarps, merges with Windy Wash fault	One trench shows multiple events, fractures and scarps in Al, basalt ash in fault plane	73° west	Oblique, left-lateral	-72 m, down to the west	2.2 m, late Quaternary	9.5 km min, 17 km max
Solitario Canyon and Iron Ridge faults	Prominent fault-line scarp, discontinuous traces, and subtle scarps in Al, Iron Ridge fault splay forms prominent fault-line scarp, merges with Stagecoach Road fault	Twelve trenches, nine of which show multiple events, fractures in Al, basalt ash in fault plane	72° west (main trace) 68° west (Iron Ridge fault)	Oblique, left-lateral	Increases to south from 61 m down to the east to >500 m down to the west	1.7-2.5 m, late Quaternary	12.5 km min, >21 km max
Stagecoach Road fault	Prominent scarp and traceable faults in Al, merges with Solitario Canyon fault and (or) Paintbrush Canyon fault	Three trenches, two of which show multiple events, fractures and scarps in Al, basalt ash in faulted Al	73° west	Dip-Slip	400 to 600 m down to the west	1.0-2.3 m, late Quaternary	4 km min, >26km max
Ghost Dance fault zone	Bedrock fault in a zone of subparallel minor faults and breccia zones	None	Near vertical	Dip-slip	Increases to south from 0 to -30 m down to the west	None	3 km min, 9 km max

Table 1-2. Summary of Characteristics of Selected Faults at Yucca Mountain (Continued)

Fault	Surface Characteristics	Evidence of Quaternary Activity	Average Dip of Fault	Sense of Displacement	Amount of Displacement (bedrock)	Amount of Displacement (Quaternary)	Fault Length
Bow Ridge fault	Fault-line scarp along Br/Al contact , subtle lineaments, may merge with Paintbrush Canyon fault	Six trenches, five of which show multiple events, fractures in Al, basalt ash in fault plane	75° west	Oblique, left-lateral	125 m down to the west	0.5-1.32m, late Quaternary	0.76 km min, 107 km max
Midway Valley fault	None, fault located on the basis of geophysical evidence	None	Unknown, west?	Unknown, Dip-slip?	40-60 m down to the west	None	1 km min, 8 km max
Paintbrush Canyon fault	Bedrock faults, bedrock scarps, lineaments, Br/Al fault contacts, faults in Al, possibly merges with Stagecoach Road fault	Four trenches and natural exposures at Busted Butte show multiple events, fractures in Al, basalt ash in fault plane (locally)	71° west	Dip-slip to oblique, left-lateral	250-500 m down to the west	1.7 to 2.7 m, 4.6-6.3 m at Busted Butte, mid to late Quaternary	10 km min, >26 km max
Northwest Trending faults	Bedrock faults with local small bedrock scarps, faults located on the basis of geophysical or drillhole evidence	None, except for one trench located on the Pagany Wash fault shows possible Quaternary displacement	>70° south to vertical	Strike-slip right-lateral	5-10 m vertical, -40 m right-lateral	None	2 km min, 8 km max

(Modified from Menges and Whitney 1996, Table 4.2.1)

NOTE: Abbreviations used in the table; Al, alluvium; Br, bedrock; >, greater than; <, less than; km, kilometer; m, meter; min, minimum; max, maximum. Faults with demonstrated Quaternary displacement are shown in **bold** font.

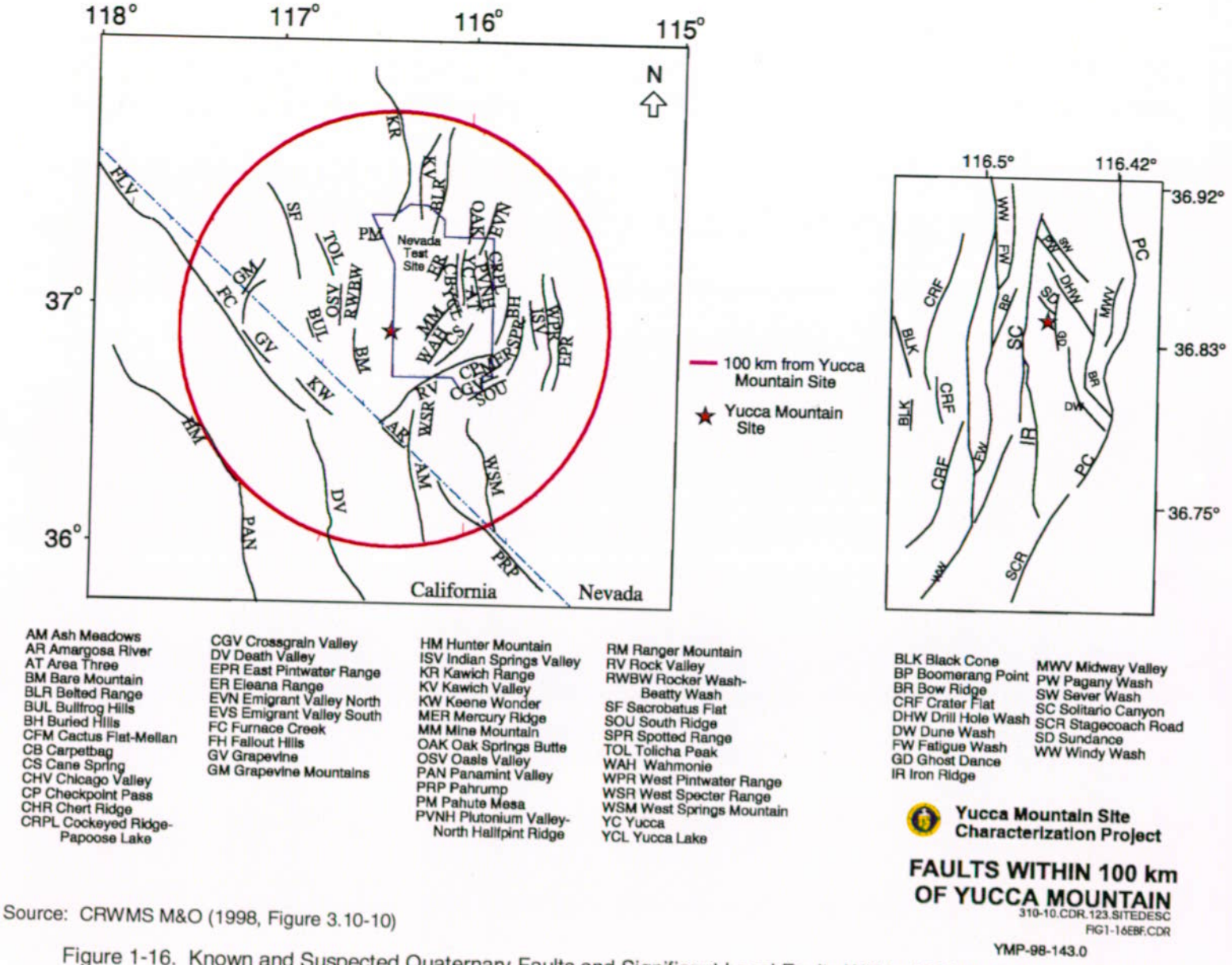

Source: CRWMS M&O (1998, Figure 3.10-10)

Figure 1-16. Known and Suspected Quaternary Faults and Significant Local Faults Within 100 km of Yucca Mountain

1.3.2.4 Fractures at Yucca Mountain

Fracture studies are discussed in detail in the *Yucca Mountain Site Description* (CRWMS M&O 1998, Sections 3.6.3 and 3.7). Section 4, below, addresses geoengineering aspects of fractures. In summary, tectonic fractures within the Paintbrush Group (Tiva Canyon, Yucca Mountain, Pah Canyon and Tonopah Spring tuffs) can be grouped into at least four sets that seem to have consistent orientation. The median orientation of tectonic fracture sets are: north-south, steeply dipping to the west; northwest striking, dipping steeply to the southwest; northeast, dipping steeply to the northwest; and east-northeast, dipping steeply to the southeast and northwest.

In addition, there is a set of subhorizontal joints that have variable strikes and dips less than 10 degrees. This set is subparallel to the flattening foliation and, at least locally, appears to have developed as a set of cooling joints. Near-vertical cooling joints developed in the welded parts of the Paintbrush Group and generally have orientations similar to the tectonic sets. They appear to pre-date the tectonic fractures.

1.3.3 Volcanism at Yucca Mountain

Volcanism is a significant aspect of the tectonics of the Yucca Mountain site. The following discussions of both the history and nature of occurrence of silicic and basaltic volcanism are presented because tectonic processes active within the Quaternary are an important part of the evaluation of the Yucca Mountain site as a potential high-level waste repository.

Volcanism in the Great Basin can generally be divided into two stages: a silicic episode involving eruption of large volume ignimbrites (Oligocene to middle Miocene) and a basaltic episode involving increasingly smaller volumes of basalt (mid-Miocene to Quaternary). These two stages of volcanism also correlate in a general way with crustal extension rate: high rate of extension during the time of the silicic episode, low and declining rate of extension during the period of basaltic volcanism (CRWMS M&O 1998, p. 3.9-1). The rocks found at Yucca Mountain, to a few kilometers depth, are predominantly Miocene silicic volcanics derived from nearby nested caldera complexes. The geochronology of these events and resulting lithologies are discussed in Section 1.2.2.2.

The initiation of true basaltic volcanism in the Great Basin and the Basin and Range tectonic province as a whole began in the early to middle Miocene (<17 Ma) (Figure 1-17) and generally postdates major silicic volcanism and periods of high extension rate in any particular region.

Basaltic volcanism in the Great Basin and adjoining regions has exhibited systematic trends in location, composition, and eruption volume through time. These trends can be related to both tectonic processes in the crust and melt generation processes in the underlying mantle. As discussed in the *Yucca Mountain Site Description* (CRWMS M&O 1998, p. 3.9-3), the eruption rate for the past 5 Ma cycle of basaltic activity near Yucca Mountain is among the lowest of volcanic fields in the western United States, and basaltic volcanism is minor compared to other regions of the western United States (Figure 1-17).

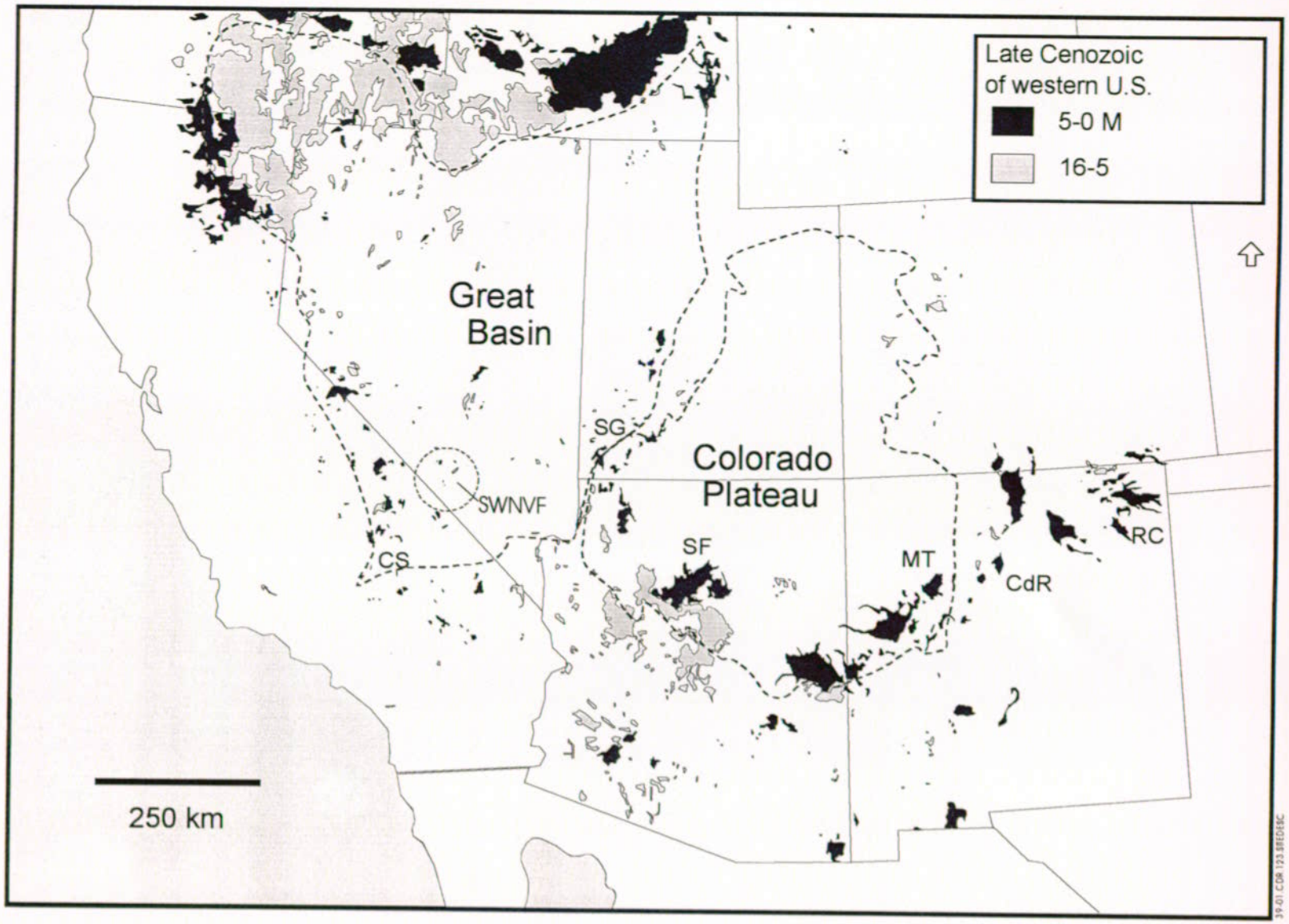

Source: CRWMS M&O (1998, Figure 3.9-1)

NOTE: The distribution of volcanic rocks of silicic and intermediate composition is not shown. The location of the Southwestern Nevada Volcanic Field (SWNVF), within which Yucca Mountain is located, is indicated as a circle of 50 km radius centered on Yucca mountain. The circle encompasses post-5 Ma basaltic centers of the Yucca Mountain region. Other labeled volcancic fields are: C: Cima, CdR: Cerros Del Rio; CS: Cosco; GC: Grand Canyon; GR Grants Ridge; LC: Lunar Crater; L: Lucero; MT: Mount Taylor; RC: Raton-Clayton; SF: San Francisco; SG: St. George; SRP: Snake River Plain; SV: Springgerville; TY: Taos; ZB: Zuni-Bandera.

Figure 1-17. Distribution of Late Cenozoic Basaltic Rocks in the Western United States

During the late Neogene (10 to 1.6 Ma) and Quaternary (1.6 to 0 Ma), small-volume, basaltic centers erupted lava flows, air falls, and cinder cones. The following discussions are intended to provide an overview of the background information available on both silicic and basaltic volcanism, which then can be used to make assessments of the likelihood of future volcanic events and, thus, their likelihood to directly or indirectly influence the performance of a potential repository at the Yucca Mountain site.

1.3.3.1 Silicic Volcanism

Silicic volcanism in the Yucca Mountain region is part of an extensive mid-Cenozoic episode that occurred throughout much of the southwest United States. Yucca Mountain is in the south-central part of the southwestern Nevada volcanic field that covered an area exceeding 11,000 square-km (Christiansen et al. 1977, p. 944). The volcanic rocks that formed Yucca Mountain were emplaced during eruptive cycles of the Timber Mountain caldera complex (Sawyer et al. 1994, pp. 1305-1306). The Yucca Mountain site, including most of the surface exposures and strata extending to the depth of the potential repository horizon, comprises volcanic units of the Paintbrush Group. The Paintbrush Group is a series of major ash flow sheets from the Timber Mountain caldera complex of the Southwestern Nevada volcanic field (Sawyer et al. 1994, pp. 1305, 1307-1308).

The time-space distribution of volcanic activity in the northern Great Basin province has been described by many authors (CRWMS M&O 1998, pp. 3.2-16, 3.9-1 to 3.9-3). Sites of Tertiary eruptive activity migrated south and southwest, progressively, in time and space across an area of Nevada and adjoining parts of Utah. The period of most voluminous silicic volcanic activity in the region occurred between 13 and 11 Ma. The site region marks the southern limit in the spread of time-transgressive volcanic activity.

Silicic volcanism produced the rocks at the site described in Section 1.2.2.2. This activity has waned and the basaltic volcanism discussed below is more important with regard to Quaternary and assessing the potential hazard from future volcanic activity.

1.3.3.2 Basaltic Volcanism

In the Yucca Mountain region, silicic volcanism of the southwestern Nevada volcanic field (see Figure 1-17) and peak extension rates in the southern Great Basin occurred simultaneously at approximately 15 to 10 Ma (Wernicke et al. 1988, pp. 1755-1756; Scott 1990, pp. 273, 279; Carr, W.J. 1990, pp. 283-284, 287). The commencement of basaltic volcanism occurred during the latter part of this period, as extension rates waned, and relatively small-volume basaltic volcanism has continued into the Quaternary Period. In terms of eruption volume, the 15 million-year history of the southwestern Nevada volcanic field is viewed as a magmatic system that peaked between 13 to 11 Ma, with the eruption of over 5,000 km^3 of ashflow tuffs, and has been in decline since, with relatively minor volumes of basalt erupted since 11 Ma (CRWMS M&O 1998, Figure 3.9-2). The last 0.1 percent of the erupted volume of the southwestern Nevada volcanic field consists entirely of basalt erupted since 7.5 Ma. In terms of relative volumes, therefore, the southwestern Nevada volcanic field is considered to have radically reduced eruptive activity since about 7.5 Ma (CRWMS M&O 1998, Figure 3.9-5).

The post-caldera basalts of the southwestern Nevada volcanic field consist of basalts erupted since formation of the Stonewall Mountain volcanic center (7.5 Ma), the furthest of the southwestern Nevada volcanic field calderas from Yucca Mountain. This definition of post-caldera basalts differs slightly from that of Crowe, Perry, Geissman et al. (1995, pp. 2-12, 2-15 to 2-16), who considered post-caldera basalts as old as approximately 9 Ma, which postdate formation of the Black Mountain caldera, the youngest caldera of the central southwestern Nevada volcanic field caldera cluster. Using the definition of Crowe, Perry, Geissman et al. (1995, pp. 2-12, 2-15, 2-16), which applies to the main portion of the southwestern Nevada volcanic field, post-caldera basalts can be divided into two episodes: older post-caldera basalts and younger post-caldera basalts. The older post-caldera basalts erupted between about 9 and 7.2 Ma, while the younger post-caldera basalts erupted between about 4.8 and 0.08 Ma. The time interval of about 2.5 Ma between these episodes is the longest eruptive hiatus of basalt in the Yucca Mountain region during the last 9 Ma. This eruptive hiatus also marks a distinct shift in the locus of post-caldera basaltic volcanism in the Yucca Mountain region to the southwest (Figure 1-18). The basalts of the older post-caldera basalts and younger post-caldera basalts are thus both temporally and spatially distinct. This observation emphasizes the importance of considering the age and location of the younger post-caldera basalts (approximately the past 5 Ma of the volcanic history of the Yucca Mountain region) when calculating the volcanic hazard to the potential Yucca Mountain repository (CRWMS M&O 1998, p. 3.9-5).

The basalts of the younger post-caldera basalts comprise at least six episodes of volcanism that occur within 50 km of the proposed Yucca Mountain repository (Figure 1-19). The total eruption volume of the younger post-caldera basalts is about 6 km^3. The volume of individual episodes has decreased progressively through time, with the three Pliocene episodes having volumes of approximately 1 to 3 km^3 each and the three Quaternary episodes having a total volume of approximately 0.5 km^3 (CRWMS M&O 1998, Figure 3.9-2, inset).

Quaternary basalt in the Yucca Mountain region erupted along a north-northwest trending alignment (Crater Flat Volcanic Zone of Crowe and Perry 1990, pp. 327-328) that lies to the south, west, and northwest of the potential repository (CRWMS M&O 1998, Figure 3.9-7). Eight Quaternary scoria cones occupy this alignment, representing either seven or eight eruptive centers. All of the Quaternary centers are similar in that they are of small volume (approximately 0.1 km^3 or less), and typically consist of a single main scoria cone surrounded by a small field of basalt flows (CRWMS M&O 1998, p. 3.9-6).

Basaltic volcanism at Crater Flat occurred in three episodes at approximately 3.7, 1, and 0.08 Ma (Figure 1-19).

Basalt of Southeast Crater Flat–The Pliocene basalt of southeast Crater Flat has been described in several publications (CRWMS M&O 1998, pp. 3.9-7 to 3.9-8). The basalt unit consists of an alignment of north-trending, dissected scoria cones, and associated moderate-volume lava flows (Figure 1-19). Recent analyses indicate an age of approximately 3.7 Ma for this basalt (Perry et al. 1998, p. 2-24 to 2-25; Fleck et al. 1996, p. 8213). The consistency of age determinations for this unit at multiple analytical laboratories suggests the chronology of this unit is well established by the existing radiometric ages. The similarity in age of the buried lava flow in Amargosa Valley and the basalt of Crater Flat suggests the units were probably erupted about the same time, but as spatially separate units.

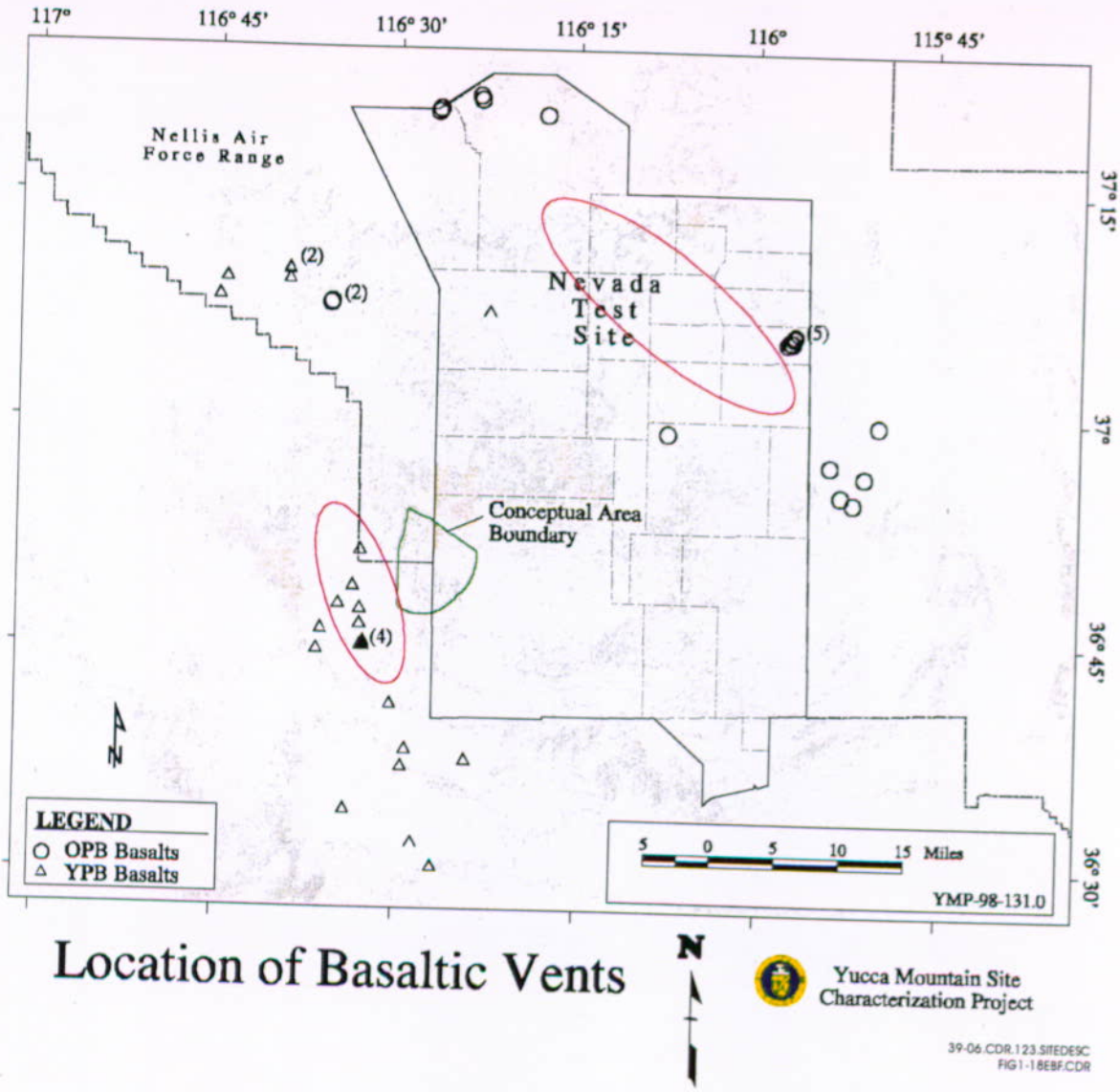

Source: CRWMS M&O (1998, Figure 3.9-6)

NOTE: Ellipses represent 95 percent confidence intervals for the location of the vents for each basalt cycle. OPB = Older Post-Caldera Basalts; YPB = Younger Post-Caldera Basalts.

Figure 1-18. Location of Vents of OPB Basalts (Circles) and YPB (post-Miocene) Basalt (Triangles)

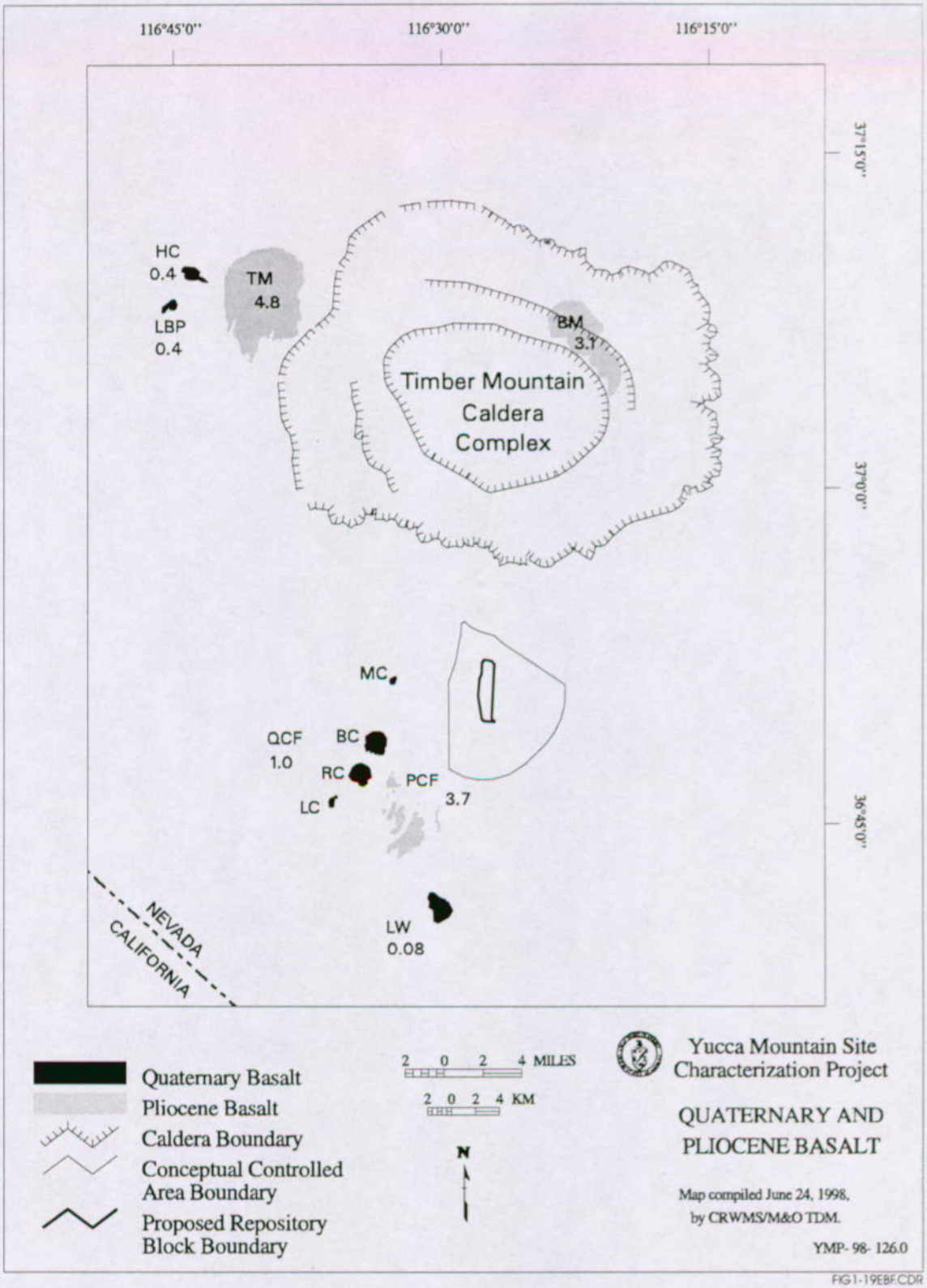

Source: CRWMS M&O (1998, Figure 3.9-7)

NOTE: HC = Hidden cone, TM = Thirsty Mesa, LBP = Little Black Peak, BM = Buckboard Mesa, LW = Lathrop Wells, MC = Makani cone, BC = Black cone, RC = Red cone, LC = Little cone, QCF = Quaternary Crater Flat, PCF = Pliocene Crater Flat

Figure 1-19. Quaternary and Pliocene Basalt Centers of the Yucca Mountain Region

Quaternary Basalt of Crater Flat–A series of four Quaternary basalt centers form a north-east trending, slightly arcuate cluster of basalt centers (Figure 1-19). From southwest to northeast, these centers consist of, respectively: Little Cones, Red Cone, Black Cone, and the Makani cone. The Little Cones have been dated at about 1.0 Ma (Crowe, Perry, Geissman et al. 1995, p. 2-21). K-Ar and Ar/Ar dates indicate that the Red and Black Cones are approximately 1 Ma (Perry et al. 1998, p. 2-28). Other age determination resulted in ages ranging from about 1 to 0.75 Ma and both have been used in the probabilistic volcanic hazard analysis (Section 1.3.3.4). The Red and Black Cone centers are analogous volcanic landforms with similar eruptive histories. Each consists of a main scoria cone surmounted by a summit crater filled with agglutinated spatter, large lava blocks, and scoria (Vaniman and Crowe 1981, pp. 15-18).

Lathrop Wells Volcanic Center–The geology and chronology of the Lathrop Wells volcanic center was described in several publications (CRWMS M&O 1998, pp. 3.9-8 to 3.9-9). The volcanic deposits of the center overlie volcanic bedrock of the Paintbrush and Timber Mountain Groups, and alluvial deposits. Early geochronological studies of the Lathrop Wells center had several problems because of the lack of ideal materials for dating and the resulting young ages. The soil horizon and cone morphology had been interpreted as indicative of a late Pleistocene or Holocene age (i.e., last 10,000 years) (Wells et al. 1990, p. 552). Subsequent studies indicated that the evolution of the center was complex and that it may have resulted from polygenetic events (Perry et al. 1998, p. 2-43). Geochronologic, geochemical, and field data obtained during 1995 and 1996 have led to a re-evaluation of previous conclusions (Perry et al. 1998, p. 2-107). Recent Argon-40/Argon-39 dates on both basalt whole-rock samples and tuff xenolith sanidine samples are reproducible and indicate an age of 75 ± 10 ka (Perry et al. 1998, pp. 2-83 to 2-85). This age determination is consistent with uranium-thorium disequilibria, Helium-3 dates, and Chlorine-36 dates obtained from samples collected at Lathrop Wells indicating that the true age of the Lathrop Wells center is between about 70 and 90 ka (CRWMS M&O 1998, p. 3.9-4).

1.3.3.3 Alternate Conceptual Models for Volcanic Activity

There are several areas of uncertainty associated with assessing hazards from future volcanic activity to a potential repository at the Yucca Mountain site. Controversy over the hazard assessment revolves around interpretation of data, choice of models, and use of analogues.

Champion (1991, pp. 63-65) suggested all Quaternary basalt centers of Crater Flat record a single, reversed, polarity remnant magnetization on the basis of field and paleomagnetic analyses of samples collected from 20 sites. These paleomagnetic data were interpreted by Champion (1991, p. 66) to permit the inference that the Quaternary basalt centers of Crater Flat formed contemporaneously (single magma-pulse) with each center being of monogenetic origin (formed in one brief eruptive cycle). However, this interpretation requires several critical underlying assumptions. For example, more information is required to determine if the centers were fed from multiple dike systems and if the geochemistry of the centers is consistent with single or multiple pulses of magma. Also, the paleomagnetic data must be considered in light of the evidence of geochemical diversity in the lavas (Perry and Crowe 1992, pp. 2358, 2362-2363). The assumptions associated with the paleomagnetic study must be more carefully evaluated before accepting the conclusion that each center is monogenetic and, especially, that all centers formed from a single magmatic event.

The recognition of time-separate events at basalt centers must be based on establishing unequivocal time-gaps between eruptive events, such as the presence of soil-bounded unconformities (Crowe, Morley et al. 1992, p. 2010). Relatively young rocks that have a low initial K content are very difficult to date because so little Ar is generated. The variable K-Ar age determinations provide permissive, but not conclusive, evidence of polygenetic events. Alternatively, the precision of the K-Ar methods is insufficient to test the polygenetic model.

The possibility of polycyclic volcanism in the Yucca Mountain region was discussed by Wells et al. (1990, pp. 549-550), who observed soils between scoria deposits south of the Lathrop Wells cone, suggesting significant time intervals between emplacement of the scoria deposits. Subsequent field, geochronologic, and geochemical studies could not disprove the hypothesis that Lathrop Wells was polycyclic (Perry et al. 1998, pp. 2-107 to 2-109), and it remains a viable alternative hypothesis to monogenetic volcanism despite vigorous scientific challenge (Turrin et al. 1992, p. 558).

The most recent studies at Lathrop Wells combining new geochronology and field studies favor a monogenetic model (Perry et al. 1998, p. 2-112), (weaken the evidence for polycyclic volcanism), and suggest that the center formed in a single complex episode about 70 to 90 ka (CRWMS M&O 1998, p. 3.9-9). Field evidence for polycylic volcanism at Lathrop Wells includes apparent erosional unconformities between eruptive units and the origin of scoria deposits on the south side of the Lathrop Wells cone. This field evidence is considered uncertain and its resolution must be considered in the volcanic hazard assessment (CRWMS M&O 1998, p. 3.9-9).

1.3.3.4 Volcanic Hazards Assessments

The probability of magmatic disruption of a repository is expressed as the annual probability that a volcanic event will disrupt (or intersect) a repository, given that a volcanic event occurs during the time period of concern. The magmatic disruption probability thus combines the recurrence rate and the disruption probability, taking into account uncertainties in each value.

Before 1996, there were three alternative sources of published probability calculations (Crowe, Perry, Geissman et al.1995, Chapter 7; Ho 1995; Connor and Hill 1995). The results of these calculations are summarized in the *Yucca Mountain Site Description* (CRWMS M&O 1998, Table 3.9-2). The calculations of Crowe et al. (1995, p. 7-91) and Connor and Hill (1995, p. 10,121, stated in events/10,000 years) result in almost identical results (approximately 10^{-8} events/year), while the calculations of Ho (1995, p. 256, stated in events/10,000 years) result in higher probabilities of disruption (bounded between 2×10^{-9} and 6.6×10^{-7} events/year). The upper end of the probability range of Ho (1995, p. 249) is predicated by restricting future volcanism to an extremely small volcanic source zone (75 km^2) that encloses the potential repository, a decision that is not justified based on the current structural understanding of the Yucca Mountain site (CRWMS M&O 1998, p. 3.9-17).

In 1995 and 1996, the U.S. Department of Energy (DOE) conducted an elicitation of recognized experts to assess uncertainties associated with the data and models used to evaluate the potential for disruption of the potential repository by volcanic processes (CRWMS M&O 1996b). The use of an expert panel ensured that a wide range of perspectives was considered in the hazard

analysis. The results of the probabilistic volcanic hazards analysis are that the aggregate expected annual frequency of intersection of the repository footprint by a volcanic event is 1.5×10^{-8}, with a 90 percent confidence interval of 5.4×10^{-10} to 4.9×10^{-8}. The mean value translates to a probability of about 1 in 7,000 that the potential repository will be disrupted by a magmatic event during the 10,000 year isolation period. The major contributions to the uncertainty in the frequency of intersection are the statistical uncertainty in estimating the rate of volcanic events from small data sets (the uncertainty in number of events) and the uncertainty in modeling the spatial distribution of future events (uncertainty in the location of future volcanic events) (CRWMS M&O 1998, p. 3.9-17).

Using most likely event count data from the probabilistic volcanic hazard assessment, Crowe, Wallmen et al. (1998, pp. 6-6, 6-14, 6-23) explored the sensitivity of the probability of intersection, assuming that aeromagnetic anomalies in the Amargosa Valley and Crater Flat, as well as the estimated number of undetected volcanic events, all represent Quaternary volcanic events. These assumptions lead to a revised count of eight Quaternary events and a revised probability of intersection of about 2.5×10^{-8} events/year, a value that is not significantly higher than previous estimates (CRWMS M&O 1998, p. 3.9-18).

The U.S. Nuclear Regulatory Commission (NRC) staff believes that the geologic evidence supports most annual probability estimates between 2×10^{-7} and 1×10^{-8} per year (Hill, B.E. et al. 1997, p. 2-26). Both the DOE and the NRC are focusing on consequence analyses as part of their total systems performance assessments.

1.4 SEISMICITY AND SEISMIC HAZARDS

1.4.1 Seismicity

1.4.1.1 Regional Seismicity

Assessment of seismic hazards at Yucca Mountain focuses on characterizing the levels of vibratory ground motion and fault displacement that will be associated with future earthquake activity in the vicinity of the site. The evaluation of these levels serves as a basis to define inputs for the preclosure seismic design of a potential geologic repository. The evaluation also provides information that can be used in evaluating the impact of different tectonic scenarios on the ability of the repository to contain and isolate waste during the postclosure period. By their nature, evaluations of seismic source characteristics, earthquake ground motions, and fault displacement involve interpretations of data. These interpretations have associated uncertainties related to parametric values and to the use of alternate models. The wide range of uncertainties must be considered to resolve competing hypotheses and alternate models. The interpretations are based on seismological, geological, geophysical, and geotechnical data specific to the Yucca Mountain site and surrounding region. Seismic hazard evaluations rely on having a description of the temporal and spatial distribution of earthquakes (both prehistoric and historic), their magnitudes, and an evaluation of how these relate to the seismotectonic processes of the region. Panels of experts used the data to evaluate and characterize seismic sources and evaluate and characterize vibratory ground motion attenuation relations. These evaluations were then used as input to a probabilistic seismic hazard analysis for both vibratory ground motion and fault displacement (see Section 1.4.3). The results of the hazard assessment provide the basis for developing ground

motion and fault displacement values appropriate for the seismic design of the potential repository.

The historical and instrumental earthquake record within 300 km of Yucca Mountain (Figure 1-20) includes the reported earthquakes of the southern Great Basin and the west-central Colorado Plateau in southwestern Utah and northeastern Arizona. The earthquake catalog is discussed in CRWMS M&O (1998, Section 3.10.2.2). The catalog contains all reported felt and instrumentally located earthquakes from the late 1800s to the present, including several of magnitude ($M > 5$) that are located slightly outside of the 300-km radius region, as discussed below. These are included because they are associated with surface ruptures that form important historical analogues for assessing fault displacement hazards at the repository site (Pezzopane and Dawson 1996, Section 9.2).

Several M_w (moment magnitude) > 5.5 events that are located within 100 km of Yucca Mountain are listed in the earthquake catalog. The earliest entry is the 1916 M_L (local magnitude) 6.1 (M_s [surface-wave magnitude] 5.9) Death Valley event (CRWMS M&O 1998, p. 3.10-7; Figures 1-20 and 1-21). Of earthquakes greater than M_w 5.5 in the 100-km compilation, only five events occurred outside of the areas of underground nuclear explosions and can be unequivocally designated as tectonic in origin. All of these tectonic $M_w > 5.5$ earthquakes, with the exception of the 1992 Little Skull Mountain earthquake, are near the Death Valley-Furnace Creek fault zone and occurred prior to 1966 (CRWMS M&O 1998, Figure 3.10-4). Many $M_w > 4$ earthquakes within 100 km also occurred near the Furnace Creek fault system, the most active tectonic feature in this region.

The significant historical seismicity of the region within 300 km of Yucca Mountain is described below and illustrated in Figures 1-20 and 1-21.

The 1932 Cedar Mountain and 1954 Fairview Peak and Dixie Valley Earthquakes

The 1932 M_L 7.2 Cedar Mountain, the 1954 M_w 7.1 Fairview Peak, and the M_w 6.8 Dixie Valley earthquakes occurred within the central Nevada seismic belt northwest of Yucca Mountain. These three events resulted in significant surface displacements (CRWMS M&O 1998, p. 3.10-8).

The Cedar Mountain earthquake produced widely distributed surface faulting recognized as 60 to 65 km in length by 8 to 17 km in width (dePolo et al. 1994, p. 50). Surface ruptures are expressed as left-stepping en echelon fissures and fractures, mole tracks, swell and depression morphology that collectively are indicative of lateral slip (Gianella and Callaghan 1934, pp. 361-363, 371-372, 377; dePolo, Ramelli et al. 1994, p. 50). Vertical displacements are generally less than 17 cm, with a maximum of 60 cm based on measurements taken by Gianella and Callaghan (1934, p. 362). Recent investigations indicate right-lateral displacements generally range from 0.5 to 1.5 m, and the maximum single-trace right-lateral displacement is 2.0 m ± 0.5 m (dePolo, Ramelli et al. 1994, p. 51). Many of the ruptures occurred along identifiable pre-existing scarps (Gianella and Callaghan 1934, pp. 358-360).

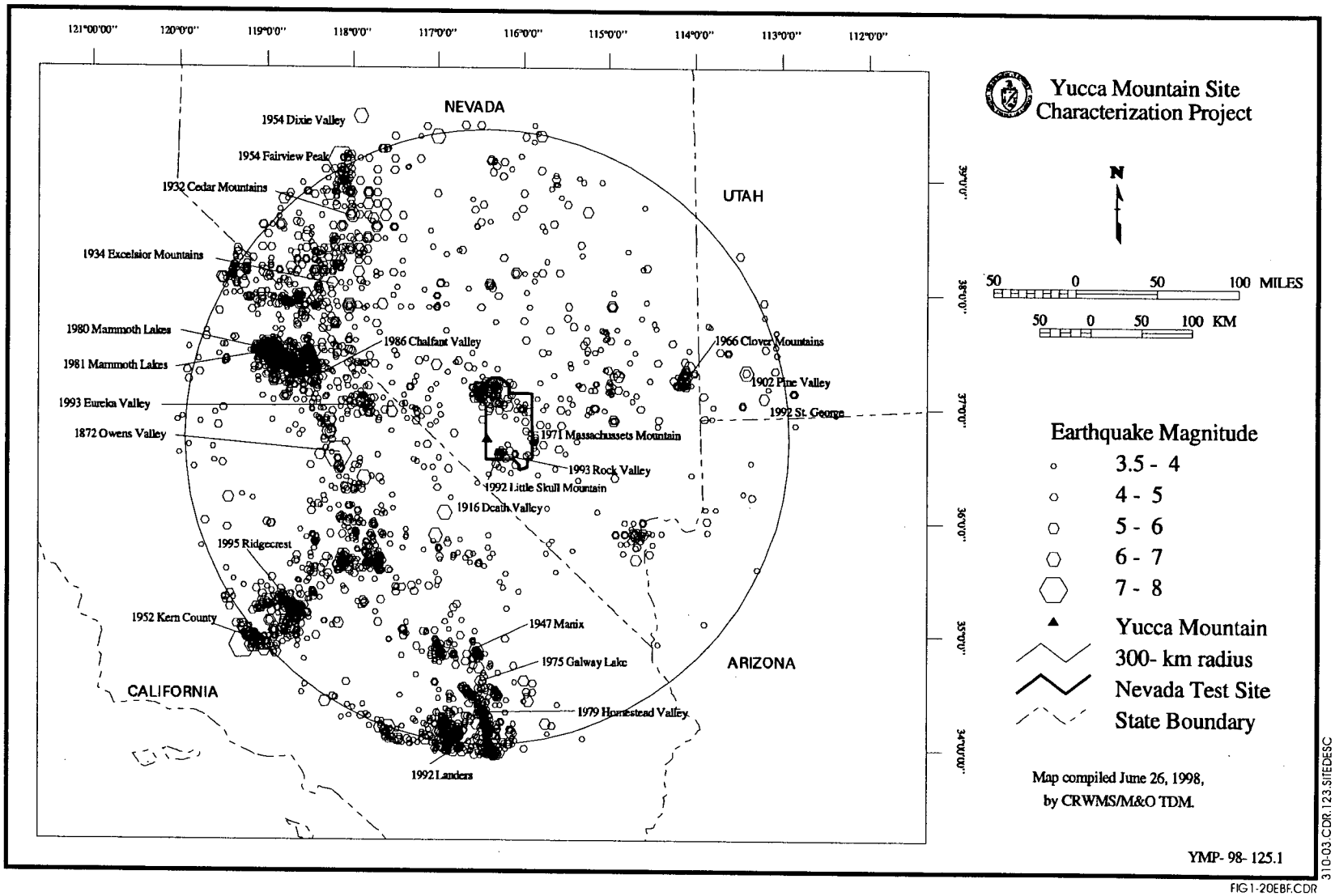

Source: CRWMS M&O (1998, Figure 3.10-3)

Figure 1-20. Historical Earthquake Epicenters within 300 km of Yucca Mountain

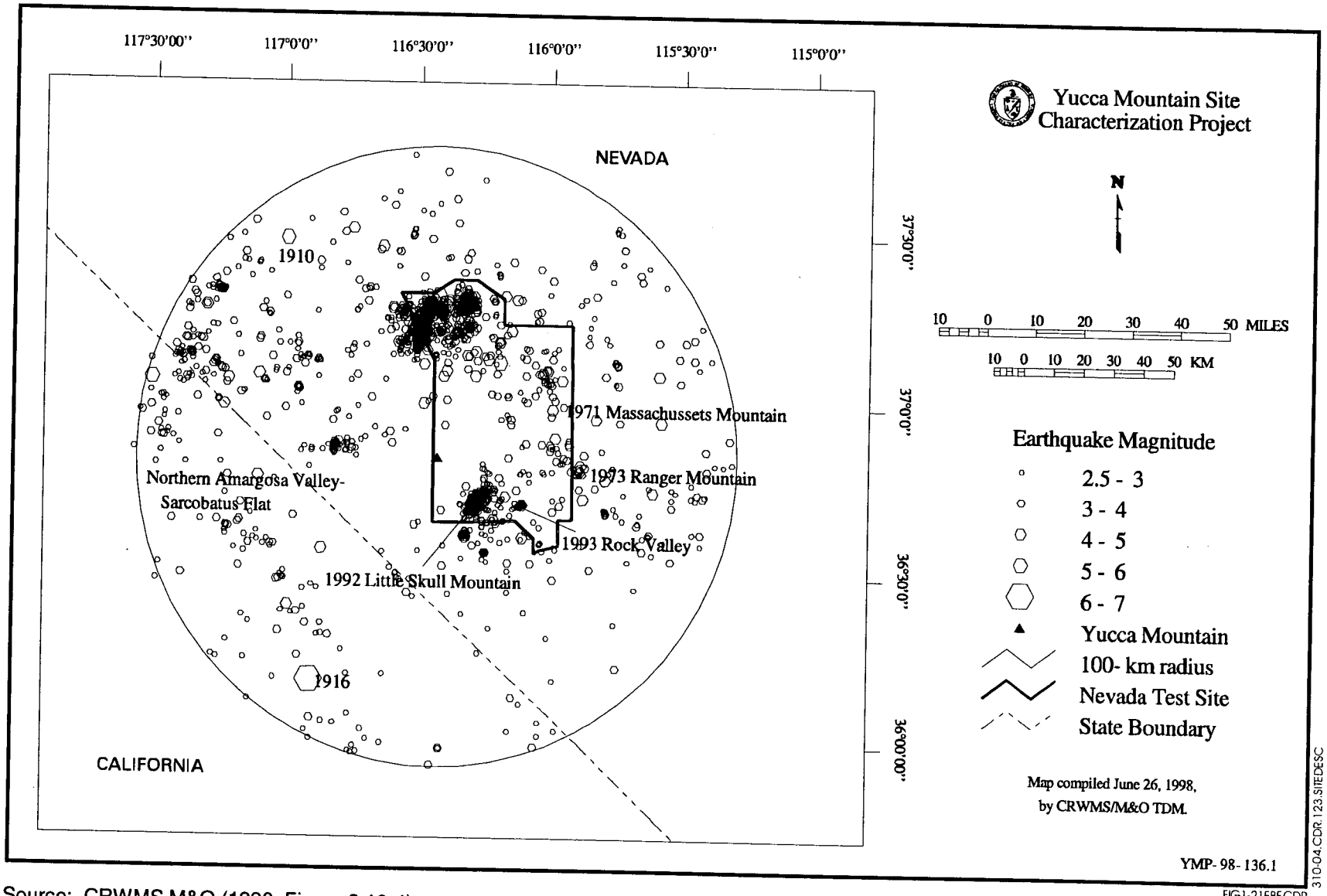

Source: CRWMS M&O (1998, Figure 3.10-4)

Figure 1-21. Historical Seismicity within 100 km of Yucca Mountain

The M_w 7.1 Fairview Peak and the M_w 6.8 Dixie Valley earthquakes (discussed below) occurred in December 1954 separated by a period of 5 minutes. The Fairview Peak earthquake ruptured several faults along a discontinuous zone that stretches for a total length of 64 km (Caskey et al. 1996, p. 785, Table 4). The longest of the individual faults is the Fairview fault, which is approximately 32 km long. The sense of displacement is dominantly normal-right-oblique, with a maximum vertical displacement of 380 cm and maximum right-lateral displacement of 290 cm along the Fairview fault (Caskey et al. 1996, p. 769). The normal-oblique slip observed for this event may represent a transition zone between dominantly right-lateral displacements observed to the south (1872 Owens Valley, 1932 Cedar Mountain) and the dominantly normal faulting seen to the north (1915 Pleasant Valley, 1954 Dixie Valley) (Caskey et al. 1996, p. 783).

The Dixie Valley earthquake ruptured the northern portion of the 100-km-long zone of surface faulting produced by the Fairview Peak-Dixie Valley earthquake sequence (Caskey et al. 1996, pp. 761, 768). Surface faulting produced by the Dixie Valley earthquake forms a 46-km-long zone which at the southern end ruptures parallel to the surface faulting formed by the Fairview Peak earthquake along the opposite side of the valley. Displacements related to the Dixie Valley earthquake are normal, down to the east, with a maximum vertical displacement of 280 cm and an average vertical surface displacement of 90 cm (Caskey et al. 1996, p. 763, Table 1). Caskey et al. (1996, p. 773) determined that the fault dips are generally steep (50° to 70°). However, in the southern part of Dixie Valley (south of the Bend), the fault appears to dip at relatively low angles (20° to 30°) within 65 m at the surface. The fault dips steeply at seismogenic depths (12 to 15 km) (Doser 1986, pp. 12,572-12,583). Other reported geologic effects included spring flow changes, water fountains, and liquefaction (Caskey et al. 1996, pp. 772-773; Slemmons 1957, p. 356). Landslides, rockfalls, mudflows, and fractures in alluvium are reported by Slemmons (1957, pp. 356-357).

The 1934 Excelsior Mountains Earthquake and the Mono Lake Region

The Mono Lake-Excelsior Mountain regions of the west-central Walker Lane in Nevada and eastern California is a continuing source of seismicity. The region is located between the seismicity in the Long Valley caldera-Mammoth Lakes area, California, and the zone defined by the 1932 and 1954 earthquake ruptures; it includes the 1934 M_L 6.3 (M_w 6.1) Excelsior Mountains, Nevada, earthquake. This earthquake produced a 1.5 to 1.7 km long fault scrap along a pre-existing bedrock fault, but may have also ruptured previously unfaulted bedrock (CRWMS M&O 1998, p. 3.10-8). The region is characterized by scattered, persistent microseismicity and northeast striking, left-lateral and left-oblique faults (dePolo, Peppin et al. 1993, pp. 279-280, 286-287).

The Mammoth Lakes-Chalfant Valley-Bishop, California, Area

The Mammoth Lakes, California, volcanic area, within and adjacent to the Long Valley caldera, has been the location of a recent series (1927 to present) of moderate sized (M 5 to 6) earthquakes, aftershock sequences, and volcanic related earthquake swarms (Hill, D.P., Wallace et al. 1985, p. 575). Several late Pleistocene and younger eruptions (the three youngest domes are about 720 years old) of the Long Valley caldera have shaped the physiography of the Mammoth Lakes-Chalfant Valley-Bishop, California, area (Bailey and Koeppen 1977, p. 5).

The *Yucca Mountain Site Description* contains a more detailed description of earthquakes in this area (CRWMS M&O 1998, pp. 3.10-10 to 3.10-11).

The 1993 Eureka Valley, California, Earthquake Sequence

The 1993 M_w 6.1 Eureka Valley, California, earthquake occurred east of the Owens Valley fault zone and just west of the structural transition between the northern Furnace Creek fault zone and the southern Fish Lake Valley fault zone (Figure 1-20). Satellite interferometry data analyzed showed a maximum displacement of 3 cm in the southeast part of the epicentral region. Surface ruptures along west-dipping faults were mostly discontinuous cracks that extended 4 to 5 km, with vertical displacement of up to 2 cm over about 100 m (CRWMS M&O 1998, p. 3.10-12).

The 1872 Owens Valley, California, Earthquake

Possibly the largest historical earthquake of the Basin and Range province, a M_w 7.8 event, occurred in 1872 along the Owens Valley fault zone in eastern California. Numerous aftershocks of probably M 6 (based on felt reports) followed the earthquake, but there is no instrumental record of the sequence. There are no seismograms with which to determine focal depth or mechanism, and the magnitude is estimated from felt area and surface rupture dimensions. Generally, there has been limited seismicity in much of the central Owens Valley.

The 1872 earthquake produced a 100 km (± 10 km) long zone of generally right lateral strike slip surface faulting along the entire length of the Owens Valley, from southern Owens Lake to north of Big Pine, California. Additional deformation is described in the *Yucca Mountain Site Description* (CRWMS M&O 1998, p. 3.10-7).

The Coso Volcanic Field and Ridgecrest, California, Area

The Ridgecrest, California, area and the Coso volcanic field north of Ridgecrest have experienced a recent series of M_L 5 earthquakes and extended aftershock sequences beginning in 1995 (Hauksson et al. 1995, p. 54). The volcanic field of the Coso geothermal area near Ridgecrest, California, has experienced ongoing small magnitude earthquakes.

A M_d (duration magnitude) 5.3 earthquake of August 17, 1995, produced a 1-km-long zone of discontinuous surface cracking along a fault trace that ruptured again in a M_d 5.4 event on September 20, 1995 (Figure 1-20). The September 20, 1995, earthquake produced surface faulting along 2.5 km of the Airport Lake fault zone, expressed mostly as left-stepping en echelon fractures and scarps with a maximum vertical displacement of 1 cm and a maximum right-lateral displacement of 0.8 cm (CRWMS M&O 1998, p. 3.10-12).

The Garlock Fault-Southern Sierra Nevada-Southeastern California Area

The trace of the Garlock fault is outlined by concentrated zones of seismicity in southeastern California. A northeast trend of seismicity, along structures at the southern end of the Sierra Nevada, includes the northeastern extent of mainshock rupture and aftershock activity of the 1952 M_w 7.5 Kern County, California, earthquake. The Garlock fault in places is marked by a high level of microseismicity. The Kern County earthquake triggered slip on certain sections of the Garlock fault, and nearby moderate to large magnitude events are sometimes associated with

increased levels of seismicity on segments of the fault that may be creeping (CRWMS M&O 1998, p. 3.10-12).

The Mojave Desert Region and 1992 Landers, California, Earthquake

The Mojave Desert contains several zones of persistent seismicity located approximately 150 to 200 km south of Yucca Mountain that include the many aftershocks of several moderate-sized (M 6 ± ½) earthquakes associated with surface faulting. The 1992 M_w 7.3 Landers earthquake is the largest surface-faulting event observed in the region. The Landers earthquake occurred in the southern Mojave Desert, a region where broad zones of primarily right-lateral and minor normal faulting splay northward from the San Andreas fault zone distributing as much as 8 to 10 mm/yr of relative right lateral motion along the Eastern California shear zone (Figure 1-20; Savage et al. 1990, p. 2116). In comparison to the Basin and Range province, seismicity in the Mojave Desert region is generally shallower and composed of more surface faulting events of predominantly strike-slip motion (CRWMS M&O 1998, p. 3.10-13).

The Lake Mead Area

Since 1936, Lake Mead, the reservoir impounded by Hoover Dam, has been the site of induced seismicity (Anderson, L.W. and O'Connell 1993, p. 85; Rogers and Lee 1976, pp. 1679-1680). Microseismicity occurs in the Colorado River area east of Las Vegas, Nevada. The *Yucca Mountain Site Description* contains more detail on earthquakes in the Lake Mead area (CRWMS M&O 1998, pp. 3.10-22 to 3.10-23).

The Nevada-Utah-Arizona Borders Area

The 1966 M_L 5.5 to 6.1 Clover Mountains earthquake occurred near the Nevada-Utah-Arizona borders and was marked by an extended aftershock sequence (Boucher et al. 1967, p. 205; Beck 1970, pp. 1, 15). No surface rupture was reported although it is unknown whether the epicentral area was investigated immediately after the event. Wallace et al. (1983, p. 610) determined a nearly pure strike slip mechanism for the mainshock from regional records.

The 1902 M_I (intensity magnitude) 6.0 Pine Valley (Smith, R.B. and Arabasz 1991, p. 198) and 1992 M_L 5.9 St. George (CRWMS M&O 1998, p. 3.10-14) earthquakes occurred east of the Clover Mountains sequence in Utah (Figure 1-20). Only one aftershock larger than M 2.5 was recorded for the St. George sequence. Smith, R.B. and Sbar (1974) discuss activity of the Intermountain Seismic belt, including activity along the Utah-Nevada-Arizona region. This is an area of generally low seismicity and the larger and moderate sized earthquakes are associated with the Colorado Plateau-Basin and Range transition zone.

The Pahranagat Shear Zone Area

The Pahranagat shear zone, located between the 1966 Clover Mountains sequence area and the northern Nevada Test Site, has been a consistent source of M 3 to M 4 earthquakes over the recent period of seismic monitoring. High angle strike-slip focal mechanisms are consistently reported in this region. The Clover Mountains and Pine Valley earthquakes and the Pahranagat shear zone activity comprise most of the events located within the eastern half of the east-west

Nevada seismic belt of the southern Great Basin (Rogers, Harmsen, Corbett et al. 1991, pp. 153-154, 163).

The Northern Nevada Test Site

The northern region of the Nevada Test Site includes the Timber Mountain caldera, Pahute Mesa, Rainier Mesa, and Yucca Flat. These areas have been the focus of considerable earthquake activity. The greater seismicity here, in contrast to the southern part of the Nevada Test Site (see below), is thought to be either directly or indirectly associated with nuclear testing (Figure 1-21).

Determining what earthquake activity is related to underground nuclear explosions, either through cavity collapse or induced by the stresses related to the explosion, is problematic. A study to determine the relative number of artificial and induced earthquakes in the testing areas suggests that the natural seismicity of the region reflects the background activity generally found in the southern Basin and Range province (Vortman 1991, pp. 11, 37-39, 42-43). In 1979 and 1983, several swarms of microearthquakes occurred in the region that are apparently unrelated to the underground nuclear explosions. Two sequences that occurred during the period of active testing took place in the vicinity of Dome Mountain and Thirsty Canyon (Rogers, Harmsen, Mermonte 1987, p. 40). Focal mechanisms for the Thirsty Canyon sequences indicate mainly right lateral strike-slip faulting on north-trending structures and normal faulting on north- or northeast-trending structures (Rogers, Harmsen, Mermonte 1987, p. 40).

The Southern Nevada Test Site

The southern portion of the Nevada Test Site is a seismically active region relative to some other areas in the southern Great Basin (Figure 1-21). Most of the seismicity that stretches across the entire southern portion of the Nevada Test Site is concentrated within and adjacent to the Rock Valley, Mine Mountain, and Cane Springs fault zones (including the 1992 M 5.6 Little Skull Mountain earthquake). This seismicity is not directly in areas of underground nuclear testing and is considered not to be induced. Some of the activity near the eastern Nevada Test Site boundary, particularly the 1971 Massachusetts Mountain earthquake and 1973 Ranger Mountain swarms, may have been triggered following the initiation of testing in the Yucca Flat area; however, there seem to be considerable numbers of small to moderate earthquakes related to natural strain release (Gomberg 1991a, Figure 10, pp. 16, 411; 1991b, pp. 16, 397). The largest event in this region is the 1992 M_L 5.6 Little Skull Mountain earthquake, which was triggered by the M_w 7.3 Landers earthquake (Anderson, J.G. et al. 1993, p. 165)

The Northern Amargosa Valley - Sarcobatus Flat

The northern Amargosa Valley-Sarcobatus Flat encompasses the areas west and northwest of the Bare Mountain fault, 25 to 90 km from the site. Seismicity in the northern Amargosa Valley is distributed in the vicinity of Beatty and the Bullfrog Hills. Some of this activity may be related to mining (Vortman 1991, pp. 11, 13-15). In Sarcobatus Flat, north and slightly west of Beatty, earthquakes have occurred in three clusters since the advent of instrumental monitoring. These clusters are spaced roughly 10 to 20 km apart in a northerly trend along the length of the valley.

The alignment of the earthquakes, and earthquake focal mechanisms, suggest right lateral strike-slip faulting on north-trending faults (Rogers, Harmsen, Carr et al. 1983, pp. 18, 20).

The Northern Death Valley Region

Seismicity along the Furnace Creek fault zone in northern Death Valley is distributed over an area much larger than the mapped surface traces of the faults (Figure 1-21). Epicenters extend northeast from northern Death Valley at the northern end of the Furnace Creek fault through the Gold Mountain-Mount Dunfee region. The largest event in this area during the modern era was a M_L 4 at Gold Mountain. The focal mechanism for this event is interpreted to have a northeast striking nodal plane consistent with left-lateral slip (Rogers, Harmsen, Carr et al. 1983, p. 20). A composite focal mechanism for a later group of earthquakes in this area suggests oblique dip-slip faulting on a northeast-striking plane (Rogers, Harmsen, Mermonte 1987, p. 48).

Depth Distribution and Focal Mechanisms

Earthquake hypocenters in the southern Great Basin are predominantly between 5 and 16 km in depth (Figure 1-22). This histogram is dominated by the Little Skull Mountain sequence which now comprises about 20 to 30 percent of the seismicity catalog for the southern Great Basin in the Nevada Test Site area. The Little Skull Mountain hypocenters were mainly between 12 and 5 km depth and the distribution peaks near the lower portion of the seismogenic zone. The sequence was well recorded and depth constraints were very good. Rogers, Harmsen, Mermonte (1987, p. 56) have shown that the seismicity in the southern Great Basin is distributed between about 15 and 2 km with a hiatus in activity at about 4 km for larger events. The 1993 Rock Valley sequence occurred at depths less than 3 km, as determined using near source (less than one focal depth) three-component digital recorders in the immediate epicentral area (Shields et al. 1995, p. F426).

Rogers, Harmsen, Carr et al. (1983, p. 21) showed that most of the seismic energy released in the southern Great Basin occurs at depths less than 12 km, but this represents a period of time (1978 to 1981) in which there was minimal moment release. Several larger magnitude earthquakes have been reported to nucleate deeper than 15 km, although these events occurred early in the instrumental record and hypocenters are not well constrained. Nucleation depths ranging from 10 to 20 km have been determined from waveform modeling for several major mainshock earthquakes in the Basin and Range province; these include the 1954 Fairview Peak and Dixie Valley, Nevada, earthquakes, the 1959 Hebgen Lake, Montana, earthquake, and the 1983 Borah Peak, Idaho, earthquake (Doser and Smith 1989, p. 1385), all of which are associated with surface-faulting on range bounding normal faults. Critical to the estimation of maximum moment from a particular structure is whether rupture can propagate to these depths, which would not necessarily correspond to hypocentral depth.

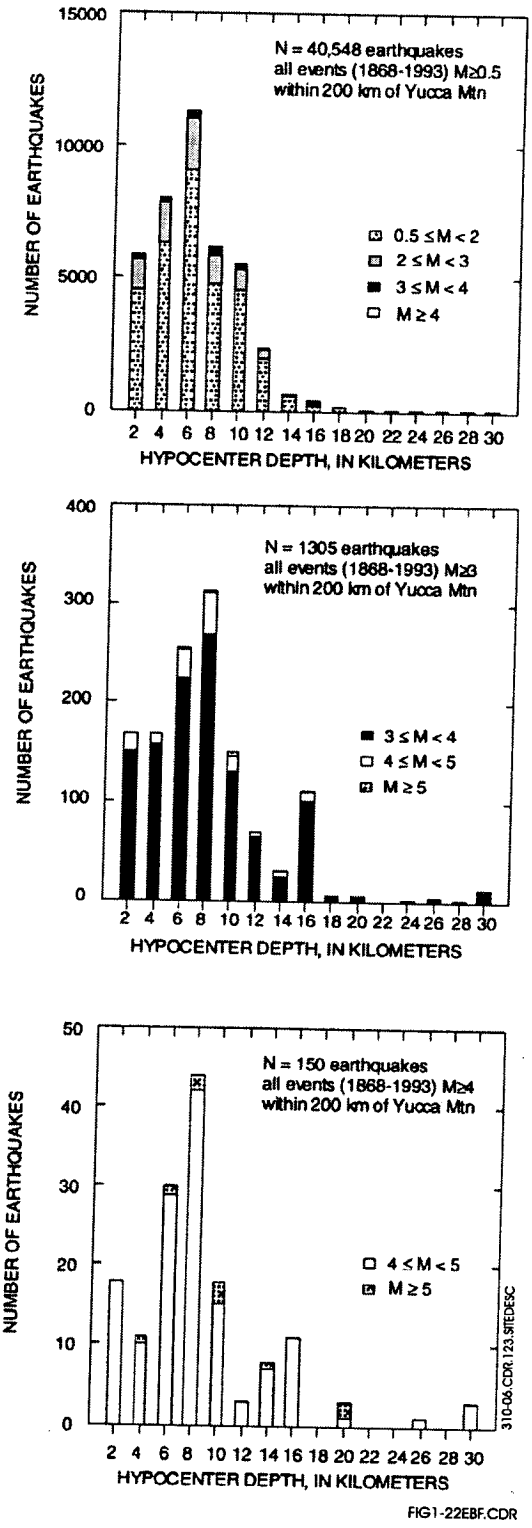

Source: CRWMS M&O (1998, Figure 3.10-6)

NOTE: Top graph: Earthquakes with M ≥ 0.5; center graph; Earthquakes M ≥ 3.0; buttom grahph; Earthquakes M ≥ 4.0.

Figure 1-22. Focal Depth Distribution of Earthquakes (1863-1993) within 200 km of Yucca Mountain

Focal mechanisms of earthquakes within approximately 100 km of Yucca Mountain exhibit strike-slip to normal oblique-slip along moderately to steeply dipping fault planes (Figure 1-23). The nodal planes are consistent with right-lateral faulting on north to north-northwest striking fault planes or normal left oblique-slip on northeast to east striking fault planes. These directions of inferred faulting are consistent with the style of Quaternary faulting in the region as well as with orientations of the principal stresses. Rogers, Harmsen, Mermonte (1987) and Bellier and Zoback (1995) discuss and analyze the modern stress field in regions of Nevada near Yucca Mountain.

Focal mechanisms of earthquakes of M_L >3.5 within the southern Great Basin from 1987 to 1997 are shown in Figure 1-23. These mechanisms plus others and hypocentral alignments indicate that right-lateral slip on northerly trending faults is today the predominant mode of stress release near the site. However, faulting on east-northeast (left-lateral) and northeast (normal) faults has been observed, as well as oblique-slip on structures of intermediate orientation with the appropriate dip angles (Figure 1-23). Geologic evidence of fault movement at Yucca Mountain reflects multiple tectonic episodes of faulting over millions of years under the influence of different stress regimes, and thus is not always consistent with these contemporary observations.

1.4.1.2 Historic Seismicity near Yucca Mountain

In the region around the potential repository site, the seismicity is distributed in a broad belt trending east-west from near the Utah border to eastern California, at a latitude of approximately 37° N. The epicenters of earthquakes within the immediate vicinity (20 km) of Yucca Mountain are shown in Figure 1-24. In this region, as elsewhere in the Great Basin, there is little correlation between the distribution of epicenters and Quaternary faults. The earthquakes generally have focal depths ranging from near-surface to 5 to 12 km. Focal mechanisms of earthquakes near Yucca Mountain are strike-slip to normal oblique-slip along moderately to steeply dipping fault planes (Figure 1-24). The nodal planes are consistent with right-lateral faulting on north to north-northwest striking planes or normal left oblique-slip on northeast to east striking faults, and thus are similar to focal mechanisms observed in the general region.

A zone of quiescence in the contemporary seismicity centered on Yucca Mountain is apparent in all studies of seismicity in the southern Great Basin (CRWMS M&O 1998, p. 3.10-17). Brune et al. (1992, p. 51) and Gomberg (1991a, pp. 16,409-16,412; 1991b, pp. 16,392, 16,396-16,398) have shown that this zone is a real feature of the seismicity and not an artifact of network design or detection capability. Other than the 1992 Little Skull Mountain event (see below), the largest earthquake to have occurred near Yucca Mountain after the installation of the Southern Great Basin Seismic Network in 1978 was an M_L 2.1 event, which occurred on November 18, 1988, and was located 12 km north-northwest of the proposed repository at a depth of approximately 11 to 12 km (Harmsen and Bufe 1992, pp. 21-23).

Paleoseismic events on a number of major faults at Yucca Mountain (see CRWMS M&O 1998, Section 3.10.6) have very long return times and strain may accumulate a long time between large surface-rupturing earthquakes on the faults. There may be little or no microseismicity on the faults during this long strain build-up. Many faults in the Great Basin with paleoseismic evidence for prehistoric surface-rupturing earthquakes have little or no associated historic seismicity.

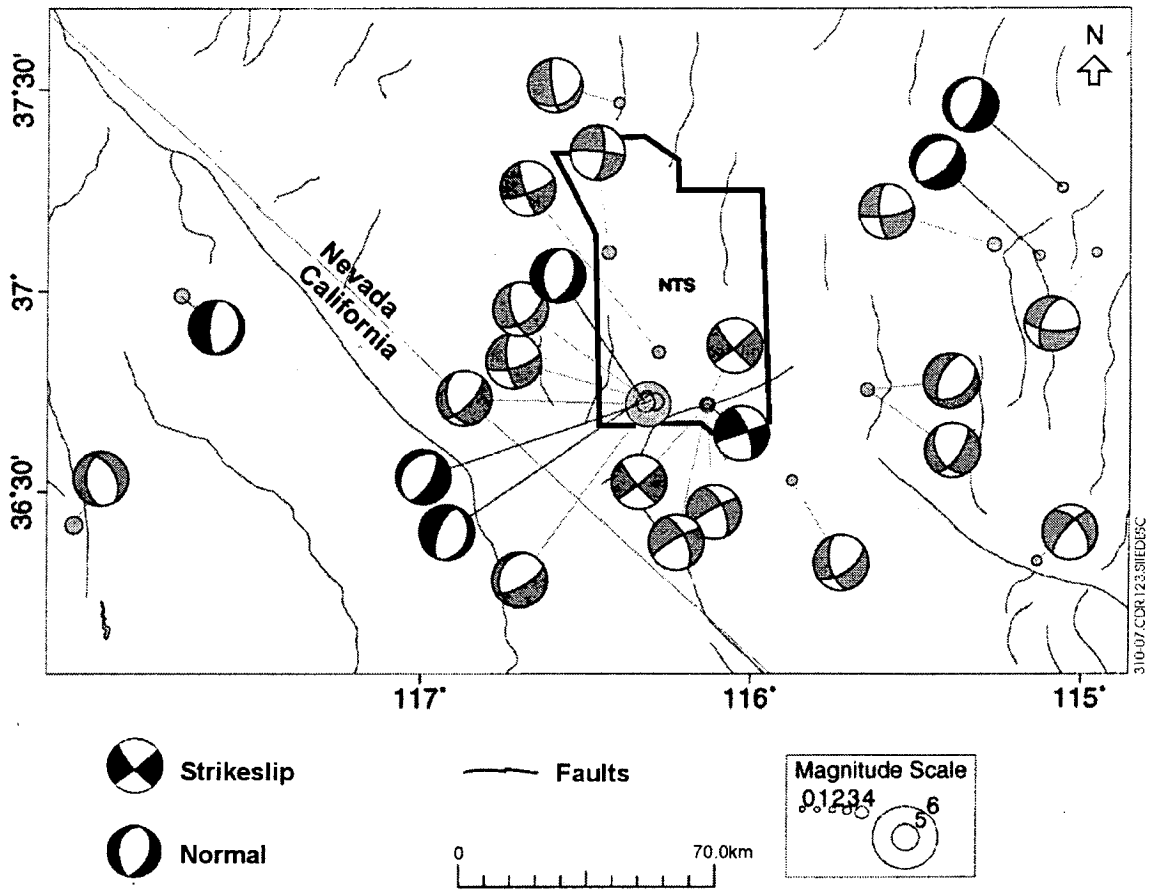

Source: CRWMS M&O (1998, Figure 3.10-7)

NOTE: Data from K. Smith, University of Nevada, Reno (written communication to I. Wong, WCFS, 1998).

Figure 1-23. Focal Mechanisms for Earthquakes of M_L > 3.5 in the Vicinity of Yucca Mountain from 1987 to 1997

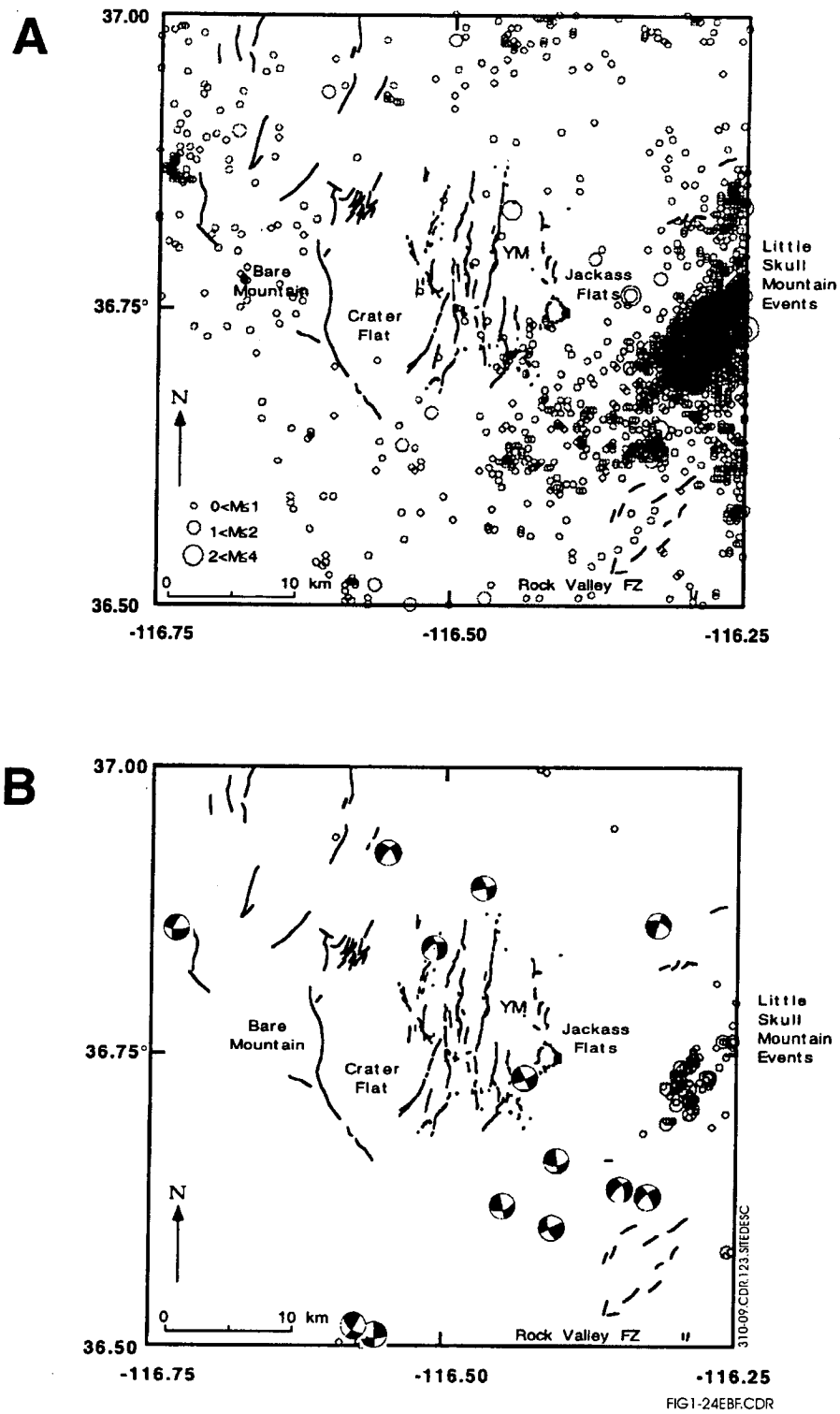

Source: CRWMS M&O (1998, Figure 3.10-9)

Figure 1-24. Epicenters and Focal Mechanisms of Earthquakes and Known and Suspected Quaternary Faults Near Yucca Mountain

The largest earthquake recorded since the regional seismic network was established in 1979 was the June 29, 1992, M_L 5.6 Little Skull Mountain earthquake (CRWMS M&O 1998, pp. 3.10-18 to 3.10-19). This event produced a horizontal ground acceleration of 0.21 g at Lathrop Wells, about 11 km from the epicenter. The earthquake caused some minor damage to the Yucca Mountain Field Operations Center in Jackass Flats, which was located nearly directly on the surface projection of the buried fault plane. The event was widely felt throughout the region. As noted previously, the earthquake appears to have been triggered by the June 27, 1992, M_w 7.3 Landers, California, event that occurred approximately 20 hours earlier. This earthquake and aftershocks are discussed in more detail in the *Yucca Mountain Site Description* (CRWMS M&O 1998, pp. 3.10-18 to 3.10-19).

Following the Little Skull Mountain earthquake, there has been an increase in earthquake activity in the southern Rock Valley fault zone (CRWMS M&O 1998, p. 3.10-19). Only two M 3+ earthquakes are included in the regional earthquake catalog prior to the Little Skull Mountain sequence. However, eight M 3+ earthquakes have occurred between May 1993 and the completion of Coe et al. (1996, Table 14.13.4).

1.4.1.3 Prehistoric Earthquakes at Yucca Mountain

Information on faults in the Yucca Mountain area suspected of having evidence of Quaternary displacements has been compiled by Piety (1996). The compilation identifies 88 faults with known or suspected Quaternary activity within a 100-km radius of the potential repository site at Yucca Mountain (Figure 1-16). Summaries of each of these faults are presented in the *Yucca Mountain Site Description* (CRWMS M&O 1998, Section 3.10.6.8).

Known and suspected Quaternary faults at and near Yucca Mountain were identified, mapped, and trenched as part of site characterization studies (Simonds et al. 1995, map; Whitney and Taylor 1996). Specific physiographic and structural evidence for Quaternary displacements was identified and mapped. Bedrock faults that lack evidence for or against Quaternary displacements also were mapped (Day et al. 1998; Simonds et al. 1995).

Reconnaissance searches for precariously balanced rocks indicate that none were found in the vicinity of historic large earthquake rupture zones (Brune and Whitney 1995, p. 39). However, numerous precarious rocks are located in Solitario Canyon to the west of the repository block. Estimates of toppling accelerations using computer models, physical models, and field tests indicate that precarious rocks would be toppled or removed by ground accelerations of a few tenths of the acceleration of gravity (g). These estimates indicate that at Yucca Mountain, ground motions have not exceeded 0.3 g for the last several tens of thousands of years. The results of these studies indicate that the immediate Yucca Mountain area has not been subjected to ground accelerations on this level for the last 40,000-80,000 years (Brune and Whitney 1995, p. 44).

Displaced or disturbed alluvial and colluvial deposits record late Quaternary faulting along nine faults in the Yucca Mountain area (Figure 1-15). These include, from west to east: the Northern and Southern Crater Flat, Windy Wash, Fatigue Wash, Solitario Canyon, Iron Ridge, Stagecoach Road, Bow Ridge, and Paintbrush Canyon faults. Paleoseisinic studies provided measurements

of fault locations, lengths, probable rupture lengths, total displacement, slip rates, and geometric relations among faults (CRWMS M&O 1998, p. 3.10-26).

Despite the uncertainties, there is good evidence for recurrent mid to late Quaternary fault displacement activity, in the form of at least two, and as many as eight, individual displacement events at most sites on the block-bounding Quaternary faults in the Yucca Mountain site area (CRWMS M&O 1998, Table 3.10-7). These events are associated with discrete fault displacements interpreted to be related to either individual paleoearthquakes or to surface rupture resulting from a single earthquake with distributive rupture on several adjacent faults (see CRWMS M&O 1998, Sections 3.10.6.1, 3.10.6.4). Paleoseismic interpretations suggest that many of the events are due to fracturing and fissuring with no detectable offset, and that such events are nearly as common as displacement events. These interpretations have led to inferences that the fracturing events, if tectonic in origin, are either the record of relatively frequent, small to moderate magnitude earthquakes that do not produce measurable rupture at the surface, or they are a record of distributed faulting and fracturing produced by rarer, larger-magnitude, surface-rupturing earthquakes on any one of several closely-spaced nearby faults (CRWMS M&O 1998, p. 3.10-26).

1.4.2 Relevant Earthquake Sources

Pezzopane (1996) carried out a preliminary evaluation of faults in the Yucca Mountain region to determine their relevance to the seismic hazard for a potential repository. He assessed whether known and suspected Quaternary faults within the region are subject to displacement and whether maximum magnitude earthquakes on these faults could produce peak ground acceleration at the potential repository site that equals or exceeds 10 percent of gravity (0.1 g). This level of ground motion was identified by McConnell et al. (1992, p. 11) as a criterion to determine faults that "may be important in the consideration of vibratory ground motion for design." Results of Pezzopane (1996) were considered in the probabilistic seismic hazard assessment discussed in Section 1.4.3.

Ninety-four individual faults and six fault combinations (assumed compound rupture on two or more faults) were identified for consideration as potential independent earthquake sources within the region (within 100 km of the Yucca Mountain site; CRWMS M&O 1998, Table 3.10-11). This evaluation was based on compilations of regional and local faults by Piety (1996) and Simonds et al (1995, map). The evidence for Quaternary displacement together with estimates of maximum fault length were tabulated for each fault. Empirical relations were used with maximum fault lengths to calculate maximum magnitude earthquakes (see CRWMS M&O 1998, Table 3.10-11). Ground motions were calculated using the maximum magnitudes and minimum fault-to-site distances with several attenuation relations to distinguish those faults capable of generating peak acceleration $\geq$ 0.1 g on rock sites at the surface at Yucca Mountain. The evaluation did not consider time-dependent data such as fault slip rates or earthquake recurrence rates. It thus provides an evaluation of the potential level of peak acceleration an estimated maximum earthquake on each fault would produce at the site. The evaluations resulted in the identification of 67 faults or fault combinations that are classified as either relevant or potentially relevant earthquake sources. Relevant earthquake sources are defined as those documented with Quaternary displacement for which the maximum magnitude earthquake can produce a peak horizontal acceleration (84th percentile) of 0.1 g or greater at the site. Potentially relevant

earthquake sources are similarly defined, except that Quaternary displacement is suspected, but not documented.

1.4.3 Probabilistic Seismic Hazard Assessment

Probabilistic seismic hazard analyses were conducted to assess the hazards at the Yucca Mountain site due to vibratory ground motion and fault displacement (USGS 1998). The objectives of the analyses are to provide quantitative hazard results to support an assessment of the potential repository's long-term performance with respect to waste containment and isolation and to form the basis for developing seismic design criteria for the License Application. The hazard results are in the form of annual exceedance probabilities for which various levels of fault displacement at selected locations in the controlled area and vibratory ground motion at a hypothetical rock outcrop at the ground surface are expected to be exceeded.

The probabilistic seismic hazard analyses consisted of three primary activities:

- Identification, evaluation, and characterization of seismic sources that would contribute to the fault displacement and vibratory ground motion hazard at Yucca Mountain.

- Evaluation and characterization of vibratory ground motion attenuation, including earthquake source, wave propagation path, and rock site effects.

- Integration of seismic source and ground motion evaluations to provide fault displacement and vibratory ground motion hazard determinations.

Both the preclosure and postclosure performance periods of the repository were addressed in the study.

By necessity, evaluations of seismic source characteristics, earthquake ground motions, and fault displacement involve interpretations of data. These interpretations have associated uncertainties related to the ability of data to fully resolve various hypotheses and models. In the probabilistic seismic hazard analyses, the input includes both estimates of the parametric variability, and uncertainty in the interpretations. To evaluate scientific uncertainty, seismic source characterizations have been made by six teams of three experts each, who together form a "composite expert" in the seismicity, tectonics, and geology of the Yucca Mountain site and region. The ground motion assessments have been made by seven individual experts.

The probabilistic seismic hazard analyses methodology for vibratory ground motions has become standard practice in evaluating seismic hazards. The use of the methodology results in calculated annual probabilities that various measures of vibratory ground motion (e.g., peak horizontal acceleration) will be exceeded at a site. The resulting "seismic hazard" curve represents the integration over all earthquake sources and magnitudes of the probability of future earthquake occurrence and, given an occurrence, its effect at a site of interest. The probabilistic methodology for evaluating fault displacement hazard is very similar to that for vibratory ground motions.

The calculation of probabilistic ground motion hazard requires three basic inputs:

- Identification of relevant seismic sources and characterization of their source geometry, probability of activity, and relation to other sources.

- Rate of earthquake occurrence and magnitude distribution for each seismic source and recurrence model.

- Attenuation relationships that provide for the estimation of a specified ground motion parameter as a function of magnitude, source-to-site distance, local site conditions, and in some cases, seismic source characteristics

For evaluating fault displacement hazard, the ground motion attenuation relationships are replaced by relationships that describe the distribution, sense, and amounts of displacement. Principal and secondary fault displacements are addressed.

An important aspect of the probabilistic seismic hazard calculations is the treatment of uncertainty. The logic tree methodology for seismic hazard analysis involves setting out a logical sequence of assessments that must be made in order to perform the analysis and addressing the uncertainties for each step in the assessment. Thus, it provides a convenient approach for breaking a large, complex assessment into a sequence of smaller, simpler components.

Vibratory ground motion hazard was computed at a defined reference rock outcrop having the properties of rock at a depth of 300 m below the ground surface at Yucca Mountain—the waste emplacement depth. Ground motion was computed at this reference location as a control motion for later determination of seismic design bases motions for surface and potential waste-emplacement level locations.

The probabilistic hazard for vibratory ground motion was calculated based on equally weighted contributions from the six seismic source expert teams and the seven ground motion experts. Results for peak ground acceleration (PGA), peak ground velocity (PGV), and accelerations at frequencies important for design are summarized in Table 1-3. This table shows the mean ground motions that are likely to be exceeded in 1,000-year (10^{-3}) and 10,000 year (10^{-4}) recurrence intervals (return periods).

For a 10,000-year recurrence interval, earthquakes smaller than M_w 6.5, occurring within 15 km of the site, dominate the higher frequency ground motions (5 to 10 Hz and higher). Dominant events for low-frequency ground motions, such as at 1 to 2 Hz, display a bimodal distribution, including large nearby events and M_w 7 and larger earthquakes beyond distances of 50 km. The latter contribution is due mainly to the relatively higher activity rates for the Furnace Creek and Death Valley faults (CRWMS M&O 1998, p. 3.10-78).

The probabilistic fault displacement hazard was calculated at nine demonstration sites within the controlled area. The integrated results provide a representation of fault displacement hazard and its uncertainty at the nine sites, based on the interpretations and parameters developed by the six seismic source expert teams. Separate results are obtained for each site in the form of summary

hazard curves. Table 1-5 summarizes the mean displacement hazard results for the two design basis annual exceedance probabilities, 10^{-4} and 10^{-5}, at the nine demonstration sites.

With the exception of the block-bounding Bow Ridge and Solitario Canyon faults (Sites 1 and 2, respectively), the mean displacements are 0.1 cm or less at 10^{-5} annual exceedance probability. At 10^{-5} probability, the mean displacements are 7.8 and 32 cm, respectively, for these two faults. Thus, sites not located on a block-bounding fault, such as sites on the intrablock faults, other small faults, shear fractures, and intact rock, are estimated to have displacements significantly less than 0.1 cm for periods up to 100,000 years (CRWMS M&O 1998, p. 3.10-81).

Table 1-3. Mean Ground Motion Hazard at 10^{-3} and 10^{-4} Annual Exceedance

Frequency	Horizontal		Vertical	
(Hz)	10^{-3}	10^{-4}	10^{-3}	10^{-4}
PGA	0.169 g	0.534 g	0.112 g	0.391 g
0.3	0.051 g	0.168 g	0.029 g	0.105 g
1.0	0.162 g	0.471 g	0.073 g	0.222 g
PGV	15.3 cm/sec	47.6 cm/sec	7.4 cm/sec	23.4 cm/sec

Source: CRWMS M&O (1998, Table 3.10-18)

Table 1-4. Mean Displacement Hazard at Nine Demonstration Sites

Site	Location	Mean Displacement (cm) Annual Exceedance Probability	
		10^{-4}	10^{-5}
1	Bow Ridge fault	<0.1	7.8
2	Solitario Canyon fault	<0.1	32
3	Drill Hole Wash fault	<0.1	<0.1
4	Ghost Dance fault	<0.1	<0.1
5	Sundance fault	<0.1	<0.1
6	Unnamed fault west of Dune Wash	<0.1	<0.1
7	100 m east of Solitario Canyon fault		
7a	2-m small fault	<0.1	<0.1
7b	10-cm shear	<0.1	<0.1
7c	fracture	<0.1	<0.1
7d	intact rock	<0.1	<0.1
8	Between Solitario Canyon and Ghost Dance faults		
8a	2-m small fault	0.1	0.1
8b	10-cm shear	0.1	0.1
8c	fracture	0.1	0.1
8d	intact rock	0.1	0.1
9	Midway Valley	<0.1	0.1

Source: CRWMS M&O (1998, Table 3.10-19)

2. HYDROLOGY

In the early planning for a national high-level radioactive waste repository, the Nevada Test Site was given high priority for a number of hydrologic reasons (DOE 1986, p. 2-12) as follows:

> "Southern Nevada is characterized by closed hydrologic basins. This means that groundwater does not discharge into rivers that flow to major bodies of surface water. It also means that water discharge points can be clearly identified.
>
> The water table is at great depth (as much as 500 m [1,640 ft] below the surface). This provides the opportunity to build a repository in the unsaturated zone where the rock containing a repository would not generally release water to drill holes or tunnels. This lack of water would minimize the corrosion of the waste canisters, the dissolution of the waste, and the transport of radionuclides from the repository.
>
> Long flow paths are present between potential repository locations and groundwater discharge points. Radionuclides would have to travel great distances before they could affect man and his surface environment.
>
> Some of the geologic materials occurring on the Nevada Test Site are highly sorptive. Radionuclides could be chemically or physically adsorbed by rock, making it extremely difficult for them to move in solution.
>
> The Nevada Test Site is located in an arid region, with an annual rainfall of less than about 150 mm (6 in). With the very low precipitation, the amount of moving groundwater is also low, especially in the unsaturated zone."

The remote location and low population, arid climate, and thick unsaturated zone make the Yucca Mountain site attractive for underground disposal of radioactive waste.

As the Yucca Mountain site investigation has evolved, hydrologic considerations continue to play a major role in planning and design of the proposed repository. Site Characterization Progress Report, Number 15 (DOE 1997, p. ES-5), identified the following attributes as most important for predicting performance of engineered and natural barriers:

- Rate of water seepage into the repository
- Waste package lifetime
- Rate of release of radionuclides from breached waste packages
- Radionuclide transport through engineered and natural barriers, including dilution in the saturated zone below the repository

It should be noted that all foregoing attributes are directly related to water movement through the unsaturated and saturated zones.

2.1 SURFACE WATER HYDROLOGY

D'Agnese et al. (1997, Figure 1, p. 59) have defined a Death Valley Regional Groundwater Flow System for the purpose of developing a regional three-dimensional conceptual and numerical groundwater flow model. The Death Valley Regional Groundwater Flow System includes the entire surface drainage basin tributary to Death Valley (Figure 2-1), plus several closed drainage basins, which are interconnected via the groundwater flow system (see D'Agnese et al. 1997, Figure 9).

The Yucca Mountain area drains mainly eastward toward Fortymile Wash, a tributary of the Amargosa River, although the western flank of Yucca Mountain drains westward toward Solitario Canyon Wash which joins the Amargosa River via Crater Flat. The main tributaries to Fortymile Wash are Yucca Wash to the north of the proposed repository, Drill Hole Wash, which drains most of the proposed repository area, and Busted Butte Wash (Dune Wash) to the south of the proposed repository (Figure 2-2).

The Yucca Mountain region is characterized by an arid to semi-arid climate, high evapotranspiration (less than 0.1 to more than 1.5 mm/day, Flint, A.L. et al. 1996, p. 77), low annual precipitation (average 165 mm/yr for the repository area, Hevesi and Flint 1998, p. 54), and infrequent storms. Stream flow results from regional storms, mostly during the winter, and from localized thunderstorms that occur mostly during the summer.

As a result of the dry climate, there are no perennial streams in the Yucca Mountain area, and even the larger streams are ephemeral; that is, they flow only in immediate response to precipitation and are dry most of the time. Throughout the Death Valley Basin, perennial flow is only observed downgradient of spring discharges and around the margins of playas and salt pans where the land surface and water table converge.

Permanent lakes in the vicinity are Crystal Reservoir, Lower Crystal Marsh, Horseshoe Reservoir, and Peterson Reservoir. These lakes are artificial impoundments that store the discharge of springs in Ash Meadows. Crystal Reservoir is the largest with a capacity of 1,836,654 m^3 (1,489 acre-feet) (Giampaoli 1986, encl. on p. 4). The major ephemeral stream in the Death Valley Basin is the Amargosa River, which originates in Oasis Valley (Figure 2-1), takes a course southeasterly 130 km, turns southwestward and then northwestward before terminating in Death Valley (Figure 2-1). The river carries floodwater occasionally following intense storms, but generally is dry except for a few short reaches that receive spring discharges, which provides low flow during the winter when evapotranspiration is at a minimum (Walker and Eakin 1963, p. 6).

As the tributary streams leave steep mountainous terrain and enter relatively flat valleys, they occupy well-defined incised floodplains, many of which contain meandering low-flow ephemeral streambeds. During major and infrequent floods, these floodplains may be inundated.

Except for the potential for flooding, surface-water hydrology has little adverse impact on siting a repository at Yucca Mountain, because of the intermittent nature of surface-water runoff and the lack of through-flowing drainages in the region. However, washes provide channels for concentrating runoff that may be significant sources of groundwater recharge (Savard 1998, pp. 2, 9).

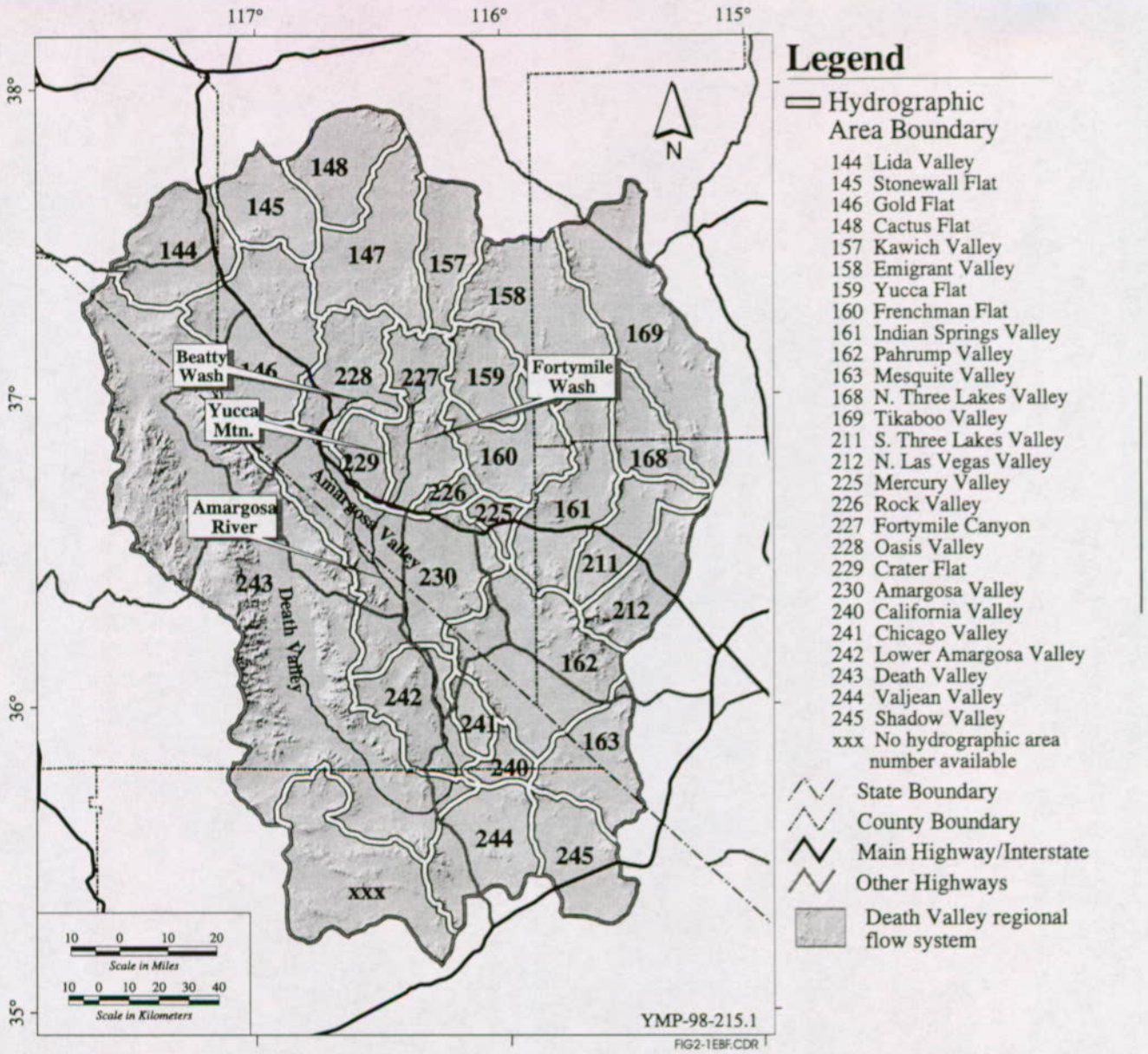

Source: CRWMS M&O (1998, Figure 5.2-10)

Figure 2-1. Death Valley Regional Groundwater Flow System Showing Hydrographic Areas (after D'Agnese et al. 1997, Figure 9)

As the major interest in streamflow in the region focuses on flood hazard, long-term stream records are mainly of crest-stage stations. As reported by Waddell et al. (1984, p. 7), the U.S. Geological Survey (USGS) has collected monthly crest-stage data in the Yucca Mountain region since the early 1960s. Flood records for 12 crest-stage sites were used by Waddell et al. (1984, p. 7) to estimate flood flow characteristics in the region. The largest flows recorded followed a storm in February 1969, when the upper Amargosa River near Beatty, Nevada, carried a maximum flow of 450 m^3/s (0.37 $m^3/s/km^2$). Other data reported by Waddell et al. (1984, Table 1, p. 7) indicate that peak flows over a 20-year period ranged from 1 $m^3/s/km^2$ for basins

larger than 100 km^2 to 3 $m^3/s/km^2$ for small basins less than 5 km^2 in area. Such higher peak flows in smaller basins are accentuated in arid zones where flash floods are common events.

As many as 41 continuous streamflow gauges and peak-flow gauges were operated in the Yucca Mountain area; however, at the end of the 1995 water year (September 30, 1995), all but three continuous gauges and most of the peak-flow gauges were discontinued (DOE 1997, p. 3-14). As of September 30, 1997, the only continuous streamflow gauges operating in the vicinity of Yucca Mountain were on Fortymile Wash; at the Narrows, near well UE-25#J13, and near Amargosa Valley, respectively (Bonner et al. 1998, pp. 105-107).

2.1.1 Flood Potential

In general, the potential for flooding must be considered in the siting of a high-level radioactive waste repository because of the risk of (1) flood damage to the repository and support facilities and (2) transport of radioactive materials away from the facility in flood waters. Initial work on prediction of flood potential at Yucca Mountain was reported in Squires and Young (1984). This study of flood hazards for a nine-mile reach of Fortymile Wash and three main southwestern tributaries in or near the Yucca Mountain site (Busted Butte, Drill Hole, and Yucca Washes) was based on records for 12 peak-flow gauging stations adjacent to the Nevada Test Site. Squires and Young (1984, Tables 2, 3, and 5) calculated discharge, area, width, mean velocity, and maximum depth of flood flows for 100-year and 500-year exceedence recurrence frequencies and maximum flood peak for a series of cross sections on Fortymile Wash and its three major tributaries within the Yucca Mountain area. Estimated peak discharges were as follows (Squires and Young 1984, p. 31).

		Peak Flood Discharge (cubic feet per second)		
Wash	Drainage Area (square miles)	100-year	500-year	Regional Maximum
Fortymile	312	12,000	58,000	540,000
Busted Butte	6.6	1,400	6,500	44,000
Drill Hole	15.4	2,300	10,000	86,000
Yucca	16.6	2,400	11,000	92,000

NOTE: 1 square mile = 2.59 square kilometers (km^2)
1 cubic foot per second = 0.02832 cubic meters per second (m^3/sec)
Busted Butte Wash is now called Dune Wash (CRWMS M&O 1998, Figure 5.1-4)

Source: CRWMS M&O (1998, Figures 5.1-9 and 5.1-13)

Figure 2-2. Flood map after Squires and Young, 1984, Plate 1; and Blanton 1992, Figures 2, 11, 16, 21, and 26

INTENTIONALLY LEFT BLANK

A recent USGS methodology (Thomas, Hjalmarson, and Waltemeyer, 1997), if applicable to the Yucca Mountain area, could result in substantial increases in the 100-year exceedence recurrence frequency peak flood discharges shown in the preceding table. However, the impact of such large peak discharges in terms of areas inundated would depend upon detailed, site specific analysis. As the new USGS methodology does not address the 500-year exceedence peak discharges or the regional maximum peak discharges, the figures shown on the preceding table for those events would remain the same, thus the areas inundated by these larger floods (Figure 2-2) would contain the revised 100-year exceedence flood-inundation areas.

Along the 15 km study area of Fortymile Wash, the flood flows would remain within the incised channel. In the Busted Butte (Dune) and Drill Hole Wash drainages, the 500-year flood would exceed stream-channel capacities at several places, and the regional maximum flood would inundate sizable areas in the central parts of the watersheds. At Yucca Wash, flood flows of all three magnitudes would remain within the stream channel. The extent of potential flooding as delineated by Squires and Young (1984, Plate 1) is shown in Figure 2-2. The potential flooding represents little hazard to the proposed underground repository, the portals of which are at higher elevation than the flood-prone areas, but flooding could represent a hazard to surface facilities, which should be designed to accommodate the flood potential.

Bullard (1992, p. 3, Figures 17-23) developed probable maximum flood hydrographs following U.S. Bureau of Reclamation procedures, which did not take into account debris bulking, for several specific sites at Yucca Mountain in connection with planning for construction of the ESF. Only local precipitation events were used to compute the probable maximum flood for the basins of interest, which ranged in drainage area from 0.052 to 11.53 km (Bullard 1992, Figures 10-16). The computed probable maximum flood peak discharges ranged from 360 to 33,500 cfs (10.2 to 949 m^3/s) and volumes ranged from 14 to 2,800 acre-feet (17,269 to 3,454,000 m^3) (Bullard 1992, Figures 17-23).

Blanton (1992, p. 7) performed a subsequent flood inundation study for Bullard's (1992, Figure 2) sites following a U.S. Bureau of Reclamation recommended approach, that took account of bulking due to entrainment of air, debris, and sediment in the stream flow. As shown on Figure 2-2, Blanton's (1992, Figures 2, 11, 16, and 21) probable maximum floods at the sites investigated were generally more extensive than the regional maximum flood zone as mapped by Squires and Young (1984, Plate 1). Although the potential flood hazard to the potential underground repository would be minimal, the surface facilities should be designed to accommodate the probable maximum floods.

2.1.2 Surface Water Quality

Streams in the immediate vicinity of Yucca Mountain are all ephemeral; that is, flow occurs rarely and only in immediate response to storms. The flow consists largely of surface runoff with little contribution from groundwater. Because of the sparse and irregular occurrence of stream flows, little data are available on the quality of stream waters.

The *Yucca Mountain Site Description* (CRWMS M&O 1998, Tables 6.2-5a and 6.2-5b) presents the available data from 19 samples from 15 sampling locations in the vicinity of Yucca Mountain collected from 1984 to 1995. These data, together with more comprehensive data from 3 Springs Basin and East Stewart Basin—sites considered representative of potential recharge areas in

Central Nevada, are interpreted in terms of the chemistry of the stream waters and evaluation of the chemical character of groundwaters (CRWMS M&O 1998, Section 6.2.4). The salient points of the interpretation of the stream water chemistry are as follows (CRWMS M&O 1998, p. 6.2-13):

- Sulfate and chloride show similar variations in concentration, suggesting that both are conservative in these dilute waters and are mainly determined by evaporation and dissolution of dry fallout salts.

- Sodium and calcium concentrations suggest these constituents are increased by dissolution of carbonate minerals and weathering reactions of soil minerals.

- Dissolution of carbonate minerals leads to large gains in bicarbonate concentration versus that of precipitation.

- Silica increases by two orders of magnitude versus precipitation, due to fast dissolution of unstable amorphous silica minerals in the soil.

The data include analyses of samples from 15 sites of common inorganic parameters (temperature, specific conductance, pH, calcium, magnesium, sodium, potassium, chloride, sulfate, fluoride, bicarbonate, and silica), trace metals (aluminum, iron, lead, manganese, bromide, iodide, and strontium), dissolved solids, tritium, and a few analyses of the stable isotopes, deuterium and Oxygen-18.

The samples ranged in total dissolved solids from 45 to 122 mg/L with the dissolved mineral matter consisting largely of sodium, calcium, and bicarbonate. Silica, which is not considered as dissolved, ranged from about 5 to 36 mg/L.

The stream samples, which have similar ionic chemistries (CRWMS M&O 1998, Figure 6.2-8), bear some resemblance to groundwaters of the saturated zone, discussed in Section 2.2.2.6, in that bicarbonate is the principal anion, and the groundwaters and stream samples are both of low to moderate mineral content, suggesting limited rock-water interaction. However, significant differences are apparent. In general, the groundwaters have higher mineral content than the stream samples and sodium is the predominant cation in the groundwaters, whereas calcium and sodium occur in about equal concentration in the stream samples.

In the stream samples, sodium ranged from 2.4 to 16 mg/L, calcium from 6.7 to 28 mg/L, and magnesium and potassium were less than 11 mg/L. Among the anion constituents, bicarbonate predominated, ranging from 32 to 109 mg/L; chloride ranged from 1.3 to 12 mg/L; and sulfate from 4.1 to 24 mg/L. The silica content ranged from 4.5 to 36 mg/L.

In summary, the distribution of constituents suggests that precipitation incorporates some soil moisture and dissolved mineral content in transit to the streams, as indicated by the moderate bicarbonate and silica concentrations; however, there is little evidence that matrix pore water contributes significantly to the stream waters as indicated by low mineral content of the stream water compared to that of pore water (Section 2.2.1.1.1).

2.2 GROUNDWATER HYDROLOGY

The regional groundwater flow system that includes Yucca Mountain is part of the Alkali Flat-Furnace Creek Groundwater Basin of the Death Valley Regional Groundwater Flow System (D'Agnese et al. 1997, Figure 30). This basin is recharged mainly by water from the high mesa areas north of Yucca Mountain, but possibly by components of interbasin flow, and discharges in the Amargosa Desert, mainly at Alkali Flat, and in Death Valley (D'Agnese et al. 1997, Table 2 and p. 68-69). Because the unsaturated zone is very thick, as much as 700 m, the term "groundwater" is applied to water moving in the unsaturated zone, as well as to water moving through the saturated zone beneath the water table (Luckey et al. 1996, p. 2).

Stratigraphic units important in discussion of groundwater at Yucca Mountain include Quaternary alluvium and colluvium, pyroclastic rocks of Miocene age, and sedimentary rocks of Paleozoic age. See Section 1.2 for a discussion of regional and site stratigraphy and Figure 2-3 for a comparison of stratigraphic subdivisions. The Miocene volcanic rocks are subdivided into (from youngest to oldest) the Timber Mountain Group, the Paintbrush Group, the Calico Hills Formation, the Crater Flat Group, the Lithic Ridge Tuff, and older tuffs, flows, and lavas beneath the Lithic Ridge Tuff. As shown in Luckey et al. (1996, Table 1), the hydrogeologic units in the Paleozoic rocks beneath the volcanic sequence consist of: (1) an upper clastic confining unit, the Eleana Formation of late Paleozoic age, which may be present beneath northern Yucca Mountain; (2) a highly permeable carbonate aquifer of early Paleozoic age, which underlies the entire Yucca Mountain area; and (3) a lower clastic confining unit of early Paleozoic and Precambrian age which probably underlies the carbonate aquifer throughout the area. An upper carbonate aquifer shown on Figure 2-3, while regionally significant, is not known to occur beneath Yucca Mountain. The pyroclastic volcanic rocks have been subdivided, as shown in Figure 2-3, into hydrogeologic units mainly on the basis of degree of welding of tuffaceous deposits.

As described by Luckey et al. (1996, p. 17), the Tertiary volcanic section at Yucca Mountain consists of a series of ash-flow and bedded ash-fall tuffs that contain minor amounts of lava and flow breccia. Individual ash-flow tuffs may be as much as several hundred meters thick, whereas bedded tuffs generally are less than a few tens of meters thick. Ash-flow tuffs range from nonwelded to densely welded, and the degree of welding varies both areally and vertically in a single flow unit. Nonwelded ash-flow tuffs, when unaltered, have moderate to small matrix permeability, but large porosity. Permeability is greatly decreased by secondary alteration, and fractures are infrequent and often closed in the low-strength nonwelded tuffs. Consequently, these rocks generally constitute laterally extensive saturated-zone confining units in the Yucca Mountain area. The properties of partly welded tuffs vary between those of fractured, welded tuffs and those of altered, nonwelded tuffs. The densely welded tuffs generally have minimal primary porosity and water-storage capacity, but they can be highly fractured. Where interconnected, fractures can easily transmit water and highly fractured units function as aquifers. In general, the bedded tuffs have large primary porosity and can store large amounts of water. Their matrix permeability is moderate to small, depending on the degree of alteration. The bedded tuffs generally function as confining units, at least when compared to less porous but densely fractured ash-flow tuffs. Lavas, flow breccias, and other minor rock types are neither

SYSTEM and Series	Stratigraphic Unit	Hydrogeologic Units		Comments
		Unsaturated	Saturated	
QUATERNARY and TERTIARY	alluvium, colluvium, eolian deposits, spring deposits, basalt lavas, lacustrine deposits, playa deposits	QAL Alluvium	QTa Valley-fill Aquifer QTc Valley-fill Confining Unit	QAL restricted to stream channels on Yucca Mountain QTa occurs mainly in Amargosa Desert; major water-supply source
TERTIARY Miocene	TIMBER MOUNTAIN GROUP Rainier Mesa Tuff	--	--	Minor erosional remnants at Yucca Mountain
	PAINTBRUSH GROUP Tiva Canyon Tuff	TCw Tiva Canyon Welded Unit	--	Mainly densely welded; caprock on Yucca Mountain. Not known in SZ at or near Yucca Mountain
	(bedded Tuff) Yucca Mountain Tuff Pah Canyon Tuff	PTn Paintbrush Nonwelded Unit	--	PTn includes bedded and non welded tuffs between basal part of Tiva Canyon Tuff unit and upper part of Topopah Spring Tuff
	Topopah Spring Tuff (Vitrophyre and non welded tuffs at base)	TSw Topopah Spring Welded Unit	uva Upper Volcanic Aquifer	About 300 m of densely welded tuff in UZ. Host rock for repository. In SZ where downfaulted to east, south, and west of site
	Calico Hills Formation	CHn Calico Hills Nonwelded Unit	uvc Upper volcanic Confining Unit	Mainly nonwelded tuff, with thin rhyolite lavas in northern site area. Varies from vitric in southwest site area to zeolitic where near or below water table
	CRATER FLAT GROUP Prow Pass Tuff Bullfrog Tuff Tram Tuff	CFu Crater Flat Undifferentiated Unit	mva Middle Volcanic Aquifer	Small occurrence in UZ. Widespread in SZ. Variably welded ashflow tuffs and rhyolite lavas. Commonly zeolitized. Most permeable zones are fracture-controlled
	Unnamed flow breccia Lithic Ridge Tuff	--	mvc Middle Volcanic Confining Unit	Nonwelded tuff, pervasively zeolitized
	Volcanics of Big Dome	--	lva Lower Volcanic Aquifer	Lava flows and welded tuff. Not known at Yucca Mountain

Source: Modified after CRWMS M&O (1998, Table 5.3-1), Czarnecki et al. (1997); Luckey et al. (1996); and Montazer and Wilson (1984)

Figure 2-3. Hydrogeologic and Stratigraphic Units

SYSTEM and Series	Stratigraphic Unit	Hydrogeologic Units		Comments
		Unsaturated	Saturated	
TERTIARY Miocene (continued) (Lower Tertiary?)	Older volcanics	--	lvc Lower Volcanic Confining Unit	Nonwelded tuff, pervasively zeolitized. Tuffaceous sediments in lower part
PERMIAN PENNSYL-VANIAN	Bird Spring Fm Tippipah Limestone	--	uca Upper Carbonate Aquifer	Limited distribution in SZ north and east of Yucca Mountain
MISSISSIPIAN-DEVONIAN	Eleana Formation (Chainman Shale)	--	ecu Eleana Confining Unit	Argillite (mudstone) and silt stone. Occurrence inferred beneath volcanics of northern Yucca Mountain
DEVONIAN SILURIAN ORDOVICIAN CAMBRIAN	Devils Gate Ls Nevada Fm Lone Mtn Dol Roberts Mtn. Fm Ely Springs Dol Eureka Qtzt. Pogonip Gp Nopah Fm Dunderberg Sh Bonanza King Fm Upper Carrara Fm	--	lca Lower Carbonate Aquifer	Mainly limestone and dolomite with relatively thin shales and quartzites. Major regional aquifer, >5 km thick
	Lower Carrara Fm	--	Zcu Precambrian Confining Unit	Dolomite, shale.
PROTEROZOIC (Upper Precambrian)	Proterozoic rocks			Quartzite, slate, marble. Fractures commonly healed by mineralization

sz = Saturated Zone; uz = Unsaturated Zone

Source: Modified after CRWMS M&O (1998, Table 5.3-1), Czarnecki et al. (1997); Luckey et al. (1996); and Montazer and Wilson (1984)

Figure 2-3. Hydrogeologic and Stratigraphic Units (Continued)

thick nor widely distributed in the Yucca Mountain area. Their hydraulic properties are probably as variable as the properties of the ash-flow tuffs, but the relatively limited areal distribution of these minor rock types makes them generally unimportant to the hydrology of Yucca Mountain.

With increasing depth, even fractured tuffs and lavas may not easily transmit water because lithostatic loading keeps the fractures closed. In addition, where volcanic glass has been partly replaced by zeolites and clays, particularly in the originally glassy nonwelded tuffs, these secondary minerals substantially decrease permeability and, thus, saturated groundwater flow through the rock. The degree of alteration can greatly affect the water-transmitting characteristics of the volcanic sequence. Alteration, particularly in the Calico Hills Formation, increases toward the north of Yucca Mountain (Moyer and Geslin 1995, p. 10) and probably accounts for the apparent decrease in hydraulic conductivity to the north. Alteration also tends to increase with depth and is pervasive below the Calico Hills Formation.

2.2.1 Unsaturated Zone Hydrology

Since the potential repository is being designed for construction in the unsaturated zone, several hundred meters above the water table, a knowledge of the physical characteristics of the natural materials and the occurrence and movement of water within the unsaturated zone are essential to planning and design of the repository facility.

The unsaturated zone, from about 500 to 750 m thick, is made up of the deposits above the regional water table. These materials include the following hydrogeologic units, from youngest to oldest:

	Hydrogeologic Unit[1,3]	Thickness, m[2]
1.	Quaternary alluvium/colluvium. Unconsolidated stream-laid deposits beneath valleys and loose slump deposits beneath slopes. Porosity and permeability medium to high.	0-30
2.	Tiva Canyon welded tuff (TCw). Mainly welded devitrified ash flow tuff, some lithophysal, some vitric. Porosity typically uniform and low, 10-30%; matrix saturation commonly 50-80% with inverse relation to porosity; matrix saturation >50% within 100 m of land surface.	0-150
3.	Paintbrush nonwelded bedded tuffs (PTn), includes non-welded basal subzone of Tiva Canyon unit (the Yucca Mountain and Pah Canyon tuffs) and uppermost non-welded to moderately welded subzone of Topopah Spring welded tuff. Porosity generally high, 30-60%; matrix saturation, 30-60%; particle density significantly lower than in welded units, 2.0-2.4 g/cm^3.	20-100
4.	Topopah Spring welded devitrified ash flow tuff (TSw), some lithophysal, some vitric, some crystal rich. Porosity generally low, <20%, but up to 40% in vitric zones; matrix saturation generally >40%, commonly >80%; particle density uniform at 2.5-2.6 g/cm^3.	290-360
5.	Calico Hills nonwelded ash flow tuff (CHn), alternating pumiceous and lithic-rich flows; uppermost of four units is pumiceous and vitric, lower three units are zeolitic, contains bedded tuff and sandstone near base; includes Prow Pass pyroclastic flow units of Crater Flat stratigraphic unit. Porosity variable, 10-40%; matrix saturation 20-90%, commonly near 100% in zeolitic zones; particle density variable 2.0-2.6 g/cm^3, but generally lower than in welded tuffs.	100-400

Hydrogeologic Unit[1,3]	Thickness, m[2]
6. Crater Flat Unit (CFu). Consists of Bullfrog welded tuff (above), and Tram nonwelded tuff (below), CFu is below water table in much of the area, only unsaturated beneath western part of Yucca Mountain. Bullfrog tuff, low porosity, <20%, high matrix saturation, close to 100%; Tram tuff porosity 20-40%, high matrix saturation; particle density 2.4 g/cm^3 in Tram tuff; 2.6 g/cm^3 in Bullfrog welded tuff.	0-200

[1]Data for porosity, matrix saturation, and particle density after L. Flint (1998, Tables 1 and 7, Figures 3-11).
[2]Thickness after Montazer and Wilson (1984, Table 1).
[3]Major subdivisions after Montazer and Wilson (1984, p. 9-19).

These major units were defined by Montazer and Wilson (1984, p. 9-19) and have been refined and subdivided by L. Flint (1998, Table 1) into 30 detailed subunits. Flint's subdivisions were based on laboratory analysis of 4,892 rock core samples collected from 23 shallow and 7 deep boreholes, and statistical analysis of hydrologic parameters to evaluate where boundaries should be adjusted to minimize variance within layers. The parameter given the greatest weight in delineating the subunits was porosity, which is well related to the lithostratigraphy and depositional and cooling history of the volcanic deposits. Generally, the hydrogeologic units agree with the major stratigraphic units (Buesch, Spengler, et al. 1996, Table 4), although in some cases the uppermost or lowermost strata of a lithostratigraphic unit, for example the Topopah Spring tuff, are grouped with the overlying or underlying unit to avoid mixing nonwelded tuffs with welded tuffs.

In addition to porosity, factors used in defining the 30 subunits included the degree of crystallization, presence of glass, presence of lithophysae (cavities), degree of welding, bedding, presence of pumice or rock fragments, and presence of alteration products, such as zeolites and clay minerals.

The distribution of samples among major units reflects the relative thickness of the major units; 43 percent were from the TSw, which is generally the thickest unit as well as the site of the potential repository; 23 percent were from the CHn; 20 percent were from the TCw; 10 percent were from the PTn; and 3 percent were from the CFu, which is in the zone of saturation in much of the area.

The mean values of the following properties are listed by L. Flint (1998, Table 7) for nearly all of the 30 hydrogeologic subunits: bulk density, porosity, particle density, volumetric water content, matrix saturation, water potential, saturated hydraulic conductivity (geometric and power law means), and estimated saturated conductivity (based on extrapolation from limited numbers of laboratory analyses). Testing methods are described by L. Flint (1998, pp. 11-18). The mean value for porosity ranged from 0.036 for the densely welded basal vitrophyre of the TSw unit to 0.499 in the Pah Canyon bedded tuff within the PTn unit. The mean value for particle density ranged from 2.24 g/cm^3 for a pumiceous pyroclastic flow of the CHn to 2.58 g/cm^3 for a welded devitrified flow within the CHn unit.

The mean value for matrix saturation ranged from a low of 0.32 in an unaltered bedded tuff near the top of the CHn to 1.00 (complete saturation) in a bedded tuff near the base of the CHn unit and a nonwelded zone in the CFu. The geometric mean for matrix saturated hydraulic conductivity, based on core analysis, ranged from $4x10^{-11}$m/s for the middle nonlithophysal zone of the TSw, part of the proposed repository zone, to $1.6x10^{-5}$m/s for an unaltered bedded tuff zone within the CHn unit (based on a single sample).

In considering the mean values cited above, it should be kept in mind, particularly for saturated hydraulic conductivity, that these figures represent tests at core (intact rock) scale and do not take into consideration fracture flow. Moreover, the hydraulic conductivity tests are under saturated condition rather than partially saturated, which is the general field situation in the unsaturated zone.

2.2.1.1 Occurrence of Unsaturated Zone Groundwater

Water in the unsaturated zone at Yucca Mountain occurs in three distinctly different regimes: (1) in pores in the rock matrix, (2) in faults and other fractures, and (3) in isolated saturated bodies of perched waters (Figure 2-4). Perched water is defined as a saturated zone separated from the water table by unsaturated materials. Various lines of evidence suggest that the matrix pore water is much older and chemically unlike that water moving in fractures, which appear to represent rapid flow paths and to feed the perched water bodies and directly recharge the water table. The perched water bodies have all been below the proposed repository horizon, and perched water has been encountered at the base of the TSw unit or in the top of the underlying nonwelded to partially welded tuffs of the CHn unit in every dry-drilled borehole that penetrated the TSw-CHn contact (Striffler et al. 1996, p. 27).

Information on pore water contained in the volcanic rock matrix is based largely on analysis of cores taken during drilling of exploratory boreholes supplemented by information collected during construction of the ESF. The core data from boreholes are summarized by L. Flint (1998, p. 54, Table 7). Chemical and isotopic data on pore and perched waters are summarized by Striffler et al. (1996, pp. 25-27), Yang, Rattray et al. (1996, p. 12-37), and Fabryka-Martin, Turin et al. (1996, pp. 60-64).

The volcanic rocks consist of alternating layers of welded and nonwelded ash flow and ash fall (bedded) tuff deposits. Each of the ash flow units is underlain by an associated bedded tuff layer. The ash flow units vary in degree of welding (or recrystallization) with the maximum welding generally found near the center of the flow, where heat was retained the longest, and the degree of welding decreasing upward and downward toward the flow boundaries.

The welded units typically have low matrix porosities and high fracture densities, whereas the nonwelded and bedded tuffs have relatively higher matrix porosities and lower fracture densities. The fracture density is correlated with the degree of welding of the volcanic rocks.

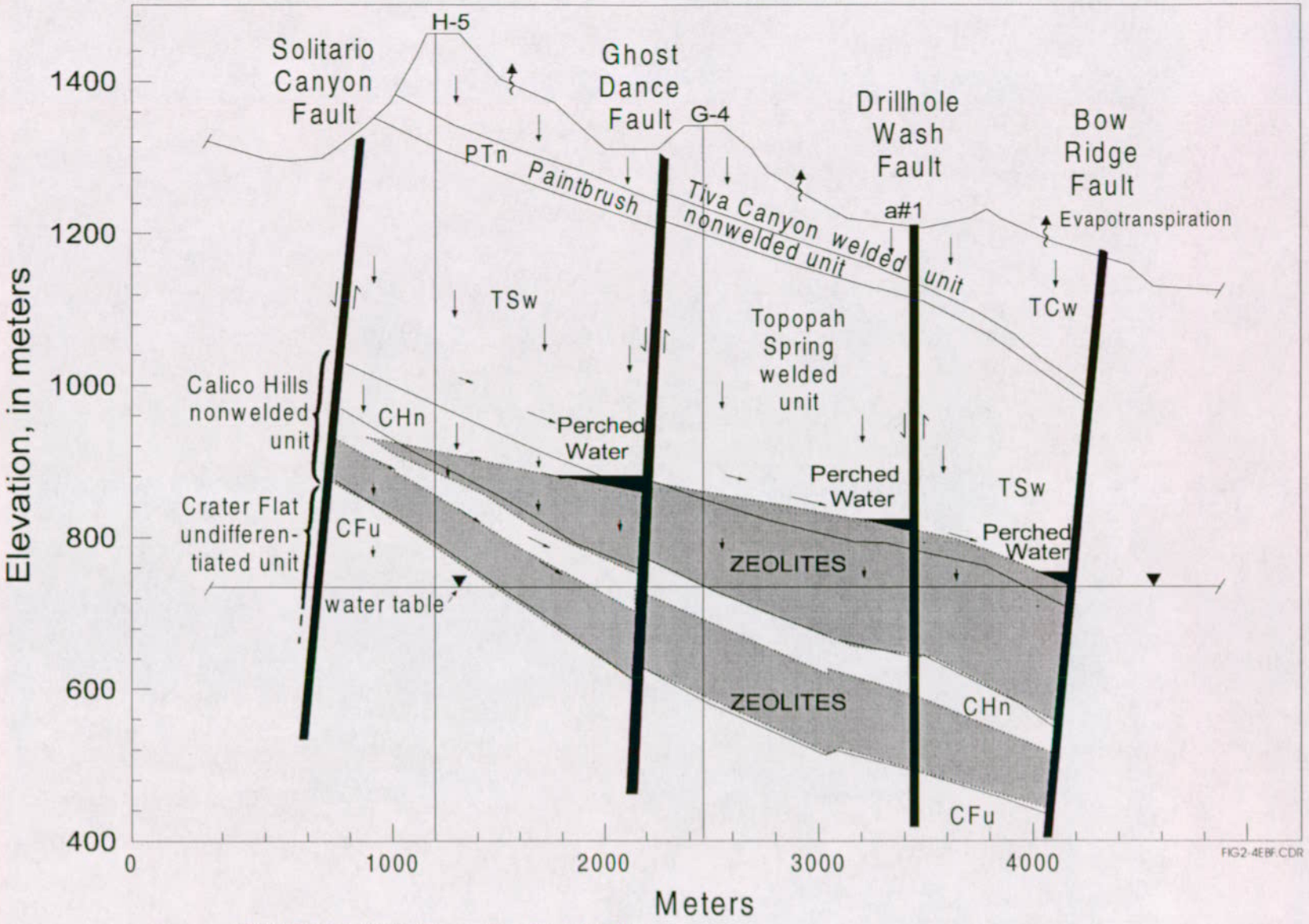

Source: CRWMS M&O (1998, Figures 5.3-175, 5.3-186b)

Figure 2-4. Schematic Conceptual Diagram of Water Flow at Yucca Mountain

Where glassy tuff has been saturated over long time periods, for example, beneath the water table, the original glassy material generally has been altered to zeolite minerals or to clay minerals. Such alteration does not affect porosity greatly, but the permeability of the rocks is greatly reduced by alteration. Alteration to zeolites or clay minerals is not a significant factor in densely welded zones where the volcanic glass was replaced by crystal mineral fragments while still hot.

Another lithologic factor affecting flow of water in the unsaturated zone is the presence of lithophysae (hollow bubble-like structures). Such cavities have the general effect of reducing the pore space through which water can flow, because water will not flow from the fine grained porous matrix into open cavities.

As noted by L. Flint (1998, p. 9), the borders of units and subunits of the volcanic sequence typically are gradational, which further complicates assignment of average properties to discrete layers for modeling purposes.

2.2.1.1.1 Pore Waters

The dissolved mineral content and isotopic character of matrix pore water indicate that the pore water is distinctly different from water of the saturated zone or perched water bodies. The latter are interpreted as being fed by fast flow through fractures rather than by water flow through the matrix porosity. Yang, Rattray et al. (1996, p. 55) observed that the unsaturated zone pore water generally had significantly higher dissolved mineral content than water of the saturated zone or perched water. They also noted frequent inversions in tritium content of pore waters, with post-1952 water interlayered with older pore water. The latter feature, Yang, Rattray et al. (1996, p. 55) interpreted as indicating that fracture flow is the dominant fluid flow mechanism in the unsaturated zone.

Chlorine-36 dating of salts leached from samples taken from the walls of the ESF were consistent with isotopic dating of water from cores in the unsaturated zone. Although some samples collected near faults apparently contained post-1952 chloride, most samples contained Chlorine-36 consistent with travel times from land surface exceeding a few thousand years, and their upper age limits ranged up to several hundred thousand years (Fabryka-Martin, Wolfsberg et al. 1996, p. 56). However, as explained in Section 2.2.1.7, more recent interpretation by Fabryka-Martin, Flint et al. (1997, p. 9-4) indicates that the groundwater everywhere in the Yucca Mountain area may have been recharged less than 10,000 years ago.

2.2.1.1.2 Fracture Flow

While various lines of evidence indicate that fractures serve as fast paths that have conducted post-1952 recharge to deep within the unsaturated zone, it is difficult to observe fracture flow directly, and reliance must be placed on indirect evidence, such as radiometric dating, to estimate the extent of fracture flow. Direct evidence of fracture flow is limited to a few televiewer images of seeps into boreholes. Fast-path fracture flow appears to be episodic, related to recharge events of short duration and having a recurrence frequency of perhaps once in 10 years (Bodvarsson and Bandurraga 1996, p. 22).

Fractures vary widely in length, orientation, connectivity, aperture width, and amounts and types of coatings, all of which may affect the flow of water. The physical parameters of fractures are characterized by outcrop mapping, borehole logging, and mapping in the ESF; however, seeps of water have not been observed in outcrop mapping or in mapping in the ESF.

Fractures at Yucca Mountain originated as a result of both initial cooling of the volcanic deposits and tectonic activity. Throckmorton and Verbeek (1995, p. 12) studied fractures at outcrops, particularly of the TCw unit, and differentiated cooling fractures from those of tectonic origin. They observed three sets of cooling fractures, two dipping nearly vertical and striking about northwest and northeast, and a third subparallel to foliation of the tuff, which form an orthogonal, three-dimensional network (see CRWMS M&O 1998, Section 3.6.3, for extensive discussions of fractures).

Throckmorton and Verbeek (1995, p. 44) also identified four sets of fractures of tectonic origin; all dip steeply and are extensional in character. Studies of fractures in the PTn unit (Rousseau et al. 1996, p. 74) indicate similar fractures to those within welded flow units; however, the overall fracture density of the PTn is low and fractures poorly connected within and between stratigraphic subunits, and most fractures in the PTn are stratabound and terminate at welding breaks or lithologic changes. Mapping in the ESF (Rousseau et al. 1996, p. 74) indicates that most of the discontinuities within the PTn are minor faults with dips less than 75° and indications of dip-slip tectonic movement. These zones generally are less than 4 cm width and have thin silica or calcite fillings.

Fracture densities in boreholes range from less than 1 to 16 per meter, and in the ESF from less than 1 to about 4 per meter (Bodvarsson and Bandurraga 1996, p. 531). The density reportedly was: (1) higher near contacts between vitric zones and non-lithophysal units in the TSw, (2) higher in non-lithophysal as compared to lithophysal zones, (3) lower within the PTn, and (4) very low in the CHn and CFu hydrogeologic units.

Fracture aperture characteristics are poorly known from direct observation, and for modeling, reliance is placed on indirect effects such as changes in air and water permeability. The available data suggest that some fracture apertures are greater than 3 mm but that the average is on the order of 0.2 mm (Bodvarsson and Bandurraga 1996, p. 532). In general, the stress due to overburden loading across high-angle fractures will be less than across low-angle fractures resulting in higher vertical than horizontal permeability.

Pneumatic pressure data (Rousseau et al. 1996, p. 104) indicated four distinct systems corresponding to the hydrogeologic units; that is, the TCw, the PTn, the TSw, and the CHn and CFu combined. Pressure signals are transmitted readily through the TCw, but are attenuated to some degree in the bedded tuffs of the PTn unit, and are little attenuated in the TSw unit.

Fracture permeabilities are controlled by aperture characteristics, which in turn are influenced by mineral coatings on the fracture walls. The fracture coatings consist of mainly tridymite, calcite, opal, and clay minerals together with lesser constituents in varying proportions, depending upon water chemistry and the history of deposition (Bodvarsson and Bandurraga 1996, p. 535). Fracture coatings are common in most units, but were lacking in cores of the Pah Canyon tuff of the PTn unit, and few coated fractures occur below the base of the TSw unit.

In general, calcite and opal fracture coatings occur in fractures having apertures greater than several millimeters. In single fractures with variable apertures, narrow intervals contain little or no mineralization, whereas wider zones are coated (Bodvarsson and Bandurraga 1996, p. 538). Dating of opal and calcite coatings on outer mineral surfaces by the uranium-series method indicated ages of 28 to >500 ka (CRWMS M&O 1998, p. 6.2-38); and of the latest calcite surfaces by the Carbon-14 method of 16 to 52 ka (the upper limit of the method) (CRWMS M&O 1998, p. 6.2-41).

The significance of fracture coatings with respect to water movement in the unsaturated zone is that they can significantly decrease travel time and increase the depth of water circulation. If a fracture face is not mineral-coated, water can be imbibed across it into the pore matrix by capillary forces once flow begins. If imbibition is restricted by mineral coating, flow down the fracture may continue without losing a significant part of the flow to the matrix.

2.2.1.1.3 Perched Water

Perched water bodies suggest that percolation rates through the unsaturated zone are locally at least as great as the hydraulic conductivity of the underlying perching layer (Striffler et al. 1996, p. 11). Typically, perched water occurs where relatively permeable nonwelded tuffs overlie partially to densely welded tuffs of lower matrix permeability, where the latter are relatively unfractured. In the fracture-flow environments of the welded tuffs, perched water occurs where a highly fractured unit overlies a relatively unfractured unit, or where fractures have been filled with precipitates (Striffler et al. 1996, p. 12). Some perched water bodies are related to faulting, where water moving down dip in the volcanic strata encounters impermeable fault fill or where a permeable layer is juxtaposed against impermeable strata.

The perched water bodies encountered to date (1997) have all been below the repository horizon (CRWMS M&O 1998, p. 5.3-162), and perched water has been encountered at the base of the TSw unit or in the top of the underlying nonwelded to partially welded tuffs of the CHn unit in every dry-drilled borehole that penetrated the TSw-CHn contact, and perched water probably exists near the base of the TSw virtually everywhere in the vicinity of the ESF (Striffler et al. 1996, p. 27). A more detailed discussion of perched water is presented in Section 2.2.1.6.

Chemical and isotopic data indicate that the perched water is distinctly different from the pore matrix water. In fact, perched water from well UZ-14 had a chloride content of 6 to 15 mg/L, while that of pore water extracted from core in the same interval had about 87 mg/L (Striffler et al. 1996, p. 26). The low chloride content of the perched water indicates little exchange between pore fluid and perched water and little rock-water interaction, suggesting the perched water results from rapid recharge through fractures.

Isotopic data are consistent with the interpretation of rapid-path recharge of the perched waters. Carbon-14 dates suggest mean residence times of about 2,200 to 6,200 years for the perched waters (Yang, Yu et al. 1997, p. 78). Tritium analyses suggest that if post-1952 recharge has reached the perched zones, it is too small in volume to be detectable (Yang, Rattray et al. 1996, p. 34).

2.2.1.2 Infiltration and Percolation

Precipitation falling on the Yucca Mountain area is partitioned into runoff across the surface to stream courses, direct evaporation from the surface, and water that infiltrates the surface soil. The water that infiltrates the soil is further partitioned into evapotranspiration, the water returned to the atmosphere through evaporation from the soil and transpiration by plants; the remaining water, that not returned to the atmosphere, is generally termed net infiltration (Flint, A.L. et al. 1996, p. 8). Percolation is defined as the downward or lateral flow of water in the unsaturated zone.

Hudson and Flint (1996, p. 2) introduced the term "shallow infiltration" for surface infiltrated water that has percolated below all unconsolidated surficial material and at least 2 m into bedrock. Water that percolates to this depth may or may not continue percolating downward through the deep unsaturated zone but is assumed to have escaped the zone of substantial evapotranspiration. Shallow infiltration is distinguished from net infiltration because some possible mechanisms exist that could prevent shallow infiltration from percolating through the unsaturated zone, including lateral flow induced at stratigraphic boundaries, barometric pumping, and large scale vapor transport. The term "recharge" is reserved for water movement from the unsaturated to the saturated zone.

Direct measurement of infiltration is not feasible at Yucca Mountain because of low precipitation and high evapotranspiration rates. Using a variety of approaches, mainly water budgeting, but including chloride mass balance, previous investigations have converged on an estimate for infiltration to the unsaturated zone of about 3 percent of the average annual precipitation (Hudson and Flint 1996, p. 3-5). Applied to an average annual precipitation of 160 mm, this suggests infiltration of about 5 mm/yr.

Shallow infiltration is spatially variable due to variability in character of subsurface material, depth to bedrock, and geomorphology, and is temporally variable due to variability in annual and seasonal precipitation, and in storm intensity, duration, and frequency (Hudson and Flint 1996, p. 6, 8).

Hudson and Flint (1996 pp. 6, 8) estimated the spatial distribution of shallow infiltration at Yucca Mountain from neutron profiles logged monthly in 69 boreholes for varying time periods between 1984 and 1995. At each borehole measured moisture profiles were made from land surface to below the unconsolidated surface material-bedrock contact. A multiple linear regression model was used to correlate annual shallow infiltration estimates to annual precipitation data, depth to bedrock, and whether the borehole was in a channel. Shallow infiltration maps were developed for a 230 km^2 study area. The calculated average infiltration for the study area was 11.6 mm/yr (Hudson and Flint 1996, p. 34). Ranges of shallow infiltration in terms of area and percentage of total are tabulated below.

Ninety-three percent of the shallow infiltration occurred in areas with less than 0.5 m of unconsolidated cover although this represents only 48 percent of the area. Very little infiltration occurs where the unconsolidated cover is thick, such as in the bottoms of channels where sediment is accumulating and holds water so that it can be returned to the atmosphere as evapotranspiration. More than half (54 percent) of the area that has more than 3 m of

unconsolidated cover accounted for less than 1 percent of the shallow infiltration at Yucca Mountain.

Shallow Infiltration Ranges at Yucca Mountain in Percentage of Area and Percentage of Total (Hudson and Flint 1996 p. 34-35)

Shallow Infiltration (mm/yr)	Percentage of Area (%)	Percentage of Total Shallow Infiltration %
0	43.7	0.0
0-<10	5.6	3.5
10-<20	26.1	37.0
20-<30	13.4	28.2
30-45	11.2	31.3

Mapped faults and associated fracture zones were delineated in a smaller 103 km^2 inner area (Hudson and Flint 1996, p. 35). Fault zones, defined as 30 m-wide zones, occupy 9.5 percent of this inner area. Of the area within these fault zones, 31.9 percent was in the >20 to 45 mm/yr shallow infiltration zone; 40 percent in the >10 to 20 mm/yr zone, and 28.1 percent in the 0 to 10 mm/yr zone. These fault zones represent potentially active pathways for conducting shallow infiltration to the proposed repository level and beyond.

Numerical models have been developed (Flint, A.L. et al. 1996, p. 91) to account for the properties and processes that govern infiltration at Yucca Mountain. These models were used to provide 100-year simulations of infiltration, which allowed for an evaluation of the temporal and spatial distribution of net infiltration throughout the area of Yucca Mountain under current climatic conditions and possible future climatic conditions (doubling precipitation increased net infiltration by a factor of four). Infiltration is temporally and spatially variable but averaged 4.5 mm/yr over the study area and 6.5 mm/yr over the potential repository area for the current climate. The most important aspect of infiltration is that temporally, it may be 0 mm/yr for several years and 10 to 20 mm/yr for one year, whereas spatially it may be 0 mm/yr for much of the area and exceed 80 mm/yr for other areas. It is not the amount of precipitation alone that determines net infiltration, but also the timing (Flint, A.L. et al. 1996, p. 91).

2.2.1.3 Water Movement

The early Montazer and Wilson (1984) conceptual model of flow of water in the unsaturated zone presumed that little vertical percolation occurred in the thick TSw unit. Evidence of post-1952 water in the form of Chlorine-36 in the ESF (Fabryka-Martin, Wolfsberg et al. 1996, p. 62) and of tritium and Carbon-14 deep in the TSw and CHn units (Yang, Rattray et al. 1996, p. 55) indicate the presence of fast pathways for rapid movement of pulses of infiltration through fractures, effectively bypassing the matrix porosity. Another aspect of this fast flow is that previous interpretations of extensive lateral flow diverted by the low permeability PTn unit may be an artifact of the numerical grid and choice of matrix and fracture properties used in modeling

(Bodvarsson and Bandurraga 1996, p. 8). The current preferred conceptual model is that while the PTn tends to attenuate the spatial and temporal variability in infiltration rate, water is conducted relatively rapidly through the PTn to the highly fractured TSw unit through faults and associated fracture systems (Bodvarsson et al. 1997, pp. I-8 to I-9).

Bodies of water perched on zeolite zones near the TSw/CHn contact, dated by the Carbon-14 method at about 2,200 to 6,200 years (Yang, Yu et al. 1997, p. 78), are much younger than could be accounted for by flow through the matrix porosity, lending further credence to the fast-flow interpretation. Although isotopic evidence indicates rapid flow paths through the unsaturated zone, it cannot be used to quantify the percolation flux, which may be quantitatively small.

The current preferred conceptual flow model (Bodvarsson and Bandurraga 1996, p. 20) suggests that a pulse type infiltration process with high infiltration occurring over short time frames and then low, steady infiltration rates over relatively long time periods is consistent with the measured saturation and moisture tension data of the unsaturated zone.

Although current interpretations do not support extensive lateral flows at the TCw/PTn contact, temperature gradient analyses (Bodvarsson and Bandurraga 1996, p. 21) indicate less vertical percolation flux in the CHn and CFu units than in the overlying TSw unit, indicating significant lateral flow above the zeolite zones near the TSw/CHn contact.

2.2.1.4 Pneumatic Pressure Effects

Pore space not occupied by water contains air and vapor-phase gases, and monitoring of transmission of barometric signals within Yucca Mountain provides important supplemental information useful in interpreting the hydrogeologic environment (Patterson et al. 1995, p. 3). For example, the permeability to air flow can be quantified from measurement of attenuation and time lag of barometric signals at different depths in boreholes, thus providing information that cannot be deduced from hydrologic measurements.

The computed phase lags and residual amplitudes of the in situ pressure data indicate that individual lithostratigraphic units can be conveniently grouped into four distinct pneumatic systems corresponding to previously defined hydrogeologic units: (1) the Tiva Canyon welded tuffs (TCw); (2) the Paintbrush Group nonwelded units that include the crystal-poor vitric base of the Tiva Canyon tuff, the Yucca Mountain and Pah Canyon tuffs (with associated bedded tuffs), and the crystal-rich top of the Topopah Spring Tuff (PTn); (3) the Topopah Spring lithophysal and nonlithophysal welded units (TSw); and (4) the pre-Topopah Spring bedded tuff, the nonwelded tuffs of the Calico Hills Formation (CHn); and the pre-Calico Hills Formation bedded tuff (CFu) (Patterson et al. 1995, p. 107).

Pneumatic pressure records for stations within the TCw unit exhibit very little attenuation or time lag of barometric signals, which indicates large bulk permeability and abundant interconnection of fractures with permeabilities ranging from hundreds to thousands of square millimeters (Patterson et al. 1995, p. 108).

Pneumatic pressure data from instrument stations located within and across various subunits of the PTn indicates that the pressure attenuation and lag of these subunits differ from one location to another, and that the variation in composite thickness is probably insufficient to account for

differences in the magnitude of the residual amplitude and phase lag of the synoptic pressure signal transmitted across the PTn. Results of one-dimensional model simulations indicate that average bulk permeability of the full thickness of the PTn ranges between 0.2 and 1 mm^2 in the vicinity of boreholes NRG-5, NRG-6, NRG-7a, SD-7, and SD-9 (Patterson et al. 1995, p. 108). These data indicate that the PTn permeability varies by a factor of five over the part of the proposed repository area monitored.

Pressure data from instrument stations located in the TSw unit exhibit negligible attenuation and lag once the pneumatic pressure signals enter those units. Pressure signals appear to be transmitted nearly instantaneously throughout the entire TSw section at most of the borehole sites, indicating that the fractures within the Topopah Spring Tuff are very permeable and highly interconnected over much of the area. The results of simulation modeling in the vicinity of boreholes NRG-5, NRG-6, and NRG-7a indicated horizontal permeabilities of the TSw unit in the range of 30 to 60 mm^2 and vertical permeabilities in the range of 70 to 100 mm^2 (Patterson et al. 1995, pp. 108, 109).

The pressure record at three stations where pressures were monitored below perched-water zones indicates that essentially all of the synoptic barometric signal was attenuated. This is consistent with the idea that a perched-water zone or highly saturated zone would have extremely low permeability to air and would effectively bar the downward propagation of the surface barometric signal (Patterson et al. 1995, p. 109).

Pressure data for several wells appear to be affected by faults that are not present at the surface or were not inferred from subsurface data. Of eight boreholes with pressure records discussed by Patterson et al. (1995, p. 109), five (NRG-5, NRG-6, SD-12, UZ-7a, and SD-7) were interpreted as having been affected by the presence of the Drill Hole Wash fault or the Ghost Dance fault both before and after the onset of ESF tunnel excavation effects. The ESF excavation effects of two other records (UZ-4 and UZ-5) were initiated when the ESF intersected a different fault connecting the tunnel pneumatically to those boreholes. These results emphasize the fact that a simple layered model that does not include detailed pneumatic characterization of faults and major fractures may fail to adequately represent the effects of many of the important pneumatic and hydraulic pathways in the vicinity of the proposed repository.

Monitoring of boreholes UZ-6 (open to both the TCw and TSw units) and UZ-6s (open only to the TSw unit) indicated a net annual exhaust of about one million cubic meters of rock gas via UZ-6s resulting from thermosyphon and wind effects in the hilly terrain near the crest of Yucca Mountain (Patterson et al. 1995, p. 89, 110). Based on chemical data, it was concluded that much of the gas exhausted at borehole UZ-6s was derived from flow from the TSw unit to the shallower TCw unit through the breach in the low permeability PTn unit created by borehole UZ-6. This air exchange was confirmed by gas tracer tests and a Modflow model. Patterson et al. (1995, p. 110) concluded from the testing at boreholes UZ-6/6s that heat generated by waste emplacement in the TSw unit would likely result in gas-phase circulation cells between the repository and the outcrop of the TSw unit that would discharge heat, moisture, and Carbon-14 to the atmosphere.

2.2.1.5 Lateral Flow and Effect of Faults

Early conceptual models of flow of moisture in the unsaturated zone (Montazer and Wilson 1984, p. 47) assumed that water percolating downward through the intensely fractured TCw unit would not infiltrate into the PTn unit due to a capillary barrier effect at the TCw/PTn contact. It was thought that transient fracture flow would end at or in the PTn unit, resulting in saturation build-up and lateral flow downdip along the TCw/PTn contact. Water would flow through fractures in the TCw along the contact until intercepted by a fault that would provide an avenue for downward flow to the water table.

The current preferred conceptual model, based on infiltration rates of about 5 mm per year, suggests little lateral flow near the TCw/PTn boundary (Bodvarsson and Bandurraga 1996, p. 21). Rather, while the PTn unit is predicted to somewhat average spatial and temporal variability in infiltration rates, it does not appear to significantly divert downward vertical moisture flow.

Lateral flow, however, is believed to occur above very low permeability zeolite zones within the CHn and CFu units (Bodvarsson and Bandurraga 1996, p. 21). Moreover, temperature gradient analysis suggests less vertical percolation flux in the CHn and CFu units than in the overlying TSw, indicating that lateral flow must occur above the zeolite zones (Bodvarsson and Bandurraga 1996, p. 21). This is consistent with the occurrence of perched water bodies near the TSw/CHn contact, which suggest very low permeability in the zeolite zones in the upper CHn unit.

The proposed repository is surrounded and crossed by numerous steeply dipping faults with varying amounts of offset (CRWMS M&O 1998, Section 3.6.2.3; Scott and Bonk 1984, map). Modeling studies have assumed the faults to be barriers to moisture movement, either capillary or permeability barriers. Limited information, based largely on pneumatic effects and the occurrence of perched water, suggest that the principal faults generally are barriers to lateral flow of water, but are highly permeable to gas or moisture flow along the fault planes (Bodvarsson and Bandurraga 1996, p. 9). The apparent lateral barrier effect may be due to low permeability fault gouge along the fault zone or to capillary barrier effects. In any event, pneumatic data suggest that above the water table most faults are permeable to gas, suggesting that they are not fully saturated with water (Bodvarsson and Bandurraga 1996, p. 21). Furthermore, the close association of nuclear bomb pulse Chlorine-36 in the ESF with mapped faults emphasizes the importance of faults as avenues for fast flow of infiltration through the PTn unit to the TSw unit and the potential repository horizon (Fabryka-Martin, Turin et al. 1996, p. 62).

2.2.1.6 Perched Water

Earlier preferred conceptual flow models of the unsaturated zone at Yucca Mountain (Montazer and Wilson 1984, p. 47) assumed that downward infiltration was controlled dominantly by matrix flow through the pores of the bedded tuff of the PTn unit. Data collected in recent years from drill holes and the ESF point to fast path flow along faults and fractures as an important and perhaps dominant flow mechanism. The existence of bodies of perched water that are younger and different in chemical and isotopic character from the matrix pore waters provide important evidence as to the flow regime.

Perched water is defined by Freeze and Cherry (1979, p. 45) as a discontinuous saturated lens with unsaturated conditions existing both above and below. The existence of perched water requires a laterally extensive zone of low permeability, sufficiently low that the average percolation flux from above exceeds the rate of transmission through the low permeability zone. In dipping strata, such as the sequence at Yucca Mountain, perched water also implies the presence downdip of a low permeability seal, such as a fault seal, which impedes downdip drainage of the perched water.

Perched water was encountered in six boreholes in the vicinity of the potential repository (USW UZ-1, UZ-14, SD-7, NRG-7A, SD-9 and SD-12; see Figure 1-5; also CRWMS M&O 1998, p. 5.3-162). The TSw-CHn contact zone is characterized by a basal vitrophyre stratum in the TSw unit above a zone of zeolitic altered tuffs in the CHn unit. Bodvarsson and Bandurraga (1996, p. 22) indicate that for a perched zone to exist, the vertical permeability of the perching units would have to be very low (less than 1 microdarcy) and fracture permeability would have to be negligible.

The chemical character of the perched water is distinctly different from matrix pore waters from the same depth interval, and the isotopic character distinguishes the perched water from the deeper groundwater of the saturated zone below. Generally, the perched waters are of sodium bicarbonate type of moderate concentration (specific conductance 224 to 518 μS/cm) similar to the saturated zone waters (Benson and Klieforth 1989, Table 1; Yang, Rattray et al. 1996, Table 7). The pore waters typically range in specific conductance from about 400 to more than 1,000 μS/cm (Yang, Rattray et al. 1996, Tables 2, 3, 4) and are notably higher in chloride content (typically 20 to 100+ mg/L) than the perched waters, which typically contained less than 10 mg/L (Yang, Rattray et al. 1996, Tables 2-6, p. 34). The low chloride content of the perched waters has been interpreted as indicating rapid fracture flow with little interchange with pore matrix water or interaction with the rocks (Yang, Rattray et al. 1996, p. 34).

The perched water has been dated by the Carbon-14 method as recharged between about 2,200 and 6,200 years, which is much younger than could be accounted for by matrix flow (Yang, Yu et al. 1997, p. 78). The stable isotope composition (deuterium and Oxygen-18) is consistent with little or no evaporation and post-Pleistocene age (Yang, Rattray et al. 1996, p. 37). The deuterium/Oxygen-18 composition of the perched water is distinctly different from that of the saturated zone water, which is indicative of recharge under colder conditions than the present climate (Benson and Klieforth 1989, p. 57) during late Pleistocene time (>10,000 years before present [BP]).

Geochemical modeling using the NETPATH model yield refined Carbon-14 residence times for perched water sampled from boreholes NRG-7a, UZ-14D, and SD-9/TS (Yang, Yu et al. 1997, p. 78). The corrected Carbon-14 residence times are 2,150 to 2,650 years for NRG-7a; 5,260 to 6,260 years for UZ-14D; and 4,040 to 5,370 years for SD-9/TS (Yang, Yu et al. 1997, p. 80). In each case the corrected residence times are substantially younger than the unadjusted Carbon-14 residence times.

Analysis of the perched waters for tritium indicates that all samples were below the detection level of 4 tritium units, which indicates that if water affected by a nuclear bomb test has reached the perched water bodies, it is quantitatively insignificant (Yang, Rattray et al. 1996, p. 34).

The significance of the perched water bodies stems largely from their implications with respect to the movement of water within the unsaturated zone as follows:

1. The widespread occurrence of perched water near the contact of the TSw and CHn units implies a laterally extensive zone of very low permeability that impedes vertical flux of water. Presumably the low permeability is related to zeolitization of glassy strata in the CHn unit and plugging of vertical structures such as faults and fractures with low permeability alteration products. The fact that perched water is not associated with zeolitized zones at shallower depth, for example in the PTn unit, suggests that the alteration leading to reduced bulk permeability was less pervasive at shallower depth. Another contributing factor maybe low permeability of the basal vitrophyre of the TSw, which is of lower matrix permeability than overlying and underlying strata (CRWMS M&O 1998, p. 5.3-163).

2. The unique chemical and isotopic character of the perched water provides strong supporting evidence for the significance of fast path flow as a mechanism for vertical percolation flux in the unsaturated zone.

3. The lateral downdip flow implied by the perched water has important implications for operation of the waste repository. If radionuclides are leached from waste canisters under future climatic and hydrologic conditions, such leachate could be expected to be diverted laterally to downdip structures such as faults rather than flowing vertically through the absorbent matrix of zeolitized deposits of the CHn and CFu units to reach the water table.

2.2.1.7 Isotopic Dating of Water and Air Flow

In an effort to refine the conceptual model of flow of water in the unsaturated zone, isotopic dating techniques have been used extensively to estimate residence time of water and rock gas since it infiltrated at land surface. Chief among these techniques are analyses of bulk rock samples for Chlorine-36 and water samples for tritium (H-3) and Carbon-14. All three isotopes are radioactive and formed naturally in the atmosphere through cosmic ray reactions with atmospheric gases and particles (Fritz and Fontes 1980, pp. 49, 79; Fabryka-Martin, Turin et al. 1996, p. 10). Moreover, the atmospheric content of all three isotopes was greatly increased through atmospheric testing of nuclear weapons during 1952 through 1963, when such testing was largely terminated by international treaty.

The half-lives and chemical properties of Chlorine-36, H-3, and Carbon-14 differ widely and this contributes to their combined use in dating of water and gases. Tritium (H-3), with a half life of 12.26 years, reached concentrations of more than 5,000 tritium units in precipitation in the western states in 1963 from a pre-1952 background level of about 6 tritium units (Yang, Rattray et al. 1996, Figure 22). By 1984, the tritium content of precipitation at Yucca Mountain had declined to about 20 tritium units (Yang, Rattray et al. 1996, p. 52). Tritium analysis of groundwater now is mainly useful as an indicator of post-1952 infiltration, because pre-bomb natural tritium has decayed to below detection levels. Tritium, an isotope of hydrogen, forms part of the water molecule and is not subject to significant chemical modification and is therefore an unequivocal indicator of post-1952 infiltration.

Carbon-14, with a half life of 5,730 years, occurs in groundwater mainly in the form of the bicarbonate ion (HCO_3). Carbon-14 reached a maximum of atmospheric concentration of about 200 percent of pre-bomb concentration in 1965 and had decayed to about 125 percent as of 1985 (Fabryka-Martin, Turin et al. 1996, Figure 4-13). Plants utilize atmospheric carbon dioxide (CO_2), containing Carbon-14, in their life cycle to form hydrocarbons. When plants die and decay, the Carbon-14 content of the hydrocarbons is incorporated into the carbon dioxide in the soil zone. This CO_2 is dissolved in infiltrating soil moisture, thus labeling the infiltration with the Carbon-14 content of the atmosphere at the time the plants died. However, other sources of carbon can contribute to the bicarbonate in groundwater, including: direct solution of atmospheric CO_2, bicarbonate dissolved from rocks of marine origin, and oxidation of methane and other hydrocarbon compounds. These other potential sources of carbon complicate the dating of groundwater by the Carbon-14 method. If such contributions can be quantified, adjusted ages can be calculated; however, this usually requires accessory information on the carbonate chemistry of the groundwater, which commonly is not available. Accordingly, Carbon-14 groundwater dates are quoted in unadjusted form, and as adjusted when confidence can be placed in the adjustment. Carbon-14 ages of groundwater are only feasible for about 40,000 years or younger because Carbon-14 decays to undetectable levels beyond that period.

Chlorine-36, with a half-life of 301,000 years, occurs in groundwater in the form of the chloride (Cl) ion. The atmospheric Chlorine-36/Cl ratio rose rapidly from about 500 x 10^{-15} prebomb background to 217,000 x 10^{-15} in 1957, and declined to about background by 1975 (Fabryka-Martin, Turin et al. 1996, p. 19, Appendix C). Chlorine-36 is produced by a number of sources (Fabryka-Martin, Turin et al. 1996, p. 10-25), including: (1) cosmogenic Chlorine-36 produced by cosmic ray reactions in the atmosphere, (2) fallout of nuclear bomb Chlorine-36, (3) local sources at the Nevada Test Site, (4) cosmogenic production in surface rocks, especially calcite, and (5) deep subsurface production as a consequence of a low but ubiquitous neutron flux.

Chlorine-36 offers several advantages as a method for calculating travel time of water, including:

1. The long half-life of 301,000 years makes dating theoretically possible over the span of 50,000 to 2 million years (Fabryka-Martin, Flint et al. 1997, p. 3-1).

2. Chloride is only transported in dissolved form, unlike H-3 and Carbon-14, which can travel in the gaseous phase as well as dissolved, and chloride is extremely conservative in water; that is, it is not subject to chemical reactions with water or rocks like Carbon-14 that cause changes in its concentration (Fabryka-Martin, Turin et al. 1996, p. 60).

3. It can be sampled by extracting the chloride from samples of bulk rock, drill cuttings, cores, or water and thus is well adapted to sampling in unsaturated materials (Fabryka-Martin, Turin et al. 1996, p. 4).

4. Chlorine-36 is a nuclear bomb fallout product, and a high concentration of Chlorine-36 is unequivocal indication of post-1952 infiltration of moisture (Fabryka-Martin, Turin et al. 1996, p. 60).

However, the Chlorine-36 methodology is still in the research and development stage and much uncertainty remains regarding quantitative input parameters, which are discussed in detail by

Fabryka-Martin, Turin et al. (1996) and Fabryka-Martin, Flint et al. (1997). In view of these uncertainties, Chlorine-36 ages of samples are given as a range from minimum to maximum, which can span very long time periods.

Chlorine-36 dating tends to indicate greater ages than Carbon-14 methods by one to two orders of magnitude (Liu et al. 1995, p. NH-52). Uncorrected Carbon-14 ages for pore water from the unsaturated zone and for perched water at Yucca Mountain have ranged from modern to 11 ka (Yang, Rattray et al. 1996, p. 34), whereas Chlorine-36 based ages have ranged from modern to 800 ka (Fabryka-Martin, Wightman et al. 1993, p. 59). The apparent discrepancies are attributed to one of the following reasons (Liu et al. 1995, pp. NH-54 to NH-58): (1) different transport mechanisms for carbon and chloride; (2) different magnitudes and timing of bomb-pulse signals; (3) mixing of waters from different flow paths with different apparent ages; and (4) inadequate methods for correcting for the effect of sample contamination by carbon or chloride from sources other than that in the infiltrating water.

For the period of the past 20,000 years, for which companion samples have been analyzed for Chlorine-36 and Carbon-14 in perched waters, Fabryka-Martin, Turin et al. (1996, p. 56) have shown that plots of Carbon-14 activity versus Chlorine-36/Cl ratio fall along a characteristic meteoric water curve. This suggests that the Chlorine-36 and Carbon-14 reconstructions are reasonable and that the perched water, at least, consists of meteoric water unaffected by geochemical processes affecting the carbon or chlorine isotopic composition (Fabryka-Martin, Turin et al. 1996, p. 56). It is expected that methodological refinements will improve the precision of isotopic dating methods, especially of Chlorine-36 dating, leading to greater consistency of dates by different methods.

Dating of recharge by the tritium, Carbon-14, and Chlorine-36 methods all produce unequivocal indication of nuclear bomb testing era infiltration, and these results have been interpreted as indicating rapid episodic moisture flow through the unsaturated zone to the ESF, the proposed repository horizon, and to deep in the TSw and CHn units (Yang, Rattray et al. 1996, p. 31; Fabryka-Martin, Turin et al. 1996, pp. 34-35).

The principal conclusions to be drawn from isotopic dating are:

1. Chlorine-36 analysis of bulk rock samples from coreholes and the ESF (Fabryka-Martin, Flint et al. 1997, p. 6-2) and tritium and Carbon-14 analyses of unsaturated zone water extracted from cores (Yang, Rattray et al. 1996, p. 31) confirm that nuclear bomb era (post-1952) infiltration has penetrated to the ESF and deep into the TSw and CHn units, evidently by fast path flow along faults and fractures. However, isotopic data do not permit direct quantification of the flux.

2. Profiles of tritium, Carbon-14, and Chlorine-36 indicate zones of old water interlayered with bomb-pulse water in the TSw unit, indicating that percolating water has bypassed the matrix pores in the TSw by fracture and/or lateral flow (Fabryka-Martin, Turin et al. 1996, p. 62).

3. Chlorine-36 and Carbon-14 ages, together with major ion analyses and stable isotope (H-2 and O-18) analyses of perched waters, indicate that water flowed episodically through fast pathways to the base of the TSw unit with little or no reaction with matrix pore water or rocks. The average ages of the perched water are all post-Pleistocene (less than about 10 ka) (Yang, Rattray et al. 1996, p. 34; Fabryka-Martin, Turin et al. 1996, p. 62; Fabryka-Martin, Flint et al. 1997, p. 9-4).

4. Chlorine-36 analysis of borehole cores and wall rocks from the ESF suggested that some matrix pore water may be very old (200,000 to 700,000 years). However, recent reinterpretation (Fabryka-Martin, Flint et al. 1997, pp. 6-3 to 6-5) of the Chlorine-36 data suggest that low Chlorine-36 values observed in some samples may be due to dilution by ancient rock chloride, rather than to radioactive decay. The cumulative results of Chlorine-36 sampling suggest that bomb-pulse moisture at the proposed repository horizon may be only a small fraction of the total moisture flux (Fabryka-Martin, Flint et al. 1997, p. 2-12; Fabryka-Martin, Turin et al. 1996, p. 64).

5. Carbon-14 ages of CO_2 in unsaturated zone gas show a systematic increase downward through the TSw unit leading to rock gas ages older than Carbon-14 dated water ages in the basal TSw unit and underlying CHn unit (Yang, Rattray et al. 1996, p. 55). This disparity in ages apparently stems from lack of isotopic Carbon-14 exchange between the liquid and gaseous phases and the fact that the gas ages result from gaseous diffusion and radioactive decay, while the water ages result from preferential flow of water through fast pathways under the force of gravity (Yang, Rattray et al. 1996, p. 55).

The following conclusions regarding the conceptual flow model for the unsaturated zone are modified from Fabryka-Martin, Turin et al. (1996, pp. 63-64).

Combining all isotopic analyses to date, the following conceptual model of flow at Yucca Mountain is developed. The widespread occurrence of bomb-pulse Chlorine-36 under zones with negligible alluvial cover indicates that water readily enters the fractured TCw unit and is transported into the underlying PTn. Due to its high porosity and low fracture density, the PTn reduces the velocity of percolating water. Residence times on the order of 10 ka in the PTn are supported by both Chlorine-36/Cl ratios in the ESF as well as by independent estimates of infiltration and Carbon-14 based perched water ages (assuming water must pass through the PTn to get to the perched water). Observations of localized occurrences of bomb-pulse Chlorine-36, tritium, and modern Carbon-14 in the TSw indicate that isolated pathways provide relatively rapid travel times through the PTn. Increased fracture permeabilities in the PTn unit as a consequence of faulting or other disturbances create pathways capable of conducting some water rapidly through this unit to the top of the TSw, where, due to increased fracturing, it then travels quickly deeper into the profile.

Modeling results show that observed isotope signals are consistent with the above site conceptual models and with existing parameter estimates. Basic parameters predict old water in the ESF, while parameter changes consistent with faults and fracturing lead to a prediction of a small component of bomb-pulse Chlorine-36 in the ESF fractures.

The overall picture emerging from the isotope studies is that infiltration is spatially variable and probably higher than previously believed, that fracture transport can be critical, permitting rapid transport through otherwise low-conductivity materials, and that isolated fast paths associated with faults and fractures may penetrate deep into the mountain. Together, these findings greatly improve the conceptual model of flow and transport at Yucca Mountain, and will thus aid in the design of the potential repository as well as development of models of radionuclide migration from the potential repository to the accessible environment or radioactivity dose to the critical population.

2.2.1.8 Temperature and Heat Flow

Under natural conditions, both liquid and gas flow in the unsaturated zone of Yucca Mountain is affected by ambient temperature changes, geothermal gradients, and atmospheric and hydrologic conditions. The thermal and hydrologic regimes are closely related due to the effects of coupling between thermal, topographic, and barometric conditions on air circulation in the mountain (Weeks 1987, p. 170). Furthermore, heat will be generated over long time periods by high-level radioactive waste emplaced in the unsaturated zone, which will greatly affect the movement of fluids.

Sass, Lachenbruch, Dudley et al. (1988, p. 24) concluded from temperature profiles in 35 boreholes near Yucca Mountain that heat flow in the unsaturated zone was primarily conductive and did not exhibit a significant convective component. However, in comparing the heart flows calculated for the entire set of drill holes at Yucca Mountain, Sass, Lachenbruch, Dudley et al. (1988, p. 47) suggested that a possible deficiency of 5-10 mW/m^2 in the unsaturated zone, relative to that in the saturated zone, could be attributed to an average water-percolation rate of 2-5 mm/yr. Repeated temperature logs in 18 boreholes indicated temperature gradients ranging from 15 to 60° C/km and that heat flow in the unsaturated zone varies systematically both spatially and as a function of thickness of the unsaturated zone. The Sass, Lachenbruch, Dudley et al. (1988, Figure 15) map of heat flow distribution in the unsaturated zone showed minimal heat flow (<35 mW/m^2) in the center of the potential repository area and increasing outward to 50 mW/m^2 around the margins of the site scale model area.

Modeling (Bodvarsson and Bandurraga 1996, p. 366) used borehole data of Sass, Lachenbruch, Dudley et al. (1988, Appendix 3) and a model developed by Rautman (1995) that correlates thermal conductivity as a function of porosity, temperature, and saturation. It was concluded from this modeling that conductive heat transfer alone cannot fully explain the observed temperature data from many boreholes, and a coupled conduction/convection model was developed which allowed for smaller observed temperature gradients due to water percolating through the unsaturated zone.

Using qualified thermal data from seven recently drilled boreholes, the percolation flux was calculated (Bodvarsson and Bandurraga 1996, pp. 376-377) assuming that the heat flux through the unsaturated zone is the sum of the conductive upward heat flow and the downward energy flux due to percolating water. These calculations indicated that almost the entire repository region has a low temperature gradient in the TSw unit, suggesting a percolation flux on the order of 5 to 12 mm per year, which is consistent with recent percolation flux estimates of Flint, A.L et al. (1996, p. 2). Similar calculations show that the temperature gradients in the CHn unit are

much greater than in the TSw, ranging from 28 to over 40°C/km, because of lower effective thermal conductivity in the CHn. This leads to calculated percolation fluxes of 2 to 7 mm per year. This latter estimate is somewhat lower than that for the TSw unit, which is consistent with the concept of lateral flow on top of the zeolites in the CHn.

2.2.2 Saturated Zone Hydrology

The concept of multiple barriers to radionuclide migration away from a repository is an important aspect of site characterization and design of a high-level radioactive waste facility. Multiple barriers include engineered barriers, such as the waste form, containment, and materials introduced in and around waste canisters, and natural barriers that include the geologic environment and its geochemical waste isolation properties. At the Yucca Mountain site, the saturated zone, the deposits below the water table, represents the final pathway and last natural barrier between the potential repository and the accessible environment (Luckey et al. 1996, p. 3), defined as the area beyond 5 km from radioactive waste. Thus, it is essential to have a good understanding of the flow and transport characteristics of the saturated zone, including groundwater time of travel, dispersive and diffusive properties of the aquifers, and geochemical retardation properties of the environment.

The water table at Yucca Mountain is generally encountered in the Calico Hills Formation and older rocks (Figure 2-4). The saturated zone has been divided by Luckey et al. (1996, p. 17, Figure 7) into three aquifers and two confining units on the basis of water bearing character (from youngest to oldest) as follows:

1. Upper volcanic aquifer, consisting of the densely welded part of the Topopah Spring Tuff of the Paintbrush Group.

2. Upper volcanic confining unit, consisting of the basal vitrophyre of the Topopah Spring Tuff, the Calico Hills Formation, and the uppermost nonwelded part of the Prow Pass tuff of the Crater Flat Group.

3. Lower volcanic aquifer, consisting of most of the Prow Pass Tuff and the underlying Bullfrog and Tram Tuffs of the Crater Flat Group.

4. Lower volcanic confining unit, consisting of bedded tuffs, lava flows, and flow breccia beneath the Tram tuff.

5. Lower carbonate aquifer, consisting of limestone and dolomite of Cambrian to Devonian age. It is inferred that locally, near the northern part of Yucca Mountain, the Eleana Formation, a clastic confining unit, overlies the carbonate aquifer, but this has not been confirmed by drilling.

Elsewhere in the region, Laczniak et al. (1996, Table 1) recognized a lava flow and welded tuff aquifer that is stratigraphically equivalent to part of the Luckey et al. (1996, p. 17) lower volcanic confining unit. To facilitate correlation between site scale and regional flow models, the lower volcanic aquifer and lower volcanic confining unit of Luckey et al. (1996, p. 17) were further subdivided in the *Yucca Mountain Site Description* (CRWMS M&O 1998, p. 5.3-4, Table 5.3-1) into middle and lower aquifers and confining units, as shown in Figure 2-3.

However, it should be noted that the lower volcanic aquifer of Figure 2-3 has not been identified in the area of the proposed repository.

As noted earlier, the densely welded tuffs have minimal porosity and water-storage capacity, but where highly fractured, function as aquifers. Conversely, the nonwelded or bedded tuffs generally have large primary porosity and can store large amounts of water, but matrix permeability is moderate to small, and they function as confining units.

2.2.2.1 Groundwater Flow

Yucca Mountain lies within the Alkali Flat-Furnace Creek groundwater basin, which is part of the Death Valley Regional Groundwater Flow System (D'Agnese et al. 1997, p. 59; Figure 2-5). The Alkali Flat-Furnace Creek basin is bordered on the east by the Ash Meadows groundwater basin and on the north and west by the Pahute Mesa-Oasis Valley groundwater basin. Collectively, these groundwater basins are designated as the Central Death Valley subregion of the regional flow system (Figure 2-5).

Recharge within the Death Valley Regional Groundwater Flow System probably occurs at higher altitudes where there is more precipitation. In the vicinity of Yucca Mountain, recharge from precipitation probably occurs at Timber Mountain, Pahute Mesa, Rainier Mesa, Shoshone Mountain, and the Spring Mountains. Some water may enter the Ash Meadows groundwater basin by subsurface flow from Pahranagat Valley on the northeastern boundary of the basin (Winograd and Thordarson 1975, p. 110-111; Thomas, B.E. et al 1996, p. C66; D'Agnese et al. 1997, Table 13). Closer to Yucca Mountain, infiltration of runoff in Fortymile Canyon and Fortymile Wash probably contributes recharge to the Alkali Flat-Furnace Creek groundwater basin (Claassen 1985, pp. F20-F21; Savard 1994, p. 1805; Savard 1998, Table 5).

Groundwater flows through Quarternary, Tertiary, and Paleozoic aquifers to discharge areas within the groundwater basins and as transfers between basins (D'Agnese et al. 1997, Table 2; Figure 2-5). The Pahute Mesa-Oasis Valley basin discharges principally as evapotranspiration in Oasis Valley, but interbasin transfer as groundwater underflow to the Alkali Flat-Furnace Creek basin also occurs. Discharge from the Ash Meadows groundwater basin at Amargosa Flat and Ash Meadows itself is largely evapotranspired, but both groundwater underflow and spring overflow on the surface transfer water to Amargosa Desert in the Alkali Flat-Furnace Creek basin. The Alkali Flat-Furnace Creek groundwater basin discharges chiefly as evapotranspiration at Alkali Flat and as underflow to Death Valley, a closed basin that is the ultimate groundwater sink for the Death Valley Regional Groundwater Flow System. There is neither surface nor subsurface flow from Death Valley; water is discharged only as evapotranspiration.

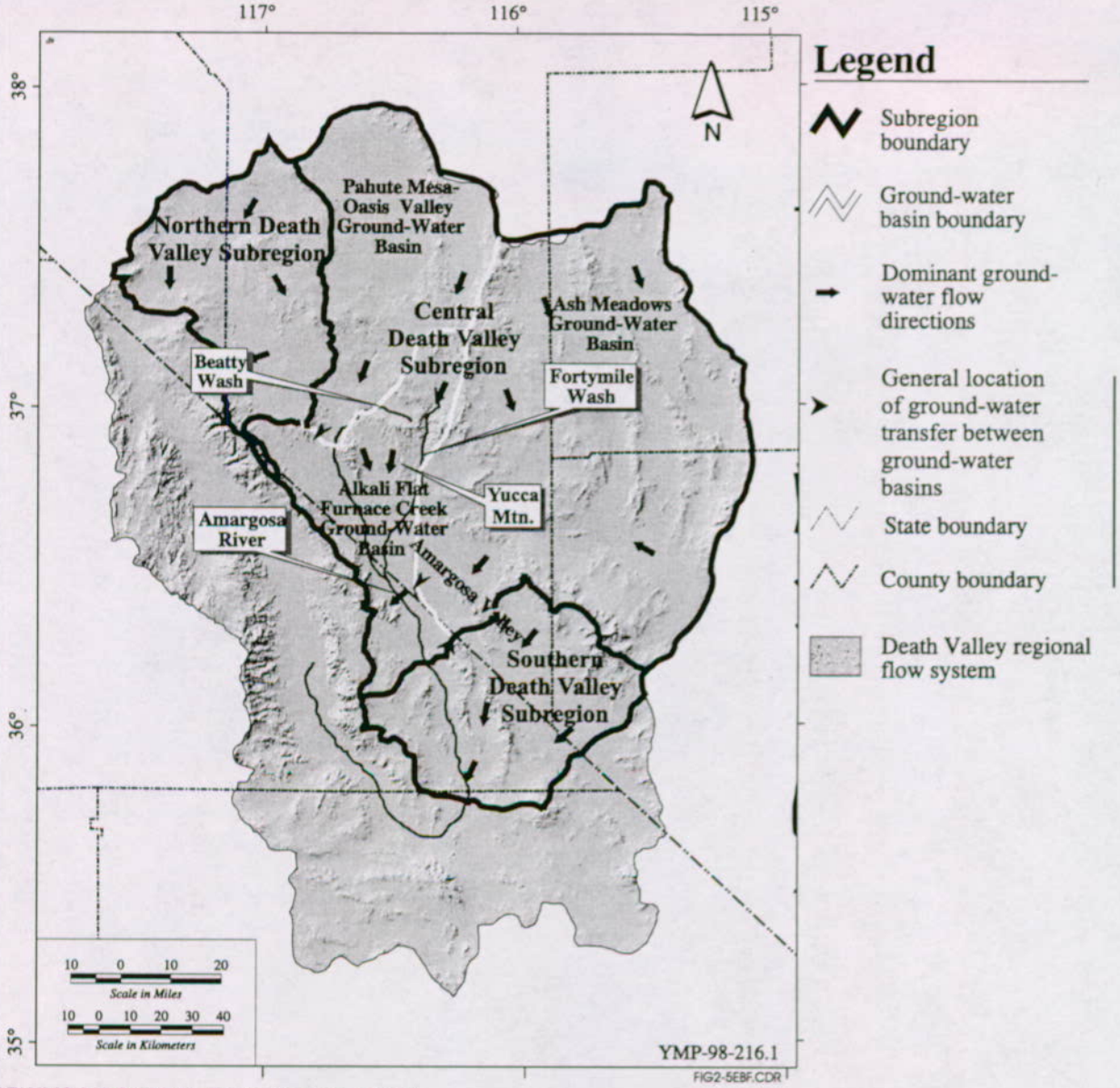

Source: CRWMS M&O (1998, Figures 5.2-25, 5.2-6)

Figure 2-5. Death Valley Regional Groundwater Flow System Showing Three Designated Subregions, Groundwater Basins, and Associated Flow Paths (Modified after D'Agnese et al. 1997, Figures 29 and 30)

In the vicinity of Yucca Mountain, groundwater flows south from recharge areas at higher altitude to the north, southerly toward basin-fill sediments (valley-fill aquifer of Winograd and Thordarson 1975, Table 1) and lacustrine deposits and carbonate rocks underlying the Amargosa Desert. Potentiometric (Claassen 1985, Figure 2; D'Agnese et al. 1997, Figure 27) and hydrochemical data indicate that groundwater flows southerly beneath the Amargosa Desert toward Alkali Flat (Franklin Lake Playa). Discharge at the playa occurs primarily through evapotranspiration. Some groundwater may flow southwesterly from the Amargosa Desert beneath the Funeral Mountains to discharge as spring flow and evapotranspiration in the vicinity of Furnace Creek Ranch in Death Valley and some flows southerly to discharge in the Shoshone/Tecopa area of the lower Amargosa Valley (D'Agnese et al. 1997, Table 2).

The site scale groundwater study area refers to an approximately 150-km^2 area around the potential repository at Yucca Mountain, extending north to about Pinnacles Ridge, east past Fortymile Wash, west past Solitario Canyon, and south to about the southern end of Yucca Mountain (Figure 1-2). The area thus defined does not have natural boundaries to groundwater flow, and different simulation models of the flow system may use different boundary conditions. In order to model groundwater flow and radionuclide transport to the assumed "critical population" in the Amargosa Farms area, the current site-area flow model is extended 20 km farther south than the boundary of Figure 2-6.

2.2.2.2 Potentiometric Surface

The Yucca Mountain site area is divided into three areal subdivisions (Luckey et al. 1996, p. 21) on the basis of the potentiometric (water table) gradient (Figure 2-6):

- An area of steep hydraulic gradient beneath the northern part of Yucca Mountain with a southward water-level decrease of 200 m in 1.5 km (gradient of 0.13)
- An area of moderate eastward gradient of 20 m in 0.4 km (gradient of 0.05) just west of Yucca Mountain in the vicinity of Solitario Canyon
- The area east of Solitario Canyon with a very small eastward gradient (0.0001 to 0.0003)

Vertical hydraulic gradients have been measured in only a few boreholes around Yucca Mountain but generally were upward. Most boreholes indicated little change in potentiometric levels with depth, however. Based on very limited data (five boreholes), Luckey et al. (1996, p. 29) infer an upward gradient from the carbonate aquifer to the volcanic aquifers, which, if valid, would indicate that for the immediate area of Yucca Mountain radionuclide transport would be restricted to the volcanic system. The foregoing conclusion is based on measurement of potentiometric levels in different depth zones and stratigraphic units in boreholes UE-25p #1 (the only hole near Yucca Mountain that penetrates into the carbonate aquifer) and in boreholes USW H-1, USW H-3, USW H-4, USW H-5, USW H-6, and UE 25b#1 (Figure 2-6), all drilled into the lower volcanic confining unit.

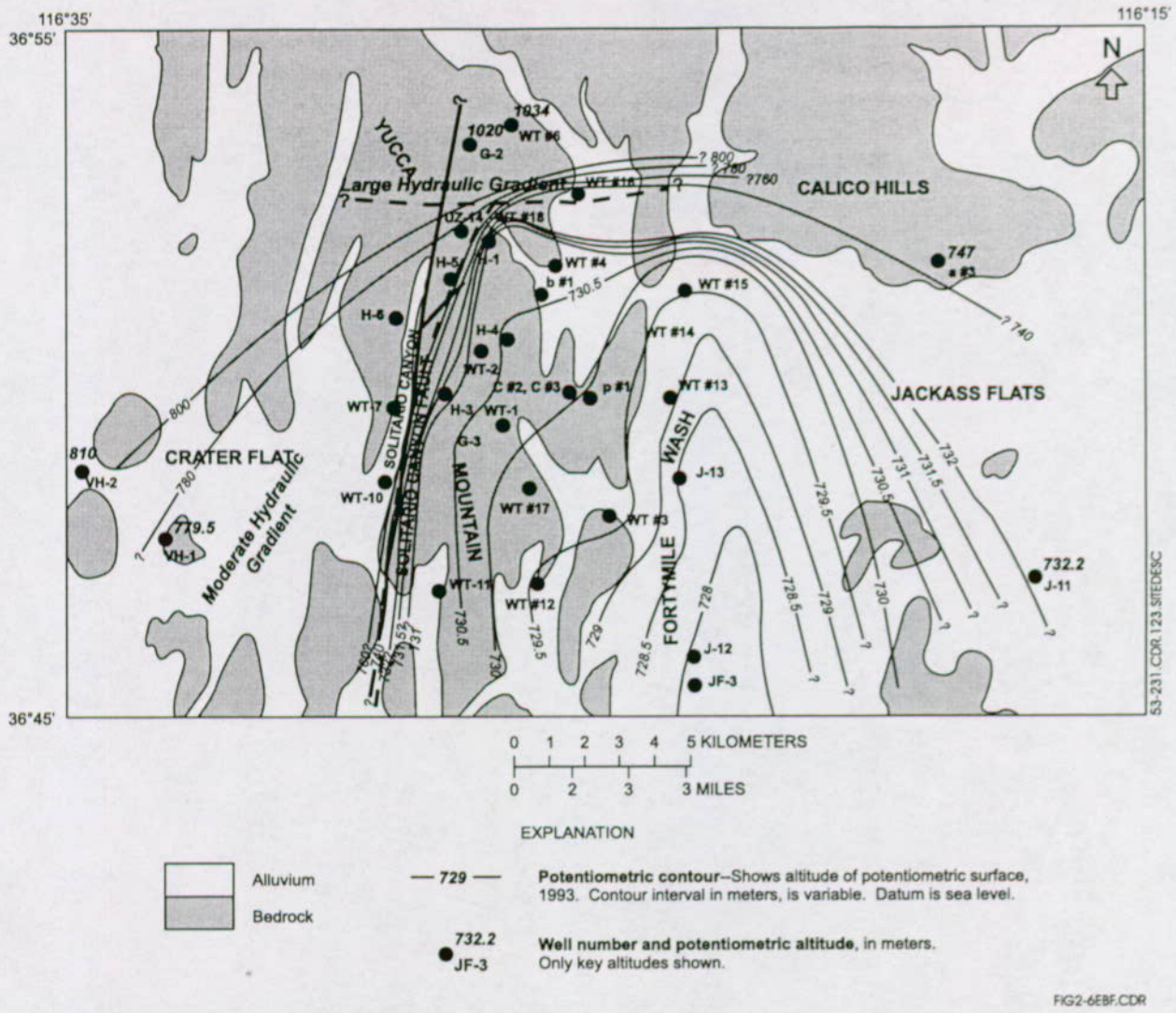

Source: CRWMS M&O (1998, Figures 5.3-222 and 5.3-231)

Figure 2-6. Piezometric Surface (Tucci and Burkhardt 1995) Based on 1993 Data

Measurements of potentiometric levels in borehole UE 25p#1 indicated (Luckey et al. 1996, p. 28):

1. Potentiometric levels gradually increased from 729.9 to 734.5 m above sea level between the water table and deep within the lower volcanic confining unit (1,114 m depth).

2. Potentiometric levels abruptly increased to 752 m in the "older tuffs" between 1,110 and 1,180 m depth.

3. Potentiometric levels remained at about 751 m through the lower volcanic confining unit and the carbonate aquifer (1,297 to 1,805 m depth).

The lower 70 m of the lower volcanic confining unit had potentiometric levels very similar to those in the carbonate aquifer, indicating that the zones were hydraulically connected. The upper 237 m of the lower volcanic confining unit had potentiometric levels similar to those of the lower volcanic aquifer (about 730 m asl).

Potentiometric levels measured in boreholes USW H-1, USW H-3, USW H-5, and USW H-6 (all of which penetrated at least 123 m of the lower volcanic confining unit) ranged between 750 and 785 m (Luckey et al. 1996, Table 3), suggesting hydraulic connection with the underlying carbonate aquifer. The table shows 54.6 m difference in head at well USW H-1 between the deepest packed-off interval, in the lower volcanic confining unit, and a shallower packed-off interval in the lower volcanic aquifier. However, potentiometric levels in boreholes UE-25 b#1 and USW H-4, which penetrated only 31 m and 64 m into the lower volcanic confining unit, respectively, had potentiometric levels (about 730 m) similar to those in the overlying lower volcanic aquifer.

In the area of steep hydraulic gradient, water levels decline southerly from about 1,020 m elevation at well USW G-2 to about 731 m at well USW H-1, over a distance of about 2.5 km (Figure 2-6). Several hypotheses have been advanced to account for this steep gradient (Luckey et al. 1996, p. 21); however, no obvious geologic cause exists, and the cause cannot be resolved on the basis of currently (1997) available data.

Based on examination of the water-level contour map (Figure 2-6), groundwater flow from west to east seems to be impeded by the Solitario Canyon fault, apparently causing the moderate hydraulic gradient west of Yucca Mountain. This may either be due to impermeable filling within the fault zone, or to juxtaposition of more permeable strata against less permeable rock units (Luckey et al. 1996, p. 25). In any event, most of the groundwater west of the fault probably flows southward either along the fault or through an aquifer beneath Crater Flat (Luckey et al. 1996, p. 25).

The area of small hydraulic gradient beneath eastern and southern Yucca Mountain includes most of the proposed repository. Here, water levels ranged from 728 to 732 m above sea level, and the small hydraulic gradient extends east as far as Fortymile Wash, where the water level is about 728 m, and probably extends into Jackass Flats where the water level at well J-11 (10 km east of well J-13) was about 732 m (Figure 2-6). The small gradient extends south at least to wells USW WT-11 and UE-25 WT#12, but may extend farther south. Ervin et al. (1993, p. 1558) suggested that the gentle gradient could indicate highly transmissive rocks, limited groundwater flow through the system, or a combination of both.

Water levels have been measured in boreholes at Yucca Mountain at varying frequencies since 1983. As of the end of 1994, the monitoring network consisted of 15 boreholes in which 16 zones were monitored monthly, and 12 boreholes in which 12 zones were monitored hourly and 4 zones were monitored continuously (Luckey et al. 1996, p. 29). Water levels at Yucca Mountain have been stable over time. After the levels have stabilized following drilling or modification of packers, they generally change very little with time. The annual range of fluctuations is on the order of tenths of a meter, and appear to be mainly in response to changes in barometric pressure and earth tides.

Short-term potentiometric fluctuations of up to 2.2 m (fluid pressure response), related to earthquakes, have been observed in wells equipped with continuous recorders at Yucca Mountain (CRWMS M&O 1998, Section 5.3.5.1.2; O'Brien 1993, Table 1). Fluctuations typically are of short duration and the piezometric level returns to its pre-earthquake trend within minutes to a few hours (O'Brien 1993, p. 7). However, a series of earthquakes on June 28 to 29, 1992 (Landers, California, M_w 7.3; Big Bear, California, M 6.6; and Little Skull Mountain, Nevada, only 23 km southeast of Yucca Mountain, M 5.6) appear to have caused longer term effects on piezometric levels at the Yucca Mountain site (CRWMS M&O 1998, p. 5.3-259). These longer term effects, which were observed in wells WT#4, WT#6, p#1, and WT-11, consisted of rises or declines in water levels (ranging from 0.25 to 1 m) in wells measured hourly, which persisted for periods of up to several months (CRWMS M&O 1998, pp. 5.3-259 to 5.3-260).

2.2.2.3 Aquifer Characteristics

The most important physical properties of aquifers for calculating travel times of groundwater and contaminants are hydraulic conductivity and effective porosity. Hydraulic conductivity is defined as the volumetric rate at which water is transmitted though a unit area (perpendicular to flow direction) of aquifer under a unit hydraulic gradient and under standard conditions. In field practice, transmissivity, the volumetric rate at which water is transmitted through a unit width of the full aquifer thickness, again under unit gradient and standard conditions, is divided by the tested thickness to obtain a first approximation of hydraulic conductivity. The degree to which this approximate, or "apparent," hydraulic conductivity is actually representative of fractured rocks requires subjective evaluations of the geologic setting and results of other tests such as flow surveys to identify productive zones within aquifers. However, tested thickness has varied within a much smaller range than is probable for actual hydraulic conductivity. Therefore, for purposes of comparing hydrogeologic units and discussing the overall distribution of rock-mass transmissive characteristics, the following discussion emphasizes transmissivity. Effective porosity is the amount of interconnected pore space available for fluid flow, expressed as a ratio of pore space to total volume. In the case of unconfined aquifers, the effective porosity approximates the specific yield, the ratio of the volume of water that after saturation can be drained by gravity to its own volume. A related parameter is storativity (or storage coefficient), which is defined as the volume of water that an aquifer releases from or takes into storage per unit surface area per unit change in head normal to that surface. In the case of unconfined aquifers, the storativity is numerically equivalent to the specific yield, or effective porosity. In the case of confined aquifers, storativity reflects an elastic response of the aquifer to an applied stress and is not a measure of volume dewatered or rewatered.

As summarized by Luckey et al. (1996, p. 32), more than 150 individual aquifer tests were conducted at 13 boreholes on and around Yucca Mountain in the early 1980s. All the tests were single-borehole tests in specific depth intervals and included constant-discharge, fluid-injection, pressure-injection, borehole flow-meter, and radioactive-tracer tests. Multiple-borehole tests have been conducted only at the C-hole complex (Boreholes UE 25c#1, #2, and #3). Results of aquifer tests usually were reported as transmissivity and hydraulic conductivity of intervals isolated with packers, but pumping-type aquifer tests were conducted in some boreholes for the entire saturated intervals. Storativity or specific yields were reported only for a few boreholes.

Transmissivity values for the hydrogeologic units in the vicinity of Yucca Mountain are listed in Table 2-1. These values were based on reported single-borehole aquifer tests and generally water was produced by a few thin, highly conductive fractures in an otherwise thick, essentially nonproductive rock matrix. Most hydraulic data are from tests conducted in the lower volcanic aquifer and in the lower volcanic confining unit. Very few data were available for the upper volcanic aquifer, the upper volcanic confining unit, and the carbonate aquifer.

Table 2-1. Estimated Transmissivity Values Obtained from Single-Borehole Aquifer Tests in the Vicinity of Yucca Mountain

Borehole Name	Transmissivity, in Meters Squared Per Day				
	Upper Volcanic Aquifer	Upper Volcanic Confining Unit	Lower Volcanic Aquifer	Lower Volcanic Confining Unit	Carbonate Aquifer
USW H-1	--	--	152	5.0×10^{-3}	--
USW H-3	--	--	<1.1	$<4.1 \times 10^{-1}$	--
USW H-4	--	--	178	23	--
USW H-5	--	--	35	--	--
USW H-6	--	--	229	6.3×10^{-2}	--
USW G-4	--	--	[1]589	--	--
UE-25 b#1	--	26	297	$<3.0 \times 10^{-3}$	--
C-hole complex	--	2.0	21	--	--
UE-25 p#1	--	--	15	2.0	118
J-13	120	[2]3.7	1.4	[3]6.3×10^{-1}	--

Source: Modified after Luckey et al. (1996, Table 5)

[--. no data; <, less than]

[1]Average determined from four tests
[2]Average determined from two tests
[3]Includes part of the lower volcanic aquifer

Hydraulic data for the upper volcanic aquifer were available only for well J-13. Thordarson (1983, Table 12) reported transmissivity of 120 m^2/d for the upper volcanic aquifer (TSw unit). The upper volcanic aquifer also was tested at borehole USW VH-1 (Thordarson and Howells 1987, p. 1); however, the tests were conducted over the entire saturated interval, which includes the lower volcanic aquifer. Most of the water produced by the borehole may be from a small part of the lower volcanic aquifer (Thordarson and Howells 1987, p. 9). Reported transmissivity values ranged from 450 to 2,400 m^2/d (Thordarson and Howells 1987, p. 14-18).

Hydraulic data for the upper volcanic confining unit were available from tests conducted at the C-hole complex, borehole UE-25 b#1, and well J-13. Reported transmissivity values for the upper volcanic confining unit ranged from 2.0 to 26 m^2/d (Luckey et al. 1996, Table 5).

Reported transmissivity values of the lower volcanic aquifer ranged from less than 1.1 to 589 m^2/d. The arithmetic mean of the 10 transmissivity values for the lower volcanic aquifer was about 152 m^2/d, and the geometric mean was about 43 m^2/d (Luckey et al. 1996, p. 35).

Reported transmissivity values of the lower volcanic confining unit ranged from less than 3.0×10^{-3} to 23 m^2/d. The arithmetic mean of the seven transmissivity values for the lower volcanic confining unit was 3.7 m^2/d and the geometric mean was 0.20 m^2/d (Luckey et al. 1996, p. 35).

Hydraulic data were available for the carbonate aquifer in the vicinity of Yucca Mountain only for borehole UE-25 p#1; Luckey et al. (1996, p. 36) indicated a transmissivity of 118 m^2/d.

In fractured-rock aquifers, such as those at Yucca Mountain, transmissivity probably is anisotropic—that is, greater in a direction parallel to the predominant fracture orientation than in other directions. Although this information is important to determining the groundwater flow paths from the potential repository, only one test has been conducted at Yucca Mountain to determine whether or not the aquifers actually are anisotropic. Erickson and Waddell (1985, p. 24-29) reported that, at borehole USW H-4, the maximum hydraulic conductivity (transmissivity divided by aquifer thickness) was from five to seven times greater than the minimum hydraulic conductivity; the maximum hydraulic conductivity was oriented in a direction 23° east of north. Czarnecki and Waddell (1984, p. 27-28), however, reported that their subregional model duplicated measured water levels more accurately when the aquifer was simulated as isotropic rather than anisotropic. Therefore, the question of whether transmissivity is anisotropic remains unresolved.

Vertical hydraulic-conductivity values were reported only for boreholes USW H-5 and the C-hole complex. Robison and Craig (1991, p. 26) reported an apparent vertical hydraulic-conductivity value of 62 m/d for the lower volcanic aquifer at borehole USW H-5. This value was about 100 times greater than the reported value for horizontal hydraulic conductivity of 0.6 m/d (Table 2-1). Data from the C-hole complex differ from the data from borehole USW H-5. The composite vertical hydraulic-conductivity value for the lower volcanic aquifer and Calico Hills aquifer were estimated to be 2 ft/d (Geldon 1996, Table 9), and were 0.067 times the values for the composite horizontal hydraulic conductivity (30 ft/d) obtained over the same intervals.

Field testing methods significantly influence transmissivity values. Geldon (1996, p. 69) reported that transmissivity determined using multiple-borehole hydraulic tests tend to be much higher—about two orders of magnitude—than values reported for single-borehole tests conducted at the same borehole. For example, a single-borehole test at borehole UE-25 c#3 resulted in a transmissivity value of 27.9 m^2/d, but results of a multiple borehole test for the same test interval in the borehole resulted in a transmissivity value of 1,860 m^2/d. Geldon (1996, p. 69) concluded that multiple-borehole tests generally sample a much larger volume of the aquifer material and incorporate a larger number of water-bearing fractures than single-borehole tests. Because most transmissivity values at Yucca Mountain were obtained from single-borehole tests, the values listed in Table 2-1 may not be representative values appropriate for scales of tens to hundreds of meters.

The hydraulic characteristics of a particular interval at a borehole are highly dependent on the fracture characteristics of that interval. A large conductive feature, such as the fault penetrated in the lower part of borehole UE-25 c#1, can contribute a large percentage of the total flow to a borehole (Luckey et al. 1996, p. 37). The tested interval containing such a feature can have a disproportionately large transmissivity compared to other intervals in the same borehole.

Intervals that have few conductive fractures generally contribute little water to the borehole and may have small transmissivity compared to other intervals in the borehole.

As summarized by Luckey et al. (1996, p. 37), specific yields ranged from 0.003 to 0.07 at the C-hole complex and from 0.15 to 0.28 at borehole USW H-5. However, the significance of such values is doubtful where most of the water is produced from a few discrete fractures.

As noted above, the water produced by wells is almost entirely from fractures, and from that standpoint, the matrix of the volcanic rocks is essentially non-productive. However, the matrix saturation constitutes by far the greatest amount of subsurface water contained in the saturated zone, and therefore must be taken into account in modeling of the hydrologic regime.

Data on matrix hydrologic properties are abundant for the unsaturated zone, but generally are sparse for the saturated zone. In the early 1980s, several wells were completed in the saturated zone and aquifer tests were conducted in numerous intervals in 13 test wells (Luckey et al. 1996, p. 32). Hydrologic investigative results through mid-1983 are summarized by Waddell et al. (1984, Table 9), who presented a table summarizing the available data on saturated matrix hydraulic conductivity and porosity by major hydrogeologic units. L.E. Flint (1998, p. 54) summarized the results of laboratory testing of the hydrologic properties of 4,892 rock samples from 30 boreholes near the potential repository site; however, most of those 30 boreholes did not penetrate into the saturated zone, as the program focus in recent years has been on characterizing the hydrologic properties of the unsaturated zone. L.E. Flint (1998, Table 7) presents summary statistics of hydrologic properties based on the 4,892 samples, including mean values of porosity, saturation, and saturated hydraulic conductivity for each of 31 hydrogeologic subunits. Comparable data on porosity and saturated hydraulic conductivity from Waddell et al. (1984, Table 9) and L. Flint (1998, Table 7) have been combined in Table 2-2 of this report for those hydrogeologic units that comprise the saturated zone at the proposed repository site, the TSw, CHn, and CFu units. The ranges cited by Waddell et al. (1984, Table 9) represent extreme values from individual wells, whereas those of L.E. Flint (1998, Table 7) represent ranges of means of numerous samples given by subunits and then aggregated by major hydrogeologic units. Thus, the data of Table 2-2 are not directly comparable; however, the two sources agree in general, namely, that the upper ranges of matrix porosity in the tuff units are fairly high, on the order of 0.30 or greater, and the saturated hydraulic conductivity is very low, ranging from 1×10^{-11} to 1×10^{-7} m/s. In referring to Table 2-2, it should be noted that core data are given only for the upper three subdivisions of Luckey et al. (1996, Table 4) of the saturated zone (see Section 2.2.2), that is, the upper volcanic aquifer, the upper volcanic confining unit, and the lower volcanic aquifer. Comparable data are not available for the lower volcanic confining unit and the lower carbonate aquifer.

Table 2-2. Hydrologic Characteristics of Saturated Zone Hydrogeologic Units at Yucca Mountain

Hydrogeologic Unit	Porosity		Saturated Hydraulic Conductivity (m/S)	
	Waddell et al. (1984)	L.E. Flint (1998)[2]	Waddell et al. (1984)[3]	L.E. Flint (1998)[4]
TSw	0.03-0.30 (J-13)[1] 0.10-0.28 (H-1)	0.036-0.157	$8x10^{-12}$ - $6x10^{-9}$	$6.2x10^{-13}$ - $2.3x10^{-10}$
CHn	0.20-0.35 (25a1) 0.45-0.48 (H-1)	0.173-0.345	$4x10^{-11}$ - $4x10^{-9}$	$7.4x10^{-11}$ - $2.1x10^{-7}$
CFu { Prow Pass Tuff }	0.10-0.30 (25a1)	0.263-0.325	$3x10^{-10}$ - $2x10^{-8}$	$9.6x10^{-11}$ - $2.9x10^{-10}$
CFu { Bull-frog Tuff }	0.15-0.25 (25a1)	0.115-0.259	$2x10^{-9}$ - $2x10^{-8}$	$2.1x10^{-12}$ - $5x10^{-11}$

[1]Range is for individual borehole indicated.
[2]Range is for means of several hydrogeologic subunits shown in L.E. Flint (1998, Tables 1 and 7).
[3]All values from borehole UE 25a#1. Values expressed as cm/s in Waddell et al. (1984, Table 9).
[4]Range is for geometric means of estimated values of several hydrogeologic subunits. Estimated values derived from correlation of measured saturated hydraulic conductivity with porosity. Grouped according to major hydrogeologic unit as shown in L.E. Flint (1998, Table 1).

2.2.2.4 Recharge to the Volcanic System

The recharge, that is, the amount of water moving from the unsaturated zone to the saturated zone in the vicinity of the proposed repository, is difficult to quantify. In part, this is due to sparsity of data, (i.e., few boreholes penetrate the deposits immediately above the water table in the vicinity of the potential repository), and in part to uncertainty regarding the continuity of the perching zone at the TSw/CHn contact, and the impact of perching upon percolation flux. The current preferred conceptual model (Bodvarsson and Bandurraga 1996, p. 20) suggests a percolation flux through the repository horizon of 5 to 10 mm/yr, which is consistent with net infiltration estimates of Flint, A.L. et al. (1996, p. 91) of 6.5 mm/yr for the proposed repository area. However, there is considerable uncertainty concerning the amount of water that may pass through the perching zone. Bodvarsson and Bandurraga (1996, pp. 371-374) calculate from thermal data a percolation flux of 5 to 12 mm/yr in the TSw unit, but 2 to 7 mm/yr in the CHn unit. This is consistent with the concept of lateral downdip flow in the perched water zones. In any event, the current recharge to the saturated zone in the vicinity of the proposed repository probably is small compared to upgradient inflows and downgradient outflows from the saturated zone.

Sources of water that enter the volcanic aquifers and confining units in the vicinity of Yucca Mountain potentially include inflow from upgradient volcanic aquifers and confining units, local recharge from Fortymile Wash, precipitation that infiltrates the surface of Yucca Mountain, especially at higher altitudes at the northern end of Yucca Mountain, and upward flow from the underlying carbonate aquifer (Luckey et al. 1996, p. 39). The magnitudes of most of the inflows to the volcanic system have not been quantified. Potentiometric levels measured in holes that penetrate to or though the lower part of the lower volcanic confining unit indicate hydraulic connection between the deep volcanic and the underlying carbonate aquifer south of the large

hydraulic gradient (see Section 2.2.2.2). Where a vertical gradient has been measured at Yucca Mountain, it is generally upward, indicating a potential for upward ground-water flow (Luckey et al. 1996, p. 28). However, no evidence of significant inflow to the volcanic rocks from the carbonates has been reported.

Potentiometric data from widely spaced boreholes upgradient from Yucca Mountain indicate that groundwater probably flows south from upland recharge areas in the volcanic terrain of Pahute and Rainier Mesas, beneath Timber Mountain, continuing southward beneath the Yucca Mountain area (Luckey et al. 1996, p. 51). However, the concept of inflow from upgradient regions is based on limited data, particularly between Yucca Mountain and Pahute Mesa.

Hydrochemical data (Benson and Kleiforth 1989, Table 1, p. 41) indicated that water in the volcanic aquifer beneath Yucca Mountain and Crater Flat was recharged during wetter climatic conditions approximately 12,000 (Well USW H-1) to 18,500 (Well USW H-6) years ago based on apparent Carbon-14 ages. However, these data do not preclude that some modern recharge occurs. Actual ages may be younger than apparent ages and the water probably is a mixture from recharge events that spanned at least a number of millennia. The data do not indicate whether the recharge occurred far upgradient or in Fortymile Wash. If most of the groundwater beneath Yucca Mountain was recharged in the distant past, the flow system may still be equilibrating from an ancient recharge pulse, resulting in a gradual decline in water levels beneath Crater Flat and Yucca Mountain over time (Luckey et al. 1996, p. 57).

Fortymile Wash is a major southward-draining channel located northeast, east, and southeast of Yucca Mountain (Figure 2-1). Fortymile Wash begins to the north of Yucca Mountain in the highlands of Pahute Mesa and ends in the Amargosa Desert to the south of the mountain. During extreme runoff, Fortymile Wash would be tributary to the Amargosa River. Osterkamp et al. (1994, Table 1, Figure 6) estimated average annual recharge along the entire 95-km length of Fortymile Wash (including Fortymile Canyon) to be about $4.22 \times 10^6 m^3$, based on channel-geometry measurements and analyses with a precipitation/runoff simulator.

Savard (1998, pp. 25-27) indicated that recharge occurred in 1983, 1992, 1993, and 1995 at borehole UE-29 UZN#91 and at nearby boreholes UE-29 a#1 and UE-29 a#2 based on rising water levels in each borehole following local precipitation and runoff. In March 1995, flow occurred in Fortymile Wash at least as far downstream as U.S. Highway 95, which was closed due to flooding. Boreholes UE-29 a#1, UE-29 a#2, and UE-29 UZN#91 located 15, 15, and 12 km, respectively, north of well J-13 on the east side of Fortymile Canyon showed significant water-level rise.

Savard (1998, p. 24) estimated long-term annual recharge to groundwater from Fortymile Wash using measured and estimated streamflow volumes and estimated streamflow infiltration losses for four reaches of Fortymile Wash between its confluence with Pah Canyon and a point in the Amargosa Valley downstream of the US Highway 95 crossing, about 18 miles downstream. The reaches were defined by the location of stream gaging stations as follows: (1) Fortymile Canyon reach between the confluence with Pah Canyon and the gage at Narrows; (2) Upper Jackass Flats reach between the Narrows gage and the gage near well J-13; (3) Lower Jackass Flats reach between the J-13 gage and the gage near U.S. Highway 95; and (4) the Amargosa Valley reach downstream of the U.S. Highway 95 gage. Savard (1998, Table 5) presents estimates of annual

average groundwater recharge rates for winter/spring and summer/fall precipitation for three time periods, 1969-95, 1983-95, and 1992-95. The seasonal average rates are combined to arrive at an estimated average annual recharge of 27,000 m^3 for the Fortymile Canyon reach, 1,100 m^3 for the Upper Jackass Flats reach, 16,200 m^3 for the Lower Jackass Flats reach, and 64,000 m^3 for the Amargosa Valley reach. The estimates total 108,600 m^3 (88 acre feet) for long-term average annual groundwater recharge from Fortymile Wash downstream of Pah Canyon.

Waddell (1984, Table 4) obtained hydrochemical samples from boreholes UE-29 a#1 and UE-29 a#2. Tritium and Carbon-14 values from these samples indicated that apparently younger water was present at shallower depths in borehole UE-29 a#1 (65.5 m deep) compared to borehole UE-29 a#2 (421.5 m deep). Younger water at shallower depth with deeper older water indicated that recharge was occurring at or near this site. In addition, the potentiometric level was about 4 m higher in the shallower borehole (UE-29 a#1) than in the deeper borehole (UE-29 a#2), which was consistent with recharge in this area.

Local infiltration from precipitation probably occurs in the Yucca Mountain area, but the amount of infiltration that reaches the water table may be inconsequential compared to the upgradient inflow and recharge from Fortymile Wash. Flint, A.L. and Flint (1994, p. 2358) estimated that near-surface infiltration ranged from 0.02 to 13.4 mm/yr and averaged 1.4 mm/yr. Higher infiltration tended to occur on the northern part of Yucca Mountain. Deep infiltration would be less than shallow infiltration because air flow through the mountain would remove some moisture. As described in Section 2.2.1.4, a natural air circulation system exists in the unsaturated zone at Yucca Mountain, which will persist after repository closure. Although accurate determination of the rate and distribution of percolation deep in the unsaturated zone at Yucca Mountain is important to predicting potential repository performance, this rate may be small enough under modern climatic conditions not to have a substantial effect on the saturated-zone flow system. If Flint, A.L. and Flint's (1994, p. 2358) average shallow infiltration of 1.4 mm/yr was assumed to reach the water table beneath the entire 150-km area of intensive unsaturated-zone hydrologic study, recharge would amount to about 200,000 m^3/year.

In a more recent analysis, Flint, A.L. et al. (1996, p. 1-2) indicate that for an average precipitation year (approximately 170 mm), net infiltration ranges from zero, where alluvial thickness is 6 m or more, to more than 80 mm/yr where thin alluvium overlies highly permeable bedrock on north-facing slopes at high elevations, and net infiltration averages 4.5 mm/yr over the Yucca Mountain study area. On a year-to-year basis, average net infiltration varies from zero in dry years to more than 20 mm/yr during years when precipitation exceeds 300 mm.

2.2.2.5 Discharge from the Volcanic Flow System

Pathways by which water may leave the volcanic aquifers and confining units in the vicinity of Yucca Mountain include outflow to downgradient volcanic aquifers and confining units and to alluvium, pumpage from wells, downward flow to the underlying carbonate aquifer, and upward flow into the unsaturated zone. The magnitudes of most of the outflows from the volcanic system have not been quantified.

Downgradient from Yucca Mountain in the Amargosa Desert, the potentiometric surface steepens gently toward the south (Czarnecki and Waddell 1984, Figure 3; D'Agnese 1994,

Figure 27), indicating southerly groundwater flow. The potentiometric surface steepens in the vicinity of the Nevada-California state line, but flattens toward Alkali Flat (Franklin Lake Playa), as it approaches and possibly even rises above the land surface. Much of the downgradient flow probably discharges at this playa, although some flow probably continues southward beyond the playa toward Death Valley (D'Agnese et al. 1997, p. 112, Table 2).

Limited evidence indicated that the carbonate aquifer may supply at least some inflow to the volcanic system at the south end of Yucca Mountain (Luckey et al. 1996, p. 41). There is no direct evidence that the volcanic system supplies outflow to the carbonate aquifer in the vicinity of Yucca Mountain. However, one explanation for the large hydraulic gradient at the northern end of Yucca Mountain assumes a major outflow from the volcanic system into the carbonate aquifer. Because of the sparseness of the data, it cannot be determined if there is any outflow from the volcanic system to the carbonate aquifer. If there is an outflow to the carbonate aquifer, it still cannot be determined whether there is a net outflow from the volcanic system to the carbonate aquifer or whether there is a net inflow to the volcanic system from the carbonate

Water is routinely pumped from wells J-12 and J-13 in Jackass Flats for use in the Yucca Mountain area and the southwestern part of the Nevada Test Site. Young (1972, p. 13) estimated that a total of about 900 million gallons ($6.9 \times 10^5 m^3/yr$) of water was pumped from wells in Jackass Flats during 1962 to 1967. LaCamera and Westenburg (1994, Table 6) estimated that a total of about 583 million gallons ($1.8 \times 10^5 m^3/yr$) of water was pumped from these wells during 1981 to 1992. The decrease in pumpage with time was due to a decrease in activity in this part of the Nevada Test Site.

Water has been pumped from various boreholes in the Yucca Mountain area to determine the hydraulic characteristics of the flow system. However, the quantities pumped were small compared to other pumpage and to natural discharge.

By far the largest amount of pumpage in the region occurs in the Amargosa Desert south of Yucca Mountain. Water is pumped from alluvial deposits for irrigation, mining, industrial, commercial, stock, and domestic use. LaCamera and Westenburg (1994, Table 6) compiled pumpage inventories made by the Nevada Division of Water Resources for the Amargosa Desert for various years. Average pumpage for 1985 to 1992 was $8.1 \times 10^6 m^3/yr$ and ranged from 4.8×10^6 to $11.9 \times 10^6 m^3/yr$. Pumpage in the Amargosa Desert is more than 40 times as large as pumpage in the Yucca Mountain area. This pumpage probably does not have a direct effect on the flow system at Yucca Mountain because of the large distances involved, but probably needs to be considered during any hydrologic modeling of the area (Luckey et al. 1996, p. 42).

2.2.2.6 Groundwater Chemistry

Water analyses from wells in the Yucca Mountain area reported by Benson and McKinley (1985, Table 1) indicate that sodium is the predominant cation and bicarbonate the predominant anion in the volcanic rocks. Among the cations, sodium (Na) ranged generally in concentration from 38 to 100 mg/L, calcium (Ca) from 1 to 20 mg/L, magnesium (Mg) from 0.01 to 2 mg/L, and potassium (K) from 1 to 5 mg/L. Among the anions bicarbonate (HCO_3) ranged generally from 110 to 275 mg/L, chloride (Cl) from 5 to 10 mg/L, and sulfate (SO_4) from 17 to 45 mg/L. Silica ranged from 40 to 57 mg/L. These values are in sharp contrast with a sample from the deep

carbonate aquifer (well UE 25 p#1, 1,257 to 1,805 m zone), which contained proportionally greater Ca, Mg, K, HCO_3, Cl, and SO_4; the concentrations (in mg/L) were as follows: Ca (100), Mg (39), Na (150), K (12), HCO_3 (569), Cl (28), and SO_4 (160). Only silica, at 41 mg/L, was in the same range as in the volcanic aquifers.

The chemical characteristics of groundwater in the Yucca Mountain area have evolved primarily from rock/water interactions. Groundwater composition is a function of recharge water chemistry and the materials with which the water interacts along its flow path. Groundwater cations in the volcanic system result from reaction with volcanic glass, primary minerals, soils, and probably to some extent, secondary phases such as calcite. In addition to being derived from rock/water interaction, anions result from solution of atmospheric, soil-zone and unsaturated-zone gases, and from precipitation. From the available information (Benson and Klieforth 1989; Thomas, J.M. et al. 1996; Yang, Rattray et al. 1996), water in the volcanic aquifers and confining units is a relatively dilute sodium bicarbonate type that would be expected to evolve in a volcanic geohydrologic system (Thomas, J.M. et al. 1996, p. C4). Water in the deep carbonate aquifer likewise is consistent with what would be expected in that environment (Thomas, J.M. et al. 1996, p. C5).

The analyses of Benson and Klieforth (1989, Table 1a and 1b) indicate significant lateral variability in chemical and isotopic characteristics of the groundwaters. An increase in Ca and Mg as compared to Na content is observed proceeding from west to east from the Yucca Mountain Crest toward Fortymile Wash. No similar systematic change is observed in anion content (HCO_3, Cl, and SO_4) or in silica content. However, Carbon-14 ages show a similar progression to the change in cation content, with the oldest waters occurring to the west, and younger to the east (an unadjusted Carbon-14 age of 18,500 years at well USW H-6 versus 9,100 years at well J-12 (Benson and McKinley 1985, Table 1). The stable isotope contents likewise show a west-east trend with the most negative values, indicative of cooler temperature of condensation, to the west and less negative values to the east. The water from the carbonate aquifer is distinctly different from water in the overlying volcanic units, in that the apparent age is significantly older (unadjusted Carbon-14 age of 30,300 years), and stable isotope content indicative of cooler ambient temperature than associated with the water in the overlying volcanics. Although the isotopic character shows a similar west-east trend to that of the relative cation concentrations, the correspondence may be fortuitous, and the progression of cation concentrations may be unrelated to age of recharge.

2.2.2.7 Dating of Recharge to the Saturated Zone

Benson and McKinley (1985, Table 1) presented results of analyses of water samples from 15 wells collected at Yucca Mountain between 1971 and 1984 including radioactive H-3, and Carbon-14 and stable H-2, Oxygen-18, and Carbon-13. The uncorrected Carbon-14 ages of recharge ranged generally from 9,100 to 18,500 years BP. Two samples from well UE 29a#2, near Fortymile Wash, indicated Carbon-14 apparent ages of 3,800 and 4,100 years BP, but these also contained nuclear-bomb H-3 at 37 pc/L indicating a component of nuclear bomb period contamination, which undermines confidence in the Carbon-14 results of those samples. Benson and Klieforth (1989, p. 57) presented interpretations of the Benson and McKinley (1985) data together with additional H-2 and Oxygen-18 analyses of precipitation in the Yucca Mountain area.

Claassen (1985) reported on the chemical and isotopic character of groundwater of the Amargosa Desert, directly south of Yucca Mountain. His report includes analyses of water samples for Carbon-14 from 28 wells and 1 spring, including 5 wells at the Yucca Mountain site previously reported by Benson and McKinley (1985, Table 1). Claassen's report (1985, Table 6) indicated uncorrected Carbon-14 ages of recharge ranging from 9,100 to 32,300 years BP. Claassen's (1985, Table 1) report also included water analyses for common inorganic constituents from 71 sources, as well as H-2 and Oxygen-18 and Carbon-13 analyses for most of the sources sampled for Carbon-14 (Claassen 1985, Table 6).

Davisson et al. (1994, Table 1) reported on a broad sampling of 31 wells at the Nevada Test Site carried out in 1992 and 1993. Two or more depth zones were sampled in three of these wells. The samples were analyzed generally for 14 common inorganic constituents, H-3, Carbon-14, Carbon-13, Chlorine-36, and Strontium-87, and selected samples were analyzed for Helium-4, Xenon-29, Krypton-82, Neon-20, Argon-36, Krypton-85, Strontium-90, Technecium-99, Cobalt-60, Antimony-125, and Cesium-137. Consistent with the findings of others, Davisson et al. (1994, p. 30) found that the major ion geochemistry of Nevada Test Site groundwaters is dominated by Na-K-HCO_3 water, related to dissolution of volcanic tuffs, and Ca-Mg-HCO_3 water, related to dissolution of Paleozoic carbonate rocks. Unadjusted Carbon-14 ages from 15 water samples showed a range from about 4,000 to 38,000 years BP, with an average age of about 20,000 years BP. They recognized that many of the samples probably contain ancient "Carbon-14 dead carbon" derived from the Paleozoic carbonate aquifers, but concluded that correction of ages, based on carbonate chemistry of the waters, would be premature until more information becomes available on Carbon-13 and Carbon-14 contents of recharge water.

Summarizing the regional information on age of recharge, it appears that most of the water in the saturated zone of the volcanic aquifers of the Yucca Mountain site, the Nevada Test Site, Amargosa Desert, and Oasis Valley was recharged in late Pleistocene time as suggested by unadjusted Carbon-14 ages in the range of 10,000 to 20,000 years BP coinciding with a period of cooler, wetter climate during the last glacial-interglacial transition (Benson and Klieforth 1989, p. 57). Recharge to the deeper Paleozoic carbonate aquifer system appears to be at least as old as that of the volcanic aquifers (Claassen 1985, Table 6; Craig and Robison 1984, p. 51), although the sampling is sparser and the ages are subject to greater corrections (to younger ages) because of probable contribution of ancient "dead or nonradioactive" carbonate from the Paleozoic rocks, which are hundreds of million years old. Somewhat younger uncorrected Carbon-14 recharge ages were noted in samples from wells near Fortymile Wash; 9,100 years BP at well J-12 and 9,900 years BP at well J-13, and 3,800 and 4,100 years BP from two different depth zones of well UE 29a#2 (Benson and Klieforth 1989, Table 1a). However, the samples from well 29a#2 contained tritium at levels suggesting contamination by a component of modern (post-1952) recharge. Claassen (1985, p. F27) observed that the youngest groundwater ages in the Amargosa Desert were in or near present-day drainageways and concluded that groundwater recharge to the valley fill occurred primarily by overland flow in or near present-day stream channels.

Sampling for Chlorine-36 has focused mainly on dating of water flow above the saturated zone (Liu et al. 1995; Fabryka-Martin, Wightman et al. 1993; Fabryka-Martin, Turin et al. 1996; Fabryka-Martin, Wolfsberg et al. 1996), as described earlier. The occurrence of bomb-pulse Chlorine-36 and tritium (Yang, Rattray et al. 1996, p. 55) in samples taken at depths below the superficial soil zone at Yucca Mountain indicates that at least some fracture zones provide paths

for rapid percolation of water. However, little information is available on quantities of water moved via fast paths and the quantitative significance of this mode of movement as related to the waters of the saturated zone.

2.3 PALEOCLIMATE AND PALEOHYDROLOGY

Proposed regulations published by the NRC (64FR8640) require the DOE to provide assurance that a total effective dose equivalent of radioactivity to the average member of a critical group located near Lathrop Wells, Nevada will not exceed 25 mrem for a performance period of 10,000 years. Accordingly, a means of predicting radioactive transport in groundwater from the proposed repository to the Lathrop Wells area (approximately 20 km) is essential to providing this assurance. The NRC has identified unsaturated and saturated flow under isothermal conditions as a Key Technical Issue to be addressed by DOE in its characterization of key site and regional scale hydrogeologic processes and features that may adversely affect performance of the proposed Yucca Mountain high-level nuclear waste repository (NRC 1997).

Subissues deemed important to the resolution of the KTI have been framed as six questions. Two of these questions relating to climate are:

(1) What is the likely range of the future climates at Yucca Mountain?
(2) What are the likely hydrologic effects of the climate change?

These questions are addressed in an Issue Resolution Status Report prepared by the NRC staff (NRC 1997, p. 2). In this IRSR, the NRC staff concludes that: (1) reasonable methods exist to bound the range of future change and the resulting consequences, and (2) enough information is currently available to reasonably estimate the range of future climates and water table rise at Yucca Mountain.

It is recognized that the earth's climate could change significantly during the period that nuclear wastes remain hazardous (NRC 1997, p. 2). Climate controls the range of precipitation and temperature, which in large part would control rates of infiltration, deep percolation, and groundwater flux through a geologic repository located in an unsaturated environment. Change in groundwater recharge will likely induce other effects, such as regional changes in the elevation of the water table. Water table rise would reduce the thickness of the unsaturated zone beneath the repository and thus affect the travel time of potential contaminants. In the unsaturated zone, it would also alter groundwater flow paths, dilution of contaminants, and transport rates. Climate is also a factor in assumptions about characteristics of the critical group and reference biosphere.

The NRC staff has determined that methods based on paleohydrologic, paleoclimatic, and geochemical information can be used to gain an adequate understanding of the range of past climates in the Yucca Mountain region (NRC 1997, p. 4). These insights can then be used to estimate the range of future climate variability. Multiple sources of data are needed to help reconstruct past environmental conditions. These include information from: paleodischarge sites; packrat middens; pollen studies; paleolake levels and sediments; groundwater isotopic data; soil properties; tree rings; erosion studies; and other sources.

2.3.1 Present Climate

The present climatic conditions in the vicinity of Yucca Mountain are described in Chapter 4 of the Yucca Mountain Site Description (CRWMS M&O 1998, p. 4.1-1) as arid to semi-arid. The following description of present climate as related to hydrology is adapted from the Yucca Mountain Site Description (CRWMS M&O 1998, p. 5.3-110 to 111).

The primary climatic parameter affecting surface hydrology and net infiltration is precipitation, including timing, frequency, duration, and intensity of precipitation. The dominant controlling factor determining the occurrence of precipitation at the site is the synoptic-scale weather circulation pattern relation to fixed-geographic moisture sources and local physiographic features. The moisture sources for the Yucca Mountain region are the Pacific Ocean, the Gulf of California, and the Gulf of Mexico. Most precipitation at the site occurs in response to low pressure systems, which are steered eastward by the jet stream and bring moisture inland from the Pacific Ocean. These weather patterns generally occur during winter, but can also occur during the winter-summer and summer-winter transition periods. Winter storms tend to result in low-intensity (light) precipitation and may occasionally last up to several days. Orographic influences tend to increase precipitation frequency and intensity for higher elevations, and precipitation often occurs as snow. On a regional scale, the orographic effects are more pronounced, particularly in the vicinity of major mountain ranges such as the Spring Mountains and the Panamint Range. The higher elevations of the mountain ranges correspond to the locations of maximum precipitation and also the locations of maximum recharge. During the summer, the jet stream migrates to the north, and weather circulation in the Yucca Mountain region tends to be dominated by high-pressure cells that cause reverse circulation, or monsoonal flow. Surface heating and convection of air masses carrying moisture from the Gulf of Mexico, the Gulf of California, and the Pacific Ocean results in sporadic but occasionally intense thunderstorms during the southwestern summer monsoon. These storms tend to be of short duration, but can produce high-intensity (heavy) precipitation, which often results in flash flooding.

The combined effect of the average winter and summer weather circulation patterns is to create zones of precipitation excess and deficit relative to the regional mean, for a given elevation, from west to east across the Southern Nevada region, with Yucca Mountain being located in an approximate transition zone between the deficit zone to the west and the excess zone to the east. The precipitation deficit (relative to the regional mean) is caused by the Sierra Nevada, which causes a regional rain-shadow during the winter and a westward diminishing of moisture from the monsoon during the summer. The combined effects of seasonal weather patterns and orographic influences cause considerable spatial variability in average annual precipitation throughout the Yucca Mountain region. Average annual precipitation estimates over the area of the Nevada Test Site range from a maximum of 370 mm in the Belted Range to a minimum of 110 mm in the Amargosa Desert. Annual precipitation within the Yucca Mountain infiltration study area averages 170 mm and ranges from a minimum of 130 mm at low elevations along the southern boundary to a maximum of 250 mm at high elevations along the northern boundary (CRWMS M&O 1998, p. 5.3-111).

In addition to the seasonal variability in precipitation, the arid climate at Yucca Mountain is characterized by considerable annual variability. Measured total annual precipitation at the site

ranged from a minimum of 12 mm for water year 1989 to a maximum of 312 mm for water year 1993 at one location (CRWMS M&O 1998, p. 5.3-111). Much of the annual variability observed in precipitation records in the Yucca Mountain region can be attributed to the effects of global circulation patterns on the position of the jet stream during the winter. In particular, the El Niño Southern Oscillation is a perturbation in the global circulation pattern that is strongly related to sea surface temperatures in the Pacific Ocean and tends to steer the jet stream south of its average winter position in the Western United States, bringing a higher frequency of storms into the Great Basin. Although the El Nino Southern Oscillation is known to significantly impact precipitation patterns across the southwestern United States, this annual-to-decade-scale variability in climates is still not completely understood, and the consistency (or lack of consistency) in its occurrence is still being evaluated (CRWMS M&O 1998, p. 5.3-111).

Another critical element relating to infiltration and groundwater recharge is evapotranspiration, the process that returns precipitation to the atmosphere, thus reducing infiltration and deep percolation. An important feature of the arid to semi-arid, warm climate of Yucca Mountain is the very high potential evaporation rate that occurs (CRWMS M&O 1998, p. 4.1-9). The typically abundant sunshine, low atmospheric relative humidity, and moderate wind speeds contribute to the great evaporation potential in the area. Actual evaporation for the desert surface is limited by availability of water in the surface layers, though evapotranspiration rates from irrigated crop areas can be large because of water availability to the crops. A limited amount of evaporation data exists for southern Nevada that would be representative of the Yucca Mountain area. An estimate of annual evaporation from a hypothetical lake is approximately 66 inches (1,650 mm), which is about a factor of ten greater than the average annual precipitation. Thus, the average annual precipitation is approximately 10 percent of the annual potential evaporation (CRWMS M&O 1998, p. 4.1-9).

Late Quaternary Climates

The late Quaternary period embraces the latter part of the Pleistocene Epoch and the Holocene Epoch up to the present. Synthesis of paleoclimatic evidence indicates that the present climate of southern Nevada exhibits a large precipitation deficit as compared to most of the Pleistocene. Wetlands are rare, few streams have perennial or intermittent flow, and springs are generally small and far apart. The following discussion is adapted largely from Forester et al. (1996, p. 1-3). Climate conditions are governed by changes in the earth's orbital properties (eccentricity, obliquity, precision) that determine insolation. Orbital properties and the resulting insolation values can be calculated for the past and future, so estimates of future conditions can be made by comparison to comparable conditions in the past. The major, insolation-controlled climate cycle of the late Pleistocene is 400 thousand years (ky) in duration with sub-cycles of approximately 100 ky. Changes in insolation are closely correlated with the major features of global climate change such as the growth and retreat of continental ice sheets. The change in insolation expected during the next 100 ky resembles change in insolation during the period from 400 ka to 300 ka.

The Devils Hole isotopic climate record shows that regional climate in southern Nevada changes in concert with global climate change. Long sedimentary records from basins such as Owens Lake provide an estimation of the character, magnitude, and frequency of local climate change, and therefore link changes in insolation to a climate response in the Yucca Mountain area.

Cores obtained from the Owens Lake basin penetrated sediments deposited during the last 500 ky. These data demonstrate that the major glacial and interglacial features of climate history are represented in this nearly continuous sediment sequence. Interpretation of the Owens Lake climate record indicates the various glacial and interglacial periods differ in their climate characteristics. The last two glacial periods (170 to 140 ka, 40 to 10 ka) appear to have been wetter and colder than the glacial from about 400 ka to 350 ka, which may serve as an analog for the next glacial period.

Interpretation of plant macrofossils found in packrat middens near Yucca Mountain indicate that mean annual precipitation (MAP) varied during the last wet period (40-10 ka), but was typically about 1.5 to 2 times the modern MAP. In particular, the midden data show short, century to millennial scale episodes when White Fir moved to lower elevations. During those episodes, MAP was probably more than twice the modern means. The variation of MAP about a mean has not been estimated, but given the diversity of dry to wet plant types within various middens, the variation in MAP was likely quite large. Episodes without White Fir often contain Limber Pine, which in addition to drier conditions, implies very cold mean annual temperature , perhaps as low as 4° to 5° C. Summer mean temperatures would also have been low, below about 16° C.

Ostracode species found in sediments from former wetlands supported by groundwater, such as those in the Las Vegas Valley, imply a higher than modern level of effective moisture. These aquatic fossils, together with the plant macrofossil data, imply that gains in effective moisture were typically due to deep depressions in temperature with only modest gains in precipitation. However, during the apparently wetter White Fir intervals, gains in effective moisture probably had a significant precipitation component in combination with temperature.

Geomorphic studies of the alluvial fans and fluvial deposits in and around Fortymile Wash show a response to past climate change. Alluvial and fluvial sediments were deposited during the wetter phases of interglacials and transitional climates, when infrequent but large storms eroded the hillslopes, including those of Yucca Mountain. Incision of these sediments occurred during cooler and wetter climate phases, when hillslopes, stabilized by vegetation, supplied little sediment to the regular flow in Fortymile Wash. Deposition (drier climate) of sediment in the wash occurred from about 120 ka to about 50 ka, and incision (wetter climate) occurred after this period and likely before the last glacial maxima period, about 18 ka radiocarbon years.

Geochronologic, isotopic, geochemical, and petrographic studies of calcite and opal minerals precipitated within fractures inside Yucca Mountain provide a direct means of comparing past regional climates to changes in infiltration, percolation, and recharge within the unsaturated zone. Stable carbon and oxygen isotopes and radiogenic strontium isotopes indicate calcite and opal formation and perched water bodies within the unsaturated zone in Yucca Mountain, come from infiltration. Stable-isotope data from unsaturated zone calcites suggest the infiltration came during glacial periods, when the regional vegetation was dominated by cool-tolerant plants. The infiltration seems to have had a maritime polar to arctic air mass signature and interacted with soil carbonates and probably other surface rocks. The data set for ages of secondary minerals, though preliminary, suggests little or no formation of secondary minerals during interglacials, consistent with a glacial mode origin for the infiltration/percolation.

Sedimentary deposits of former wetlands and springs found in valleys down the flow gradient from Yucca Mountain provide records of ground water discharge during both the last and probably the penultimate major wet-climate period. Spring deposits at Crater Flat and at the Lathrop Wells Diatomite, respectively 17 and 20 km south of Yucca Mountain, and paleo-wetland deposits near the Amargosa River, about 40 km south of Yucca Mountain, show discharge occurred between about 40 ka and 8 ka. The discharge, at least in part, came from the regional aquifer when the water tables rose to a maximum of about 100 m above present levels, as indicated from the depth to groundwater at the Lathrop Wells Diatomite site.

2.3.2 Paleohydrology

The principal hydrologic effects of cooler, wetter climates during the Pleistocene include higher precipitation and lower evaporation (increased effective moisture), which in turn resulted in greater infiltration, deep percolation, and recharge to groundwater. These latter effects resulted in significant rise in the water table, and increased surface discharge in the form of gaining streams, springs, and increased wetland areas (CRWMS M&O 1998, p 5.2-57). A wide variety of evidence cited in NRC (1997, p. 26) suggests that the water table was 10 to 130 m higher than the present throughout the Yucca Mountain region at times during the late Quaternary. The 10-m rise was observed at Devils Hole near the present discharge area of the regional carbonate aquifer at Ash Meadows; elsewhere the water table rise was at least 60 m.

The rise of the water table in response to increased effective moisture was reflected in surface discharge at springs and marshlands in topographically low areas. Some of the discharge areas in Fortymile Canyon northeast of Yucca Mountain sustained perennial flow. The Lathrop Wells Diatomite is a known paleospring deposit just to the south of Crater Flat, only 20 km southwest of Yucca Mountain (NRC 1997, p. 20). Currently, the water table there is about 115 m below the spring deposits (NRC 1997, p. 22).

At the Yucca Mountain site, the principal quantitative evidence of former higher water-table levels is marked by the occurrence of zeolite minerals above the present water table. Zeolite minerals form from glassy materials in tuffs due to extended periods of saturation (such as below the water table). At Yucca Mountain, the contact of the zeolitic altered zone in the Calico Hills non-welded tuff with unaltered glassy tuffs is found about 80-100 m above the present water table. This suggests that the water table stood about 100 m higher than at present over the thousands of years required for zeolitization of the glassy tuffs (NRC 1997, p. 22).

Evidence of perennial flow about 50 ka in Fortymile Canyon was found in samples from a packrat midden about 12 km northeast of Yucca Mountain. These data consist of the remains of willow, knotweed, and wild rose, which require damp soil or a shallow water table for survival. The site is about 60 m above the canyon floor where the water table currently is about 27 m deep. This evidence suggests that the water table was 75 to 95 m higher during the interval from 73 ka to 47 ka (NRC 1997, p. 24).

2.3.4 Future Climate at Yucca Mountain

The NRC staff have adopted the position that past climatic records from the Yucca Mountain area can serve as an index to future climate at the site (NRC 1997, p. 2). The NRC staff has determined that anthropogenic changes to the atmosphere, such as the greenhouse effect, are detectable and likely to increase with time (NRC 1997, p. 8), but that a greenhouse warming will last no more than about 3 ka, and that thereafter the climate of Yucca Mountain will resume cooling in accord with the Milankovich orbital theory of climate. Accordingly, the staff will postulate that full pluvial (cooler and wetter) conditions will dominate during at least several thousand years of the next 10 ka. Thus, anthropogenic effects will be assumed to delay but not prevent a return to pluvial conditions at Yucca Mountain with hydrologic effects similar to those of past pluvial phases (NRC 1997, p. 8).

INTENTIONALLY LEFT BLANK

3. NATURAL RESOURCES

The purpose of this section is to identify and evaluate or assess the potential for natural resources within the geologic setting of the Yucca Mountain Conceptual Controlled Area (see Figure 3-1 for a delineation of the controlled area). This section on natural resources includes a brief description of the resources (including metallic minerals, industrial rocks and minerals, hydrocarbons [petroleum, natural gas, oil shale, tar sands, and coal], and geothermal energy) currently known in the region or that could reasonably be postulated to be present based on models of natural resource occurrence. Resource potential is difficult to predict since it is dependent upon many factors, including economics, the potential discovery of new uses for resources, or the discovery of synthetics to replace natural resource use. This evaluation is based on present use and economic values of the resources. It does not predict future market trends or undiscovered uses for resources. This section is based on Section 3.11 of the *Yucca Mountain Site Description* (CRWMS M&O 1998).

Nevada ranked approximately second in the United States in value of nonfuel mineral production in 1996 (Nevada Bureau of Mines and Geology 1997, p. 3). Nonfuel minerals exclude oil, gas, coal, uranium, and geothermal resources. Nevada leads the nation in the production of gold, silver, mercury, and barite (Nevada Bureau of Mines and Geology 1997, p. 3). Gold is Nevada's leading commodity in terms of value (Nevada Bureau of Mines and Geology 1997, p. 3). Brucite, magnesite, clays, gemstones, gypsum, iron ore, lead, sand, gravel, and crushed stone are some of the commodities that also were, or are, produced in Nevada.

Previous Project Studies–Numerous investigations have been supported by the DOE in pursuing the assessment of natural resources at Yucca Mountain and the southern Great Basin. These include an early mineral resources assessment (Bell and Larson 1982), an environmental assessment (DOE 1986), the Site Characterization Plan (DOE 1988), a mineral withdrawal evaluation of the Yucca Mountain Addition (Castor et al. 1990), and a regional compilation of mineral resources (Berquist and McKee 1991).

The Yucca Mountain Project has supported numerous natural resources investigations; most were carried out under the natural resources study plan (USGS 1992). Isotope geochemistry studies were carried out by the U.S. Geological Survey (Neymark et al. 1995; Marshall et al. 1996; Peterman et al. 1994). Preliminary petroleum investigations were reported by the U.S. Geological Survey (Grow et al. 1994). Some preliminary natural resources information was included in the License Application Annotated Outline (YMP 1995).

Reports on the various commodities were prepared from 1994 through 1997. The commodity reports included geothermal resources (CRWMS M&O 1996c), industrial rocks and minerals (Castor and Lock 1995), metallic and mined energy resources (Castor, S.B.; Garside, L.J.; Tingley, J.V.; LaPointe, D.D.; Desilets, M.O.; Hsu, L-C.; and Goldstrand, P.M., *Assessment of Metallic and Mined Energy Resources in the Yucca Mountain Conceptual Controlled Area, Nye County, Nevada,* in review, Nevada Bureau of Mines and Geology), and hydrocarbon resources (French, D.E., *Assessment of Hydrocarbon Resources of the Yucca Mountain Vicinity, Nye County, Nevada*, in review).

Assumptions, Methods, and Procedures–The basic assumption used in this assessment is that resources throughout the Great Basin, including the Yucca Mountain study area, are defined on the basis of geological, geophysical, structural, and geochemical attributes, and that these attributes can be measured and compared. It is also assumed that natural resources within the study area occur within the same geologic environments as those in other parts of the Great Basin. The final assumption is that natural resource development is based on established engineering and economic principles and that the present conditions provide a valid projection for the foreseeable future.

3.1 METALLIC MINERAL AND MINED ENERGY RESOURCES

The Yucca Mountain region in the southern Great Basin contains valuable or potentially valuable metallic mineral deposits, including deposits with past or current production of gold, silver, mercury, base metals, and uranium (Figure 3-1). The presence of these deposits in the region and the identification of geologic features, including veins and normal faults at Yucca Mountain that are similar to those in mineralized areas, have led some writers to propose that the Yucca Mountain Conceptual Controlled Area may have potential for metallic mineral deposits (Johnson and Hummel 1991, p. 15; Weiss et al. 1996, p. 2081). There is no evidence, however, of any mining activity in the Yucca Mountain Conceptual Controlled Area.

3.1.1 Identified Metallic Resources in the Yucca Mountain Conceptual Controlled Area

On the basis of chemical analyses of samples collected in the Yucca Mountain Conceptual Controlled Area by Castor et al. (*Assessment of Metallic and Mined Energy Resources in the Yucca Mountain Conceptual Controlled Area, Nye County, Nevada*, in review, Nevada Bureau of Mines and Geology, p. 176), no ore-grade resources of metallic commodities have been identified, with the exception of tin. The estimated reserve of tin, however, is very low. On the basis of field examination, the amount of the type of rock in which the tin was detected appears to be minor in the Yucca Mountain Conceptual Controlled Area (see Castor et al., *Assessment of Metallic and Mined Energy Resources in the Yucca Mountain Conceptual Controlled Area, Nye County, Nevada,* in review, Nevada Bureau of Mines and Geology; Sections 5.7.2 [p. 142] and 6.2.10 [p. 165]).

3.1.1.1 Comparison of the Geology of the Yucca Mountain Conceptual Controlled Area with Mineralized Areas in the Region

The evaluation of the Yucca Mountain site relies on a comparison of the geology of the Yucca Mountain Conceptual Controlled Area to models of mineral deposition, along with geophysical and geochemical analysis of the area. Weiss et al. (1996, p. 2088) noted that Yucca Mountain is not attractive for present-day mineral exploration when compared to the nearby Bare Mountain, Calico Hills, and Wahmonie areas, but stated that similarities in stratigraphy, structure, some vein and alteration mineral assemblages, and geochemistry between the Yucca Mountain Conceptual Controlled Area and some mineralized areas are evidence that precious-metal deposits could be present in the Yucca Mountain Conceptual Controlled Area (Weiss et al. 1995,

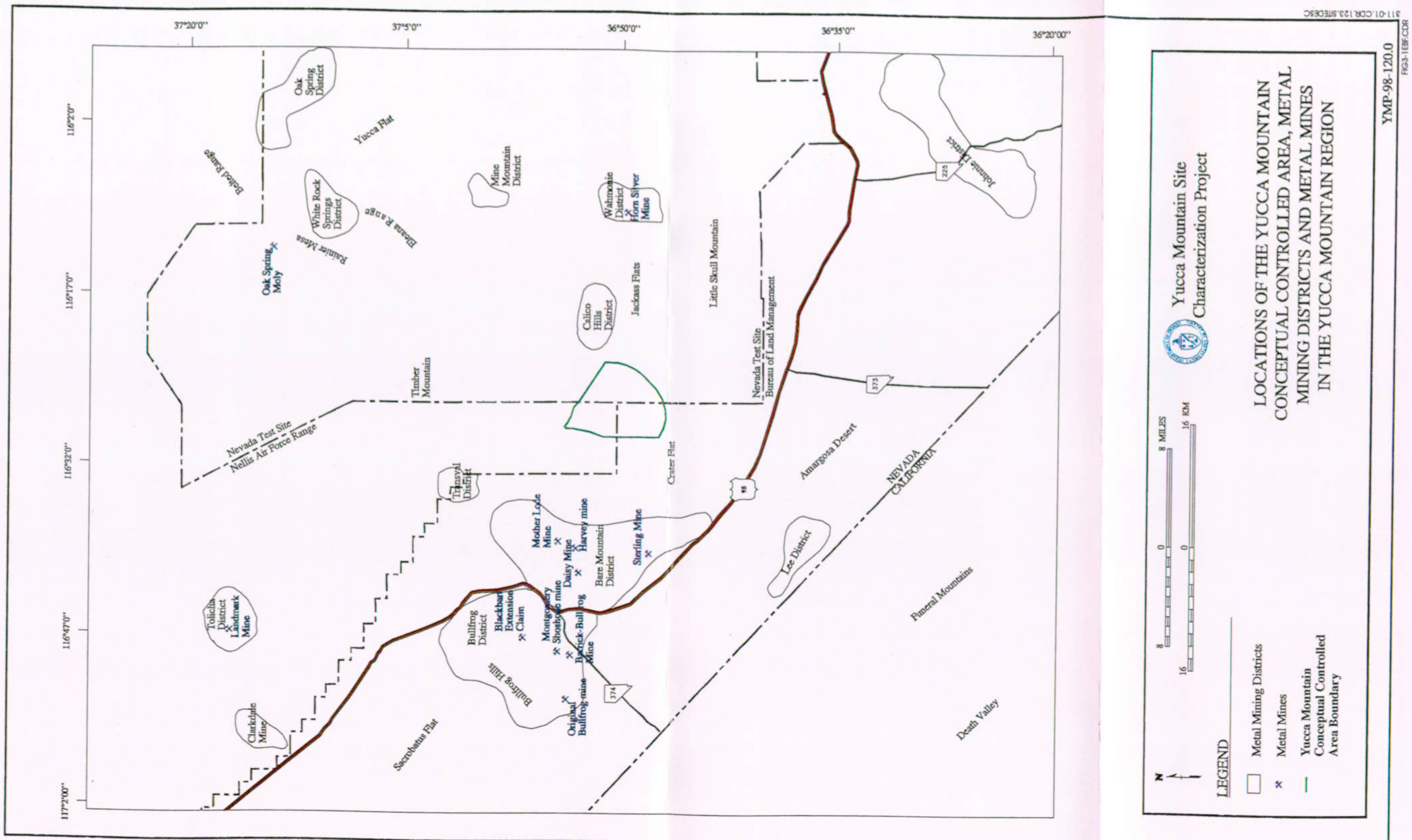

Source: CRWMS M&O (1998, Figure 3.11-1), and Castor, S.B.; Garside, L.J.; Tingley, J.V.; LaPointe, D.D.; Desilets, M.D.; Hsu, L-C.; Goldstrand, P.M. (*Assessment of Metallic and Mined Energy Resources in the Yucca Mountain Conceptual Controlled Area, Nye County, Nevada,* in review, Nevada Bureau of Mines and Geology)

Figure 3-1. Locations of the Yucca Mountain Conceptual Control Area, Metal Mining Districts, and Metal Mines in the Yucca Mountain Region

INTENTIONALLY LEFT BLANK

pp. 3-13; 1996, p. 2088). An evaluation of such comparisons was presented in Castor et al. (*Assessment of Metallic and Mined Energy Resources in the Yucca Mountain Conceptual Controlled Area, Nye County, Nevada,* in review, Nevada Bureau of Mines and Geology; Section 5.3 [pp. 76-81]).

Based on the discussions in Castor et al. (*Assessment of Metallic and Mined Energy Resources in the Yucca Mountain Conceptual Controlled Area, Nye County, Nevada,* in review, Nevada Bureau of Mines and Geology, p. 177), the potential for volcanic rock-hosted epithermal precious metal deposits at depth (in excess of 700 m or more) in the Yucca Mountain Conceptual Controlled Area cannot be completely ruled out. However, it probably could not be economically mined at such depths.

Castor et al. (1990, p. 69) argued that the pattern of faulting in the southwest part of the Yucca Mountain Conceptual Controlled Area was substantially different from that in precious-metal mining districts in the region. The data indicate that faults exposed at the surface in the Yucca Mountain Conceptual Controlled Area are generally subparallel and, therefore, that fault intersections, which are commonly important mineralization controls, are relatively rare in the Yucca Mountain area (Castor et al., *Assessment of Metallic and Mined Energy Resources in the Yucca Mountain Conceptual Controlled Area, Nye County, Nevada,* in review, Nevada Bureau of Mines and Geology, p. 77).

It appears that the alteration and mineralization which followed the deposition of the Paintbrush Group (see Section 1.2.2.2) and is present within a few kilometers of the Yucca Mountain Conceptual Controlled Area in the Calico Hills and in Claim Canyon does not extend into the Yucca Mountain Conceptual Controlled Area (Castor et al., *Assessment of Metallic and Mined Energy Resources in the Yucca Mountain Conceptual Controlled Area, Nye County, Nevada,* in review, Nevada Bureau of Mines and Geology, p. 158).

The presence of pre-Paintbrush Group hydrothermal activity in the northern Yucca Mountain area has been suggested by Weiss et al. (1996, p. 2081) as an important factor in the evaluation of the Yucca Mountain Conceptual Controlled Area for epithermal precious-metal deposits. The implication of these occurrences is that Paintbrush Group rocks in the Yucca Mountain Conceptual Controlled Area may overlie, and thus mask, areas of mineralized rocks in the Crater Flat Group and older rocks. However, the trace element chemistry of samples from the northern Yucca Mountain area do not include elevated precious metal contents, and while such occurrences demonstrate that local hydrothermal activity took place during Crater Flat Group magmatism, they do not provide direct evidence for an episode of precious-metal mineralization at that time.

Although hydrothermal activity that has produced economic or potentially economic mineralization occurs in volcanic rocks to the west, north, and east of the Yucca Mountain Conceptual Controlled Area, no clear evidence exists for extension of these episodes of mineralization into the Yucca Mountain Conceptual Controlled Area. Although Tertiary volcanic rocks at depth in the north part of the Yucca Mountain Conceptual Controlled Area contain features such as clay mineral assemblages, pyrite and barite in veins and alkali feldspar alteration that are suggestive of hydrothermal activity, there is no direct evidence for mineralized rocks containing potentially economic precious-metal deposits. (Castor et al., *Assessment of*

Metallic and Mined Energy Resources in the Yucca Mountain Conceptual Controlled Area, Nye County, Nevada, in review, Nevada Bureau of Mines and Geology, pp. 157-159). Drill hole samples from areas with suggestive alteration, vein mineralogy, and pathfinder (an element used in assessments that would indicate the possible existence of certain metallic minerals) element abundance have low gold, silver, and base metal contents.

3.1.2 Mined Energy Resources (Uranium)

It is not unusual to find a few elevated uranium values in hydrothermally altered rocks or vein material from volcanic-hosted epithermal mineral deposits. Occurrences of sparse uranium minerals or of anomalous amounts of uranium or radioactivity are not uncommon in Nevada's mining districts (Garside 1973, p. 1). It is likely that such sporadic uranium concentrations are related to redistribution by hydrothermal fluids in these districts, especially in those hosted by volcanic rocks that may have uranium available in amounts that could be moved and concentrated. In the majority of cases, these anomalous uranium concentrations from Nevada's precious- and base-metal mining districts are not known to form ore bodies (Castor et al., *Assessment of Metallic and Mined Energy Resources in the Yucca Mountain Conceptual Controlled Area, Nye County, Nevada,* in review, Nevada Bureau of Mines and Geology, p. 168).

Castor et al. (*Assessment of Metallic and Mined Energy Resources in the Yucca Mountain Conceptual Controlled Area, Nye County, Nevada,* in review, Nevada Bureau of Mines and Geology, p. 170) do not consider the anomalous amounts of uranium found in samples from Yucca Mountain as indicators of uranium deposits, but more likely, as indicators of uranium redistribution in ash-flow tuffs related to near-surface hydrologic processes. Fumarolic activity and high-temperature devitrification that took place shortly after eruption of the ash-flow tuffs (Stimac et al. 1996, pp. 263-264) or selective leaching later during weathering (Zielinski 1978, p. 413) may have made uranium more readily available for distribution. The highest amount of uranium found at the site (65 ppm) is far below what would be considered ore in today's market (at least 1,000 ppm) and the likelihood of economically mineable, concealed uranium deposits in the Yucca Mountain Conceptual Controlled Area is extremely low (Castor et al., *Assessment of Metallic and Mined Energy Resources in the Yucca Mountain Conceptual Controlled Area, Nye County, Nevada,* in review, Nevada Bureau of Mines and Geology, p. 177).

3.1.3 Conclusions

On the basis of extensive sampling and geochemical and mineralogical analyses by Castor et al. (*Assessment of Metallic and Mined Energy Resources in the Yucca Mountain Conceptual Controlled Area, Nye County, Nevada,* in review, Nevada Bureau of Mines and Geology) and previous work, the Yucca Mountain Conceptual Controlled Area contains no identified metallic mineral or uranium resources. In addition, on the basis of detailed study of the geology, geochemistry, mineralogy, mineral alteration, geophysical data, and remote sensing, the Yucca Mountain Conceptual Controlled Area is considered to have little or no potential for deposits of metallic minerals or uranium resources that could be mined economically now or in the foreseeable future. Simple statistical analyses indicate substantial differences between geochemical patterns for precious metals, base metals, and pathfinder elements between the Yucca Mountain Conceptual Controlled Area and metal mining districts in the region.

The highest metallic commodity values in the Yucca Mountain Conceptual Controlled Area occur in scattered occurrences of mineralized rock and alteration that are considered to be of fumarolic origin. These occurrences are thought to be of minimal size and have little potential for depth extension. A select sample containing about 0.003 percent tin was collected from one occurrence in the south part of the Yucca Mountain Conceptual Controlled Area; however, examination of the occurrence suggested that only very minor amounts of similar rock were present.

3.2 INDUSTRIAL ROCKS AND MINERALS RESOURCES

The Yucca Mountain region contains many occurrences of valuable or potentially valuable industrial rocks and minerals (Castor and Lock 1995, p. 1). Deposits with past or current production in the region include those of borate minerals, building stone, clay, construction aggregate, fluorspar, silicate, and zeolites (Figure 3-2; Castor and Lock 1995, p. 1). Clay minerals, zeolites, fluorite, and barite have been identified in samples from drill holes at Yucca Mountain (Caporuscio et al. 1982, pp. 1, 4, 6; Scott and Castellanos 1984, pp. 58-62; Bish 1989, pp. 1-2; Broxton, Bish et al. 1987, p. 89). The potential for industrial mineral resources in the Yucca Mountain Conceptual Controlled Area was assessed by Castor and Lock (1995) and the following discussion is summarized from their report.

3.2.1 Industrial Minerals in the Great Basin

Most of the industrial mineral production in the region surrounding the Yucca Mountain Conceptual Controlled Area has originated from four mining districts: the Bare Mountain, Bullfrog, Ash Meadows, and Death Valley mining districts (Castor and Lock 1995, p. 3). The first two had primarily precious metal production, whereas the Ash Meadows and Death Valley districts are solely industrial mineral districts (Castor and Lock 1995, p. 3).

3.2.2 Industrial Rocks and Minerals at Yucca Mountain

Many of the industrial rock and mineral commodities that occur in the Great Basin do not occur in geologic settings similar to that at Yucca Mountain; they include alunite, basalt, feldspar, gemstones, gypsum, kyanite, lithium, mica, pyrophyllite, quartz and quartzite, salt (salines and brines), sandstone, silica sand, sodium compounds (sodium carbonate and sulfate), sulfur, turquoise, and wollastonite. Barite, clay minerals, fluorite, and zeolites, have been identified in samples from Yucca Mountain (e.g., Caporuscio et al. 1982, p. 1; Scott and Castellanos 1984, pp. 58-62; Bish 1989, pp. 1-2; Broxton, Bish et al. 1987, p. 89). Building stone, construction aggregate, limestone, pumice, silica, and vitrophyre/perlite can also be found at Yucca Mountain and will also be discussed here.

3.2.2.1 Barite

Barite occurs sparingly in core from boreholes in the Yucca Mountain Conceptual Controlled Area (Castor and Lock 1995, p. 60). Minor amounts of barite occur in some thin veins in volcanic rock at depths of 1,200 m or more under Yucca Mountain. However, the Yucca Mountain Conceptual Controlled Area is considered to have little or no potential for barite production because these barite occurrences are minor and at such great depths.

3.2.2.2 Building Stone

In the Yucca Mountain Conceptual Controlled Area, considerable amounts of Tertiary tuff are accessible at the surface for use as building stone (Castor and Lock 1995, p. 55). The likelihood of excavation of this ash-flow tuff for building stone is dependent on intangible factors, including future demand for particular colors and textures of stone. The tuff in the Yucca Mountain Conceptual Controlled Area does not appear to have unique properties, either physical or aesthetic, that would make it especially valuable as a decorative dimension stone when compared with tuffs outside the Yucca Mountain Conceptual Controlled Area that are abundant in the region.

3.2.2.3 Clay

Although large amounts of smectite clay are clearly present in the Yucca Mountain Conceptual Controlled Area, most of the calculated subeconomic resource is too deep to make acceptable strip ratios for clay mining. In addition, the grade of most of the material is insufficient to compete with regional sources of clay (Castor and Lock 1995, p. 28).

3.2.2.4 Construction Aggregate

The canyons and alluvial fans in the Yucca Mountain Conceptual Controlled Area contain minor amounts of high-quality construction sand and gravel in comparison to regional resources (Castor and Lock 1995, p. 47). Most of the detritus in these sands and gravels is probably sound, durable welded ash-flow tuff; however, some structurally inferior nonwelded and bedded tuff fragments are probably also present. Abundant welded ash-flow tuff bedrock exposures in the Yucca Mountain Conceptual Controlled Area undoubtedly include material that has adequate soundness and durability for many of the uses of crushed stone. For concrete aggregate, alkaline reactivity problems that are commonly associated with silicic rhyolite may make both sand and gravel and bedrock deposits in the Yucca Mountain Conceptual Controlled Area less desirable. It should be noted that any use of these materials would only involve surface disturbing activities and will not result in potential inadvertent human intrusion into the repository. Under present circumstances, the Yucca Mountain Conceptual Controlled Area has little or no potential for production of construction aggregate except for internal use by the DOE or its contractors during repository construction or other activities in the vicinity.

3.2.2.5 Fluorite

Fluorite-bearing veins in the volcanic stratigraphic sequence at the site are thin and contain only small amounts of fluorine. No fluorite was identified during the surface appraisal of the Yucca Mountain Addition, and although fracture-coating fluorite was found in core at depths as shallow as 318 m, thicker veins that carry fluorite (up to 1 cm thick) occur at depths at or below 970 m. None of the reported occurrences of fluorite identified in small amounts in core and cuttings from the Yucca Mountain Conceptual Controlled Area are of sufficient grade or tonnage or of shallow enough depth to constitute an economic resource (Castor and Lock 1995, pp. 20-21).

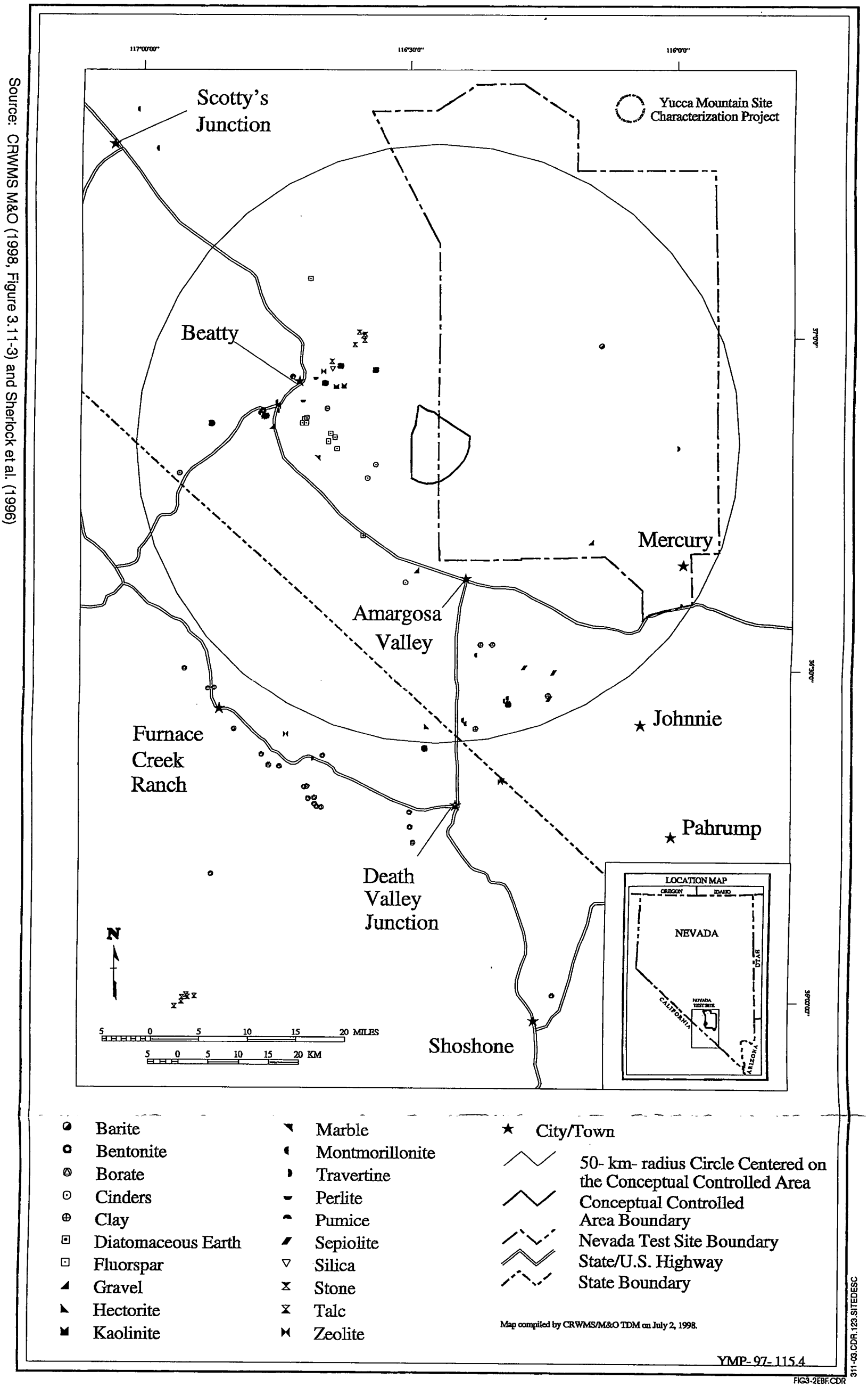

Source: CRWMS M&O (1998, Figure 3.11-3) and Sherlock et al. (1996)

Figure 3-2. Industrial Mineral Occurrences in the Vicinity of Yucca Mountain

INTENTIONALLY LEFT BLANK

3.2.2.6 Limestone

Limestone or dolomite, although abundant in the surrounding region, does not crop out in the Yucca Mountain Conceptual Controlled Area (Day et al. 1998). Given its low unit value, economic extraction of limestone and dolomite is not possible at the depths greater than 1,240 m which is where it occurs in the Yucca Mountain Conceptual Controlled Area (Carr, M.D. et al. 1986, pp. 16-17). The Yucca Mountain Conceptual Controlled Area is considered to have no potential for production of limestone or dolomite (Castor and Lock 1995, p. 89).

3.2.2.7 Pumice

The potential for pumice or pumicite production from the Yucca Mountain Conceptual Controlled Area is considered to be low (Castor and Lock 1995, p. 71). No occurrences of economic pumice or pumicite are known, and the pumiceous material that is present in the Paintbrush Group appears to be too consolidated or impure for commercial use. In addition, large resources of domestic pumice and pumicite are available for sale in a relatively stable, long-term market. Therefore, it is highly unlikely that new pumice or pumicite mines will be opened in the near future.

3.2.2.8 Silica

Neither the thin silica veins encountered in drill holes, or the impure siliceous breccia found on the surface, can be considered to have commercial significance as sources of silica (Castor and Lock 1995, p. 77). Volumetrically significant deposits of high-grade silica are not known to occur in the Yucca Mountain Conceptual Controlled Area and it is not considered to have any potential for silica production.

3.2.2.9 Vitrophyre/Perlite

No exposures or drill hole intercepts of glassy silicic domes, flows, or intrusions, which is the geologic environment for vitrophyre/perlite, have been recorded in the Yucca Mountain Conceptual Controlled Area, although these rocks are present a few kilometers to the north in the rhyolite of Forty Mile Canyon (Scott and Bonk 1984, p. 1). The Yucca Mountain Conceptual Controlled Area contains some dense vitrophyric welded ash-flow tuff layers that may contain expandable perlite; however, it is unlikely that these layers will be mined because of the large amount of overburden (Castor and Lock 1995, pp. 65-67).

3.2.2.10 Zeolites

A large subeconomic resource of zeolite is present at Yucca Mountain (Castor and Lock 1995, p. 40); however, the stratigraphic units that contain this estimated resource do not crop out within the Yucca Mountain Conceptual Controlled Area (Day et al. 1998). Although zeolitized rock may reach the surface along the northeast border of the Yucca Mountain Conceptual Controlled Area, the zeolite is covered by considerable thickness of tuff containing little or no zeolite (about 500 m) a short distance to the south. Because zeolite deposits are mined by open-pit methods, the amount of overburden is an important factor, and the zeolite subeconomic resource in the Yucca Mountain Conceptual Controlled Area occurs at depths that render commercial extraction

unlikely. The deposit is economically unattractive when compared with the large amounts of readily extractable higher-grade zeolite elsewhere in the western United States.

As noted by Papke (1972, pp. 27-28), zeolite deposits of the type that are present in tuff at Yucca Mountain are extensive in Nevada, and only have economic potential for uses that require impure materials of relatively low unit value. Given their low commercial value, relatively low grades, and the unfavorable mining situation, it is not likely that zeolites in the Yucca Mountain Conceptual Controlled Area will be commercially attractive in the foreseeable future (Castor and Lock 1995, p. 41).

3.3 HYDROCARBON RESOURCES

Brief discussions on oil and gas potential are presented as part of general resource evaluations in Bell and Larson (1982, p. 19) and Castor et al. (1990, pp. 72-73). Papers by Aymard (1989), Grow et al. (1994), Barker (1994), Cashman and Trexler (1995), and Trexler et al. (1996) have presented information aimed more directly at making an evaluation. Numerous papers on commercial and non-commercial occurrences are in Schalla and Johnson (1994) and other publications of the Nevada Petroleum Society. Subsection 3.3 is based primarily on French, D.E., *Assessment of Hydrocarbon Resources of the Yucca Mountain Vicinity, Nye County, Nevada*, in review.

3.3.1 Oil and Gas

The four components necessary for generation, migration, and preservation of hydrocarbons are source rocks, reservoir rocks, seals, and traps. These four components characterize the habitat of oil in the Great Basin and will be described in this section. This information can then be compared to the Yucca Mountain area to assess its potential for hydrocarbon resources.

Source rocks of Mississippian and Tertiary age have generated the oil that is commercially produced in the Great Basin (French, D.E., *Assessment of Hydrocarbon Resources of the Yucca Mountain Vicinity, Nye County, Nevada*, in review, p. 18). Likewise, source beds have been identified in the Mississippian and Tertiary stratigraphy of the Yucca Mountain area. However, Mississippian-age source rocks at Yucca Mountain are at an advanced state of maturity compared to counterparts in the area of Railroad and Pine valleys. This complicates the identification of a generation site in the vicinity of Yucca Mountain. Whereas the generation of oil is a relatively recent and an ongoing process in the producing areas, accumulations at Yucca Mountain that originated from Mississippian source rocks would likely be a product of generation from a site that is no longer intact. Tertiary-age source rocks are present in the Yucca Mountain area but the state of knowledge about them is meager. They may be present in the basin of Crater Flat where they could be buried adequately for generation to occur. Comparable circumstances exist in Railroad Valley where early Tertiary source rocks have generated the oil produced at Eagle Springs Field and in the Great Salt Lake where oil from Neogene source rocks is produced.

Reservoir rocks of the Yucca Mountain area compare favorably with those of the producing areas of the region. Paleozoic carbonate rocks, early Tertiary limestone, middle Tertiary ash-flow tuffs, and late Tertiary debris slides and basalt are proven reservoirs in the region and

have counterparts in the vicinity of Yucca Mountain. In addition, cavernous porosity is present in a wider range of stratigraphy around Yucca Mountain than exists in the producing areas.

The most important sealing horizon in the Great Basin, the unconformity at the base of the valley fill, is absent at Yucca Mountain. The unconformity is present in Crater Flat where it could act as a seal for accumulations in volcanic rocks, but it is dissimilar to the unconformity of the producing areas. Because the basin of Crater Flat began to form during the deposition of the Tertiary volcanic sequence, these rocks became part of the basin-fill section. Consequently, the unconformity is difficult to identify as a discrete horizon representing a single continuous span of time at Crater Flat. This contrasts sharply with Railroad Valley where there is a significant time break between the cessation of deposition of volcanic strata and the onset of deposition of syntectonic basin-fill sediments (French, D.E., *Assessment of Hydrocarbon Resources of the Yucca Mountain Vicinity, Nye County, Nevada*, in review, p. 10).

Fault-block traps similar to those that produce elsewhere in the Great Basin are also present at Yucca Mountain. Certain special circumstances, like the faulted debris slides that produce at Kate Spring Field, have been eroded from Yucca Mountain, but are present in the Crater Flat basin adjacent to the west.

The basic elements of a viable petroleum system are present in the Yucca Mountain area; therefore, the petroleum potential is not zero (French, D.E., *Assessment of Hydrocarbon Resources of the Yucca Mountain Vicinity, Nye County, Nevada*, in review, p. 20). In comparing the Yucca Mountain area to known producing fields in the region, the area of a potential generation site and volume of potential source rock are limited compared with the productive basins in the region, and one of the important seals of the region is not well developed in the Yucca Mountain area. The conditions of source, reservoir, trap, and seal that characterize petroleum accumulations of the Great Basin are present, with variations, in the Yucca Mountain area. Most of the variations, however, have negative implications for the accumulation of hydrocarbons at the repository site (French, D.E., *Assessment of Hydrocarbon Resources of the Yucca Mountain Vicinity, Nye County, Nevada*, in review, p. 18).

3.3.2 Tar Sands

It is extremely unlikely that tar sands are concealed at depth below Yucca Mountain but not exposed in rocks of the surrounding area (Castor et al., *Assessment of Metallic and Mined Energy Resources in the Yucca Mountain Conceptual Controlled Area, Nye County, Nevada,* in review, Nevada Bureau of Mines and Geology, p. 172). There is no evidence for the accumulation of such deposits in the region, and the area of Yucca Mountain is considered to have low potential for the accumulation and preservation of liquid petroleum as well (Grow et al. 1994, p. 1314). In the unlikely event that tar sands were present at Yucca Mountain, they would most likely be found in the Paleozoic marine rocks which occur at depths of 1,200 m or more. Conventional recovery methods for tar sands require surface mining and processing of large volumes of rock. Mass mining underground at such depths is certainly not economically feasible now or in the foreseeable future.

3.3.3 Oil Shale

It is not certain if rocks with a depositional environment compatible with oil shales are present at depth under Yucca Mountain. Even if rocks containing oil shales are present beneath Yucca Mountain, they have probably been heated, with consequent loss of hydrocarbons. In the unlikely event that oil shales of some richness do occur under Yucca Mountain, the minimum depth to such rocks below Yucca Mountain is 1,200 m (Castor et al., *Assessment of Metallic and Mined Energy Resources in the Yucca Mountain Conceptual Controlled Area, Nye County, Nevada,* in review, Nevada Bureau of Mines and Geology, p. 173; Section 1.2.2.1). Such speculative deposits would have to be mined by underground methods at those depths and that is unlikely until other more cost-effective energy sources (including rich surface oil shales in the United States) are near exhaustion in the distant future. Economic conditions in the United States have not yet warranted exploitation of rich oil shales such as those exposed at the surface in the Green River Formation of Wyoming. Thus, oil shales are unlikely in the Yucca Mountain Conceptual Controlled Area, and if any are present, exploitation is not economically feasible for the foreseeable future (Castor et al., *Assessment of Metallic and Mined Energy Resources in the Yucca Mountain Conceptual Controlled Area, Nye County, Nevada,* in review, Nevada Bureau of Mines and Geology, p. 173).

3.3.4 Coal

There are no reports of coal from southern Nevada in the vicinity of Yucca Mountain (Castor et al., *Assessment of Metallic and Mined Energy Resources in the Yucca Mountain Conceptual Controlled Area, Nye County, Nevada,* in review, Nevada Bureau of Mines and Geology, p. 174). Because coal was actively sought during early mining and mineral exploration, it seems unlikely that any coal beds of significance were not discovered; during this period prospectors had access to areas now excluded from mining and prospecting (the Nevada Test Site and the Nellis Air Force Range).

Economic coal deposits are usually found in lacustrine deposits. No coal or coal-bearing Tertiary sedimentary rocks have been encountered in drillholes on and adjacent to Yucca Mountain (Castor et al., *Assessment of Metallic and Mined Energy Resources in the Yucca Mountain Conceptual Controlled Area, Nye County, Nevada,* in review, Nevada Bureau of Mines and Geology, p. 175). In the Yucca Mountain area, rocks younger than about 15 Ma are almost entirely volcanic in character, consisting of Miocene ash-flow tuffs, flows, and associated bedded pyroclastic rocks. No significant lacustrine units are known from this sequence in the site area (CRWMS M&O 1996d).

3.4 GEOTHERMAL RESOURCES

The *Yucca Mountain Site Description* (CRWMS M&O 1998, Section 3.11.5) contains a detailed discussion of geothermal resources and a comparison of characteristics indicative of geothermal activity to the characteristics of the Yucca Mountain Area. In summary, this comparison indicates the following: recent volcanism is only of small volume and is isolated; the temperature gradient at Yucca Mountain is low or below average; there are no geysers, fumaroles, or hot springs nearby; there is no siliceous sinter present; the high silica water anomaly, na/k anomaly, and geophysical anomaly are all non-thermal; the only appreciable

porosity or permeability is in the deep carbonate aquifer; there are no geothermal discoveries nearby; and there are no competitive interests present.

3.4.1 Absence of a Heat Source

Magma bodies below larger calderas (>10 km diameter) cool slowly and may be heat sources for up to 2 Ma (Wohletz and Heiken 1992, p. 160). Silicic volcanism located close enough to Yucca Mountain to have provided heat to the local hydrologic regime ended more than 11 Ma. Thus, there is no potential heat source to drive exploration for geothermal resources at Yucca Mountain.

3.4.2 Hydrology and Heat Flow

Heat flow at Yucca Mountain is less than 60 and as low as 30 mW/m^2 (Sass, Lachenbruch, Dudley 1988, pages 36-37, Table 5) which is much less than the Basin and Range average (100 ± 20 mW/m^2), or the regional heat flow (about 85 mW/m^2; Sass, Lachenbruch, Dudley 1988, page 44). For deep holes (approximately 300 meters to 600 meters deep) with minimal hydrologic disturbance, the temperature gradient is on the order of 30°C/km (Sass, Lachenbruch, Dudley 1988, pages 38-39, Table 6). The highest temperature measured at Yucca Mountain is 62°C, at about 1,800 meters depth in borehole USW H-1 (Sass, Lachenbruch, Dudley 1988, Appendix I, page 73, Figure 1-13). Temperatures, thermal gradients, and heat flow at Yucca Mountain vary greatly over small distances vertically and laterally (i.e., small wavelength), indicating dominance of relatively shallow hydrologic factors (Sass, Lachenbruch, Dudley 1988, pages 24, 31, 42). The water table at Yucca Mountain is generally 500 to 700 meters beneath the irregular land surface, and the temperature at the water table ranges between 29°C and 39°C (Sass, Lachenbruch, Dudley 1988, Appendix I, pp 66, 67, 69-81, Figures 1-6, 1-7, 1-9 through 1-21).

3.4.3 Indirect Indications of Potential Geothermal Systems

In addition to direct observations of a geothermal system, the presence of a potential geothermal system can be assessed through indirect observations of thermal springs and spring deposits, stable isotopes, and chemical geothermometers.

The lack of siliceous spring deposits at Yucca Mountain suggests that no thermal fluids from high-temperature reservoirs have discharged to the surface in the study area in the last 1.6 Ma (Section 1.2.2.4, Table 1-2; CRWMS M&O 1996c, p. 28).

Available information on spring deposits in the southern Great Basin indicates that presently flowing or pre-existing springs were or are only moderately warm (probably 30 to 40°C). There is no indication from geological, geophysical, geochemical, and drilling data that the area surrounding the Yucca Mountain site, including the Yucca Mountain Conceptual Controlled Area, has potential for anything but low-temperature geothermal resources (and those only at depth) (CRWMS M&O 1996c, p. 92).

3.4.4 Conclusions

Results documented in CRWMS M&O (1996c, p. 92) indicated that thermal resources at Yucca Mountain are classed as low temperature (defined as being within the range from 25 to 90°C) and occur at depths in excess of 400 m. Chemical analyses of fluids throughout the area and in various lithologic formations indicate that the water is non-thermal in origin. Geophysical data, including gravity, magnetic, seismic, and heat flow data failed to delineate any systematic structural evidence for a thermal anomaly. Hydrological data indicate that thermal fluids, where they exist, are restricted to faults, fractures, breccia zones, and the deep Paleozoic carbonate aquifers. Compared with the physical attributes of geothermal systems that have been developed in other parts of the Great Basin, no economically viable resources were identified within the Yucca Mountain area. Some surface geothermal manifestations were identified within a 50-mile radius of Yucca Mountain, but, based on the present level of development, recreational uses are the only likely applications (CRWMS M&O 1996c, p. 92)

4. GEOENGINEERING

4.1 INTRODUCTION

This section summarizes the geoengineering properties of the site with specific focus on the potential repository block (Figure 4-1). Geoengineering properties include the physical, mechanical, thermal, thermal/mechanical, and other relevant special properties of the various units of geologic material constituting the site. Figure 4-1 shows the location of boreholes, the ESF, and test alcoves that were sources of data. This section is based on Section 3.7 of the *Yucca Mountain Site Description* (CRWMS M&O 1998).

The primary emphasis in this section is on the description of the geoengineering properties in the potential repository block. Investigations were focused on the lithostratigraphic units proposed as the repository host horizon. However, the planned location of the repository host horizon has been adjusted during the course of design and investigation. Geoengineering properties of near-surface geologic materials have been investigated outside the repository block for the design of surface facilities (Figure 4-1). This information is also summarized below.

Data from laboratory testing of intact (borehole) samples and in situ testing at larger scales were analyzed to determine the geoengineering properties of the site. Testing and analyses were conducted in the context of other site properties. Experimental observations are the primary source of the geoengineering properties database.

4.2 STRATIGRAPHIC FRAMEWORK FOR TESTING

The general stratigraphy of the area is illustrated in Figure 4-2, which has been abstracted from the more extensive stratigraphy described in Section 1.2 and CRWMS M&O (1998, Tables 3.5-1 and 3.5-2). Cross-sections along the north ramp, main drift, and the south ramp of the ESF are shown on Figures 4-3, 4-4, and 4-5, respectively. Rocks that are important to repository design are mainly within the Miocene age Paintbrush Group, which consists of welded and nonwelded ashflow deposits. The formations within the Paintbrush Group, as shown on Figure 4-2 and described in greater detail in Section 1.2, include, in ascending order, the Topopah Spring Tuff, the Pah Canyon Tuff, the Yucca Mountain Tuff, and the Tiva Canyon Tuff. Below the rocks of the Paintbrush Group is the Calico Hills Formation. Overlying the Paintbrush in local areas near Exile Hill are younger, nonwelded ashflow and air-fall tuffs, including tuff unit "X" and the Rainier Mesa and Ammonia Tanks tuffs of the Timber Mountain Group.

The late Tertiary and Quaternary surficial sedimentary deposits of the Yucca Mountain area consist of colluvium; alluvium; wind blown (eolian) sand sheets, ramps, and dunes; and spring deposits (CRWMS M&O 1998, Section 3.4). These range in age from late Pliocene to Holocene. Surficial deposits are described in greater detail in Section 1.2 and in CRWMS M&O (1998, Sections 3.4 and 3.7.7).

The Yucca Mountain project developed a thermal/mechanical stratigraphy to provide a systematic basis for characterizing the rock mass in the site area based on geoengineering properties of the rock units and to facilitate analysis of the response of the rock to repository construction, operation, and long-term performance. This stratigraphic system is based on

thermal and mechanical rock characteristics that are important to repository design, and was developed by designating lithologic units, in whole or part, or a group of contiguous units or parts, as thermal/mechanical units. Ortiz et al. (1985, p. 3) proposed this nomenclature to group rocks with similar thermal and mechanical properties. The stratigraphy was based on the observation (Lappin et al. 1982, p. 20) that thermal and mechanical properties can be correlated directly to grain density and porosity. The stratigraphy of Ortiz et al. (1985, p. 10, Table 1) includes 16 thermal/mechanical units, seven of which are shown on Figure 4-2. The thermal/mechanical units were originally identified megascopically in terms of their welding and lithophysal cavity content.

The definition of thermal/mechanical units reflects to a large extent the general degree of welding (see CRWMS M&O 1998, Section 3.5, Table 3.5-2, p. 3.7-2). The thermal/mechanical units correlate generally with groups of lithostratigraphic units, or in the case of the Topopah Spring Tuff, parts of a lithostratigraphic unit (Figure 4-2; CRWMS M&O 1998, p. 3.7-2, Tables 3.5-2 and 3.7-1). The upper two Topopah Spring Tuff welded units, TSw1 and TSw2, are both within the densely welded, devitrified Topopah Spring Tuff. Originally, Ortiz et al. (1985, p. 11) defined the TSw1 as containing more than 10 percent void space from lithophysal cavities and TSw2 as containing less than 10 percent void space from lithophysal cavities. However, the change in percentage of lithophysae does not occur at a consistent stratigraphic position in the crystal-poor upper lithophysal zone and can be difficult to identify. For this reason, the Tptpul (upper lithophysal zone)-Tptpmn (middle nonlithophysal zone) lithostratigraphic contact is now used to define the TSw1-TSw2 thermal/mechanical contact and the top of the proposed repository host horizon is now aligned with the horizon below which lithophysae content is less than 10 percent (CRWMS M&O 1997d, Section 7.3, pp. 36-38). This may be up to 30 m above the Tptpul-Tptpmn lithostratigraphic contact (Spengler and Fox 1989, pp. 26-27). Recently, CRWMS M&O (1997d, p. 45) indicated that the top of the repository host horizon is up to 45 m above the contact north of the proposed emplacement area. It appears to be up to 30 to 35 m above the contact within the proposed emplacement area.

The uppermost identified thermal/mechanical unit is the undifferentiated overburden unit. This is a collection of various rock and soil types that overlie the welded, devitrified Tiva Canyon Tuff. The overburden unit includes alluvium, colluvium, nonwelded, and vitric portions of the Tiva Canyon Tuff, and other tuff units such as the Rainier Mesa Tuff of the Timber Mountain Group, tuff unit "X," and their associated bedded tuff units (See Figure 4.2; and Ortiz et al. 1985, Table 1).

Most of the Tiva Canyon Tuff is contained in the Tiva Canyon welded thermal/mechanical unit (TCw). This unit includes rock between and including the densely welded subzone of the vitric zone of the crystal-rich member and the densely welded subzone of the vitric zone of the crystal-poor member. The unit is exposed on top of Yucca Crest and the ridges on the eastern flank of Yucca Mountain.

Below the TCw is the Paintbrush Tuff nonwelded thermal/mechanical unit (PTn). This unit consists of partially welded to nonwelded, vitric and, in places, devitrified tuffs. The nonwelded and moderately welded tuffs at the base of the Tiva Canyon Tuff, the Yucca Mountain Tuff, the Pah Canyon Tuff, the nonwelded and moderately welded tuffs at the top of the Topopah Spring Tuff, and the associated bedded tuffs are included in this unit.

Source: CRWMS M&O (1998, Figure 3.7-1)

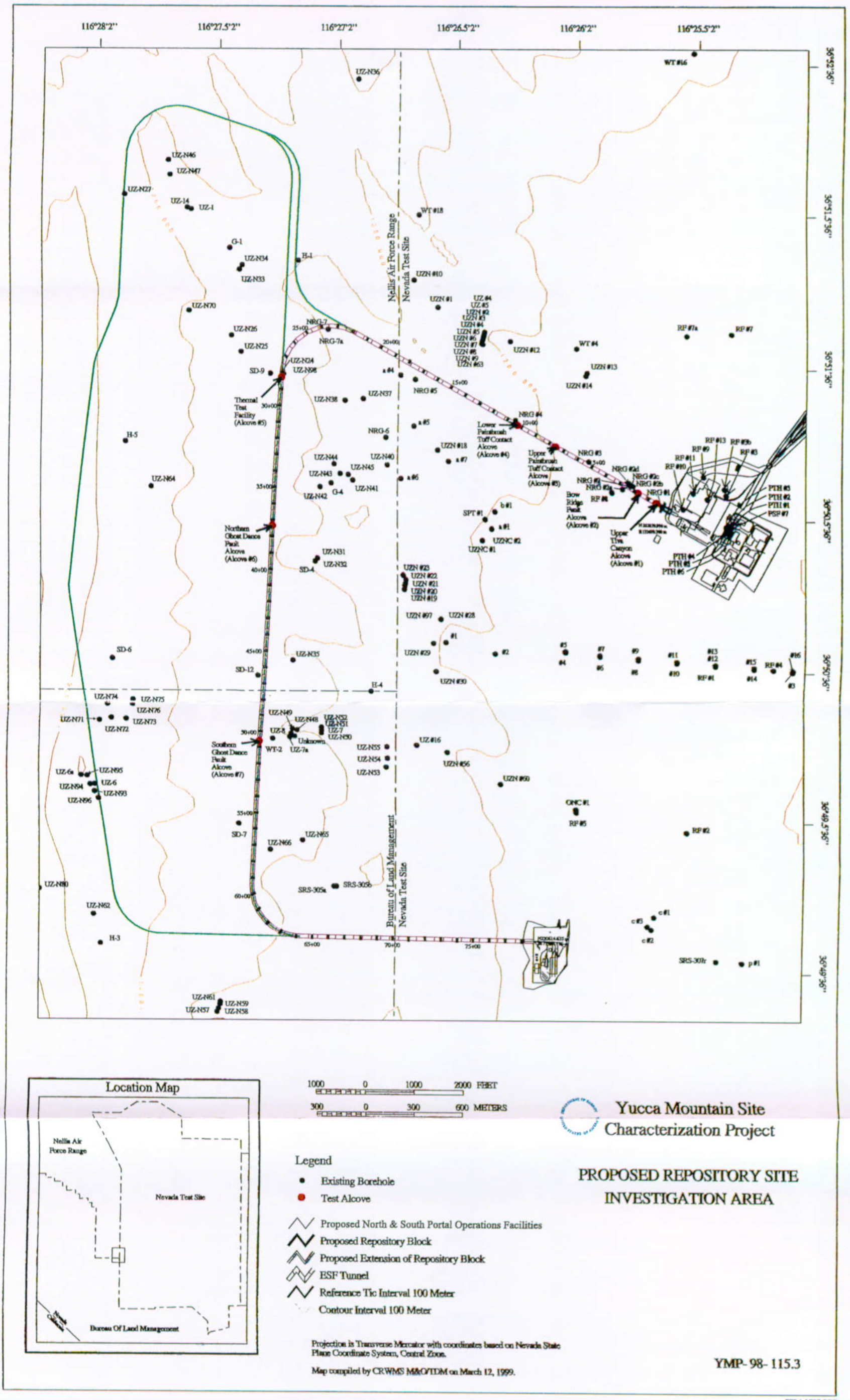

Figure 4-1. Proposed Repository Site Investigation Area

INTENTIONALLY LEFT BLANK

Lithostratigraphic Units[1,5,6,7]		Thermal/Mechanical Units[1,2]	Hydrogeologic Units[3]
Timber Mountain Tuff (Tm)	Rainier Mesa member (Tmr)	Undifferentiated overburden (UO)	Unconsolidated Surficial Materials (UO)
	Pre- Rainier Mesa bedded tuff (Tmbt1)		
PAINTBRUSH GROUP (Tp)			
	rhyolite of Comb Peak (Tpk); includes the pyroclastic flow deposit (Tpki) that is informally referred to as tuff unit "X" (Tpki)		
	post-Tiva Canyon bedded tuff (Tpbt5)		
Tiva Canyon Tuff (Tpc)	crystal-rich member (Tpcr) vitric zone (Tpcrv) -nonwelded subzone (Tpcrv3) -moderately welded subzone (Tpcrv2) -densely welded subzone (Tpcrv1) nonlithophysal zone (Tpcrn) lithophysal zone (Tpcrl)	Tiva Canyon welded (TCw)[4]	Tiva Canyon welded (TCw)
	crystal-poor member (Tpcp) upper lithophysal zone (Tpcpul) middle nonlithophysal zone (Tpcpmn) lower lithophysal zone (Tpcpll) lower nonlithophysal zone (Tpcpln) -hackly subzone (Tpcplnh) -columnar subzone (Tpcpinc) vitric zone (Tpcpv) -densely welded subzone (Tpcpv3) -moderately welded subzone (Tpcpv2) -nonwelded subzone (Tpcpv1)	Paintbrush Tuff nonwelded (PTn)	Paintbrush nonwelded (PTn)
	pre-Tiva Canyon bedded tuff (Tpbt4)		
Yucca Mountain Tuff (Tpy)	Yucca Mountain Tuff (Tpy)		
	pre-Yucca Mountain bedded tuff (Tpbt3)		
Pah Canyon Tuff (Tpp)	Pah Canyon Tuff (Tpp)		
	pre-Pah Canyon bedded tuff (Tpbt2)		
Topopah Spring Tuff (Tpt)	crystal-rich member (Tptr) vitric zone (Tptrv) -nonwelded subzone (Tptrv3) -moderately welded subzone (Tptrv2) -densely welded subzone (Tptrv1) nonlithophysal zone (Tptrn) lithophysal zone (Tptrl)	Topopah Spring welded, lithophysae-rich (TSw1)	Topopah Spring welded (TSw)
	crystal-poor member (Tptp) upper lithophysal zone (Tptpul) [upper part]		
REPOSITORY HOST HORIZON[5]	upper lithophysal zone (Tptpul) [lower part] middle nonlithophysal zone (Tptpmn) lower lithophysal zone (Tptpll) lower nonlithophysal zone (Tptpln)	Topopah Spring welded, lithophysae-poor (TSw2)	
	vitric zone (Tptpv) -densely welded subzone (Tptpv3) -moderately welded subzone (Tptpv2) -nonwelded subzone (Tptpv1)	Topopah Spring welded, vitrophyre (TSw3)	Topopah Spring basal vitrophyre (TSbv)
	pre-Topopah Spring bedded tuff (Tpbt1)	Calico Hills Nonwelded (CHn)	Calico Hills nonwelded (CHn)
Calico Hills (Tac)	Calico Hills Formation (Tac)		
	pre-Calico Hills bedded tuff (Tacbt)		

1) Buesch, Spengler et al. (1996)
2) Ortiz et al. (1985)
3) Arnold et al. (1995)
4) Where preserved, the base of the crystal-poor densely welded subzone (Tpcpv3) forms the base of the TCw thermal-mechanical and hydrogeologic units (Buesch, Spengler et al. 1996)
5) CRWMS M&O (1997d)
6) Moyer et al. (1995)
7) Geslin et al. (1995)

Source: CRWMS M&O (1998, Table 3.7-1)

Figure 4-2. Comparison of Several Stratigraphic Subdivisions of Mid-Tertiary Volcanic Rocks at Yucca Mountain

The Topopah Spring welded thermal/mechanical unit (TSw) underlies the PTn. This unit is subdivided into three subunits based on the percentage of total rock volume occupied by lithophysae and the identification of the crystal-rich vitrophyre. The top subunit (TSw1) is lithophysae-rich. This subunit includes several parts of the Topopah Spring crystal-rich member (Tptr) plus the upper part of the Topopah Spring crystal-poor member, as shown on Figure 4-2. This upper subunit ranges from about 49 to 113 m thick (CRWMS M&O 1998, p. 3.7-3). The middle subunit (TSw2) is lithophysae-poor and consists of the middle nonlithophysal, lower lithophysal, and lower nonlithophysal zones. The TSw2 sub-unit ranges in thickness from 175 to 229 m. The vitrophyre subunit (TSw3) at the base of the Topopah Spring welded unit is about 7 to 25 m thick (CRWMS M&O 1998, p. 3.7-3, Table 3.5-2).

The Calico Hills nonwelded unit (CHn) underlies the TSw unit. This unit consists of the lower nonwelded to partially welded portion of the Topopah Spring Tuff, the Calico Hills Formation, the underlying pre-Calico Hills bedded tuff, and the upper nonwelded portions of the underlying Prow Pass Tuff of the Crater Flat Group.

As shown in Figure 4-2, the TSw2 thermal/mechanical unit and the lower portion of the TSw1 thermal/mechanical unit have been identified as the proposed repository host horizon (CRWMS M&O 1997c, pp. 2-3, 3-5; 1997d, p. 37). This includes the lower portion of the Tptpul (upper lithophysal zone) lithostratigraphic unit, and the whole of the Tptpmn (middle nonlithophysal zone), Tptpll (lower lithophysal zone), and Tptpln (lower nonlithophysal zone) lithostratigraphic units.

4.3 ROCK STRUCTURE PROPERTIES FROM FIELD STUDIES

A description and analysis of rock structural geological data from surface mapping of fractures, detailed line surveys, and underground scanline mapping in the ESF are presented in CRWMS M&O (1998, Section 3.6). The data synthesis includes fracture orientation distributions, trace length distributions, fracture intensity for various stratigraphic units, fracture connectivity, and fracture aperture and mineralization. A brief summary is presented here.

Joints within the Paintbrush Group have been subdivided into early cooling joints, later tectonic joints, and joints due to erosional unloading. Each type of joint exhibits different characteristics that may impact trace length, connectivity, and orientation. Cooling joints and tectonic joints are similar in orientation but differ in surface roughness. Joints due to erosional unloading have a different orientation and tend to be cross joints terminating at pre-existing joints (Sweetkind and Williams-Stroud 1996, p. 71).

Cooling joints are identified in every unit that is at least moderately welded. They occur as two nearly orthogonal sets of steeply dipping joints, with a third, subhorizontal joint set that occurs irregularly. Very general information on fracture intensity and connectivity indicates that the highest joint frequencies and connectivities occur in the nonlithophysal units of the Tiva Canyon and Topopah Spring tuffs. Nonwelded tuffs of the PTn had the lowest joint frequencies and lowest observed connectivities.

ESF North Ramp As-Built Cross Section
Looking North

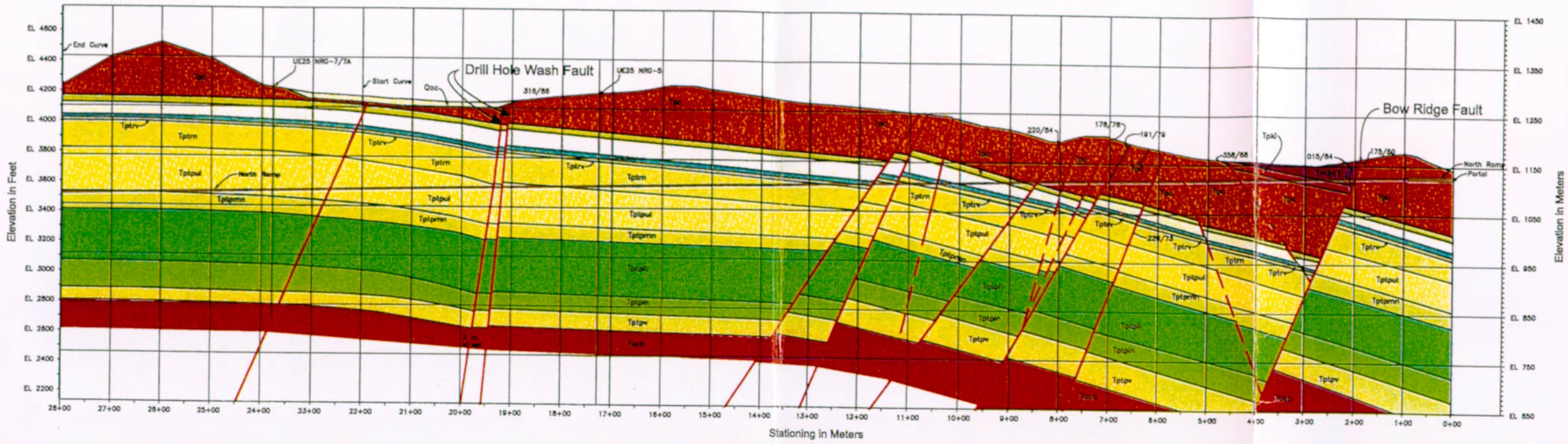

EXPLANATION

Quaternary

Qac — Alluvial and colluvial deposits

Timber Mountain Group

Rainier Mesa Tuff

Tmbt1 — Pre-Rainier Mesa Tuff bedded tuff

Paintbrush Group

Tpki — Rhyolite of Comb Peak, ignimbrites (tuff unit "x") and includes post-Tiva Canyon Tuff bedded tuff (Tpbt5)

Tiva Canyon Tuff

Tpc — undifferentiated

Paintbrush Group

Yucca Mountain Tuff

Tpy — includes pre-Tiva Canyon Tuff bedded tuff (Tpbt4)

Pah Canyon Tuff

Tpp — non- to moderately welded, includes pre-Yucca Mountain Tuff bedded tuff (Tpbt3)

Tpbt2 — Pre-Pah Canyon bedded tuff

Paintbrush Group

Topopah Spring Tuff

Crystal-rich member

Tptr — Crystal-rich member

Crystal-poor member

Tptpul — Upper lithophysal zone

Tptpmn — Middle nonlithophysal zone

Tptpll — Lower lithophysal zone

Tptpln — Lower nonlithophysal zone

Tptpv — Vitric zone

Calico Hills Group

Tacb — Calico Hills undifferentiated

FIG4-3ESF.CDR

Source: CRWMS M&O (1998, Figure 3.7-2)

Figure 4-3. Stratigraphic Cross Section Along the Exploratory Studies Facility North Ramp

INTENTIONALLY LEFT BLANK

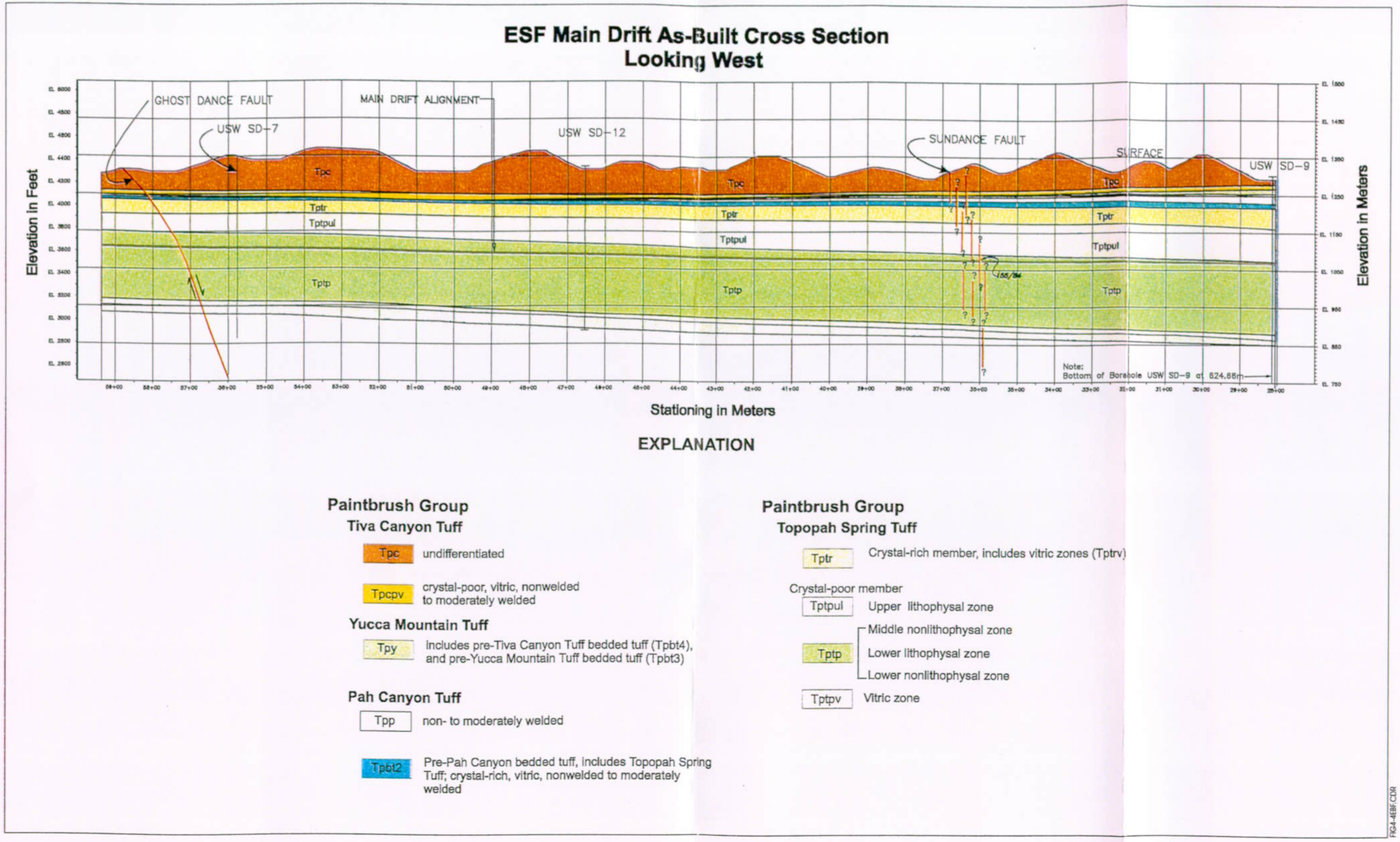

Source: CRWMS M&O (1998, Figure 3.7-4)

Figure 4-4. Stratigraphic Cross Section Along the Exploratory Studies Facility Main Drift

INTENTIONALLY LEFT BLANK

ESF South Ramp As-Built Cross Section
Looking North

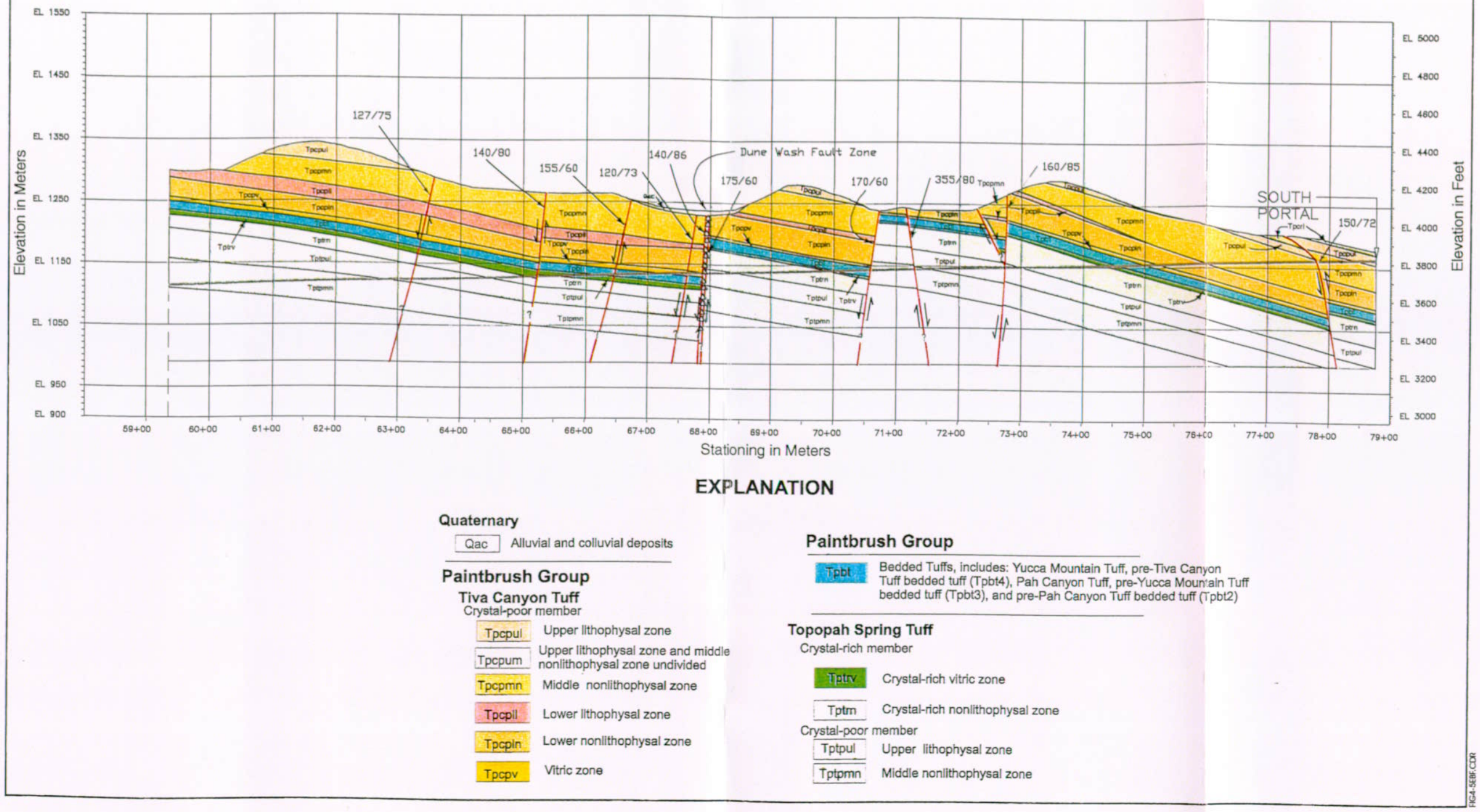

EXPLANATION

Quaternary

- Qac — Alluvial and colluvial deposits

Paintbrush Group

Tiva Canyon Tuff

Crystal-poor member

- Tpcpul — Upper lithophysal zone
- Tpcpum — Upper lithophysal zone and middle nonlithophysal zone undivided
- Tpcpmn — Middle nonlithophysal zone
- Tpcpll — Lower lithophysal zone
- Tpcpln — Lower nonlithophysal zone
- Tpcpv — Vitric zone

Paintbrush Group

- Tpbt — Bedded Tuffs, includes: Yucca Mountain Tuff, pre-Tiva Canyon Tuff bedded tuff (Tpbt4), Pah Canyon Tuff, pre-Yucca Mountain Tuff bedded tuff (Tpbt3), and pre-Pah Canyon Tuff bedded tuff (Tpbt2)

Topopah Spring Tuff

Crystal-rich member

- Tptrv — Crystal-rich vitric zone
- Tptrn — Crystal-rich nonlithophysal zone

Crystal-poor member

- Tptpul — Upper lithophysal zone
- Tptpmn — Middle nonlithophysal zone

FIG4-5EBF.CDR

Source: CRWMS M&O (1998, Figure 3.7-3)

Figure 4-5. Stratigraphic Cross Section Along the Exploratory Studies Facility South Ramp

INTENTIONALLY LEFT BLANK

Data from borehole studies indicate that rock quality calculated from core data was relatively low for all stratigraphic units. Substantial amounts of core in all lithostratigraphic units was either lost or recovered as rubble. Combining data from each of the boreholes, the amount of lost core for the Tptpmn lithostratigraphic unit was 15 percent of the total core length. Rubble zones accounted for 20 percent of the total length. The high proportion of lost core and rubble is attributed to the degree of small-scale fracturing of the welded rocks and the presence of other inhomogeneities such as lithophysae and vapor-phase alteration. Fracturing also may have been induced along a subhorizontal fabric or foliation by drilling. These inhomogeneities had a large influence on core recovery and core quality, but have much less significance at the tunnel scale. Lost core and rubble zones did, however, limit description of core in places where individual features could not be reconstructed.

While core recovery is related to the quality of rock encountered in a boring, it also is influenced to some degree by the drilling technique and type and size of core barrel used. The rock quality designation (Deere 1968, p.15) is a recovery ratio that provides an alternative estimate of in situ rock quality. This ratio is determined by considering only pieces of core that are at least 100 mm (4 inches) long. Rock quality designation is calculated as the percentage ratio between the total length of such core recovered and the length of core drilled on a given run.

This index has been widely used as a general indicator of rock mass quality and is an input for determination of indices of rock mass quality, such as rock mass rating and rock mass quality index, discussed in Section 4.5.1, below.

The rock quality designation used for geotechnical design purposes considered all breaks in the core, including those identified by geological/geotechnical staff as drilling-induced and those indeterminate as to their natural or drilling-induced origin. Rock quality designation was generally not high in any unit, due to the relatively low recovery of intact core, the high frequency of core fractures, and the consideration of drilling-induced mechanical breaks as fractures. Using the relative rock quality descriptions based on rock quality designation developed by Deere (1968, pp. 15-16), rock quality of core in the Tptpmn stratigraphic zone of the TSw2 thermal/mechanical unit ranges from poor to very poor among the boreholes evaluated. Within the Tptpmn are two intervals of generally higher rock quality designation bounding a lower rock quality designation interval defined by the lithophysal subzone of the Tptpmn lithostratigraphic unit. The portion of the TSw2 unit intersected by the Main Drift is characterized by very low rock quality designations, and these low values are consistent from hole to hole. Based on rock quality designation values, core from the TCw and PTn thermal/mechanical units are classified as poor quality rock, and core from the TSw1 is classified as very poor quality rock (Brechtel et al. 1995, p. 2-9). Locally, however, the nonlithophysal portion of the TSw1 was of higher quality and is classified as poor instead of very poor rock. Rock mass properties are discussed in Section 4.5.1.

Rock quality designation data assessed in the ESF were higher than those data obtained from borehole samples. This is due the greater extent of fractures on the scale of core samples, core data including smaller-scale features not counted on the ESF scale, and drilling-induced fractures.

Qualitative rock weathering descriptors were applied to describe the average condition of the core in each core run interval. These standard descriptors are based on recommendations of the International Society for Rock Mechanics (ISRM 1981) and are listed in Table 4-1. All rock from the Tptpmn in the TSw2 unit was either fresh or slightly weathered, constituting 51 percent and 49 percent, respectively, of the total recovered core (Kicker et al. 1996, pp. 4-5).

Table 4-1. Rock Weathering Descriptions

Weathering Class	Log Abbreviation	Description
Fresh	F	Rock and fractures not oxidized or discolored; no separation of grains, change of texture, or solutioning.
Slightly Weathered	S	Oxidized or discolored fractures and nearby rock; some dull feldspars; no separation of grains; minor leaching.
Moderately Weathered	M	Fractures and most of the rock oxidized or discolored; partial separation of grains; rusty or cloudy crystals; moderate leaching of soluble minerals.
Intensely Weathered	I	Fractures and rock totally oxidized or discolored; extensive clay alteration; leaching complete; extensive grain separation; rock is friable.
Decomposed	D	Grain separation and clay alteration complete.

Source: Sandia National Laboratories Technical Procedure SNL TP-233, *Geotechnical Logging of Core by Examination of Core and Video Records*
CRWMS M&O (1998, Table 3.7-3)

Rock hardness is a general descriptor of the strength of the rock material. The estimated hardness classification ratings used are listed in Table 4-2. Above the Repository Host Horizon, the estimated hardness of the TSw1 lithophysal thermal/mechanical unit is 3 percent very hard, 79 percent hard, 12 percent moderately hard, and 4 percent moderately soft. The estimated hardness for most of the Repository Host Horizon, the TSw2 unit, is 16 percent very hard, 79 percent hard, and 5 percent moderately hard (CRWMS M&O 1998, Figure 3.7-8 and Table 3.7-1)

Table 4-2. Estimated Rock Hardness Descriptions

Hardness Class	Log Abbreviation	Description
Extremely Hard	1	Cannot be scratched; chipped only with repeated heavy hammer blows.
Very Hard	2	Cannot be scratched; broken only with repeated hammer blows.
Hard	3	Scratched with heavy pressure; breaks with heavy hammer blow.
Moderately Hard	4	Scratched with light-moderate pressure; breaks with moderate hammer blow.
Moderately Soft	5	Grooved (1/16th inch) with moderate heavy pressure; breaks with light hammer blow.
Soft	6	Grooved easily with light pressure; scratched with fingernail; breaks with light-moderate manual pressure.
Very Soft	7	Readily gouged with fingernail; breaks with light pressure.
Soil-Like	8	Cohesive
Soil-Like	9	Non-Cohesive

Source: Sandia National Laboratories Technical Procedure SNL TP-233, *Geotechnical Logging of Core by Examination of Core and Video Records*
CRWMS M&O (1998, Table 3.7-4)

4.4 LABORATORY PROPERTIES OF INTACT ROCK

4.4.1 Physical Properties

4.4.1.1 Density and Porosity

Density, a physical property defined as mass per unit volume at a specific temperature, can vary substantially within a rock mass because of variations in mineralogic composition, porosity, and welding. Average grain density is controlled by the composition of the rock, and variations in average grain density are attributable to variations in mineral composition and rock-forming processes. Porosity is a measure of the volume of voids in a solid material such as rock. It can be calculated from the relationship of average grain density and dry bulk density and also from the relationship of saturated bulk density and dry bulk density. Effective elastic constants, rock fracture, and rock rheological behavior are controlled in large part by the size, shape, and distribution of pores throughout the rock.

Techniques for obtaining dry and saturated bulk densities, average grain density, and calculated porosity for specimens from the NRG boreholes are presented in CRWMS M&O (1997c, Section 5.1.1) and in earlier reports cited in CRWMS M&O (1998, pp. 3.7-12 to 3.7-13). The data are summarized by thermal/mechanical unit in CRWMS M&O (1998, Tables 3.7-5, 3.7-6, 3.7-7, and 3.7-8). As shown, nonwelded rocks of the undifferentiated overburden and PTn units have significantly lower bulk density and higher porosity than rocks of welded units TCw, TSw1, and TSw2. Because of the relatively uniform composition of the tuffs, average grain density shows only small variability among different rock units. Mean dry bulk density was 1.28 g/cc in both the nonwelded units undifferentiated overburden and PTn. Mean bulk density in the other, welded units was substantially higher and ranged from 2.12 to 2.35 g/cc (CRWMS M&O 1998, p. 3.7-13).

As part of the pre-heating, ambient characterization of hydrologic properties, density and porosity measurements were also performed on cores from wet-drilled and dry-drilled underground boreholes in the Single Heater Test block and the Drift Scale Test block of the ESF. Grab samples from the Observation Drift of the Drift Scale Test were also tested. All tested samples were from the TSw2 thermal/mechanical unit. Results are summarized in the *Yucca Mountain Site Description* (CRWMS M&O 1998, Table 3.7-9) and are generally consistent with TSw2 results from surface-based boreholes. As shown, mean bulk density ranged from 2.20 to 2.26 g/cc, mean particle density ranged from 2.49 to 2.51 g/cc, and mean porosity ranged from 9.3 to 12.5 percent (CRWMS M&O 1998, p. 3.7-13).

Porosity, bulk density, and particle density were measured in additional core samples from drill holes SD-7, SD-9, and SD-12 in support of hydrologic measurements. Samples were collected at a nominal 3-ft, regularly spaced sampling interval on core from these boreholes. Results from SD-7, SD-9, and SD-12 are presented in Rautman and Engstrom (1996a, pp. 141-159), Engstrom and Rautman (1996, pp. 108-126), and Rautman and Engstrom (1996b, pp. 118-130), respectively.

L.E. Flint (1998) divided the unsaturated zone at the site into 30 hydrogeologic subunits based on hydrogeologic properties and laboratory analyses of 4,892 core samples obtained from 23

shallow and 7 deep boreholes and statistical analyses of the results (similar hydrogeologic properties within limited ranges). This study measured porosity, bulk density, and particle density. Section 2.2.1 and L.E. Flint (1998, Table 7) contain additional discussions and data.

4.4.1.2 Mineralogy

The mineralogy and petrology of the volcanic sequence at Yucca Mountain have been described extensively in both studies of drill core and outcrop samples (see CRWMS M&O 1998, Section 6.1, for a summary). In brief, both the Tiva Canyon Tuff and the Topopah Spring Tuff are zoned ash-flow tuffs with crystal-poor rhyolitic units at the base and crystal-rich quartz latite units at the top. Both units have devitrification, welding zones, and secondary crystallization imposed upon their primary features (see CRWMS M&O 1998, Section 6.1, for a description of these features).

A suite of 97 samples from borehole NRG-6 was studied to understand the mineralogy and petrology of samples tested for thermal expansion, thermal conductivity, and mechanical properties (CRWMS M&O 1997c, Section 5.1.2). Borehole NRG-6 was selected because it provides a relatively complete stratigraphic section from the lower part of the Tiva Canyon Tuff through most of the lower lithophysal zone of the Topopah Spring Tuff of the Paintbrush Group (Figure 4-2; see CRWMS M&O 1998, Table 3.5-2). Depths ranged from 6.77 to 330.7 m (22.2 to 1,085.0 ft).

Petrographic and mineralogical data were obtained by an examination of all 97 core samples from NRG-6 (CRWMS M&O 1998, Table 3.7-10). More detailed mineralogical and chemical analyses were performed for selected samples using different laboratory analytical methods, including optical microscopy of thin-sections with modal point counts of identified constituents to determine composition, X-ray diffraction analysis of prepared powders to identify and estimate proportions of finely crystalline minerals, and whole-rock chemical analysis to determine the chemical composition and water content of samples (CRWMS M&O 1997c, Section 5.1.2).

Results of laboratory testing of mineral abundances for samples from the Single Heater Test region of the Thermal Test Facility are presented in CRWMS M&O (1998, Table 3.7-11). Quartz and cristobalite averaged about 8 and 19 percent of the sample, respectively. Smectite was found in all the samples, but was generally present at less than 3 percent. The greatest variability was shown in the abundance of albite and sanidine. Clinoptilolite was present in small amounts in three of the samples. Because the method used to estimate mineral abundance is not normalized to 100 percent, the total mineral abundance do not add up to 100 percent. The average of the total is 96±4. This low value suggests that an unidentified phase may be present. The observed mineralogy is generally consistent with previous measurements of mineral abundance in core samples of Topopah Spring devitrified tuff (Bish and Chipera 1986, pp. 11-18).

Results of laboratory testing of mineral abundances for samples from the Drift Scale Test block are summarized in CRWMS M&O (1998, Table 3.7-12). All samples were from the TSw2 thermal/mechanical unit. The total abundance of the silica polymorphs is fairly uniform, although the cristobalite component varies from 4 to 31 percent, suggesting potential variability in thermal/mechanical properties at the temperatures at which cristobalite undergoes a phase

change. In most samples, albite, sanidine, and cristobalite are the dominant phases, with lesser amounts of quartz. Tridymite is significant in three samples, with cristobalite being less abundant in these samples. Zeolite phases were observed in three samples, clinoptilolite in two samples, and stilbite in one sample. No samples contained detectable mica phases (CRWMS M&O 1998, p. 3.7-16).

4.4.2 Thermal Properties

4.4.2.1 Thermal Conductivity

Thermal conductivity is a measure of the ability of a material to transmit heat, and so relates to the ability of the host rock to conduct heat away from waste containers. Thus, thermal conductivity is an important parameter for numerically simulating the transient temperature field from heat generated by emplaced radioactive waste.

CRWMS M&O (1998, p. 3.7-17) summarizes sampling and testing for thermal conductivity in the ESF. Variation of thermal conductivity with saturation averaged for the NRG boreholes is illustrated for thermal/mechanical units for low temperatures (<100°C) in CRWMS M&O (1998, p. 3.7-17 to 3.7-18). Variations for high temperatures (>100°C) are shown in CRWMS M&O (1998, p. 3.7-17 to 3.7-18). The data were compiled in this manner rather than for each 25°C interval because thermal conductivity is not strongly temperature dependent. No data were available for tuff rocks in the undifferentiated overburden unit, or for an upper portion of the TCw unit (CRWMS M&O 1998, p.3.7-18). Additional thermal conductivity data from the TSw2 unit (Tptpmn) from the Single Heater Test block are shown in CRWMS M&O (1998, p. 3.7-17 to p. 3.7-18). These specimens were all tested in the air-dried state, that is, in the as-received condition. Results are consistent with results from the specimens from NRG boreholes. Thermal conductivity data from the TSw2 unit in the Drift Scale Test block are presented in CRWMS M&O (1998, p. 3.7-17 to 3.7-18). The specimens were all tested in the saturated condition, and results are also consistent with specimens from NRG boreholes (CRWMS M&O 1998, p. 3.7-17 to 3.7-18).

Thermal conductivities are lower for dried specimens and highest for saturated specimens. Thermal conductivities, averaged over all boreholes, ranged, depending upon temperature and saturation state, from 1.2 to 1.9 W/(mK) for TCw, from 0.4 to 0.9 W/(mK) for PTn, from 1.0 to 1.7 W/(mK) for TSw1, and from 1.5 to 2.3 W/(mK) for TSw2. The data show distinct differences between the nonwelded tuffs of the PTn and the welded tuffs of the TCw, TSw1, and TSw2. PTn consistently shows the lowest conductivities, while the TCw and TSw2 units have the highest values. TSw1 specimens span a larger range of thermal conductivities and are intermediate in value (CRWMS M&O 1998, p. 3.7-18).

Evaluation of the mean values in CRWMS M&O (1998, Tables 3.7-13, 3.7-14, 3.7-15, and 3.7-16) indicates that thermal conductivity was affected by saturation and, to a lesser degree, temperature. Thermal conductivity generally increased with increasing saturation and temperature. Sharp increases in thermal conductivity are observed near 100°C for several oven-dried specimens. These increases are as yet unexplained, but may be associated with a change in instrumentation at 100°C or with the vaporization of remaining water. For ESF Single Heater Test block specimens, thermal conductivity appeared to increase sharply at 70°C. This response

is probably associated with the change in instrumentation at that temperature. At temperatures above 100°C, thermal conductivity shows little temperature dependence. Thermal conductivity of specimens containing moisture decreased with increasing temperature, presumably as the specimens dehydrated (Brodsky et al. 1996, p.27); this was frequently not the case as shown by an extensive database (Brodsky et al. 1996, Appendix E; CRWMS M&O 1997c, p. 5-48).

Comparison of qualified data from NRG-4, NRG-5, NRG-6, and NRG-7 and previous unqualified data from USW G-1, USW G-2, USW G-3, and USW G-4 reported by Brodsky et al. (1996, p. 34) indicates that the two sets of data compare very well for TSw1 and TSw2. For PTn data, the nonqualified values are higher by approximately a factor of two than those reported in Brodsky et al. (1996, p. 34) and CRWMS M&O (1997c, p. 5-48). However, the non-qualified database for PTn consisted of only two tests from hole USW G-2, which is almost 3 km from the nearest NRG borehole (CRWMS M&O 1998, p. 3.7-18).

4.4.2.2 Thermal Expansion

Thermal expansion is the tendency of a material to undergo a nearly proportional degree of volume or length change as a result of a change in temperature. The coefficient of thermal expansion is usually recorded as a change in strain (linear dimension per unit original length), per degree Celsius.

Mean coefficients of thermal expansion are presented by thermal/mechanical unit and saturation in CRWMS M&O (1998, Tables 3.7-17 and 3.7-18) for heating phases and cooling phases, respectively. Qualified thermal expansion data only exist for the TCw, PTn, TSw1, and TSw2 thermal/mechanical units. The mean thermal expansion coefficient does show some borehole-to-borehole variation, which is obscured by the data averaging in these tables; complete data are presented in Brodsky et al. (1996, Appendix D). The mean thermal expansion coefficient was highly temperature dependent and ranged, depending upon temperature and saturation state, from 6.6×10^{-6}/°C to 50×10^{-6}/°C for TCw, from negative values to 16×10^{-6}/°C for PTn, from 6.3×10^{-6}/°C to 44×10^{-6}/°C for TSw1, and from 6.7×10^{-6}/°C to 37×10^{-6}/°C for TSw2. Data also are summarized by lithostratigraphic unit and are plotted as strain versus temperature in CRWMS M&O (1997c, p. 5-60) and Brodsky et al. (1996, Appendix D). Additional data for TSw2 thermal/mechanical unit (Tptpmn) samples from the Single Heater Test region of the ESF Thermal Test Facility are presented in CRWMS M&O (1998, Table 3.7-19). The mean thermal expansion coefficients for these samples ranged from 7.5 to 52 $\times 10^{-6}$/°C, and, as shown, were temperature dependent during the heating cycle. Complete data and analyses are presented in CRWMS M&O (1996a).

CRWMS M&O (1998, Table 3.7-20) contains statistical summaries for mean coefficients of thermal expansion for specimens from the Drift Scale Test block for heating and cooling. Single Heater Test and Drift Scale Test values are generally consistent. The data presented in CRWMS M&O (1998, Tables 3.7-17 through 3.7-20) indicate that at a "transition temperature" of 150 to 200°C, the mean thermal expansion coefficient increases more steeply for the welded tuff (TCw, TSw1, TSw2) but decreases for the nonwelded tuff (PTn). Some specimens that displayed sensitivity to transition temperature were analyzed to assess the role of the maximum test temperature. Specimens from approximately the same depth and same borehole were tested to different temperatures. The results showed that as long as the maximum test temperature

remained below the transition temperature, the specimens did not permanently change dimension (Brodsky et al. 1996, p. 44).

Additional results of testing indicate: thermal expansion was independent of saturation state for welded specimens but did depend upon saturation state for the nonwelded specimens; the data were insufficient to formulate conclusions regarding the effect of test specimen size on test results; and the correlation between thermal properties and mineralogy was very poor (see CRWMS M&O 1998, Section 3.7.3.2.2, for details).

4.4.2.3 Heat Capacity

Heat capacity is the amount of heat required to change the temperature of a substance by a given amount. Bulk chemical analyses of 20 tuff samples from Yucca Mountain were used to calculate heat capacities of the solid components of the tuffs as a function of temperature. The data were combined with grain density, matrix porosity, lithophysal-cavity abundance, mineral abundance, in situ saturation, and the properties of water to estimate rock-mass thermal capacitance. Calculations were completed for nine thermal/mechanical units (TCw, PTn, TSw1, TSw2, TSw3, CHn1v, CHn2v, CHn1z, and CHn2z) over the temperature range of 25 to 275°C. Summary mineralogic and chemical data are reported in Connolly and Nimick (1990) and thermal capacitance calculations and results are presented in Nimick and Connolly (1991).

Thermal capacitance for TSw1 and TSw2, which is heat capacity multiplied by specimen density, is summarized in CRWMS M&O (1998, Table 3.7-21). A complete data presentation is included in CRWMS M&O (1997c, pp. 5-67 to 5-68). Thermal capacitance is higher for TSw2 than for TSw1. Mean thermal capacitance ranges from 1.6 to 2.1 J cm^{-3} K^{-1} for TSw1 and from 1.8 to 2.5 J cm^{-3} K^{-1} for TSw2 (CRWMS M&O 1998, Table 3.7-21).

4.4.3 Mechanical Properties

4.4.3.1 Static and Dynamic Elastic Constants

Young's modulus and Poisson's ratio are the primary mechanical deformation indices of rock and are indicators of the elastic response of the rock to stress. Static Young's modulus and Poisson's ratio were computed from the stress-strain data obtained for the specimens tested in confined and unconfined compression. In addition, dynamic elastic moduli were computed from compressional and shear wave velocities measured under ambient laboratory conditions.

Detailed results of experiments conducted on specimens from cores recovered from boreholes UE-25 NRG-2, UE-25 NRG-3, UE-25 NRG-4, UE-25 NRG-5, USW NRG-6, and USW NRG-7/7A are presented in Martin et al. (1994, Tables 1-4, pp. 25-35; 1995, Tables 1-4, pp. 26-38) and Boyd et al. (1996a, Tables 1-4, pp. 29-44; 1996b, Tables 1-4, pp. 26-36). CRWMS M&O (1998, Tables 3.7-22 and 3.7-23) lists the mean and standard deviation of static Young's modulus (elastic modulus) and Poisson's ratio for thermal/mechanical units and for individual lithostratigraphic units. In general, the Young's modulus of the tuff depends on welding. Nonwelded tuff is weak and exhibits low Young's moduli. In contrast, the welded tuffs are stronger and exhibit significantly greater Young's moduli. In borehole NRG-6, for example, the moduli range from less than 1 Gpa for the nonwelded units to near 40 Gpa for the

welded units. The greatest moduli are observed for specimens recovered from units TCw and TSw2. The Young's moduli observed on specimens from TSw1 are somewhat lower than those for the other welded units. The standard deviation in the Young's moduli for each thermal/mechanical unit is large. Specimens separated by very small vertical distances, having nominally the same texture and composition, exhibited large changes in moduli (CRWMS M&O 1997c, p. 5-97).

For specimens from the TSw2 thermal/mechanical unit in the Single Heater Test region of the ESF Thermal Test Facility, elastic constants calculated from unconfined compression tests were fairly consistent, with a mean Young's modulus of 32.4 GPa and a mean Poisson's ratio of 0.17. Complete test results and analysis are presented in CRWMS M&O (1996a).

Elastic constants calculated from unconfined compression tests on specimens from the TSw2 thermal/mechanical unit (Tptpmn lithostratigraphic unit) in the Drift Scale Test block were slightly higher than values from the Single Heater Test block, but generally consistent with values from NRG borehole samples. The mean Young's modulus was 36.8 GPa and the mean Poisson's ratio 0.201. Standard deviations for both constants were slightly smaller than either of the other two test suites (CRWMS M&O 1998, p. 3.7-25).

4.4.3.2 Compressive Strength

Compressive strength of a rock is its ability to withstand compressive stress without failure. Compressive strength of intact rock is measured in the laboratory by subjecting a cylindrical test piece to a compressive load parallel to its axis until it fails. Compressive strength is the maximum stress at failure and is computed from the maximum load and the cross-sectional area of the test piece. Confined (or triaxial) compressive strength is determined by subjecting the cylindrical test specimen to a uniform lateral confining pressure in addition to the axial load.

Results of unconfined compression tests indicate that the unconfined compressive strengths vary depending on the welding, porosity, and fabric of the rock. Welded tuffs exhibited higher strengths than nonwelded tuffs. Within the welded units, the variations in strengths are related to the presence and size of lithophysae and vapor-phase altered zones. CRWMS M&O (1998, Table 3.7-25) compares the mean and standard deviation of uniaxial compressive strength for thermal/mechanical units and individual lithostratigraphic units. The data are described in greater detail in CRWMS M&O (1997c, pp. 5-102 to 5-111).

Specimens from TCw typically exhibit the greatest strengths (i.e., in excess of 300 Mpa). In contrast, the weakest specimens are from the PTn unit, with strengths generally less than 10 Mpa. Large variability is observed for TSw1 and TSw2. The strengths for these units vary from 25 to 250 Mpa and show no consistent trend between strength and depth.

Results of unconfined compression tests on TSw2 samples from the Single Heater Test region of the ESF Thermal Test Facility (CRWMS M&O 1996a) showed a large scatter in strengths similar to that observed in other testing of Yucca Mountain tuffs (Brechtel et al. 1995, pp. 6-3 to 6-4; CRWMS M&O 1997c, p. 5-102). Unconfined compressive strengths ranged from 75.1 to 243.8 Mpa, with a mean of 143.2 Mpa and a standard deviation of ±50.3 Mpa (CRWMS M&O 1996a). Moisture contents for these specimens were not controlled and differences in moisture

contents may have contributed to the scatter in strengths. The mode of failure for all specimens was dominated by brittle axial cracking. There was no correlation between strength and mode of failure, and all of the specimens failed explosively (CRWMS M&O 1996a, p. 4-9).

Results of confined compression tests indicate that the axial stress difference at failure increases with increasing confining pressure. Strength parameters calculated from confined compression test results are listed in CRWMS M&O (1998, Table 3.7-26). The specimens tested in confined compression failed in shear; that is, the fractures formed on shear planes with little evidence of axial splitting. In most cases, a visibly evident shear plane developed. However, there was no evidence of conjugate fracture sets forming in any of the specimens. The lack of a conjugate set would be consistent with failure along a pre-existing fabric. Complete data and analysis are presented in CRWMS M&O (1997c, pp. 5-102, 5-112 to 5-119).

Seventeen confined compression experiments were also performed at a nominal temperature of 150°C on specimens recovered from borehole USW SD-9. All of the measurements were conducted on specimens from thermal/mechanical unit Tsw2. These high temperature confined compression test data indicate a clear increase in strength between 1 and 5 Mpa confining pressure, but no apparent increase in strength between 5 and 10 Mpa confining pressure. This range in confining pressure is roughly coincident with the static load of 7 Mpa at the repository horizon (see Section 4.6). Comparison of room and elevated temperature tests suggests that the effect of temperature on the strength of welded tuff from Tsw2 is small. Similarly, Young's modulus and Poisson's ratio measured at elevated temperatures (150°C) were not significantly different from those measured at room temperature (CRWMS M&O 1998, p. 3.7-28).

4.4.3.3 Tensile Strength

Tensile strengths generally range from 0.2 to 16 Mpa. The weakest specimens are from the nonwelded PTn thermal/mechanical unit. The greatest strengths are observed in the TCw welded tuff. In general, TSw1 is weaker than TSw2. However, there is significant scatter in TSw2 data. Results are summarized in CRWMS M&O (1998, Table 3.7-27) and presented in greater detail in CRWMS M&O (1997c, p. 5-119).

4.4.3.4 Time-Dependent (Creep) Behavior

If a solid is subjected to a load (stress) within its elastic limit, it instantaneously experiences an amount of deformation (strain), which disappears on the removal of the load. If the load is maintained at the same level, the solid will continue to deform beyond the instantaneous deformation at a slow rate depending on the level of the applied stress. This continuing deformation with time in spite of no increase in stress is referred to as time-dependent deformation or creep deformation.

Results of creep measurements on specimens from the TSw2 thermal/mechanical unit (tptpmn lithostratigraphic unit) are presented in CRWMS M&O (1998, Table 3.7-28). The experiments were conducted at nominal differential stresses of 40, 70, 100, and 130 Mpa, at a fixed confining pressure of 10 Mpa, and at a temperature of 225°C. The duration of the experiments ranged from 2.55×10^6 s to 5.90×10^6 s (30 to 68 days). At higher stress differences, the data show very small increases in the axial strain. The experiments conducted at stress differences between

40 and 100 Mpa show smaller strain accumulations, and for the test conducted at a differential stress of 40 Mpa, no strain accumulation was observed. Each test was terminated before failure of the specimen.

4.4.3.5 Hardness

Schmidt hammer rebound hardness measurements were conducted on samples from the NRG holes to produce early strength estimates and to supplement the rock mechanics test data. Results of Schmidt hammer measurements are summarized in CRWMS M&O (1998, Table 3.7-29).

4.5 ROCK MASS PROPERTIES

Analyses to support the design of the repository are required to address the potential impacts of seismic, thermal, and mechanical loading. These analyses require knowledge of rock properties at the rock mass scale as inputs. Mechanical properties are known to be very different for strong, jointed, in situ rock masses than for small, intact samples tested in the laboratory. These differences are termed "scale effects" and are attributed to the influence of the size of the rock mass affected and to inhomogeneities such as jointing.

4.5.1 Rock Mass Classification

Rock mass classification systems were employed in ESF construction activities as the basis of empirical design of excavation ground support and empirical correlation with rock mass properties. The rock mass rating system (Bieniawski 1979) and the rock mass quality system (Barton et al. 1974) are rock classification methods that consider characteristics of the rock mass such as the degree of jointing, the interaction of joints to form blocks, joint surface frictional characteristics, rock strength, rock stress, and hydrologic conditions. Rock mass quality indices and the parameters used to determine the indices are not primary data, but they are derived from direct observations of rock mass characteristics.

The calculation of rock mass rating requires six parameters that consider the strength of the rock, the rock quality designation, the joint spacing, the condition of joint surfaces, the groundwater environment, and a factor for the adjustment of joint orientation toward the excavation. The rock mass quality index is calculated from parameters related to joints, block size, interblock shear strength, and the effect of active stress. Both of these indices are discussed in detail in CRWMS M&O (1998, Section 3.7.4.1).

Lowest rock mass quality was observed in the TCw thermal/mechanical unit. The TCw also had the greatest variability. Rock mass quality was lowest in the most densely welded lithostratigraphic units, Tpcpul and Tpcpmn, in the Tiva Canyon tuff. It was higher in the less densely welded upper and lower portions. This correlates with analysis of the fracture mapping for TCw, which consistently indicates more joint sets and higher joint frequency. In addition, the North Ramp penetrates the TCw in a zone of normal faulting, which contributed to the broken character of the TCw rocks.

The PTn unit showed consistently high rock mass quality ratings. Typically, only one set of joints was evident in the PTn and had very limited impact on the excavation. Rock strength was

low in this unit, with some intervals being nonlithified. Shear failures were observed on the sides of the tunnels in some of the weaker PTn materials. However, they were localized and have not affected the long-term character of the excavation.

Poor rock mass quality, anticipated in the upper lithophysal zone (Tptpul) of the TSw1 thermal/mechanical unit, was not observed. Jointing was not well developed and was generally limited to one set. The inhomogeneities in the Tptpul caused by large lithophysae and relatively small cracking of the rock had little effect on the rock mass at the excavation scale. Where the middle nonlithophysal zone (Tptpmn) in the TSw2 was exposed in excavations of the Main Drift, rock mass quality was relatively high.

Rock mass quality indices are affected by the value of the rock quality designation parameter. Rock quality designation data obtained from boreholes was much lower than the rock quality designation assessed at the tunnel scale. This is due to the greater extent of fractures on the scale of core samples. Core data include smaller-scale fractures that were not counted at the tunnel scale, as well as drilling-induced fractures.

4.5.2 Thermal Properties

Correlations have been developed or proposed for thermal/mechanical properties at the rock mass scale. Thermal conductivity at the intact scale has been shown to be a function of porosity, saturation, and temperature. Differences at the rock mass scale are projected to be related to the additional fracture porosity, which should be a small effect. Similarly, the heat capacity of intact rock is expected to be an adequate analogue at the rock mass scale.

Preliminary thermal/mechanical analyses for design have been performed in an attempt to project laboratory thermal expansion data to the rock mass scale, as described in Jung et al. (1993). The preliminary thermal/mechanical analyses indicate a maximum upward displacement of almost 30 cm at the surface, 300 years after waste emplacement. Most of this displacement would originate in the TSw2 unit. The rock in the immediate vicinity of the repository was predicted to be in compression, but the tensile stress nearer the surface (TCw thermal/mechanical unit) was predicted to be relatively high (approximately 5 Mpa). This behavior could potentially result in the opening of preferential pathways for water infiltration or gas migration (CRWMS M&O 1997c, p. 7-16). However, thermal expansion data for the analyses in Jung et al. (1993, p. 4-10) came primarily from borehole laboratory thermal expansion testing results. Data from the in situ thermal tests being conducted in the ESF are anticipated to be more representative of rock mass behavior than the laboratory test results and will be used for updating and expanding the three-dimensional thermal/mechanical analysis for the repository. The resulting more realistic material models would probably predict lower stresses (Jung et al. 1993; CRWMS M&O 1998, p. 3.7-38).

Rock mass thermal properties are related to rock mass hydrologic properties. Sass, Lachenbruck, Dudley et al. (1988, p. 24) concluded from temperature profiles in 35 boreholes near Yucca Mountain that heat flow was primarily conductive and did not exhibit a significant convective component. More recently, Bodvarsson and Bandurraga (1996, p. 366) used borehole data (Sass, Lachenbruck, Dudley et al. 1988, Appendix 3) and a model developed by Rautman (1995, pp. 83-84) that correlates thermal conductivity as a function of porosity,

temperature, and saturation. Bodvarsson and Bandurraga (1996, p. 368) concluded that conductive heat transfer alone cannot fully explain the observed temperature data and a coupled conduction/convection model was developed to explain the temperature data obtained from boreholes (see previous, more detailed discussion in Section 2.2.1.8). In addition, using qualified thermal data and assumptions regarding heat flux, Bodvarsson and Bandurraga (1996, p. 371) calculated a percolation flux of approximately 5 to 12 mm/yr through the TSw unit, which is consistent with recent percolation flux estimates of Flint, A.L. et al. (1996, p. 91).

4.5.3 Mechanical Properties

4.5.3.1 Rock Mass Strength

Rock mass mechanical properties have been estimated using the approach proposed by Hardy and Bauer (1991). The approach uses laboratory test data and rock mass quality rating to estimate mechanical properties at the rock mass scale for use in equivalent continuum analyses. The estimated properties are listed in CRWMS M&O (1998, Table 3.7-40) for each thermal/mechanical unit and rock mass rating values at 40 percent cumulative frequency of occurrence. Ranges of the rock mass properties are estimated based on rock mass rating from scanline data and the average of the appropriate intact rock property. Complete analysis is presented in CRWMS M&O (1997c, pp. 7-2 to 7-12, Appendix B). Two sets of empirical rock mass strength criteria, Yudhbir and Prinzl (1983) and Hoek and Brown (1988), were adopted for the Drift Design Methodology, and are discussed in CRWMS M&O (1998, Section 3.7.4.3.1). Complete design rock mass strength envelopes for the thermal/mechanical units and resulting power law constants are given for all rock mass classes in each thermal/mechanical unit in CRWMS M&O (1997c, pp. 7-6 to 7-12).

4.5.3.2 Rock Mass Elastic Moduli

Complete results of rock mass elastic moduli testing are presented in CRWMS M&O (1997c, p. 7-13). Empirical relationships to estimate Poisson's ratio from rock mass quality are not available. The mean values for intact rock Poisson's ratios from the laboratory tests for each thermal/mechanical unit were adopted as the rock mass Poisson's ratios.

4.6 IN SITU STRESS CONDITIONS

Design of the Yucca Mountain repository requires knowledge of the magnitude, direction, and variability of the preconstruction in situ state of stress for the analysis and design of stable underground openings as well as for the prediction of short-term and long-term rock mass deformation. Detailed results of in situ stress measurements in tuffs at Yucca Mountain are contained in several references cited in CRWMS M&O (1998, p. 3.7-44). These references also discuss details of testing techniques and potential limitations and errors.

Table 4-3 presents a summary of the estimated in situ stress at the repository horizon. The direction of the maximum principal stress is vertical, due to lithostatic load. At the repository elevation, the vertical stress has been assumed to be 7.0 Mpa on the average (CRWMS M&O 1998, Table 3.7-43). In situ stress calculated for the ESF test area in borehole G-4 (DTN: MO9007RIB00022.003, Figure 4) showed a vertical stress of 6.0 Mpa at a depth of 300 m. Horizontal stress for the same depth ranged from 2.2 to 4.4 Mpa.

Table 4-3. Summary of In Situ Stresses at the Repository Horizon

Parameter	Average Value	Range of Values
Vertical Stress	7.0 MPa	5.0 - 10.0 MPa
Minimum Horizontal/Vertical Stress Ratio	0.5	0.3 - 0.8
Maximum Horizontal/Vertical Stress Ratio	0.6	0.3 - 1.0
Bearing of Minimum Horizontal Stress	N57°W	N50°W - N65°W
Bearing of Maximum Horizontal Stress	N32°E	N25°E - N40°E

Source: Advanced Conceptual Design Report (CRWMS M&O 1996f)
CRWMS M&O (1998, Table 3.7-43)

Horizontal in situ stresses at the repository site are expected to be generally low. Consequently, failure modes around underground openings during construction are expected to be primarily controlled by geologic structures. Minimum and maximum horizontal/vertical stress ratios are close, indicating a weak horizontal stress anisotropy. Lateral stresses and their effects would thus be expected to be similar for all drift orientations (CRWMS M&O 1998, p. 3.7-45).

Hydraulic fracturing tests, which were performed for ambient characterization of the Drift Scale Test block, measured in situ stresses in the TSw2 unit (SNL 1996, p. 2; CRWMS M&O 1997a, p. 13). Results were generally consistent but revealed somewhat lower in situ stresses than previously estimated. Reliable results from a hydraulic fracturing test conducted in the Drift Scale Test block indicate that the largest horizontal compressive stress is 2.9 (±4) MPa acting in the N15°E (±14°) direction and the least horizontal principal stress is 1.7 (±0.1) MPa acting in the N75°W (±14°) direction. Based on the depth of these tests, the vertical stress was not measured but was approximated as 4.7 Mpa, due to the weight of the overburden (CRWMS M&O 1998, p. 3.7-45).

Although the measured horizontal stresses are only moderately differential, both are smaller than the vertical stress. This measured stress regime, one of low horizontal magnitudes, is in accord with the dominant local normal faults. The north-northeastern maximum horizontal stress direction is subparallel to the average strike of these faults and is supported by previous measurements in the Yucca Mountain area (Zoback and Healy 1984, pp. 691-692).

4.7 EXCAVATION CHARACTERISTICS OF THE ROCK MASS

Geotechnical monitoring data were developed during excavation of the North Ramp Starter Tunnel and Upper Tiva Canyon Alcove to provide the basis for design verification (SNL 1995, abstract). The North Ramp Starter Tunnel was constructed to launch the 7.6-m diameter tunnel boring machine being used to construct the ESF North Ramp, Main Drift, and South Ramp. The Upper Tiva Canyon Alcove was excavated off the North Ramp Starter Tunnel to provide access for site characterization testing. Design verification studies are being performed to monitor and observe the long-term behavior of openings in the range of rock conditions to be encountered in the potential repository host rock, to observe and evaluate the construction of the ESF with respect to implications for repository construction and performance, and to collect information for design of the ventilation systems in the repository.

Specific safety and health concerns related to rock mass mineralogies at Yucca Mountain include respiratory effects of erionite and silica minerals (including quartz and crystobalite) during daily

underground activities. These minerals occur in varying proportions in the different lithologies and geochemical environments at Yucca Mountain. Hazards include erionite, a carcinogen, and crystalline silica, which can produce respiratory ailments upon becoming airborne. Occurrence of these minerals is discussed in detail in CRWMS M&O (1998, Section 6).

Safety and health concerns for the Yucca Mountain Project are summarized in CRWMS M&O (1998, p. 3.7-46).

Excavation methods and excavation characteristics are described in CRWMS M&O (1998, Sections 3.7.6.1 and 3.7.6.2).

4.8 ENGINEERING PROPERTIES OF SURFICIAL MATERIALS

4.8.1 Surficial Sedimentary Deposits

The late Tertiary and Quaternary surficial sedimentary deposits of the Yucca Mountain area consist of colluvium, alluvium, eolian sand sheets, ramps and dunes, and spring deposits (Section 1.2; CRWMS M&O 1998, Section 3.4.3.3). These range in age from late Pliocene to Holocene. The deposits are grouped into eight major units plus locally important eolian and marsh deposits.

Late Pliocene and early Pleistocene deposits consist predominantly of debris flows with sparse, bedded fluvial sediments. They occur as dissected fans and fan remnants that are adjacent to bedrock ranges and, less commonly, as isolated outcrops several kilometers from the ranges. These deposits are moderately indurated, coarse, angular, unsorted gravel with minor amounts of sand- to clay-sized material (Wesling et al. 1992; Lundstrom, S.C., Mahan, S.A., and Paces, J.B., *Preliminary Surficial Deposits Map of the Northwest Quarter of the Busted Butte 7.5-Minute Quadrangle,* USGS-OFR-95-133, in press).

Middle to late Pleistocene deposits consist of alluvium, fluvial and eolian sands, and local lenses of volcanic ash. These deposits generally overlie older alluvial deposits on middle to upper pediment slopes, and they occur in larger stream valleys.

Eolian deposits occur as dunes and sand sheets in and adjacent to the Amargosa Valley. Ramps of fine, well-sorted sand as much as 50 m thick flank many of the hills bordering the Amargosa Valley and near Yucca Mountain at Busted Butte. Fluvial sand sheets occur along major streams and along drainages downstream from dunes.

Holocene deposits in the Yucca Mountain area consist of fluvial sand and gravel and eolian sand. Holocene deposits occur mainly as thin, broad fans downstream from incised stream channels on pediment slopes. Eolian sand deposits consist of well-sorted fine sand that occurs as small dunes and irregularly-shaped sheets in the Amargosa Valley.

4.8.2 Soil Investigations

Investigations to determine the physical properties of soils in the site area have been conducted in Midway Valley in the general area of potential repository surface facilities and in the North Ramp surface facility area for the ESF. The Bureau of Reclamation study of the North Ramp

area found that topsoil typically ranges from 0 to 3 ft (0 to 1m) of silty sand, silty sand with gravel, poorly graded gravel with sand, and silty gravel with sand; is relatively loose; and contains roots. The soil at the site is primarily colluvium and alluvium, generally composed of silty sand and silty gravels with fines ranging from 4 to 30 percent. Some clayey sand and clayey gravel with fines ranging from 29 to 40 percent are present but in very limited amounts. Physical property data and test pit logs for seven portal pad test pits and 39 road alignment test pits are provided by the U.S. Bureau of Reclamation (USBR 1992). These seven portal pad test pits are representative of materials and foundation conditions for the ESF North Ramp Surface Facility. The soil is caliche-cemented from just below the surface to several feet deep adjacent to and decreasing away from Exile Hill. All the soil in the North Ramp Surface Facility pad area is carbonate-cemented to some degree. The carbonate-cemented soil may be ripped to facilitate excavation. The prevalence of secondary carbonate-cementation throughout the pad area indicates that foundation bearing capacities determined by disturbed sampling methods or physical properties will be conservative. Practical methods to sample and test the gravelly materials at the site do not exist. Soil material had to be jack-hammered for removal for tests because of the soil cementation. However, in-place and relative densities were determined and can be used to assess the bearing capacity of the material. The material appears to be adequate for founding the relatively temporary, low-load structures contemplated. A suggested design value for bearing capacity is 1.1 ton/ft^2 (105.3 kPa) per foot of footing width plus 1.9 ton/ft^2 (181.9 kPa) per foot of depth. Calculations, estimated settlement, and references are contained in U.S. Bureau of Reclamation (USBR 1992, p. 13) and CRWMS M&O (1998, p. 3.7-51).

INTENTIONALLY LEFT BLANK

5. REFERENCES

NOTE: Each listed reference is followed by a number indicating where it can be found in the Yucca Mountain Project records systems. Numbers consisting of three letters followed by a period, eight numbers, another period, and finally four more numbers (e.g., MOL. 19980212.0002) are accession numbers for the YMP Records Information System. Numbers consisting of the letters "TIC" followed by six numbers are catalog numbers for the YMP Technical Information Center (e.g., TIC 242720). For some references, an additional number is given that provides traceability to data used or developed in the document. These Data Tracking Numbers are preceded by the letters "DTN:" and indicate the location of the data in the YMP Technical Data Management System.

5.1 REFERENCES CITED

Albers, J.P. and Stewart, J.H. 1972. "Geology and Mineral Deposits of Esmeralda County, Nevada." *Nevada Bureau of Mines and Geology Bulletin 78.* Reno, Nevada: University of Nevada-Reno, Mackay School of Mines. TIC 219270.

Anderson, J.G.; Brune, J.N.; dePolo, D.; Gomberg, J.; Harmsen, S.C.; Savage, M.K.; Sheehan, A.K.; and Smith, K.D. 1993. "Preliminary Report: The Little Skull Mountain Earthquake, June 29, 1992." *Dynamic Analysis and Design Considerations for High Level Nuclear Waste Repositories,* 162-175. New York, New York: American Society of Civil Engineers. DTN: GS920883117412.028; TIC 233289.

Anderson, L.W. and O'Connell, D.R. 1993. *Seismotectonic Study of the Northern Portion of the Lower Colorado River, Arizona, California and Nevada.* USBR-SR-934. Denver, Colorado: U.S. Department of the Interior, Bureau of Reclamation. TIC 237904.

Arnold, B.W.; Altman, S.J.; Robey, T.H.; Barnard, R.W.; and Brown, T.J. 1995. *Unsaturated-Zone Fast-Path Flow Calculations for Yucca Mountain Groundwater Travel Time Analyses (GWTT-94).* SAND95-0857. Albuquerque, New Mexico: Sandia National Laboratories. MOL.19960327.0336.

Axen, G.J.; Taylor, W.J.; and Bartley, J.M. 1993. "Space-Time Patterns and Tectonic Controls of Tertiary Extension and Magmatism in the Great Basin of the Western United States." *Geological Society of America Bulletin, 105,* 56-76. Boulder, Colorado: Geological Society of America. TIC 224970.

Aymard, W.H. 1989. *Hydrocarbon Potential of Yucca Mountain, Nevada.* U.93. Master's thesis. Reno, Nevada: University of Nevada-Reno. TIC 222219.

Bailey, R.A. and Koeppen, R.P. 1977. *Preliminary Geologic Map of Long Valley Caldera, Mono County, California.* USGS-OFR-77-468. Denver, Colorado: U.S. Geological Survey. MAPI-1933. TIC 242720.

Barker, C.E. 1994. *Thermal and Petroleum Generation History of the Mississippian Eleana Formation and Tertiary Source Rocks, Yucca Mountain Area, Southern Nye County, Nevada.* USGS-OFR-94-161. Denver, Colorado: U.S. Geological Survey. TIC 234479.

Barton, N.R.; Lien, R.; and Lunde, J. 1974. "Engineering Classification of Rock Masses for the Design of Tunnel Support." *Rock Mechanics, 6,* 189-236. New York, New York: Springer-Verlag. TIC 219995.

Beck, P. 1970. *The Southern Nevada-Utah Border Earthquakes, August to December 1966.* U.54. Master's thesis. Salt Lake City, Utah: University of Utah. TIC 216837.

Bell, E.J. and Larson, L.T. 1982. *Overview of Energy and Mineral Resources for the Nevada Nuclear Waste Storage Investigations, Nevada Test Site, Nye County, Nevada.* NVO-250. Las Vegas, Nevada: U.S. Department of Energy Nevada Operations Office. NNA.19870406.0078.

Bellier, O. and Zoback, M.L. 1995. "Recent State of Stress Change in the Walker Lane Zone, Western Basin and Range Province, United States." *Tectonics, 14,* 564-593. Washington, D.C.: American Geophysical Union. TIC 233037.

Benson, L.V. and Klieforth, H. 1989. "Stable Isotopes in Precipitation and Groundwater in the Yucca Mountain Region, Southern Nevada: Paleoclimatic Implications." *American Geophysical Union Geophysical Monograph 55,* 41-59. Washington, D.C.: American Geophysical Union. TIC 224413.

Benson, L.V. and McKinley, P.W. 1985. *Chemical Composition of Ground Water in the Yucca Mountain Area, Nevada, 1971-84.* USGS-OFR-85-484. Denver, Colorado: U.S. Geological Survey. NNA.19900207.0281.

Berquist, J.R. and McKee, E.H. 1991. *Mines, Prospects, and Mineral Occurrences in Esmeralda and Nye Counties, Nevada, near Yucca Mountain.* U.S. Geological Survey Administrative Report (Mineral Resource Data System). Denver, Colorado: U.S. Geological Survey. NNA.19920131.0434.

Bieniawski, Z.T. 1979. *Engineering Rock Mass Classification.* Wiley-Interscience Publication. New York, New York: John Wiley & Sons. TIC 226350.

Bish, D.L. 1989. *Evaluation of Past and Future Alterations in Tuff at Yucca Mountain, Nevada, Based on the Clay Mineralogy of Drill Cores USW G-1, G-2, and G-3.* LA-10667-MS. Los Alamos, New Mexico: Los Alamos National Laboratory. NNA.19890126.0207.

Bish, D.L. and Chipera, S.J. 1986. *Mineralogy of Drill Holes J-13, UE-25A#1, and USW G-1 at Yucca Mountain, Nevada.* LA-10764-MS. Los Alamos, New Mexico: Los Alamos National Laboratory. NNA.19890523.0057.

Blanton III, J.O. 1992. *Nevada Test Site Flood Inundation Study: Part of a Geological Survey Flood Potential and Debris Hazard Study, Yucca Mountain Site.* For U.S. Department of Energy, Office of Civilian Radioactive Waste Management. Denver, Colorado: U.S. Bureau of Reclamation. TIC 205029.

Bodvarsson, G.S. and Bandurraga, T.M. (eds.) 1996. *Development and Calibration of the Three-Dimensional Site-Scale Unsaturated Zone Model of Yucca Mountain, Nevada.* LBNL Milestone Report. Berkeley, California: Lawrence Berkeley National Laboratory. MOL.19970211.0176.

Bodvarsson, G.S.; Bandurraga, T.M.; and Wu, Y.S. (eds.) 1997. *The Site Scale Unsaturated Zone Model of Yucca Mountain, Nevada, for the Viability Assessment.* LBNL-40376. Berkeley, California: Lawrence Berkeley National Laboratory. MOL.19971014.0232.

Bonner, L.J.; Elliott, P.E.; Etchemendy, L.P.; and Smallwood, J.R. 1998. *Water Resources Data, Nevada, Water Year 1997.* U.S. Geological Survey Water Data Report NV-97-1. Denver, Colorado: U.S. Geological Survey. TIC 242466.

Boucher, G.; Seeber, L.; Ward, P.; and Oliver, J. 1967. "Microearthquake Observations at the Epicenter of a Moderate-sized Earthquake in Nevada." *EOS Transactions of the American Geophysical Union, 48,* 205. Washington, D.C.: American Geophysical Union. TIC 234477.

Boyd, P.J.; Price, R.H.; Martin, R.J.; and Noel, J.S. 1996a. *Bulk and Mechanical Properties of the Paintbrush Tuff Recovered From Boreholes UE25 NRG-2, 2A, 2B, and 3.* SAND94-1902. Albuquerque, New Mexico: Sandia National Laboratories. MOL.19970102.0002.

Boyd, P.J.; Price, R.H.; Noel, J.S.; and Martin, R.J. 1996b. *Bulk and Mechanical Properties of the Paintbrush Tuff Recovered From Boreholes UE25 NRG-4 and -5.* SAND94-2138. Albuquerque, New Mexico: Sandia National Laboratories. MOL.19970102.0004.

Brechtel, C.E.; Lin, M.; Martin, E.; and Kessel, D.S. 1995. *Geotechnical Characterization of the North Ramp of the Exploratory Studies Facility.* SAND95-0488/1, SAND95-0488/2. Albuquerque, New Mexico: Sandia National Laboratories. MOL.19950502.0004; MOL.19950502.0005.

Brocher, T.M. and Hunter, W.C. 1996. "Seismic Reflection Evidence Against a Shallow Detachment Beneath Yucca Mountain, Nevada." *High Level Radioactive Waste Management, Proceedings of the Seventh Annual International Conference, Las Vegas, Nevada, April 29-May 3, 1996,* 148-150. La Grange Park, Illinois: American Nuclear Society. TIC 231911.

Brodsky, N.S.; Riggins, M.; Connolly, J.; and Ricci, P. 1996. *Thermal Expansion, Thermal Conductivity, and Heat Capacity Measurements for Boreholes UE25 NRG-4, UE25 NRG-5, USW NRG-6, and USW NRG-7/7A.* SAND95-1955. Albuquerque, New Mexico: Sandia National Laboratories. MOL.19970723.0039.

Broxton, D.E.; Bish, D.L.; and Warren, R.G. 1987. "Distribution and Chemistry of Diagenetic Minerals at Yucca Mountain, Nye County, Nevada." *Clays and Clay Minerals, 35,* n. 2, 89-110. Long Island City, New York: Pergamon Press. TIC 203900.

Brune, J.N.; Nicks, W.; and Aburto, A. 1992. "Microearthquakes at Yucca Mountain, Nevada." *Seismological Society of America Bulletin, 82,* 164. El Cerrito, California: Seismological Society of America. TIC 212563.

Brune, J.N. and Whitney, J.W. 1995. "Precarious Rocks and Seismic Shaking at Yucca Mountain, Nevada." U.S. Geological Survey report prepared in cooperation with the U.S. Department of Energy. Denver, Colorado: U.S. Geological Survey. MOL.19960415.0356.

Buesch, D.C.; Spengler, R.W.; Moyer, T.C.; and Geslin, J.K. 1996. *Proposed Stratigraphic Nomenclature and Macroscopic Identification of Lithostratigraphic Units of the Paintbrush Group Exposed at Yucca Mountain, Nevada.* USGS-OFR-94-469. Denver, Colorado: U.S. Geological Survey. DTN: GS931208314211.049; MOL.19970205.0061.

Bullard, K.L. 1992. Nevada Test Site Probable Maximum Flood Study, Part of U.S. Geological Survey Flood Potential and Debris Hazard Study, Yucca Mountain Site. Denver, Colorado: U.S. Bureau of Reclamation. TIC 205030.

Burchfiel, B.C. and Davis, G. 1988. "Mesozoic Thrust Faults and Cenozoic Low-Angle Normal Faults, Eastern Spring Mountains, Nevada and Clark Mountains Thrust Complex, California." Weide D.L. and Faber, M.L. (eds.), "This Extended Land: Geological Journeys in the Southern Basin and Range." *Field Trip Guidebook. Geological Society of America, Cordilleran Section, Meeting, Las Vegas, Nevada. Special Publication No. 2,* 87-106. Las Vegas, Nevada: Department of Geoscience, University of Nevada Las Vegas. TIC 234473.

Burchfiel, B.C.; Fleck, R.J.; Secor, D.T.; Vincelette, R.R.; and Davis, G.A. 1974. "Geology of the Spring Mountains, Nevada." *Geological Society of America Bulletin, 85,* 1013-1022. 1:62,000-scale map. Boulder, Colorado: Geological Society of America. TIC 217346.

Byers, Jr., F.M.; Carr, W.J.; Orkild, P.P. 1989. "Volcanic Centers of Southwestern Nevada: Evolution of Understanding, 1960-1988." *Journal of Geophysical Research, 94,* 5908-5924. Washington, D.C.: American Geophysical Union. TIC 224013.

Byers, Jr., F.M.; Carr, W.J.; Orkild, P.P.; Quinlivin, W.D.; and Sargent, K.A. 1976. *Volcanic Suites and Related Cauldrons of Timber Mountain-Oasis Valley Caldera Complex, Southern Nevada.* U.S. Geological Survey Professional Paper 919. Denver, Colorado: U.S. Geological Survey. NNA.19870406.0239.

Caporuscio, F.A.; Vaniman, D.T.; Bish, D.L.; Broxton, D.E.; Arney, B.; Heiken, G.H.; Byers Jr., F.M.; Gooley, R.; and Semarge, E. 1982. *Petrologic Studies of Drill Cores USW G-2 and UE25b#1H, Yucca Mountain, Nevada.* LA-9255-MS. Los Alamos, New Mexico: Los Alamos National Laboratory. HQS.19880517.1110.

Carr, M.D.; Waddell, S.J.; Vick, G.S.; Stock, J.M.; Monsen, S.A.; Harris, A.G.; Cork, B.W.; and Byers Jr., F.M. 1986. *Geology of Drillhole UE25p#1: A Test Hole into Pre-Tertiary Rocks Near Yucca Mountain, Southern Nevada.* USGS-OFR-86-175. Denver, Colorado: U.S. Geological Survey. DTN: GS930283117461.002; HQS.19880517.2633.

Carr, W.J. 1984. *Regional Structural Setting of Yucca Mountain, Southwestern Nevada, and Late Cenozoic Rates of Tectonic Activity in Part of the Southwestern Great Basin, Nevada and California.* USGS-OFR-84-854. Denver, Colorado: U.S. Geological Survey. DTN: GS900983117435.001; NNA.19870325.0475.

Carr, W.J. 1990. "Styles of Extension in the Nevada Test Site Region, Southern Walker Lane Belt; an Integration of Volcano-Tectonic and Detachment Fault Models." *Basin and Range Extensional Tectonics Near the Latitude of Las Vegas, Nevada.* Wernicke, B.P. ed. Geological Society of America Memoir 176, 283-303. Boulder, Colorado: Geological Society of America. TIC 222540

Carr, W.J. 1992. "Structural Model for Western Midway Valley Based on RF Drillhole Data and Bedrock Outcrops (Appendix A)," in Gibson, J.D.; Swan, F.H.; Wesling, J.R.; Bullard, T.F.; Perman, R.C.; Angell, M.M.; and DiSilvestro, L.A. (eds.), "Summary and Evaluation of Existing Geological and Geophysical Data near Prospective Surface Facilities in Midway Valley, Yucca Mountain Project, Nye County, Nevada." SAND90-2491. Albuquerque, New Mexico: Sandia National Laboratories. DTN: SNSAND90249100.000; NNA.19910709.0001.

Cashman, P.H. and Trexler, J.H. 1995. "Evaluation of Hydrocarbon Potential," in *Evaluations of the Geologic Relations and Seismotectonic Stability of the Yucca Mountain Area, Nevada,* Nuclear Waste Site Investigation Progress Report. Reno, Nevada: Center for Neotectonic Studies, Mackay School of Mines, University of Nevada-Reno. TIC 224579.

Caskey, S.J.; Wesnousky, S.G.; Zhang, P.; and Slemmons, D.B. 1996. "Surface Faulting of the 1954 Fairview Peak (M_s=7.2) and Dixie Valley (M_s=6.8) Earthquakes, Central Nevada." *Bulletin of the Seismological Society of America, 86,* 761-787. El Cerrito, California: Seismological Society of America. TIC 234277.

Castor, S.B. and Lock, D.E. 1995. "Assessment of Industrial Minerals and Rocks in the Controlled Area." DOE/NV/10872-T272. Reno, Nevada: Nevada Bureau of Mines and Geology. TIC 237919.

Castor, S.B.; Feldman, S.C.; and Tingley, J.V. 1990. *Mineral Evaluation of the Yucca Mountain Addition, Nye County, Nevada.* Nevada Bureau of Mines and Geology Open-File Report 90-4. Reno, Nevada: University of Nevada-Reno, Mackay School of Mines. TIC 229055.

Cemen, I.; Wright, L.A.; Drake, R.E.; and Johnson, F.C. 1985. "Cenzoic Sedimentation and Sequence of Deformational Events at the Southeastern End of the Furnace Creek Strike-Slip Zone, Death Valley Region, California." Biddle, K.T. and Christie-Blick, N. (eds). Strike-slip Deformation, Basin Formation, and Sedimentation, *Society of Economic Paleontologists and Mineralogists Special Publication*, 37, 127-139. Tulsa, Oklahoma: Society of Economic Paleontologists and Mineralogists. TIC 225911.

Champion, D.E. 1991. "Volcanic Episodes Near Yucca Mountain as Determined by Paleomagnetic Studies at Lathrop Wells, Crater Flat, and Sleeping Butte, Nevada." *High Level Radioactive Waste Management, Proceedings of the Second Annual International Conference, Las Vegas, Nevada, April 28-May 3, 1991, 1,* 61-67. La Grange Park, Illinois: American Nuclear Society. TIC 217295.

Christiansen, R.L.; Lipman, P.W.; Carr, W.J.; Byers Jr., F.M.; Orkild, P.P.; and Sargent, K.A. 1977. "Timber Mountain-Oasis Valley Caldera Complex of Southern Nevada." *Geological Society of America Bulletin, 88,* 943-959. Boulder, Colorado: Geological Society of America. TIC 201802.

Claassen, H.C. 1985. *Sources and Mechanisms of Recharge for Ground Water in the West-Central Amargosa Desert, Nevada—A Geochemical Interpretation.* U.S. Geological Survey Professional Paper 712-F. Denver, Colorado: U.S. Geological Survey. NNA.19900124.0031.

Coe, J.A.; Yount, J.C.; and O'Leary, D.W. 1996. "Preliminary Results of Paleoseismic Investigations on the Rock Valley Fault System," in *Seismotectonic Framework and Characterization of Faulting at Yucca Mountain, Nevada.* (Whitney, J.W., report coordinator). U.S. Geological Survey Milestone Report 3GSH100M, Chapter 4.13. Denver, Colorado: U.S. Geological Survey. DTN: GS960583117441.001; MOL.19970129.0041.

Connolly, J.R. and Nimick, F.B. 1990. *Mineralogic and Chemical Data Supporting Heat Capacity Determination for Tuffaceous Rocks.* SAND88-0882. Albuquerque, New Mexico: Sandia National Laboratories. NNA.19890928.0125.

Connor, C.B. and Hill, B.E. 1995. "Three Nonhomogeneous Poisson Models for the Probability of Basaltic Volcanism: Application to the Yucca Mountain Region, Nevada." *Journal of Geophysical Research, 100,* 10,107-10,125. Washington, D.C.: American Geophysical Union. TIC 237682.

Craig, R.W. and Robison, J.H. 1984. *Geohydrology of Rocks Penetrated by Test Well UE25p#1, Yucca Mountain Area, Nye County, Nevada.* U.S. Geological Survey Water Resources Investigations Report 84-4248. Denver, Colorado: U.S. Geological Survey. NNA.19870317.0157.

Crowe, B.M. and Perry, F.V. 1990. "Volcanic Probability Calculations for the Yucca Mountain Site: Estimation of Volcanic Rates." *Proceedings Nuclear Waste Isolation in the Unsaturated Zone, Focus '89, Symposium,* 326-334. La Grange Park, Illinois: American Nuclear Society. TIC 225000.

Crowe, B.M.; Morley, R.; Wells, S.; Geissman, J.; McDonald, E.; McFadden, L.; Perry, F.; Murrell, M.; Poths, J.; and Forman, S. 1992. "The Lathrop Wells Volcanic Center: Status of Field and Geochronology Studies." *High Level Radioactive Waste Management, Proceedings of the Third Annual International Conference, Las Vegas, Nevada, April 12-16, 1992,* 1997-2013. La Grange Park, Illinois: American Nuclear Society. TIC 224346.

Crowe, B.M.; Perry, F.V.; Geisman, J.; McFadden, L.; Wells, S.; Marrell, S.; Potts, J.; Valentine, G.A.; Bowker, L.; and Finnegan, K. 1995. *Status of Volcanism Studies For The Yucca Mountain Site Characterization Project.* LA-12908-MS. Los Alamos, New Mexico: Los Alamos National Laboratory. MOL.19951127.0107.

Crowe, B.M.; Wallmann, P.; and Bowker, L. 1998. "Probabilistic Modeling of Volcanism Data: Final Volcanic Hazard Studies for the Yucca Mountain Site." Perry, F.V.; Crowe, B.M.; Valentine, G.A.; and Bowker, L.M. (eds.), *Synthesis of Volcanism Studies for the Yucca Mountain Site Characterization Project.* Los Alamos, New Mexico: Los Alamos National Laboratory Deliverable Report 3781MR1. MOL.19980722.0048.

CRWMS M&O 1996a. *Characterization of the ESF Thermal Test Area.* B00000000-01717-5705-00047 REV 01. Las Vegas, Nevada: CRWMS M&O. MOL.19970116.0187.

CRWMS M&O 1996b. *Probabilistic Volcanic Hazard Analysis for Yucca Mountain, Nevada.* BA0000000-01717-2200-00082 REV 00. Las Vegas, Nevada: CRWMS M&O. MOL.19961119.0034.

CRWMS M&O 1996c. *Geothermal Resource Assessment of the Yucca Mountain Area, Nye County, Nevada.* BA0000000-03255-5705-00002. Las Vegas, Nevada: CRWMS M&O. MOL.19960903.0027.

CRWMS M&O 1996d. *Yucca Mountain Project Stratigraphic Compendium.* BA0000000-01717-5700-00004 REV 01. Las Vegas, Nevada: CRWMS M&O. MOL.19970113.0088.

CRWMS M&O 1996e. *Mined Geologic Disposal System Advanced Conceptual Design Report, Volume II of IV, Repository.* B00000000-01717-5705-00027 REV 00. Las Vegas, Nevada: CRWMS M&O. MOL.19960826.0095.

CRWMS M&O 1997a. *Confirmation of Empirical Design Methodologies.* BABEE0000-01717-5705-00002 REV 00. Las Vegas, Nevada: CRWMS M&O. MOL.19980219.0104.

CRWMS M&O 1997b. *ISM2. 0: A 3D Geologic Framework Integrated Site Model of Yucca Mountain.* B00000000-01717-5700-00004 REV 00. Las Vegas, Nevada: CRWMS M&O. MOL.19970625.0119.

CRWMS M&O 1997c. *Yucca Mountain Site Geotechnical Report.* B00000000-01717-5705-00043 REV 01. Las Vegas, Nevada: CRWMS M&O. MOL.19980212.0354.

CRWMS M&O 1997d. *Determination of Available Volume for Repository Siting, Las Vegas, Nevada.* BCA000000-01717-0200-00007 REV 00. Las Vegas, Nevada: CRWMS M&O. MOL.19971009.0699.

CRWMS M&O 1998. *Yucca Mountain Site Description.* B00000000-01717-5700-00019 REV 00. Las Vegas, Nevada: CRWMS M&O. MOL.19980729.0047; MOL.19980729.0048; MOL.19980729.0049; MOL.19980729.0050; MOL.19980729.0051; MOL.19980729.0052; and MOL.19980729.0053.

Czarnecki, J.B. and Waddell, R.K. 1984. *Finite-Element Simulation of Ground-Water Flow in the Vicinity of Yucca Mountain, Nevada-California.* U.S. Geological Survey Water Resources Investigations Report 84-4349. Denver, Colorado: U.S. Geological Survey. NNA.19870407.0173.

Czarnecki, J.B.; Faunt, C.C.; Gable, C.W.; and Zyvolski, G.A. 1997. *Hydrogeology and Preliminary Calibration of a Preliminary Three-Dimensional Finite Element Ground-Water Flow Model of the Site Saturated Zone, Yucca Mountain, Nevada.* U.S. Geological Survey Administrative Report. Denver, Colorado: U.S. Geological Survey. MOL.19980204.0519.

D'Agnese, F.A. 1994. *Using Geoscientific Information Systems for Three-Dimensional Modeling of Regional Ground-Water Flow System, Death Valley Region, Nevada and California.* Doctoral dissertation. Golden, Colorado: Colorado School of Mines. TIC 236958.

D'Agnese, F.A.; Faunt, C.C.; Turner, A.K.; and Hill, M.C. 1997. *Hydrogeologic Evaluation and Numerical Simulations of the Death Valley Regional Ground-Water Flow System, Nevada and California.* U.S. Geological Survey Water Resources Investigation Report 96-4300. Denver, Colorado: U.S. Geological Survey. MOL.19980306.0253.

Davis, J.L.; Bennett, R.A.; Wernicke, B.P. 1998. "Geodetic Evidence for Deformation near Yucca Mt., Nevada," *EOS, Transactions, American Geophysical Union, 79,* n. 45, F203. Washington, D.C.: American Geophysical Union. TIC 243123.

Davisson, M.L.; Kenneally, J.M.; Smith, D.K.; Hudson, G.B.; Nimz, G.J.; and Rego, J.A. 1994. *Preliminary Report on the Isotope Hydrology Investigations at the Nevada Test Site.* UCRL-ID-116112. Livermore, California: Lawrence Livermore National Laboratory. MOL.19950406.0041.

Day, W.C.; Potter, C.J.; Sweetkind, D.S.; Dickerson, R.P.; and San Juan, C.A. 1998. *Bedrock Geologic Map of the Central Block Area, Yucca Mountain, Nevada.* U.S. Geological Survey Miscellaneous Investigations Series Map I-2601. Denver, Colorado: U.S. Geological Survey. TIC 237019.

Deere, D.U. 1968. "Geological Considerations." *Rock Mechanics in Engineering Practice.* Staff, R.G. and Zienkiewicz, D.C. (eds.), 1-20. New York, New York: John Wiley Publishing. TIC 234672.

dePolo, C.M.; Peppin, W.A.; and Johnson, P.A. 1993. "Contemporary Tectonics, Seismicity, and Potential Earthquake Sources in the White Mountains Seismic Gap, West-Central Nevada and East-Central California." *Tectonophysics, 225,* 271-299. Amsterdam, Netherlands: Elsevier Science Publishers. TIC 234521.

dePolo, C.M.; Ramelli, A.R.; and Bell, J.W. 1994. "The 1932 Cedar Mountain Earthquake, Central Nevada, U.S.A.—A Major Basin and Range Province Earthquake That Had a Widely Distributed Surface Faulting Pattern." Prentice, C.S.; Schwartz, D.P.; and Yeats, R.S., convenors, Proceedings of the Workshop on Paleoseismology. USGS-OFR-94-568 p. 50-52. Denver, Colorado: U.S. Geological Survey. TIC 234666.

Diehl, P. 1976. "Stratigraphy and Sedimentology of the Wood Canyon Formation, Death Valley Area, California," in Troxel, B. and Wright, L. (eds.), "Geologic Features of Death Valley, California." *California Division of Mines and Geology Special Report 106.* Sacramento, California: State of California, Division of Mines and Geology. TIC 232853.

DOE (U.S. Department of Energy) 1986. *Nuclear Waste Policy Act Environmental Assessment, Yucca Mountain Site, Nevada Research and Development Area, Nevada.* DOE/RW-0073. Washington, D.C.: U.S. Department of Energy. TIC 202189.

DOE 1988. *Site Characterization Plan, Yucca Mountain Site, Nevada Research and Development Area, Nevada.* DOE/RW-0199. Washington, D.C.: U.S. Department of Energy, Office of Civilian Radioactive Waste Management. HQO.19881201.0002.

DOE 1997. *Site Characterization Progress Report: Yucca Mountain, Nevada.* Number 15. DOE/RW-0498. Washington, D.C.: Office of Civilian Radioactive Waste Management. HQO.19970428.0001.

DOE 1998. Quality Assurance Requirements and Description. DOE/RW-0333P, Rev. 8. Washington, D.C.: Offfice of Civilian Radioactive Waste Management.

Doser, D.I. 1986. "Earthquake Processes in the Rainbow Mountain-Fairview Peak-Dixie Valley, Nevada, Region (1954-1959)." *Journal of Geophysical Research, 91,* 12,572–12,586. Washington, D.C.: American Geophysical Union. TIC 223278.

Doser, D.I. and Smith, R.B. 1989. "An Assessment of Source Parameters of Earthquakes in the Cordillera of the Western United States." *Bulletin of the Seismological Society of America, 79,* 1383-1409. El Cerrito, California: Seismological Society of America. TIC 236846.

Duebendorfer, E.M. and Black, R.A. 1992. "Kinematic Role of Transverse Structures in Continental Extension: An Example from the Las Vegas Valley Shear Zone, Nevada." *Geology, 20,* 1107-1110. Boulder, Colorado: Geological Society of America. TIC 236844.

Engstrom, D.A. and Rautman, C.A. 1996 . *Geology of the USW SD-9 Drill Hole, Yucca Mountain, Nevada.* SAND96-2030. Albuquerque, New Mexico: Sandia National Laboratories. MOL.19970508.0288.

Erickson, J.R. and Waddell, R.K. 1985. *Identification and Characterization of Hydrologic Properties of Fractured Tuff Using Hydraulic and Tracer Tests—Test Well USW H-4, Yucca Mountain, Nye County, Nevada.* U.S. Geological Survey Water Resources Investigations Report 85-4066. Denver, Colorado: U.S. Geological Survey. NNA.19870407.0184.

Ervin, E.M.; Luckey, R.R.; and Burkhardt, D.J. 1993. "Summary of Revised Potentiometric-Surface Map for Yucca Mountain and Vicinity, Nevada." *High Level Radioactive Waste Management, Proceedings of the Fourth Annual International Conference, Las Vegas, Nevada, April 26-30, 1993, 2,* 1554-1558. La Grange Park, Illinois: American Nuclear Society. TIC 235056.

Fabryka-Martin, J.T.; Flint, A.L.; Sweetkind, D.S.; Wolfsberg, A.V.; Levy, S.S.; Roemer, C.J.C.; Roach, J.L.; Wolfsberg, L.E.; and Duff, M.C. 1997. *Evaluation of Flow and Transport Models of Yucca Mountain, Based on Chlorine-36 Studies for FY97.* LANL Milestone Report SP2224M3. Los Alamos, New Mexico: Los Alamos National Laboratory. MOL.19980204.0916.

Fabryka-Martin, J.T.; Turin, H.J.; Wolfsberg, A.V.; Brenner, D.; Dixon, P.R.; and Musgrave, J.A. 1996. *Summary Report of Chlorine-36 Studies.* LANL Milestone Report 3782. Los Alamos, New Mexico: Los Alamos National Laboratory. MOL.19980429.0123.

Fabryka-Martin, J.T.; Wightman, S.J.; Murphy, W.J.; Wickham, M.P.; Caffee, M.W.; Nimz, G.J.; Southern, J.R.; Sharma, P. 1993. "Distribution of Chlorine-36 in the Unsaturated Zone at Yucca Mountain: An Indicator of Fast Transport Paths." *Proceedings of Topical Meeting on Site Characterization and Model Validation, Focus '93, Las Vegas, Nevada, September 26-29, 1993,* 58-67. Los Alamos, New Mexico: Los Alamos National Laboratory. TIC 233133.

Fabryka-Martin, J.T.; Wolfsberg, A.V.; Dixon, P.R.; Levy, S.; Musgrave, J.; and Turin, H.T. 1996. *Summary Report of Chlorine-36 Studies: Sampling, Analysis, and Simulation of Cl-36 in the Exploratory Studies Facility.* LANL Milestone Report 3783M. Los Alamos, New Mexico: Los Alamos National Laboratory. MOL.19970211.0036.

Faulds, J.E.; Bell, J.W.; Feuerbach, D.L.: and Ramelli, A.R. 1994. *Geologic Map of the Crater Flat Area, Nevada.* Nevada Bureau of Mines and Geology Map 101. Reno, Nevada: Mackay School of Mines, University of Nevada-Reno. TIC 211484.

Fleck, R.J.; Turrin, B.D.; Sawyer, D.A.; Warren, R.G.; Champion, D.E.; Hudson, M.R.; and Minor, S.A. 1996. "Age and Character of Basaltic Rocks of the Yucca Mountain Region, Southern Nevada." *Journal of Geophysical Research, 101,* 8205-8227. Washington, D.C.: American Geophysical Union. TIC 234626.

Flint, A.L. and Flint, L.E. 1994. "Spatial Distribution of Potential Near Surface Moisture Flux at Yucca Mountain." *High Level Radioactive Waste Management, Proceedings of the Fifth Annual International Conference, Las Vegas, Nevada, May 22-26, 1994, 4,* 2352–2358. La Grange Park, Illinois: American Nuclear Society. TIC 224142.

Flint, A.L.; Hevesi, J.A.; and Flint, L.E. 1996. *Conceptual and Numerical Model of Infiltration for the Yucca Mountain Area, Nevada.* U.S. Geological Survey. Milestone Report 3GUI623M. Denver, Colorado: U.S. Geological Survey. MOL.19970409.0087.

Flint, L.E. 1998. *Characterization of Hydrogeologic Units Using Matrix Properties, Yucca Mountain, Nevada.* U.S. Geological Survey Water Resources Investigations Report 97-4243. Denver, Colorado: U.S. Geological Survey. DTN: GS960908312231.004; MOL.19980429.0512.

Forester, R.M.; Bradbury, J.P.; Carter, C.; Elvidge, A.B.; Hemphill, M.L.; Lundstrom, S.A.; Mahan, S.A.; Marshall, B.D.; Neymark, L.A.; Paces, J.B.; Sharpe, S.E.; Whelan, J.F.; and Wigand, P.E. 1996. *Synthesis of Quarternary Response of the Yucca Mountain Unsaturated and Saturated Zone Hydrology to Climate Change.* U.S. Geological Survey Milestone Report 3GCA102M. Denver, Colorado: U.S.Geological Survey. MOL.19970211.0026.

Freeze, R.A. and Cherry, J.A. 1979. *Groundwater.* Englewood Cliffs, New Jersey: Prentice-Hall. TIC 217571.

Fritz, P. and Fontes, J.C. 1980. *Handbook of Environmental Chemistry.* Amsterdam, Netherlands: Elsevier Scientific Publishing Company. TIC 243187.

Garside, L.J. 1973. "Radioactive Mineral Occurrences in Nevada." *Nevada Bureau of Mines and Geology Bulletin 81,* 121. Reno, Nevada: Nevada Bureau of Mines and Geology. TIC 217104.

Geldon, A.L. 1996. *Results and Interpretation of Preliminary Aquifer Tests in Boreholes UE-25c #1, UE-25c#2, and UE-25c #3, Yucca Mountain, Nye County, Nevada.* U.S. Geological Survey Water-Resources Investigations Report 94-4177. Denver, Colorado: U.S. Geological Survey. MOL.19980724.0389.

Geslin, J.K.; Moyer, T.C. and Buesch, D.C. 1995. *Summary of Lithologic Logging of New and Existing Boreholes at Yucca Mountain, Nevada, August 1993 to February 1994.* U.S. Geological Survey Open File Report 94-342. Denver, Colorado: U.S. Geological Survey. DTN: GS940308314211.009; TIC 215172.

Giampaoli, M.C. 1986. "Trip Report." *Hydrologic Field Reconnaissance led by Robert Coache, Water Resources Division, Nevada Department of Conservation and Natural Resources, April 24, 1986.* M86-GEO-MEG-054. Las Vegas, Nevada: Science Applications International Corporation. HQS.19880517.1765; TIC 218738.

Gianella, V.P. and Callaghan, E. 1934. "The Cedar Mountain, Nevada, Earthquake of December 20, 1932." *Bulletin of the Seismological Society of America, 24,* 345-383. El Cerrito, California: Seismological Society of America. TIC 217009.

Gibson, J.D.; Swan, F.H.; Wesling, J.R.; Bullard, T.F.; Perman, R.C.; Angell, M.M.; and DiSilvestro, L.A. 1992. *Summary and Evaluation of Existing Geological and Geophysical Data Near Prospective Surface Facilities in Midway Valley, Yucca Mountain Project, Nye County, Nevada.* SAND-90-2491. Albuquerque, New Mexico: Sandia National Laboratories. DTN: SNSAND90249100.000; NNA.19910709.0001.

Gomberg, J.S. 1991a. "Seismicity and Detection/Location Threshold in the Southern Great Basin Seismic Network." *Journal of Geophysical Research, 96,* 16,401-16,414. Washington, D.C.: American Geophysical Union. TIC 212627.

Gomberg, J.S. 1991b. "Seismicity and Shear Strain in the Southern Great Basin of Nevada and California." *Journal of Geophysical Research, 96,* 16,383-16,399. Washington, D.C.: American Geophysical Union. TIC 225033.

Grow, J.A.; Barker, C.E.; and Harris, A.G. 1994. "Oil and Gas Exploration Near Yucca Mountain, Southern Nevada." *High Level Radioactive Waste Management, Proceedings of the Fifth Annual International Conference, Las Vegas, Nevada, May 22-26, 1994,* 1298-1315. New York, New York: American Nuclear Society. TIC 210984.

Hardy, M.P. and Bauer, S.J. 1991. *Drift Design Methodology and Preliminary Application for the Yucca Mountain Site Characterization Project.* SAND89-0837. Albuquerque, New Mexico: Sandia National Laboratories. NNA.19910808.0105.

Hardyman, R.F. and Oldow, J.S. 1991. "Tertiary Tectonic Framework and Cenozoic History of the Central Walker Lane, Nevada." Raines, G.L.; Lisle, R.E.; Schafer, R.W.; and Wilkinson, W.H. (eds.), "Geology and Ore Deposits of the Great Basin." *Geological Society of Nevada Symposium Proceedings, 1,* 279-301. Reno, Nevada: Geological Society of Nevada. TIC 233074.

Harmsen, S.C., and Bufe, C.G. 1992. *Seismicity and Focal Mechanisms in the Southern Great Basin of Nevada and California: 1987 through 1989.* USGS-OFR-91-572. Denver, Colorado: U.S. Geological Survey. NNA.19920408.0001.

Harrington, C.D. and Whitney, J.W. 1987. "Scanning Electron Microscope Method for Rock-Varnish Dating." *Geology, 15,* 967-970. Boulder, Colorado: Geological Society of America. TIC 203298.

Hauksson, E.; Hutton, K.; Kanamori, H.; Jones, L.; Mori, J.; Hough, S.; and Roquemore, G. 1995. "Preliminary Report on the 1995 Ridgecrest Earthquake Sequence in Eastern California." *Seismological Research Letters, 66,* 54-60. El Cerrito, California: Seismological Society of America. TIC 234445.

Hevesi, J.A. and Flint, A.L. 1998. *Geostatistical Model for Estimating Precipitation and Recharge in the Yucca Mountain Region, Nevada - California.* U.S. Geological Survey Water Resources Investigations Report 96-4123. Denver, Colorado: U.S. Geological Survey. MOL.19981209.0399.

Hill, B.E.; Conner, C.B.; and Trapp, J.S. 1997. "Igneous Activity". Sagar, B. (ed.), NRC High-Level Radioactive Waste Program Annual Progress Report: Fiscal Year 1996, NUREG/CR-6513, No. 1, 2-1 - 2-32. Washington, D.C.: U.S. Nuclear Regulatory Commission. TIC 242355.

Hill, D.P.; Wallace, R.E.; and Cockeram, R.S. 1985. "Review of Evidence on the Potential for Major Earthquakes and Volcanism in the Long Valley-Mono Craters-White Mountains Regions of Eastern California." *Earthquake Prediction Research, 3,* 571-594. Tokyo, Japan: Terra Scientific Publishing Company. TIC 217846.

Ho, C-H. 1995. "Sensitivity in Volcanic Hazard Assessment for the Yucca Mountain High-Level Nuclear Waste Repository Site: The Model and the Data." *Mathematical Geology, 27,* 239-258. New York: Plenum. TIC 234736.

Hoek, E. and Brown, E.T. 1988. "The Hoek-Brown Failure Criterion - A 1988 Update." *Proceedings of the Canadian Rock Mechanics Symposium,* 31-38. Toronto, Canada: University of Toronto Press. TIC 240286.

Hudson, D.B. and Flint, A.L. 1996. *Estimation of Shallow Infiltration and Presence of Potential Fast Pathways for Shallow Infiltration in the Yucca Mountain Area, Nevada.* Draft U.S. Geological Survey Water Resources Investigation Report. Denver, Colorado: U.S. Geological Survey. MOL.19970116.0025.

ISRM (International Society for Rock Mechanics) 1981. "Basic Geotechnical Description of Rock Masses," *International Journal of Rock Mechanics and Mining Sciences & Geomechanics Abstracts, 18,* 85-110. Great Britain: Pergamon Press Ltd. TIC 234727.

Jayko, A.S. 1990. "Shallow Crustal Deformation in the Pahranagat Area, Southern Nevada," in "Basin and Range Extensional Tectonics Near the Latitude of Las Vegas, Nevada." Wernicke, B.P. (ed.), *Geological Society of America Memoir 176,* 213-236. Boulder, Colorado: Geological Society of America. TIC 241469.

Johnson, C. and Hummel, P. 1991. "Yucca Mountain, Nevada—Nuclear Waste or Resource Rich." *Geotimes, 36,* n. 8, 14-16. Falls Church, Virginia: American Geological Institute. TIC 234741.

Jung, J.; Ryder, E.E.; Boucheron, E.A.; Dunn, E.; Holland, J.F.; and Miller, J.D. 1993. *Design Support Analyses: North Ramp Design Package 2C.* Albuquerque, New Mexico: Sandia National Laboratories. DTN: SNT01122093001.001; NNA.19940607.0103.

Kicker, D.C.; Martin, E.R.; Brechtel, C.E.; Stone, C.A.; and Kessel, D.S. 1996. *Geotechnical Characterization of the Main Drift of the Exploratory Studies Facility.* SAND95-2183. Albuquerque, New Mexico: Sandia National Laboratories. MOL.19970806.0296.

LaCamera, R.J. and Westenburg, C.L. 1994. *Selected Ground-Water Data for the Yucca Mountain Region, Southern Nevada and Eastern California, through December 1992.* USGS-OFR-94-54. Denver, Colorado: U.S. Geological Survey. MOL.19980410.0299.

Laczniak, R.J.; Cole, J.C.; Sawyer, D.A.; and Trudeau, D.A. 1996. *Summary of Hydrogeologic Controls on Ground-Water Flow at the Nevada Test Site, Nye County, Nevada.* U.S. Geological Survey Water Resources Investigations Report 96-4109. Carson City, Nevada: U.S. Geological Survey. TIC 226157.

Lappin, A.R.; VanBuskirk, R.G.; Enniss, D.O.; Butters, S.W.; Prater, F.M.; Muller, C.B.; and Bergosh, J.L. 1982. *Thermal Conductivity, Bulk Properties, and Thermal Stratigraphy of Silicic Tuffs from the Upper Portion of Hole USW-G1, Yucca Mountain, Nye County, Nevada.* SAND81-1873. Albuquerque, New Mexico: Sandia National Laboratories. HQS.19880517.1669.

Liu, B.; Fabryka-Martin, J.; Wolfsburg, A.; Robinson, B.; and Sharma, P. 1995. "Significance of Apparent Discrepancies in Water Ages Derived from Atmospheric Radionuclides at Yucca Mountain, Nevada." *Proceedings of 1995 American Institute of Hydrology Annual Meeting, May 14-18, 1995, Denver, Colorado.* LA-UR-95-572. Los Alamos, New Mexico: Los Alamos National Laboratory. TIC 222140.

Luckey, R.R.; Tucci, P.; Faunt, C.C.; Ervin, E.M.; Steinkampf, W.C.; D'Agnese, F.A.; and Patterson, G.L. 1996. *Status of Understanding of the Saturated-Zone Ground-Water Flow System at Yucca Mountain, Nevada, as of 1995.* U.S. Geological Survey Water Resources Investigations Report 96-4077. Denver, Colorado: U.S. Geological Survey. TIC 227084.

Maldonado, F.Y. and Koether, S.L. 1983. *Stratigraphy, Structure, and Some Petrographic Features of Tertiary Volcanic Rocks at the USW G-2 Drill Hole, Yucca Mountain, Nye County, Nevada.* USGS-OFR-83-732. Denver, Colorado: U.S. Geological Survey. NNA.19870506.0143.

Marrett, R.; Stamatakos, J.A.; Ferrill, D.A.; Connor, C.B.; Hill, B.E. 1998. "Extension Rate Estimates From Faults, Fracture Opening, and Earthquakes near Yucca Mountain, Nevada," *EOS, Transactions, American Geophyical Union, 79*, n. 45, F203. Washington, D.C.: American Geophysical Union. TIC 243125.

Marshall, B.D.; Kyser, T.K.; and Peterman, Z.E. 1996. *Oxygen Isotopes and Trace Elements in the Tiva Canyon Tuff, Yucca Mountain and Vicinity, Nye County, Nevada.* USGS-OFR-95-431. Denver, Colorado: U.S. Geological Survey. MOL.19970804.0096.

Martin III, R.J.; Price, R.H.; Boyd, P.J.; and Noel, J.S. 1994. *Bulk and Mechanical Properties of the Paintbrush Tuff Recovered from Borehole USW NRG-6.* SAND93-4020. Albuquerque, New Mexico: Sandia National Laboratories. MOL.19940811.0001.

Martin III, R.J.; Price, R.H.; Boyd, P.J. and Noel, J.S. 1995. *Bulk and Mechanical Properties of the Paintbrush Tuff Recovered from Borehole USW NRG-7/7A.* SAND94-1996. Albuquerque, New Mexico: Sandia National Laboratories. MOL.19950316.0087.

McConnell, K.I.; Blackford, M.E.; and Ibrahim, A.K. 1992. *Staff Technical Position on Investigations to Identify Fault Displacement Hazards and Seismic Hazards at a Geological Repository.* NUREG-1451. Washington D.C.: U.S. Nuclear Regulatory Commission. TIC 204829.

Menges, C.M. and Whitney, J.W. 1996. "Distribution of Quaternary Faults at Yucca Mountain," in *Seismotectonic Framework and Characterization of Faulting at Yucca Mountain, Nevada* (Whitney, J.W., report coordinator). U.S. Geological Survey Milestone Report 3G5H100M, Chapter 4.2. Denver, Colorado: U.S. Geological Survey. MOL.19970129.0041.

Montazer, P. and Wilson, W.E. 1984. *Conceptual Hydrologic Model of Flow in the Unsaturated Zone, Yucca Mountain, Nevada.* U.S. Geological Survey Water Resources Investigations Report 84-4345. Lakewood, Colorado: U.S. Geological Survey. NNA.870519.0109.

Moyer, T.C. and Geslin, J.K. 1995. *Lithostratigraphy of the Calico Hills Formation and Prow Pass Tuff (Crater Flat Group) at Yucca Mountain, Nevada.* USGS-OFR-94-460. Denver, Colorado: U.S. Geological Survey. DTN: GS940608314211.028; MOL.19941208.0003.

Moyer, T.C.; Geslin, J.K. and Buesch, D.C. 1995. *Summary of Lithologic Logging of New and Existing Boreholes at Yucca Mountain, Nevada, July 1994 to November 1994.* U.S. Geological Survey Open File Report 95-102. Denver, Colorado: U.S. Geological Survey. DTN: GS941208314211.060; TIC 224224.

Nevada Bureau of Mines and Geology 1997. "The Nevada Mineral Industry 1996." *Nevada Bureau of Mines and Geology Special Publication MI-1996.* Reno, Nevada: Nevada Bureau of Mines and Geology. TIC 240403.

Neymark, L.A.; Marshall, B.D.; Kwak, F.K.; Futa, K.; and Mahan, S.A. 1995. *Geochemical and Pb, Sr, and O Isotopic Study of the Tiva Canyon Tuff and Topopah Spring Tuff, Yucca Mountain, Nye County, Nevada.* USGS-OFR-95-134. Denver, Colorado: U.S. Geological Survey. MOL.19960531.0087.

Nimick, F.B. and Connolly, J.R. 1991. *Calculation of Heat Capacities for Tuffaceous Units from the Unsaturated Zone at Yucca Mountain, Nevada.* SAND88-3050. Albuquerque, New Mexico: Sandia National Laboratories. TIC 201604.

Noble, D.C.; Weiss, S.I.; and McKee, E.H. 1991. "Magmatic and Hydrothermal Activity, Caldera Geology, and Regional Extension in the Western Part of the Southwestern Nevada Volcanic Field." Raines, G.L.; Lisle, R.E.; Shafer, R.W.; and Wilkinson, W.W. (eds.), *Geology and Ore Deposits of the Great Basin: Symposium Proceedings,* 913-934. Reno, Nevada: Geological Society of Nevada. TIC 222751.

NRC (Nuclear Regulatory Commission) 1997. *Issue Resolution Status Report on Methods to Evaluate Climate Change and Associated Effects at Yucca Mountain* (Key Technical Issue: Unsaturated and Saturated Flow Under Isothermal Conditions). Washington, D.C.: U.S. Nuclear Regulatory Commission. MOL. 19971117.0697.

O'Brien, G.M. 1993. *Earthquake-Induced Water-Level Fluctuations at Yucca Mountain, Nevada, June 1992.* USGS-OFR-93-73. Denver, Colorado: U.S. Geological Survey. NNA.19930326.0022.

O'Neill, J.M.; Whitney, J.W.; and Hudson, M.R. 1992. *Photogeologic and Kinematic Analysis of Lineaments at Yucca Mountain, Nevada—Implications for Strike-slip Faulting and Oroclinal Bending.* USGS-OFR-91-623. Denver, Colorado: U.S. Geological Survey. DTN: GS920783117461.002; TIC 205807.

Ortiz, T.S.; Williams, R.L.; Nimick, F.B.; Whittet, B.C.; and South, D.L. 1985. *A Three-Dimensional Model of Reference Thermal/Mechanical and Hydrological Stratigraphy at Yucca Mountain, Southern Nevada.* SAND84-1076. Albuquerque, New Mexico: Sandia National Laboratories. NNA.19890315.0013.

Osterkamp, W.R.; Lane, L.J.; and Savard, C.S. 1994. "Recharge Estimates Using a Geomorphic/Distributed-Parameter Simulation Approach, Amargosa River Basin." *Water Resources Bulletin, 30,* n. 3, 493-507. Minneapolis, Minnesota: American Water Resources Association. TIC 237428.

Paces, J.D.; Whelan, J.F.; Forester, R.M.; Bradbury, J.P.; Marshall, B.D.; and Mahan, S.A. 1997. *Summary of Discharge Deposits in the Amargosa Valley.* U.S. Geological Survey Milestone Report SPC33M4 prepared for the U.S. Department of Energy. Denver, Colorado: U.S. Geological Survey. MOL. 19981104.0151.

Papke, K.G. 1972. "Erionite and Other Associated Zeolites in Nevada." *Nevada Bureau of Mines and Geology Bulletin 79.* Reno, Nevada: University of Nevada-Reno, Mackay School of Mines. TIC 219484.

Patterson, G.L.; Weeks, E.P.; Rousseau, J.P.; and Oliver, T.A. 1995. *Interpretation of Pneumatic and Chemical Data from the Unsaturated Zone near Yucca Mountain, Nevada.* U.S. Geological Survey Deliverable 3GGP605M. Denver, Colorado: U.S. Geological Survey. MOL.19970324.0058.

Perry, F.V. and Crowe, B.M. 1992. "Geochemical Evidence for Waning Magmatism and Polycyclic Volcanism at Crater Flat, Nevada." *High Level Radioactive Waste Management, Proceedings of the Third Annual International Conference, Las Vegas, Nevada, April 12-16, 1992,* 2356-2365. La Grange Park, Illinois: American Nuclear Society. TIC 225113.

Perry, F.V.; Crowe, B.M.; Wells, S.G.; McFadden, L.D.; Geissman, J.W.; Poths, J.; Murrell, M.T.; Heizler, M.T.; Bowker, L.M.; Finnegan, K.P.; and Valentine, G.A. 1998. "Geology and Geochronology of Basaltic Volcanism in the Yucca Mountain Region." Chapter 2. Perry, F.V.; Crowe, B.M.; Valentine, G.A.; and Bowker, L.M. (eds.), *Synthesis of Volcanism Studies for the Yucca Mountain Site Characterization Project.* LA13478. Los Alamos, New Mexico: Los Alamos National Laboratory. MOL.19980722.0048.

Peterman, Z.E.; Widmann, B.L.; Marshall, B.D.; Aleinikoff, J.N.; Futa, K.; and Mahan, S.A. 1994. "Isotopic Tracers of Gold Deposition in Paleozoic Limestones, Southern Nevada." *High Level Radioactive Waste Management, Proceedings of the Fifth Annual International Conference, Las Vegas, Nevada, May 22-26, 1994, 3,* 1316-1323. La Grange Park, Illinois: American Nuclear Society. TIC 226990.

Pezzopane, S.K. 1996. "Relevant Earthquake Sources," in *Seismotectonic Framework and Characterization of Faulting at Yucca Mountain, Nevada* (Whitney, J.W., report coordinator). U.S. Geological Survey Milestone Report 3GSH100M, Chapter 11. Denver, Colorado: U.S. Geological Survey. MOL.19970129.0041.

Pezzopane, S.K. and Dawson, T.E. 1996. "Fault Displacement Hazard: A Summary of Issues and Information," in *Seismotectonic Framework and Characterization of Faulting at Yucca Mountain, Nevada.* (Whitney, J.W., report coordinator). U.S. Geological Survey Milestone Report 3GSH100M, Chapter 9. Denver, Colorado: U.S. Geological Survey. MOL.19970129.0041.

Piety, L.A. 1996. *Compilation of Known or Suspected Quaternary Faults within 100 km of Yucca Mountain, Nevada and California.* USGS-OFR-94-112. Denver, Colorado: U.S. Geological Survey. MOL.19971009.0003.

Potter, C.J.; Dickerson, R.P.; and Day, W.C. 1995. "Nature and Continuity of the Sundance Fault, Yucca Mountain, Nevada." USGS Administrative Report to the U.S. Department of Energy. Denver, Colorado: U.S. Geological Survey. DTN: GS950808314221.004; MOL.19960403.0161.

Rautman, C.A. 1995. "Modeling Spatial Heterogeneity of Thermal Conductivity Using a Surrogate Property." *High-Level Radioactive Waste Management, Proceedings of the Sixth Annual International Conference, Las Vegas, Nevada, April 30-May 5, 1995,* 83-84. La Grange Park, Illinois: American Nuclear Society. TIC 238768.

Rautman, C.A. and Engstrom, D.A. 1996a. *Geology of the USW SD-7 Drill Hole, Yucca Mountain, Nevada.* SAND 96-1474. Albuquerque, New Mexico: Sandia National Laboratories. MOL.19971218.0442.

Rautman, C.A. and Engstrom, D.A. 1996b. *Geology of the USW SD-12 Drill Hole, Yucca Mountain, Nevada.* SAND96-1368. Albuquerque, New Mexico: Sandia National Laboratories. MOL.19970613.0101.

Reynolds, M.W. 1969. *Stratigraphy and Structural Geology of the Titus and Titanothere Canyons Area, Death Valley, California.* University of California-Berkeley, doctoral dissertation. Map Scale 1:62,500. Berkeley, California: University of California-Berkeley. TIC 204144.

Robison, J.H. and Craig, R.W. 1991. *Geohydrology of Rocks Penetrated by Test Well USW H-5, Yucca Mountain, Nye County, Nevada.* U.S. Geological Survey Water Resources Investigations Report 88-4168. Denver, Colorado: U.S. Geological Survey. NNA.19900110.0400.

Rogers, A.M. and Lee, W.H.K. 1976. "Seismic Study of Earthquakes in the Lake Mead, Nevada-Arizona Region." *Bulletin of the Seismological Society of America, 66,* 1657–1681. El Cerrito, California: Seismological Society of America. TIC 218413.

Rogers, A.M.; Harmsen, S.C.; Carr, W.J.; and Spence, W.J. 1983. *Southern Great Basin Seismological Data Report for 1981 and Preliminary Data Analysis.* USGS-OFR-83-669. Denver, Colorado: U.S. Geological Survey. DTN: GS900983117411.003. NNA.19870518.0053.

Rogers, A.M.; Harmsen, S.C.; Corbett, E.J.; Priestly, K.; and dePolo, D. 1991. "The Seismicity of Nevada and Some Adjacent Parts of the Great Basin." Slemmons, D.B.; Engdahl, E.R.; Zoback, M.D.; and Blackwell, D.D. (eds.), *Neotectonics of North America.* DMV 01, 153-184. Boulder, Colorado: Geological Society of America. TIC 243190.

Rogers, A.M.; Harmsen, S.C.; and Mermonte, M.E. 1987. *Evaluation of the Seismicity of the Southern Great Basin and Its Relationship to the Tectonic Framework of the Region.* USGS-OFR-87-408. Denver, Colorado: U.S. Geological Survey. DTN: GS900983117411.006; MOL.19980330.0439.

Rousseau, J.P.; Kwicklis, E.M.; and Gilles, D.C. (eds.) 1996. *Hydrogeology of the Unsaturated Zone, North Ramp Area of the Exploratory Studies Facility, Yucca Mountain, Nevada.* Draft Milestone Report 3GUP431M. (Final Report to be published as Water Resources Investigations Report 98-4050). Denver, Colorado: U.S. Geological Survey. MOL.19980220.0164.

Sargent, K.A. and Stewart, J.H. 1971. *Geologic Map of the Spector Range NW Quadrangle, Nye County, Nevada.* U.S. Geological Survey Geological Quadrangle Map GQ-884, Scale 1:24,000. Washington, D.C.: U.S. Geological Survey. TIC 205650.

Sass, J.H.; Lachenbruch, A.H.; Dudley Jr., W.W.; Priest, S.S.; and Munroe, R.J. 1988. *Temperature, Thermal Conductivity, and Heat Flow near Yucca Mountain, Nevada: Some Tectonic and Hydrologic Implications.* USGS-OFR-87-649. Denver, Colorado: U.S. Geological Survey. NNA.19890123.0010; MOL.19971027.0303.

Savage, J.C.; Lisowski, M.; Gross, W.K.; King, N.E.; and Svarc, J.L. 1994. "Strain Accumulation Near Yucca Mountain, Nevada, 1983-1993," *Journal of Geophysical Research, 99,* 18103-18107. Washington, D.C.: American Geophysical Union. TIC 235681.

Savage, J.C.; Lisowski, M.; and Prescott, W.H. 1990. "An Apparent Shear Zone Trending North-Northwest Across the Mojave Desert into Owens Valley, Eastern California." *Geophysical Research Letters, 17,* 2113–2116. Washington, D.C.: American Geophysical Union. TIC 235680.

Savage, J.C.; Svarc, J.L.; and Prescott, W.H. 1998. "Strain Accumulation at Yucca Mountain, Nevada, 1983-1998." *EOS, Transactions, American Geophysical Union, 79,* n. 45, F203. Washington, D.C.: American Geophysical Union. TIC 243124.

Savard, C.S. 1994. "Ground-water Recharge In Fortymile Wash Near Yucca Mountain, Nevada, 1992-93." *High Level Radioactive Waste Management, Proceedings of the Fifth Annual International Conference, Las Vegas, Nevada, May 22-26, 1994,* 1805-1813. La Grange Park, IIIinois: American Nuclear Society. TIC 236603.

Savard, C.S. 1998. *Estimated Ground-Water Recharge from Streamflow in Fortymile Wash near Yucca Mountain, Nevada.* U.S. Geological Survey Water Resources Investigation Report 97-4273. Denver, Colorado: U.S. Geological Survey. TIC 236848.

Sawyer, D.A.; Fleck, R.J.; Lanphere, M.A.; Warren, R.G.; Broxton, D.E.; and Hudson, M.R. 1994. "Episodic Caldera Volcanism in the Miocene Southwestern Nevada Volcanic Field: Revised Stratigraphic Framework, 40-Ar/39-Ar Geochronology, and Implications for Magmatism and Extension." *Geological Society of America Bulletin, 106,* 1304-1318. Boulder, Colorado: Geological Society of America. TIC 222523.

Schalla, R.A. and Johnson, E.H. (eds.) 1994. "Oil Fields of the Great Basin." *Nevada Petroleum Society Symposium.* Reno, Nevada: Nevada Petroleum Society, Inc. TIC 211290.

Scott, R.B. 1990. "Tectonic Setting of Yucca Mountain, Southwest Nevada." *Basin and Range Extensional Tectonics Near the Latitude of Las Vegas, Nevada.* Wernicke, B.P. ed. Geological Society of America Memoir 176, 251-282. Boulder, Colorado: Geological Society of America. TIC 222230

Scott, R.B. and Bonk, J. 1984. *Preliminary Geologic Map of Yucca Mountain, Nye County, Nevada, with Geologic Cross-Sections.* USGS-OFR-84-494. Scale 1:12,000. Denver, Colorado: U.S. Geological Survey. TIC 203162.

Scott, R.B. and Castellanos, M. 1984. *Stratigraphic and Structural Relations of Volcanic Rocks in Drill Holes USW GU-3 and USW G-3, Yucca Mountain, Nye County, Nevada.* USGS-OFR-84-491. Denver, Colorado: U.S. Geological Survey. MOL.19980403.0203.

Scott, R.B.; Bath, G.D.; Flanigan, V.J.; Hoover, D.B.; Rosenbaum, J.G.; and Spengler, R.W. 1984. *Geological and Geophysical Evidence of Structures in Northwest-trending Washes, Yucca Mountain, Southern Nevada, and Their Possible Significance to a Nuclear Waste Repository in the Unsaturated Zone.* USGS-OFR-84-567. Denver, Colorado: U.S. Geological Survey. DTN: GS900908314212.006; NNA.19890715.0538.

Sherlock, M.G.; Cox, D.P.; and Huber, D.F. 1996. "Known Mineral Deposits and Occurrences in Nevada." Singer, D.A. (ed.), *An Analysis of Nevada's Metal-Bearing Mineral Resources.* Nevada Bureau of Mines and Geology OFR 96-2. Reno, Nevada: Nevada Bureau of Mines and Geology. TIC 233941.

Shields, G.; Smith, K.D.; and Brune, J.N. 1995. "Source Parameters of a Sequence of Very Shallow Earthquakes in the Rock Valley Fault Zone, Southern Nevada Test Site." *EOS Transactions, American Geophysical Union-Abstract, 76,* F426. Washington, D.C.: American Geophysical Union. TIC 235738.

Simonds, F.W.; Whitney, J.W.; Fox, K.F.; Ramelli, A.R.; Yount, J.C.; Carr, M.D.; Menges, C.M.; Dickerson, R.P.; and Scott, R.B. 1995. *Map Showing Fault Activity in the Yucca Mountain Area, Nye County, Nevada.* U.S. Geological Survey Miscellaneous Investigation Series Map I-2520, Scale 1:24,000. Denver, Colorado: U.S. Geological Survey. DTN: GS931183117461.004; MOL.19980618.0033.

Smith, R.B. and Arabasz, W.J. 1991. "Seismicity of the Intermountain Seismic Belt." Slemmons, D.B.; Engdahl, E.R.; Zoback, M.D.; and Blackwell, D., (eds.), *Neotectonics of North America, DMV 01,* 185-228. Boulder, Colorado: Geological Society of America. TIC 240998.

Smith, R.B. and Sbar, M.L. 1974. "Contemporary Tectonics and Seismicity of the Western United States with Emphasis on the Intermountain Seismic Belt." *Geological Society of America Bulletin, 85,* 1205-1218. Boulder, Colorado: Geological Society of America. TIC 238890.

SNL (Sandia National Laboratories) 1995. *Evaluation of Geotechnical Monitoring Data from the ESF North Ramp Starter Tunnel, April 1994 to June 1995.* SAND95-1675, Rev. 1. Albuquerque, New Mexico: Sandia National Laboratories. MOL.19960508.0117.

SNL 1996. *Hydraulic Fracturing Stress Measurements in Test Hole ESF-AOD-HDFR#1, Thermal Test Facility, Exploratory Studies Facility at Yucca Mountain.* Albuquerque, New Mexico: Sandia National Laboratories. MOL.19970717.0008.

SNL 1995. "Geotechnical Logging of Core by Examination of Core and Video Records," SNL-TP-233, Technical Procedure, Section 3.5.1 of *Geotechnical Logging of Core By Examination of Core and Video Records from Coreholes and Procedures for Establishing QA Records.* Albuquerque, New Mexico: Sandia National Laboratories. MOL. 19981026.0209.

Spengler, R.W. and Fox Jr., K.F. 1989. "Stratigraphic and Structural Framework of Yucca Mountain, Nevada." *Radioactive Waste Management and the Nuclear Fuel Cycle. 13,* n. 1–4, 21-36. Denver, Colorado: Hardwood Academic Publishers. TIC 222668.

Spengler, R.W.; Braun, C.A.; Martin, L.G.; and Weisenberg, C.W. 1994. *The Sundance Fault—A Newly Recognized Shear Zone at Yucca Mountain, Nevada.* USGS-OFR-94-49. Denver, Colorado: U.S. Geological Survey. DTN: GS940108314221.002; TIC 210718.

Squires, R.R. and Young, R.L. 1984. *Flood Potential of Fortymile Wash and Its Principal Southwestern Tributaries, Nevada Test Site, Southern Nevada.* U.S. Geological Survey Water Resources Investigations Report 83-4001. Denver, Colorado: U.S. Geological Survey. NNA.19890511.0110.

Stewart, J.H. 1970. *Upper Precambrian and Lower Cambrian Strata in the Southern Great Basin, California and Nevada.* U.S. Geological Survey Professional Paper 620. Washington, D.C.: U.S. Geological Survey. TIC 232997.

Stewart, J.H. 1980. "Geology of Nevada, A Discussion to Accompany the Geologic Map of Nevada." *Nevada Bureau of Mines & Geology Special Publication No. 4.* Reno, Nevada: University of Nevada-Reno, Nevada Bureau of Mines and Geology. TIC 219557.

Stewart, J.H. 1988. "Tectonics of the Walker Lane Belt, Western Great Basin - Mesozoic and Cenozoic Deformation in a Zone of Shear." Ernst, W.G. (ed.), *Metamorphism and Crustal Evolution of the Western United States, VII,* 684-713. Englewood Cliffs, New Jersey: Prentice-Hall, Inc. TIC 218183.

Stewart, J.H. and Diamond, D.S. 1990. "Changing Patterns of Extensional Tectonics; Overprinting of the Basin of the Middle and Upper Miocene Esmeralda Formation in Western Nevada by Younger Structural Basins." *Basin and Range Extensional Tectonics Near the Latitude of Las Vegas, Nevada.* Wernicke, B.P. ed. Geological Society of America, Memoir 176, 447-475. Boulder, Colorado: Geological Society of America. TIC 222540

Stimac, J.; Hickmott, J.; Abell, R.; Larocque, A.C.L.; Broxton, D.E.; Gardner, J.; Chipera, S.; Wolff, J.; and Gaueke, E. 1996. "Redistribution of Pb and Other Volatile Trace Metals During Eruption, Devitrification, and Vapor-Phase Crystallization of the Bandelier Tuff, New Mexico." *Journal of Volcanology and Geothermal Research, 73,* 245-266. Amsterdam, Netherlands: Elsevier Science Publishers. TIC 234905.

Stock, J.M.; Healy, J.H.; Hickman, S.H.; Zoback, M.D. 1985. "Hydraulic Fracturing Stress Measurements at Yucca Mountain, Nevada, and Relationship to the Regional Stress Field," *Journal of Geophysical Research, 90,* 8691-8706. Washington, D.C.: American Geophysical Union. DTN: GS930583117481.005; TIC 219009.

Striffler, P.; O'Brien, G.M.; Oliver, T.; and Burger, P. 1996. *Perched Water Characteristics and Occurrences, Yucca Mountain, Nevada.* Milestone Report 3GUS600M. Denver, Colorado: U.S. Geological Survey. MOL.19980224.0105.

Sweetkind, D.S. and Williams-Stroud, S. 1996. *Characteristics of Fractures at Yucca Mountain, Nevada: Synthesis Report.* Administrative Report. Denver, Colorado: U.S. Geological Survey. MOL.19961213.0181.

Taylor, W.J. 1990. "Spatial and Temporal Relations of Cenozoic Volcanism and Extension in the North Paroc and Seaman Ranges, Eastern Nevada." *Basin and Range Extensional Tectonics Near the Latitude of Las Vegas, Nevada.* Wernicke, B.P. ed. Geological Society of America Memoir 176, 181-193. Boulder, Colorado: Geological Society of America. TIC 241468

Thomas, B.E.; Hjalmarson, H.W.; and Waltemeyer, S.D. 1997. *Methods for Estimating Magnitude and Frequency of Floods in the Southwestern United States.* USGS Water Supply Paper 2433. TIC 243122.

Thomas, J.M.; Welch, A.H.; and Dettinger, M.D. 1996. Geochemistry and Isotope Hydrology of Representative Aquifers in the Great Basin Region of Nevada, Utah, and Adjacent States. USGS Professional Paper 1409-C. Denver, Colorado: U.S. Geological Survey. TIC 235070.

Thordarson, W. 1983. *Geohydrologic Data and Test Results from Well J-13, Nevada Test Site, Nye County, Nevada.* U.S. Geological Survey Water Resources Investigations Report 83-4171. Denver, Colorado: U.S. Geological Survey. NNA.19870518.0071.

Thordarson, W. and Howells, L. 1987. *Hydraulic Tests and Chemical Quality of Water at Well USW VH-1, Crater Flat, Nye County, Nevada.* U.S. Geological Survey Water Resources Investigations Report 86-4359. Denver, Colorado: U.S. Geological Survey. NNA.19890922.0289.

Throckmorton, C. K. and Verbeek, E.R. 1995. *Joint Networks in the Tiva Canyon and Topopah Spring Tuffs of the Paintbrush Group, Southwestern Nevada.* USGS-OFR-95-2. Denver, Colorado: U.S. Geological Survey. TIC 235000.

Trexler, J.H.; Cole, J.C.; and Cashman, P.H. 1996. "Middle Devonian-Mississippian Stratigraphy On and Near the Nevada Test Site: Implications for Hydrocarbon Potential." *American Association of Petroleum Geologists Bulletin, 80,* n. 11, 1736-1762. Tulsa, Oklahoma: American Association of Petroleum Geologists. TIC 233004.

Tschanz, C.M. and Pampeyan, E.H. 1970. "Geology and Mineral Deposits of Lincoln County, Nevada." *Nevada Bureau of Mines and Geology Bulletin 73.* Reno, Nevada: University of Nevada-Reno, Mackay School of Mines. TIC 232876.

Tucci, P. and Burkhardt, D.J. 1995. *Potentiometric Surface Map, 1993, Yucca Mountain and Vicinity, Nevada.* U.S. Geological Survey Water Resources Investigations Report 95-4149. Denver, Colorado: U.S. Geological Survey. MOL.19960924.0517.

Unruh, J.R. 1991. "The Uplift of the Sierra Nevada and Implications for Late Cenozoic Epeirogeny in the Western Cordillera." *Geological Society of America Bulletin 103,* 1395-1404. Boulder, Colorado: Geological Society of America. TIC 241710.

USBR (U.S. Bureau of Reclamation) 1992. *Soil and Rock Geotechnical Investigations, Field and Laboratory Studies, North Ramp Surface Facility, Exploratory Studies Facility, Yucca Mountain Project, Nevada.* Technical Memorandum No. 3610-92-35. Denver, Colorado: Department of Interior, U.S. Bureau of Reclamation. TIC 208867.

USGS 1992. *Study Plan for Study 8.3.1.9.2.1, Natural Resource Assessment of Yucca Mountain, Nye County, Nevada, Rev. 0.* Washington, D.C.: U.S. Department of Energy, Office of Civilian Radioactive Waste Management. NNA.19920826.0147.

USGS 1998. *Probabilistic Seismic Hazard Analyses for Fault Displacement and Vibratory Ground Motion at Yucca Mountain, Nevada.* Wong, I.G. and Stepp, J.C., Report Coordinators. Final Report prepared by the CRWMS M&O for the U.S. Geological Survey. Volumes 1-3. Oakland, California: CRWMS-M&O. MOL.19980619.0640.

Vaniman, D.T. and Crowe, B.M. 1981. *Geology and Petrology of the Basalts of Crater Flat: Applications to Volcanic Risk Assessment for the Nevada Nuclear Waste Storage Investigations.* LA-8845-MS. Los Alamos, New Mexico: Los Alamos National Laboratory. HQS.19880517.1541.

Vortman, L.J. 1991. *An Evaluation of the Seismicity of the Nevada Test Site and Vicinity.* SAND86-7006, UC-814. Albuquerque, New Mexico: Sandia National Laboratories. NNA.19911118.0084.

Waddell, RK. 1984. *Hydrologic and Drill-Hole Data for Test Wells UE-29a #1 and UE-29a #2, Fortymile Canyon, Nevada Test Site.* USGS-OFR-84-142. Denver, Colorado: U.S. Geological Survey. HQS.19880517.1861.

Waddell, R.K.; Robison, J.H.; and Blankennagel, R.K. 1984. *Hydrology of Yucca Mountain and Vicinity, Nevada-California—Investigative Results Through Mid-1983.* U.S. Geological Survey Water Resources Investigations Report 84-4267. Denver, Colorado: U.S. Geological Survey. NNA.19870406.0343.

Walker, G.E. and Eakin, T.E. 1963. "Geology and Ground Water of Amargosa Desert, Nevada-California." *Ground-Water Resources Reconnaissance Series Report 14.* Carson City, Nevada: State of Nevada Department of Conservation and Natural Resources. TIC 208665.

Wallace, T.C.; Helmberger, D.V.; and Engen, G.R. 1983. "Evidence of Tectonic Release from Underground Nuclear Explosions in Long-period P Waves." *Bulletin of Seismological Society of America, 73,* 593-613. El Cerrito, California: Seismological Society of America. TIC 218114.

Weeks, E.P. 1987. "Effect of Topography on Gas Flow in Unsaturated Fractured Rock." *Geophysical Monograph 42,* 165-170. Washington, D.C.: American Geophysical Union. TIC 223605.

Weiss, S.I., Noble, D.C.; and Larson, L.T. 1995. "Multiple Episodes of Hydrothermal Activity and Epithermal Mineralization in the Southwestern Nevada Volcanic Field and Their Relations to Magmatic Activity, Volcanism and Regional Extension." *Task 3: Evaluation of Mineral Resource Potential, Caldera Geology and Volcano-tectonic Framework at and near Yucca Mountain: Report for October 1994 – September 1995.* Reno, Nevada: Center for Neotectonic Studies, University of Nevada-Reno. TIC 243162

Weiss, S.I.; Noble, D.C.; and Larson, L.T. 1996. "Hydrothermal Origin and Significance of Pyrite in Ash-Flow Tuffs at Yucca Mountain, Nevada." *Economic Geology, 90,* 2081-2090. El Paso, Texas: Economic Geology Publishing Co. TIC 234950.

Wells, S.G.; McFadden, L.D.; Renault, C.E.; and Crowe, B.M. 1990. "Geomorphic Assessment of Late Quaternary Volcanism in the Yucca Mountain Area, Southern Nevada: Implications for the Proposed High-Level Radioactive Waste Repository." *Geology, 18,* 549-553. Boulder, Colorado: Geological Society of America. TIC 218564.

Wernicke, B.; Axen, G.J.; and Snow, J.K. 1988. "Basin and Range Extensional Tectonics at the Latitude of Las Vegas, Nevada." *Geological Society of America Bulletin, 100,* 1738-1757. Boulder, Colorado: Geological Society of America. TIC 233007.

Wernicke, B.; Davis, J.L.; Bennett, R.A.; and Elosegui, P. 1998. "Anomalous Strain Accumulation in the Yucca Mountain Area, Nevada." *Science, 279,* 2096-2098. Washington, D.C.: American Association for the Advancement of Science. TIC 235956.

Wesling, J.R.; Bullard, T.F.; Swan, F.H.; Perman, R.C.; Angel, M.M.; and Gibson, J.D. 1992. *Preliminary Mapping of Surficial Geology of Midway Valley, Yucca Mountain, Nye County, Nevada.* SAND91-0607. Albuquerque, New Mexico: Sandia National Laboratories. DTN: SNF12000000001.000; NNA.19920410.0053.

Whitney, J.W. and Harrington, C.D. 1993. "Relict Colluvial Boulder Deposits as Paleoclimatic Indicators in the Yucca Mountain Region, Southern Nevada." *Geological Society of America Bulletin, 105,* 1008-1018. Boulder, Colorado: Geological Society of America. TIC 208099.

Whitney, J.W. and Taylor, E.M. (eds.) 1996. "Quaternary Paleoseismology and Stratigraphy of the Yucca Mountain Area," *in Seismotectonic Framework and Characterization of Faulting at Yucca Mountain, Nevada.* (Whitney, J.W., Report Coordinator). "U.S. Geological Survey Milestone Report 3GSH1OOM, Chapter 4." Denver, Colorado: U.S. Geological Survey. MOL.19970129.0041.

Winograd, I.J. and Thordarson, W. 1975. *Hydrogeologic and Hydrochemical Framework, South-Central Great Basin, Nevada-California, with Special Reference to the Nevada Test Site.* U.S. Geological Survey Professional Paper 712-C. Denver, Colorado: U.S. Geological Survey. HQS.19880517.2908; NNA.19870406.0201.

Wohletz, K.H. and Heiken, G.H. 1992. *Volcanology and Geothermal Energy.* Berkeley, California: University of California Press. TIC 241603.

Yang, I.C.; Rattray, G.W.; and Yu. P. 1996. *Interpretation of Chemical and Isotopic Data from Boreholes in the Unsaturated Zone at Yucca Mountain, Nevada.* U.S. Geological Survey Water Resources Investigation Report 96-4058. Denver, Colorado: U.S. Geological Survey. MOL.19970715.0408.

Yang, I.C.; Yu, P.; Rattray, G.W.; and Thorstenson, D.C. 1997. *Hydrochemical Investigations and Geochemical Modeling in Characterizing the Unsaturated Zone at Yucca Mountain, Nevada.* U.S. Geological Survey Milestone Report 3GUH607M. Denver, Colorado: U.S. Geological Survey. MOL.19970415.0393.

YMP (Yucca Mountain Site Characterization Project) 1993. *Topical Report: Evaluation of the Potentially Adverse Condition Evidence of Extreme Erosion During the Quaternary Period at Yucca Mountain, Nevada.* YMP/92-41-TPR. Vol. 4. Las Vegas, Nevada: Yucca Mountain Site Characterization Office. NNA.19930316.0208.

YMP 1995. *Mined Geologic Disposal System License Application Annotated Outline.* YMP/94-05, Rev. 0. Las Vegas, Nevada: Yucca Mountain Site Characterization Office. TIC 236270

Young, R.A. 1972. *Water Supply for the Nuclear Rocket Development Station at the U.S. Atomic Energy Commission's Nevada Test Site.* U.S. Geological Survey Water-Supply Paper 1938. Washington, D.C.: U.S. Geological Survey. TIC 200544.

Yudhbir, W.L. and Prinzl, F. 1983. "An Empirical Failure Criterion for Rock Masses." *Proceedings of the 5th Congress of the International Society for Rock Mechanics, held in Melbourne, Australia,* B1-B8. Rotterdam, Netherlands: A.A Balkema for the International Society for Rock Mechanics. TIC 226278.

Zielinski, R.A. 1978. "Uranium Abundances and Distribution in Associated Glassy and Crystalline Rhyolites of the Western United States." *Geological Society of America Bulletin, 89,* 409–414. Boulder, Colorado: Geological Society of America. TIC 241708.

Zoback, M.D. and Healy, J.H. 1984. "Friction, Faulting, and In Situ Stress." *Annales Geophysicae, 2,* n. 6, 689-698. Paris, France: European Geophysical Society, Gauthier-Villars. TIC 234995.

Zoback, M.L. 1989. "State of Stress and Modern Deformation of the Basin and Range Province," *Journal of Geophysical Research, 94,* 7105-7128. Washington, D.C.: American Geophysical Union. TIC 225191.

Zoback, M.L.; Anderson, R.E.; and Thompson, G.A. 1981. "Cainozoic Evolution of the State of Stress and Style of Tectonism of the Basin and Range Province of the Western United States." *Philosophical Transactions of the Royal Society of London, Series A, 300,* 407-434. London, England: Royal Society of London. TIC 218137.

5.2 CODES, STANDARDS, AND REGULATIONS

64 FR 8640. Disposal of High-Level Radioactive Waste in a Proposed Geologic Repository at Yucca Mountain. Proposed rule: 10 CFR 63. Washington, D.C.: U.S. Government Printing Office. TIC: 242725.

5.3 PROCEDURES

M&O Procedures

QAP -2-0, *Conduct of Activities*

PRO-TS-003, *Development of Technical Documents Not Subject to QARD Requirements*

INTENTIONALLY LEFT BLANK